AD-A159 039 THE ATTENUATION OF FLEXURAL WAVES IN MASS LOADED BEAMS (U) MASSACHUSETTS INST OF TECH CAMBRIDGE DEPT OF OCEAN ENGINEERING T L SMITH MAY 85 N66314-70-A-0073 1/2

UNCLASSIFIED F/G 20/11 NL

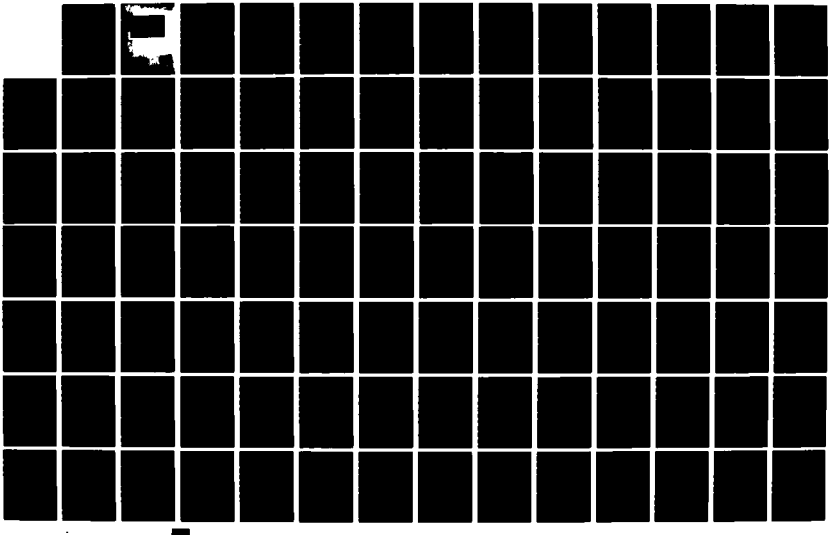

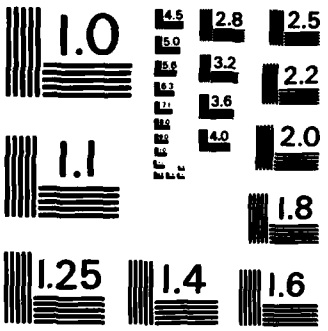

MICROCOPY RESOLUTION TEST CHART
NATIONAL BUREAU OF STANDARDS-1963-A

AD-A159 039

DEPARTMENT OF OCEAN ENGINEERING

MASSACHUSETTS INSTITUTE OF TECHNOLOGY

CAMBRIDGE, MASSACHUSETTS 02139

THE ATTENUATION OF FLEXURAL WAVES IN MASS LOADED BEAMS

TIMOTHY L. SMITH

MAY 1985

COURSE XIIIA

N66314-70-A-0073

THE ATTENUATION OF FLEXURAL WAVES IN MASS LOADED BEAMS

by

TIMOTHY L. SMITH LT/USN

B.S. Mech. Eng., Auburn University
(1981)

SUBMITTED TO THE DEPARTMENT OF
OCEAN ENGINEERING
IN PARTIAL FULFILLMENT OF THE REQUIREMENTS
FOR THE DEGREES OF

MASTER OF SCIENCE IN NAVAL ARCHITECTURE AND MARINE ENGINEERING

AND

MASTER OF SCIENCE IN MECHANICAL ENGINEERING

at the

MASSACHUSETTS INSTITUTE OF TECHNOLOGY
May, 1985

© Timothy L. Smith, 1985

DTIC
ELECTE
SEP 10 1985
S D

The author hereby grants to M.I.T. and the U.S. Government permission to reproduce and to distribute copies of this thesis document in whole or in part.

Signature of Author. . . . . Timothy L. Smith LT/USN.
Department of Ocean Engineering
May, 1985

Certified by . . . . . .
Professor Ira Dyer
Thesis Supervisor

Certified by . . . . . J. Kim Vandiver
Professor J. Kim Vandiver
Thesis Reader

Accepted by . . . . . A. Douglas Carmichael
Professor Douglas A. Carmichael
Chairman, Dept. Graduate Committee
Department of Ocean Engineering

Accepted by . . . . . .
Professor Ain Ants Sonin
Chairman, Dept. Committee on
Graduate Studies
Department of Mechanical Engineering

THE ATTENUATION OF FLEXURAL WAVES IN MASS LOADED BEAMS

by

TIMOTHY L. SMITH, LT/USN

Submitted to the Department of Ocean Engineering in May 1985 in partial fulfillment of the requirements for the Degrees of Master of Science in Naval Architecture and Marine Engineering and Master of Science in Mechanical Engineering

ABSTRACT

This thesis experimentally tests the effect of resiliently mounted, independent masses on the propagation of flexural waves in a rectangular beam. The flexural waves are attenuated over a wide frequency band, and the magnitude and band of the attenuation is determined by the attached mass per unit length and the spring constant and resistance per unit length of the mounting material. The experimental results are compared with analytical predictions for the flexural wave attenuation. The results confirm the analytical model used and that the attached mass system acts as a dynamic absorber.

Thesis Supervisor: Professor Ira Dyer, Ph.D.
Professor of Ocean Engineering

Accession For
NTIS
DTIC
Unannounced
Justification
By
Distribution/
Availability Codes
Dist
A-1
perform 50 on file.
DTIC
COPY
INSPECTED

ACKNOWLEDGEMENTS

I wish to thank and recognize those who have helped me along the way and made this thesis possible. First, I would like to thank Professor Ira Dyer for his time, effort and patience. His ideas and physical intuition were invaluable. I would also like to thank Professor Kim Vandiver for the loan of his spectral analyzer.

I also want to thank Kodali Rao and Greg Chisholm for their assistance. Greg was especially helpful in providing me with access to the Vibrations Laboratory and the lab equipment.

I want to recognize Anna Markowitz for her cheerful assistance in preparing this thesis. She was very patient with me even though I sometimes made the work difficult.

Finally, I wish to thank my wife, Linda, and children, Lee, Kristin and Jill, for their personal sacrifices they were forced to make on my behalf. Certainly without their love and patience, this thesis would not have been possible.

Sincerely,

Timothy L. Smith

TABLE OF CONTENTS

LIST OF FIGURES

LIST OF FIGURES

(continued)

GLOSSARY OF SYMBOLS

A	Cross sectional area of beam
A_o	Attenuation for a distance λ_o
E	Young's Modulus
F_o	Exciting force magnitude
I	Cross sectional moment of inertia of beam
K	Propagation constant
K_o	Propagation constant of untreated beam
K_i	Imaginary part of the propagation constant
K'	Normalized propagation constant, K/K_o
M	Main Mass
R	Resistance per unit length
R'	Loss factor
f	Frequency
g	Gravitational acceleration
k	Spring constant per unit length
l	Length
m	Mass per unit length added to beam, dynamic absorber mass
t	Time
x	Longitudinal dimension of beam
y	Displacement of beam, displacement of main mass

GLOSSARY OF SYMBOLS

(continued)

α Mode shape factor

β Ratio of added mass per unit length to beam mass per unit length

λ_o Wave length in untreated beam

η Displacement of added mass

ρ Mass per unit volume

ω Radian frequency

ω_o Natural frequency of added mass-spring system

ω' Normalized radian frequency, ω/ω_o

1. INTRODUCTION

This thesis deals with the attenuation of flexural waves in a rectangular beam loaded with many independent masses mounted on it with a resilient material. The fundamental difference between this thesis and other known works is that attenuation or damping is achieved by many individual spring-mass-damper systems distributed along the beam. This is in contrast to the usual constrained layer or free-surface layer damping treatments which are commonly used in structural vibration damping.

The motivation for this thesis is the need to better understand and be able to predict vibration levels in ship and submarine hulls which contain resiliently mounted equipment. For example, it is known that as flexural waves propagate along a submarine hull, more attenuation takes place than can be accounted for with current models such as submerged shells without internal equipment. One possible explanation is that the resiliently mounted equipment inside the hull contribute to the wave attenuation, yielding the higher than expected results.

To date, the primary reason for using resilient mountings is to isolate the internal equipment from the hull thereby reducing the transmission of unwanted vibration to the hull. Now it appears that a secondary

effect may be that of an unintentional 'dynamic absorber'. The intent of this thesis is to experimentally test in a preliminary fashion the effect of resiliently mounted equipment on the propagation of flexural waves along the hull.

The hull of a ship or submarine, while at first glance a regular pattern of plates and frames, is actually a highly inhomogeneous system. This leads to some very complex modelling which would quickly overshadow the problem to be evaluated here. So, it is desirable to study a system which possesses both the important features of the real structure and yet be simple enough to treat experimentally. To this end, this thesis, intended as a preliminary study of the problem, models the hull and its internally mounted equipment as a uniform beam with a simple distribution of resiliently attached masses. Furthermore, the dimensions of the attached masses used was small enough to make the distribution continuous. This is a natural starting point as ship structures are frequently modelled as some type of beam system.

First the analytical solution of the problem was addressed by the thesis supervisor and students working with him. Using elementary beam theory and assumptions about the distribution and behavior of the attached masses, an analytical model was derived. Then, this model is used to predict the attenuation for given mass

distributions and resilient materials. A summary of the derivation is given in this thesis.

Next, an experiment was devised and carried out by the author to verify the analytical results. This experiment is the principal focus of this thesis. It consisted of a uniform beam on which an approximately continuous mass distribution was resiliently mounted. A white noise flexural wave input was used at one end of the beam. Then the difference in vibration levels between the "input end" and "output end" of the beam was measured. The difference in vibration levels or attenuation was then compared with that predicted by the analytical model. The agreement between the two results are quite good.

2. ANALYTICAL MODEL

For the purpose of this investigation, a uniform beam with an attached uniform distribution of spring-mass-damper systems is used as the model (see Figure 1). The beam is assumed to vibrate in flexure (bending) only with the attached masses vibrating in the same plane of motion as the beam. Note that Figure 1 shows the attached masses on both sides of the beam. This symmetry is required so that no longitudinal waves are created during vibration through asymmetric coupling effects. Figure 2 shows the coordinates and parameters used in this derivation.

If the attached masses are not present, elementary beam theory yields the familiar result

$$EI \frac{\partial^4 y}{\partial x^4} + \rho A \frac{\partial^2 y}{\partial t^2} = 0 \qquad (1)$$

as the governing equation for the free, flexural vibration of a uniform beam. Assume an $e^{-i\omega t}$ time dependence and a solution of the form e^{iKx}, and then recall that the general solution for equation (1) becomes

$$y=C_1\sin(Kx)+C_2\cos(Kx)+C_3\sinh(Kx)+C_4\cosh(Kx) \qquad (2)$$

with the $e^{-i\omega t}$ time dependence omitted. Also recall that

the propagation constant

$$K^4 = \left(\frac{\rho A \omega^2}{EI}\right). \qquad (3)$$

For this case, K is purely real and no attenuation takes place as the flexural waves propagate along the beam. However, if the attached mass systems are included in the derivation, K will turn out to have an imaginery part and the flexural wave will be attenuated as it propagates along the beam.

Again, referring to Figure 2, the double-sided configuration shown is used in the derivation[2] to simplify the algebra, but the results are valid for comparison with practical single-sided configurations, at least approximately. Ignoring any rotation of the attached mass and using elementary beam theory, two simultaneous differential equations governing the free vibration of the system are obtained.

These equations are:

$$EI \frac{\partial^4 y}{\partial x^4} + \rho A \frac{\partial^2 y}{\partial t^2} + R\left(\frac{\partial y}{\partial t} - \frac{\partial \eta}{\partial t}\right) + k(y-\eta) = 0 \qquad (4)$$

for the beam and

$$m \frac{\partial^2 \eta}{\partial t^2} + R\left(\frac{\partial \eta}{\partial t} - \frac{\partial y}{\partial t}\right) + k(\eta - y) = 0 \qquad (5)$$

for the attached masses.

Again, assuming $e^{-i\omega t}$ time dependence, equations (4) and (5) become

$$EI \frac{\partial^4 y}{\partial x^4} - \omega^2 \rho A - i\omega R(y-\eta) + k(y-\eta) = 0 \qquad (6)$$

and

$$-\omega^2 m\eta - i\omega R(\eta-y) + k(\eta-y) = 0. \qquad (7)$$

Now solving equation (7) for $(y-\eta)$ leads to

$$(y-\eta) = y \left(\frac{\omega^2 m}{\omega^2 m + i\omega R - k}\right). \qquad (8)$$

All that remains is to substitute equation (8) into equation (6) and assume a solution of the form e^{iKx} as before. This yields the new propagation constant

$$K^4 = \left(\frac{\rho A \omega^2}{EI}\right) + \left(\frac{m\omega^2}{EI}\right) \left(\frac{i\omega R - k}{\omega^2 m + i\omega R - k}\right). \qquad (9)$$

Looking back to the propagation constant for the beam alone, note that

$$K^4 = \left(\frac{\rho A \omega^2}{EI}\right). \qquad (3)$$

So now by defining an "untreated" beam propagation constant as

$$K_o^4 = K^4 = \left(\frac{\rho A \omega^2}{EI}\right) \qquad (10)$$

and substituting K_o into equation (9), the "treated" beam propagation constant becomes

$$K^4 = K_o^4 \left[1 + \left(\frac{m}{\rho A}\right) \left(\frac{i\omega R - k}{\omega^2 m + i\omega R - k}\right)\right]. \qquad (11)$$

Equation (11) is the heart of the problem. Since the propagation constant can now have an imaginary part (whether or not R=0), attenuation will occur as the flexural waves propagate along the beam.

All that remains to be done is to find the magnitude of the attenuation, which requires taking the imaginary part of the fourth root of equation (11). This was done by Mr. Kodali Rao*. He devised a computer program that would generate the magnitude of the real and imaginary parts of equation (11) given the input parameters of the beam-mass system.

Rao's equation for the non-dimensional propagation

*Center for Advanced Engineering Study, M.I.T., working with Professor Ira Dyer.

constant is

$$K'^4 = \frac{R'^2 + \left(\frac{1}{\omega'^2}\right)(1-\omega'^2) + \left(\frac{\beta}{\omega'^2}\right)[R'^2\omega'^2 + (1-\omega'^2)] + i\omega'\beta R'}{R'^2 + \left(\frac{1}{\omega'^2}\right)(1-\omega'^2)} \qquad (12)$$

where

$K' = \left(\frac{K}{K_o}\right)$, $\omega' = \left(\frac{\omega}{\omega_o}\right)$, $R' = \left(\frac{R}{\omega m}\right)$ and $\beta = \left(\frac{m}{\rho A}\right)$. Here ω_o is defined as the natural frequency of the attached mass-spring system.

Note that in non-dimensional form, the only system parameters needed are the normalized frequency ω', the loss factor of the resilient material, R', and the mass ratio of the attached mass to the beam mass, β.

The output of Rao's program is of the form (K_i/K_o) which, for the purpose of this thesis, has been converted to an attenuation, A_o, for the distance of λ_o measured in dB, where λ_o is the wavelength of the flexural wave in the untreated beam. This is accomplished by recognizing that the attenuation arises from $e^{-K_i x}$. Attenuation in dB is then

$$(8.686)K_i x. \qquad (13)$$

Attenuation in the distance λ_o then becomes

$$(8.686)K_o\lambda_o\left(\frac{K_i}{K_o}\right) = (8.686)(2\pi)\left(\frac{K_i}{K_o}\right). \qquad (14)$$

Or

$$A_o = 54.5 \left(\frac{K_i}{K_o}\right). \qquad (15)$$

Figure 3 is a typical attenuation curve predicted by this model. In the figure, β=0.50, and R'=0.46. The mass-spring-damper distribution assumed produces attenuation over a frequency band with the maximum attenuation near $\omega=\omega_o$. (In Figure 3, $A_{o,max}$=11.3 dB at ω/ω_o=1.1). It can be shown that the attenuation attained increases with β and (1/R'). Also, the width of the attenuation band increases with R'.

This behavior is recognized as that of a dynamic absorber. To show this, the derivation for a dynamic absorber is included here[5]. Figure 3A shows a symmetric dynamic absorber. The coordinates used are the same as in Figure 2. The equations of motion for this system are:

$$M\frac{\partial^2 y}{\partial t^2} + R\left(\frac{\partial y}{\partial t} - \frac{\partial \eta}{\partial t}\right) + k(y-\eta) = F_o e^{-i\omega t} \qquad (16)$$

and

$$m\frac{\partial^2 \eta}{\partial t^2} + R\left(\frac{\partial \eta}{\partial t} - \frac{\partial y}{\partial t}\right) + k(\eta-y) = 0 \qquad (17)$$

where F_o is the amplitude of the exciting force.

As before, assume a solution of the form $e^{-i\omega t}$, solve equation (17) for $(y-\eta)$ and substitute back into equation (16). The result of this is

$$\left(\frac{Y}{F_o}\right) = \left[\frac{\omega^2 m + i\omega R - k}{-\omega^2 M(\omega^2 m + i\omega R - k) - \omega^2 m(i\omega R - k)}\right]. \qquad (18)$$

Equation (18) can be written in the form A+iB so that the magnitude of the ratio (y/F_o) is $(A^2+B^2)^{1/2}$. The algebra yields

$$\left|\frac{Y}{F_o}\right| = \left[\frac{\omega^2 R^2 + (\omega^2 m - k)^2}{[\omega^2 M(\omega^2 m - k) - \omega^2 mk]^2 + \omega^2 R^2 (\omega^2 M + \omega^2 m)^2}\right]^{1/2}. \qquad (19)$$

Now, nondimensionalizing equation (19),

$$\left|\frac{Y}{F_o}\right| = \left[\frac{R'^2 + \left(1 - \frac{1}{\omega'^2}\right)^2}{\left(\frac{m}{M}\right)^2 \left[R'^2 + \left(\frac{1}{\omega'^2}\right)^2\right]}\right]^{1/2}. \qquad (20)$$

Equation (20) is very similar to equation (12) for the beam system. Reduction of the main mass vibration amplitude is a function of the mass ratio and loss factor as before. The behavior of equation (20) is shown in Figure 3B.

When there is no resistance, R'=0 and the main mass vibration amplitude goes to zero at $(\omega / \omega_o)=1$. The main mass stands still because the attached mass-spring vibration produces an infinite force opposing the exciting force. As ω moves away from ω_o, the main mass vibration amplitude increases with $(\omega / \omega_o)^2$. The result is a very narrow attenuation band about $\omega = \omega_o$.

If resistance is introduced, R'≠0 and the main mass vibration amplitude is no longer zero at $(\omega/\omega_o)=1$, but some small value dependent upon R' and the mass ratio. The main mass vibration is reduced because the attached mass-spring-damper vibration produces a finite force which opposes the exciting force and limits the main mass motion. The presence of resistance also causes the attenuation band to widen. Therefore, resistance in the dynamic absorber results in a wider attenuation band, but a reduced peak attenuation. Both effects are shown in Figure 3B.

The beam-mass system used in this thesis is an application of a two-dimensional dynamic absorber. The attached mass-spring-damper systems vibrate locally to produce a force opposing the force created by the flexural waves moving along the beam. Thus, the vibrating attached masses reduce the vibratory motion of the beam, producing an attenuation band around $\omega = \omega_o$.

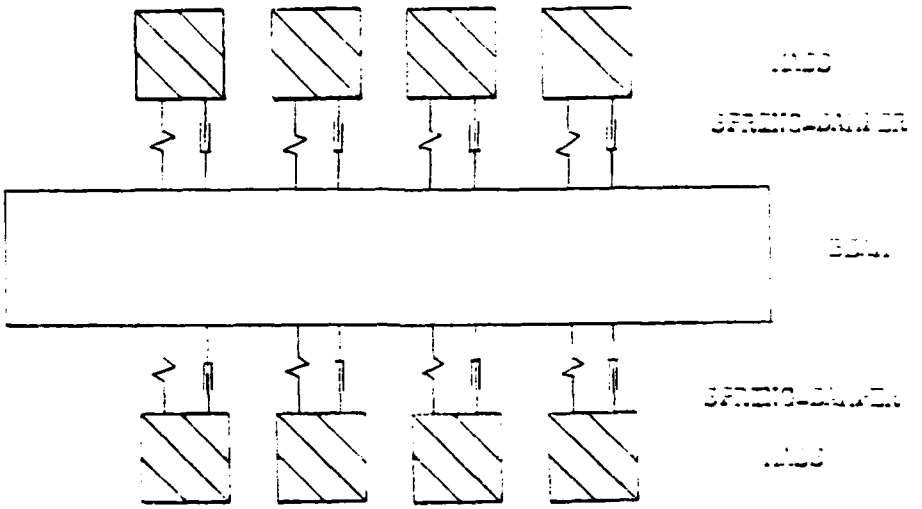

FIGURE 1

Beam with Attached Mass-Spring-Damper Distribution

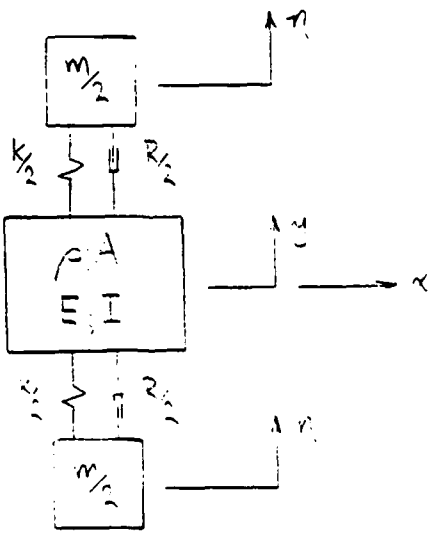

FIGURE 2

Coordinates and Parameters for Beam-Mass Systems

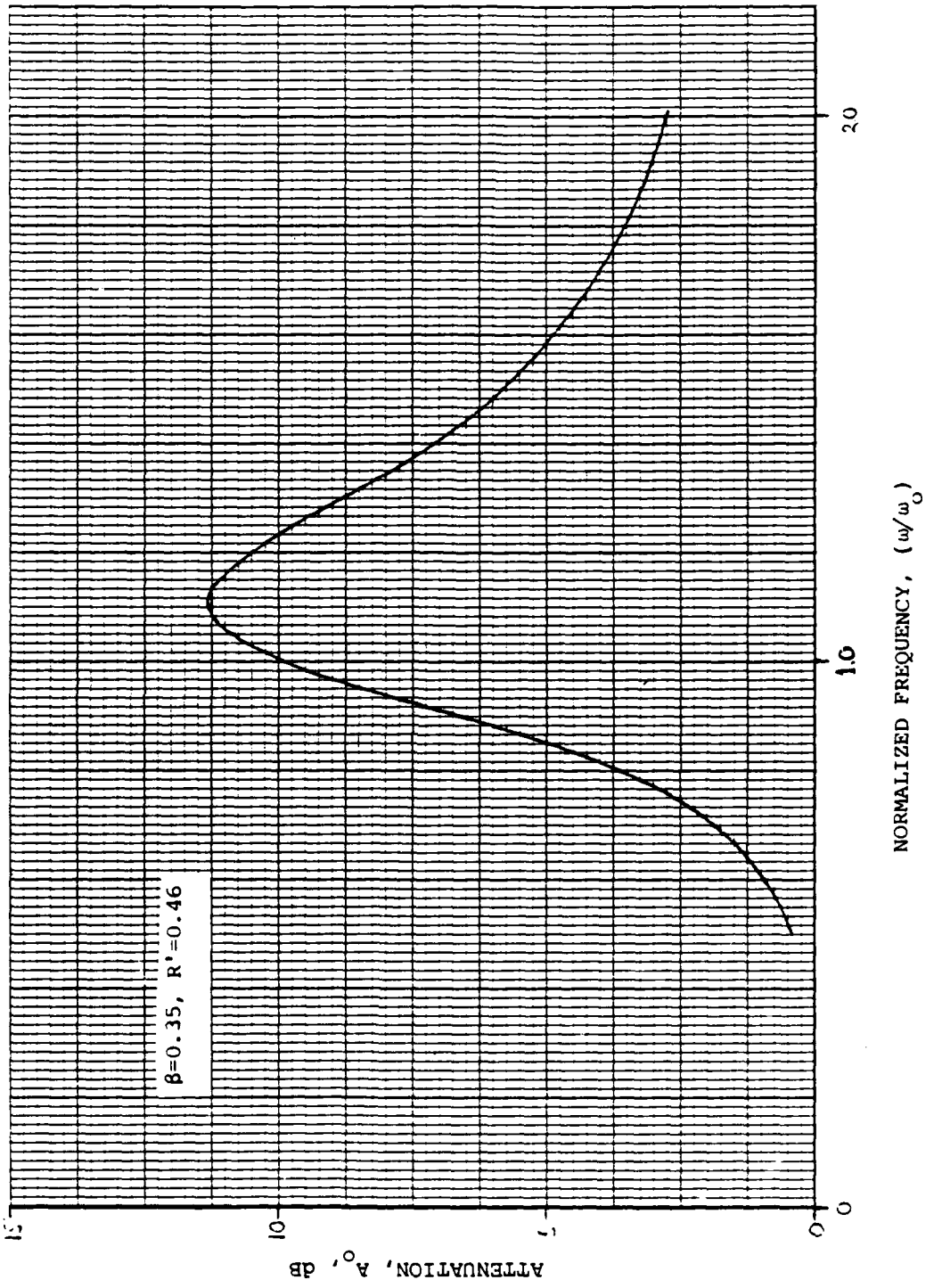

FIGURE 3

Typical Attenuation Curve for Beam-Mass System Predicted by Analytical Model

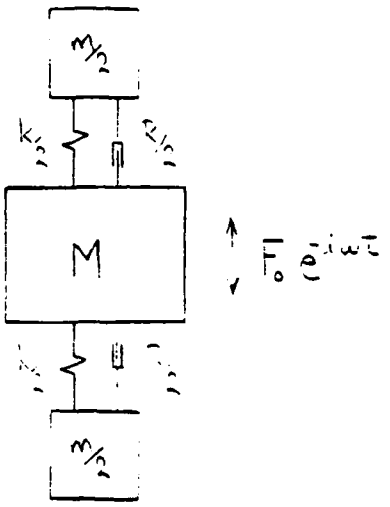

FIGURE 3a

SYMMETRIC DYNAMIC ABSORBER

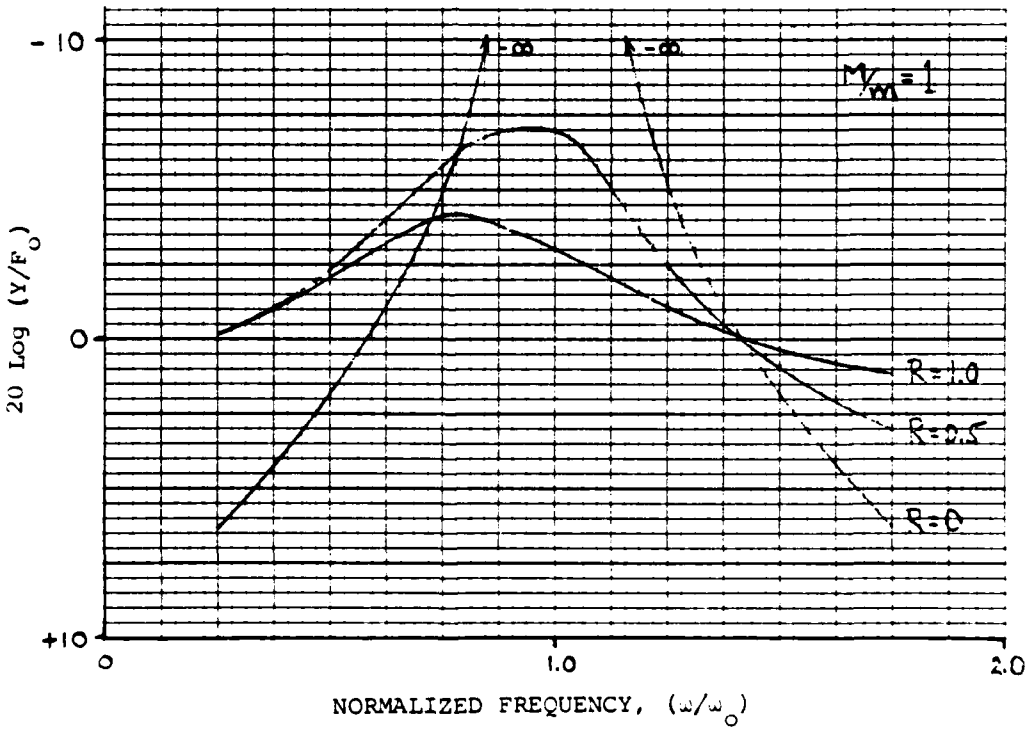

FIGURE 3b

Main Mass Vibration Amplitude Versus
Normalized Frequency for Various
Values of Loss Factor

3. EXPERIMENTAL VERIFICATION

3.1 DEVISING AN EXPERIMENT

The author's principal purpose was to devise an experimental method of testing the analytical model. The beam part of the system was simple enough: use a beam. The more difficult problem was how to attach a distribution of independent masses to it and meet all the conditions imposed by the assumptions made in the analytical model.

Some of the more important considerations were:

1) How to support the beam and attached masses such that the beam would not sag under its weight and the supports would not interfere with the wave propagation?

2) How to drive or excite the beam such that flexural waves propagate down the beam only and no reflected or standing waves are created?

3) How to attach the masses to the beam such that a mass-spring-damper system is set up which vibrates in the same plane as the beam? Side coupling between and rotation of the masses was to be avoided.

4) How small must the longitudinal dimension of the mass-spring-damper system be

so that the distribution appears continuous?

5) How to accurately measure the attenuation of the propagating flexural waves?

The type of beam selected was a uniform, rectangular beam. Beams of this type have many advantages in this application. They are cheap and readily available. They are symmetric. And, since they are much stiffer in one dimension, it is fairly easy to cause the beam to vibrate in pure bending. Also, the flat surfaces provide a convenient place to attach the masses. The beam material and size were selected somewhat arbitrarily. An aluminum beam with rectangular dimensions of 1/2 by 1/4 inch was used.

But, how can the beam be supported and flexural waves generated so that only they propagate down the beam? One way to support the beam so that the supports don't interfere with the propagating waves is to suspend the beam by threads. For this experiment, the beam was suspended horizontally from the ceiling by thin, monofilament fishing line. The line does not restrict the motion of the beam horizontally and transmits very little energy away from the system. And by suspending the beam with its stiffer dimension in the vertical plane, it will not sag appreciably.

However, a finite beam with free ends readily

resonates. To overcome this, the beam must be damped at one end to absorb the waves as they propagate toward it. Suitable damping can be achieved using a box of sand in which the end of the beam is buried.

It was decided that a good way to excite the beam in flexure was to drive it horizontally with white noise. Thus, a known input over a broad range of frequency could be easily achieved.

So, at this point, the experiment consisted of a horizontally suspended, uniform, rectangular beam, driven at one end with white noise and damped at the other end by burying it in sand. Now how can a continuous mass-spring-damper system be added to the beam?

Since the wide dimension of the beam is in the vertical plane to prevent sagging and the beam is to be driven in flexure horizontally, the attached masses must be on the vertical sides of the beam. The method used to accomplish this was to stick a resilient material onto both sides of the beam to simulate the spring-damper, and then stick the masses to the resilient material.

For the resilient material, a closed-cell foam weather stripping was selected because it was readily available, about the right size and had appropriate stiffness and damping qualities. As for the masses to be attached, nuts and/or washers were used. These were chosen again because of availability and also because of

the range in mass and physical size they provided. And, being mass produced items, their uniformity was good.

The experimental set up of the beam-mass system is shown in Figure 4. All that remains to be done is to measure the attenuation. The approach adopted here was to drive the beam with white noise at an arbitrary but fixed level. Then, using an accelerometer, one can measure the acceleration spectrum level on the input or driven side of the attached masses and on the output or damped side of the attached masses. The difference between the spectrum levels would then be a measure of the attenuation caused by the attached masses.

3.2 EXPERIMENTAL SET UP

The first thing set up in the lab was the equipment needed to drive the beam and measure its vibration. A block diagram of the equipments used is shown in Figure 5.

The beam was driven with white noise from a random noise generator, through a power amplifier, shaker and impedance head. The impedance head was primarily used to monitor the drive point acceleration level so that the input level could be kept constant.

The beam vibration level was measured with an accelerometer. The accelerometer output was processed and monitored using an amplifier and a filter in series with a

spectrum analyzer. The accelerometer was fixed to the beam using bee's wax so that the measurement position could be easily changed.

With the drive and measurement equipment ready, the next step was to obtain a measured spectrum on the beam alone that was relatively smooth in frequency. With white noise driving the beam, if the measured beam spectrum was smooth, it would mean that the desired unidirectional wave propagation existed. That is, all the flexural wave input by the shaker was travelling down the beam and being absorbed by the sand making the beam appear semi-infinite. This ideal case wasn't obtained.

There were two significant departures from the desired smooth spectrum. One was that there were significant resonance peaks present below 800 Hz. The other was that there were two zones of non-propagation at 525 and 4200 Hz.

The resonance peaks at low frequencies were the result of the beam-sand interface reflecting rather than absorbing waves at these frequencies. The non-propagation zones were caused by the method and point of attachment of the shaker. Essentially, the shaker was driving the beam at a nodal point corresponding to waves at the non-propagating frequencies.

Even with these problems, a trial run with the mass-spring-damping system attached was conducted. The

closed-cell foam was attached to both sides beam with double-sided stick tape. Then, quarter inch nuts were placed side-by-side on the exposed sticky surface of the foam weather stripping. The length of the mass-spring-damper system was about 30cm.

The treated beam was then driven and acceleration measurements were made on the driven side and damped side of the treatment. A very broad attenuation zone was detected by comparing the input and output measurements. Appreciable attenuation had taken place from about 200 to 700 Hz. The general shape of the attenuation curve was as expected. Now the experimental set up and procedure needed refining.

Changes in the experimental set up were aimed at achieving a smoother beam spectrum. The first change was to use a longer beam and have a sand box for damping each end of the beam thereby simulating an infinite, vice a semi-infinite beam. The primary motivation for this was to eliminate the beam end discontinuity.

Another was that a much greater length of beam was placed into the sand. The idea was that by burying more beam length in the sand the absorption of waves with longer wavelengths would be increased, thus smoothing the spectrum at lower frequencies. In the initial arrangement, about 30cm of the beam was placed in the sand and in the final arrangement about 90cm on each end was

placed in sand. For comparison, at 300 Hz λ_o=44cm and at 200 Hz, λ_o=54cm.

The driving point attachment was also altered. The first connection consisted of a bolt through the center of the beam. The beam was secured by a nut and a small washer on each side. The final connection used two large washers to clamp the beam from below. The intent was to have a more rigid drive connection with larger contact area. This connection had the drawback that it may have introduced torsional waves because it was off-center. However, it was judged that this effect was of minor importance and did not invalidate the results.

With these changes, the beam spectrum was again measured. Based on the preliminary treated beam measurement, the useful frequency range became 300 to 2000 Hz. Improvement had been made in both the low frequency region and the non-propagation zones.

Since the foregoing changes made improvements, could more of the same be better? At this point, a lot of time was expended trying to further improve the beam spectrum to no positive end.

The sand was worked with first, and the following conclusions were reached:

1) The length of the beam in the sand had no noticable effect beyond about 50 or 60 cm.

2) The low frequency resonance peaks were

reduced more when the beam was merely "nestled" in the sand instead of being buried. Burying the beam causes more of a discontinuity and consequently, more reflection.

3) Very dry, fine sand was far superior to wet sand. The beam spectrum was very sensitive to moisture. The wetter the sand, the worse the low frequency resonance peaks became. Again, this was due to a greater discontinuity at the beam-sand interface. Moist sand does attenuate high frequencies better, but this was not the issue here.

4) Adding damping materials to the beam ends in addition to the sand had no noticable effect. The damping material was good for high frequency absorption which, again, was not a problem.

The drive point connection was also varied to find a better method. The size of the area clamped was further increased and found to have little effect. Varying the horizontal location of the drive point caused the frequency of the non-propagation zone to shift by as much as 100 Hz. Moving the drive point closer to the sand caused the frequency of the non-propagating zone to shift upward indicating that it was a function of the beam end

length. But since the frequency shift was limited, this could not be used to move the non-propagating zone out of the frequency range of interest.

For comparison, Figures 6 through 9 show various measured frequency spectra. Figure 6 shows the response of the beam alone. The beam was suspended horizontally by thin lines and struck lightly with a small metal rod. The first five resonance peaks were verified using elementary beam theory (see Appendix A). Figure 7 shows the white noise input to the beam from the shaker. There is a 60 Hz peak present, but above 100 Hz the spectrum is quite good. Figure 8 shows the driven response of the beam with the ends free. And Figure 9 shows the driven response of the beam with both ends in the sand. This spectrum is quite good above 350 Hz. It would have been nice to have the spectrum shown in Figure 9 for all the experimental runs, but as can be seen in the figures in the appendices, the spectrum was different for each run. The mass loading of the beam and the resonance of the mass-spring-damper system added unwanted wrinkles to the spectrum. However, the input and output spectrum irregularities usually subtracted or averaged out and the resulting data were acceptable.

3.3 EXPERIMENTAL PROCEDURES

The equipment was calibrated with all components connected as a unit including the sensor, amplifier, filter, analyzer and connecting cables. Then, no instrument, setting or cables were changed during the experiment.

The accelerometer used for the beam, a Wilcoxon Research #91 (2gm), and the accelerometer portion of the impedance head, a Wilcoxon Research Model Z-602, and their respective system components were calibrated using a General Radio vibration calibrator Model 1557-A. The amplifier and filter settings for both systems were 10 dB gain, 20 Hz high pass and 3150 Hz low pass.

The force portion of the impedance head was calibrated by a mass comparison procedure. Two known masses were each attached to the impedance head and then driven sinusoidally. The force voltage output and known acceleration level were used to determine the force level.

The point input impedance of the beam was determined and compared to the impedance of the accelerometer. This was done to ensure that the accelerometer impedance was small compared to the beam impedance and would not affect the measurements taken.

Finally, the desired attenuation data were taken. The procedure was simplified by the fact that this was not

a phase coherent vibration study. The only parameter of interest was the amplitude of the acceleration spectrum at the input and output sides of the beam treatment.

For ease in data comparison, an arbitrary reference acceleration level was chosen. The acceleration at the drive point as measured by the impedance head was maintained at -50 ± 0.5 dB re 4.35g at 1000 Hz. This level was checked before each data set was taken.

Data were taken for eight different mass ratios and for two systems containing a combination of mass ratios. For each mass ratio, data were taken for different lengths of beam treatment. By measuring several different lengths, the attenuation per unit length of beam treatment could be determined from the slope of the data obtained.

The input and output amplitude frequency spectra were taken using a Spectral Dynamics SD345 spectrum analyzer. The input and output measurements were each RMS values averaged over three locations 2 cm apart to submerge uncertainties due to residual phase coherent effects as in standing waves. This was done by moving the accelerometer and taking 21 time averages at location one, 22 at location two and 21 at location three. Sixty-four time averages was a convenient setting that gave good results.

The input and output spectra were plotted using a Hewlett-Packard 7470A digital plotter. A typical plot is shown in Figure 10. The difference between the two

spectra was taken every 50 Hz to get the insertion loss.

The attenuation for various treatment lengths was taken and reduced to an attenuation per unit length by finding the slope of the insertion loss curve for each frequency. The slope was determined by a least squares fit of the data. From the slope, A_o, the attenuation in the distance of one untreated wavelength, was computed by multiplying the slope by λ_o. This could then be compared with the analytical model predictions.

There is a common difficulty in using the insertion loss. As the attenuation level increases beyond a certain value, the insertion loss curve flattens out or saturates. The saturation in this experiment became more evident as the mass ratio and, therefore, the attenuation levels increased. An example of a saturated insertion loss curve and its effect on the attenuation curve obtained are shown schematically in Figures 11 and 12. The insertion loss saturation is caused by a bypassing or short circuiting of the wave energy around the beam treatment. The effect was corrected for by taking the slope through the unsaturated portion of the attenuation versus length curve.

The loss factor and stiffness values of the closed cell foam used as the resilient material are needed for comparison of the experimental and analytical results. In particular, the loss factor, R', and the stiffness, k, versus frequency were determined.

The apparatus used to measure R' and k is shown in Figure 13. The foam was mounted on a plate and a known mass was placed on top of the foam. The plate was then driven with white noise and the response of the mass measured with an accelerometer. A typical amplitude response curve is shown in Figure 14. From the amplitude response curve, the natural frequency, ω_o, and the half-power bandwidth can be determined. With these two parameters and the known mass, the values of R' and k are easily computed.

Difficulty was experienced in determining R' and k values to be used however. This was caused by the differing areas of contact of the masses used. The R' and k experiment used a plate on top of the foam to simulate a continuous distribution, but the attenuation experiment used individual nuts and washers on the foam. And since the foam's material properties are greatly affected by the geometries involved, some uncertainty existed. There was also considerable spread in the R' and k data before it was averaged. Plots of R' and k versus frequency are shown in Figures 15 and 16.

The analytical model does not account for variation of R' and k with frequency. However, the change with frequency is small and has little effect on the predicted attenuation curve. The effects of the experimentally determined frequency variation of R' and k are shown in

Figures 17 and 18 (in these figures, the constant R' and k curve is the same as that in Figure 3 with β=0.50 and R'=0.46). The effects are small compared to the experimental errors, and can be neglected.

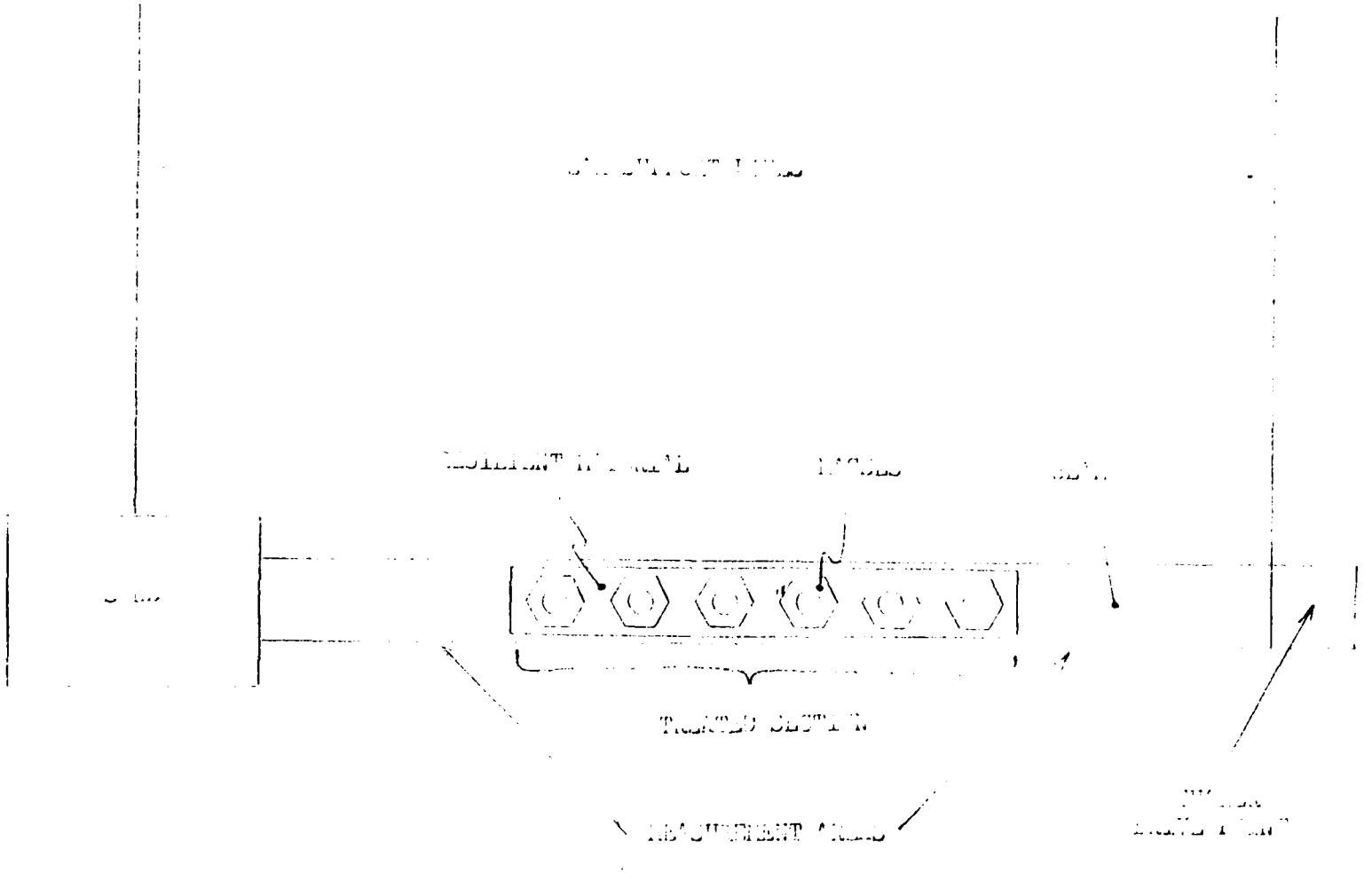

FIGURE 4

Experimental Beam-Mass Setup

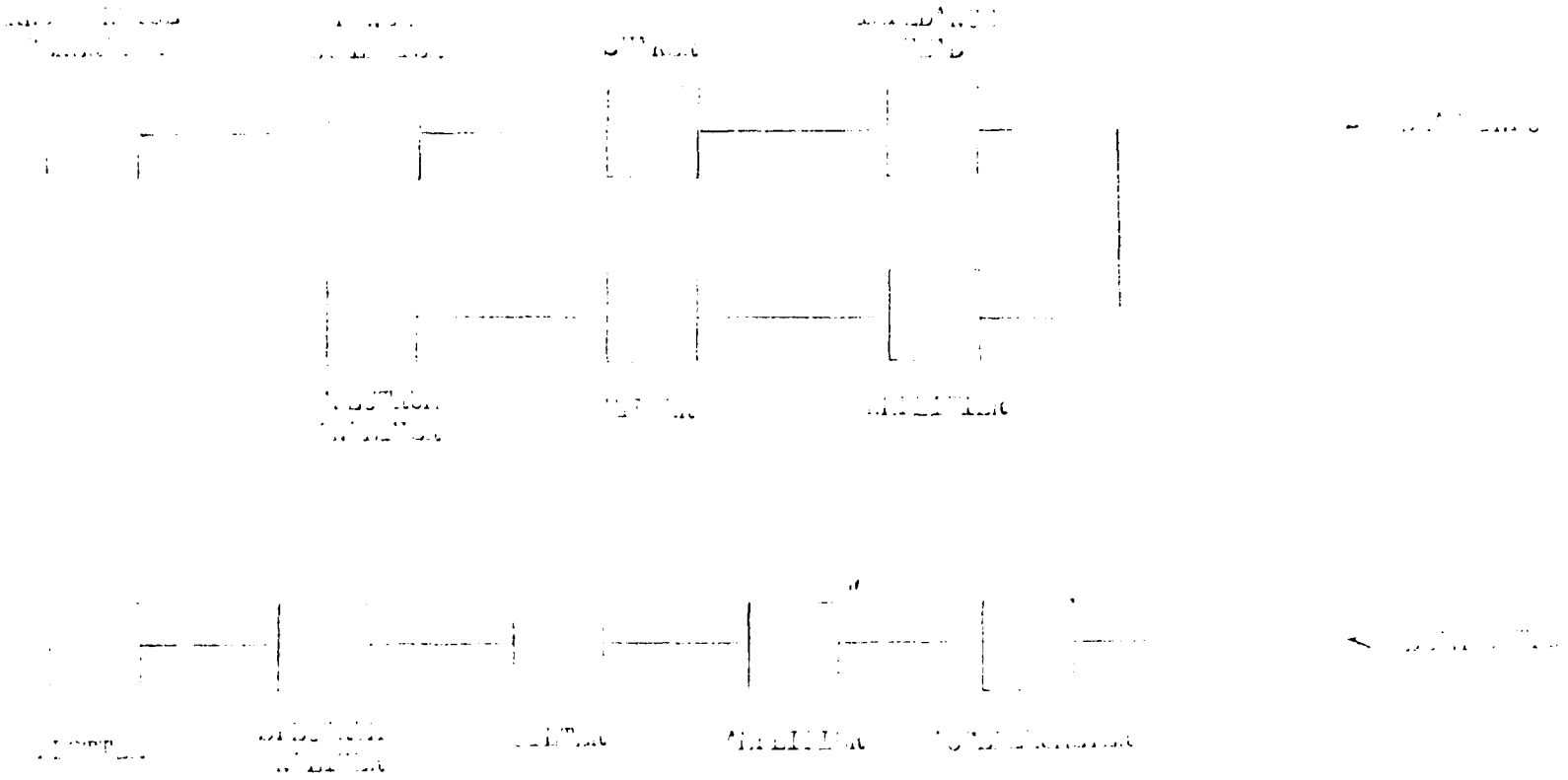

FIGURE 5

Block Diagram of Lab Equipment

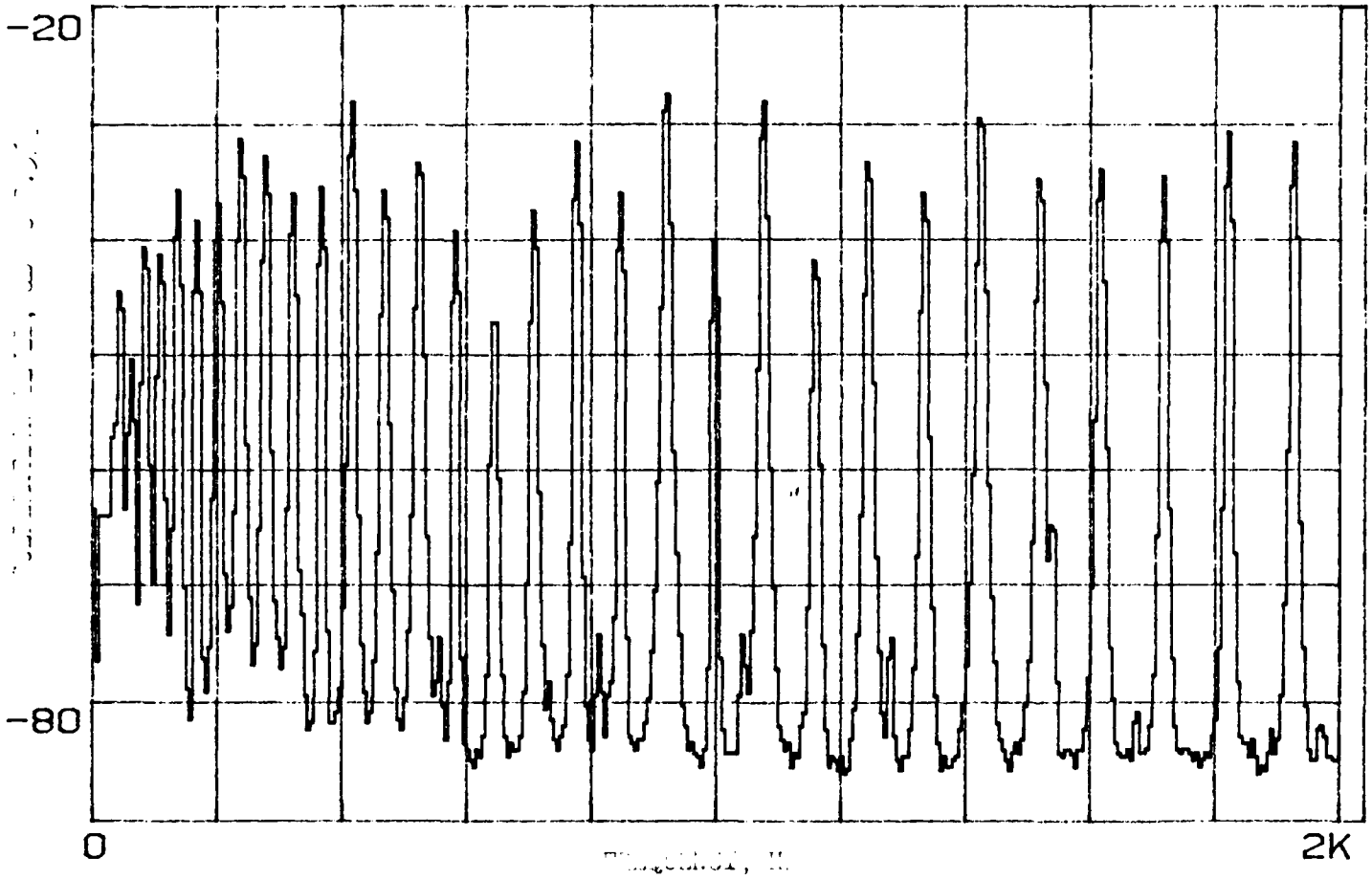

FIGURE 6

Measured Response of Free-Free Beam

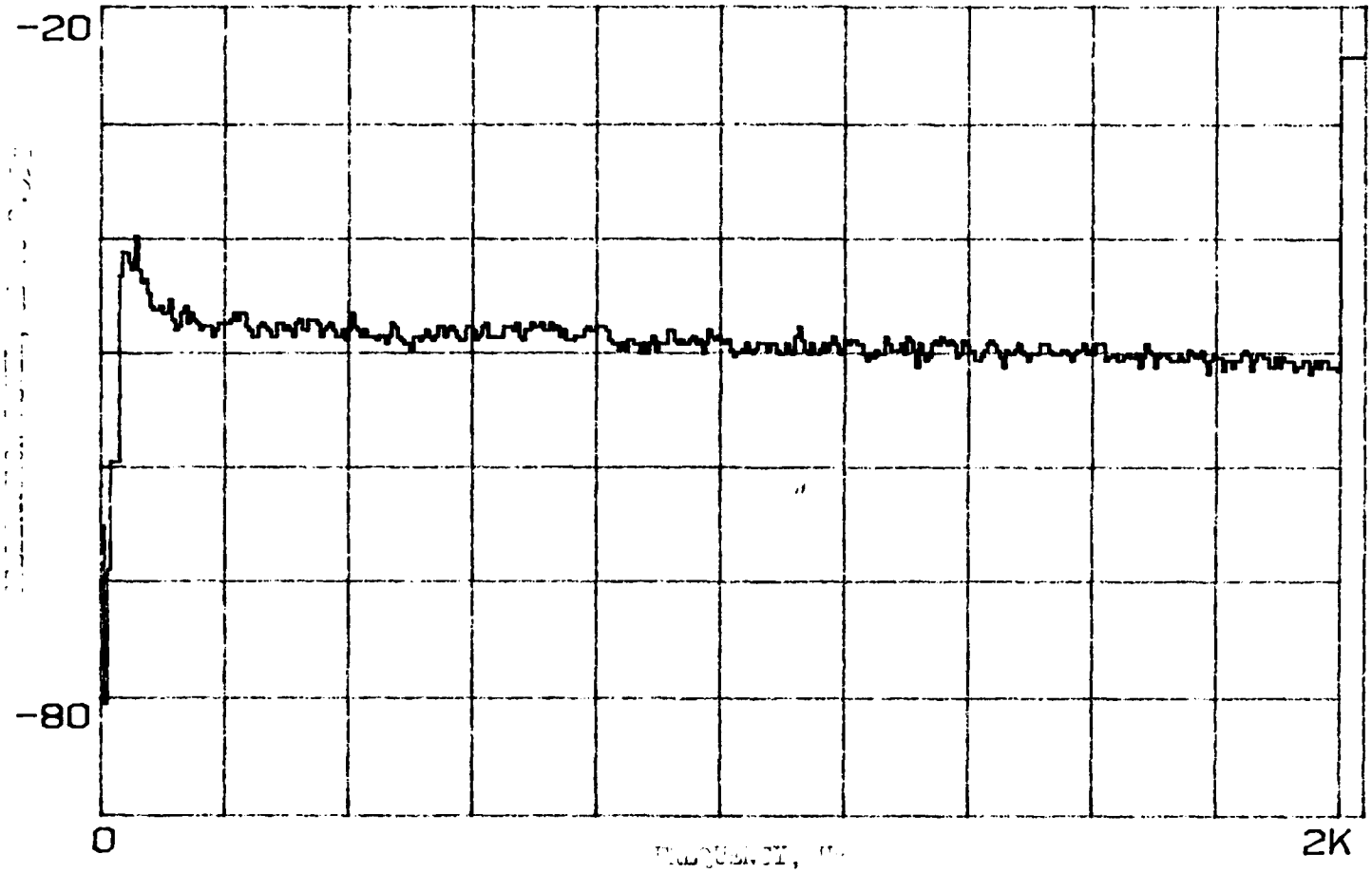

FIGURE 7

White Noise Input to Beam From Shaker

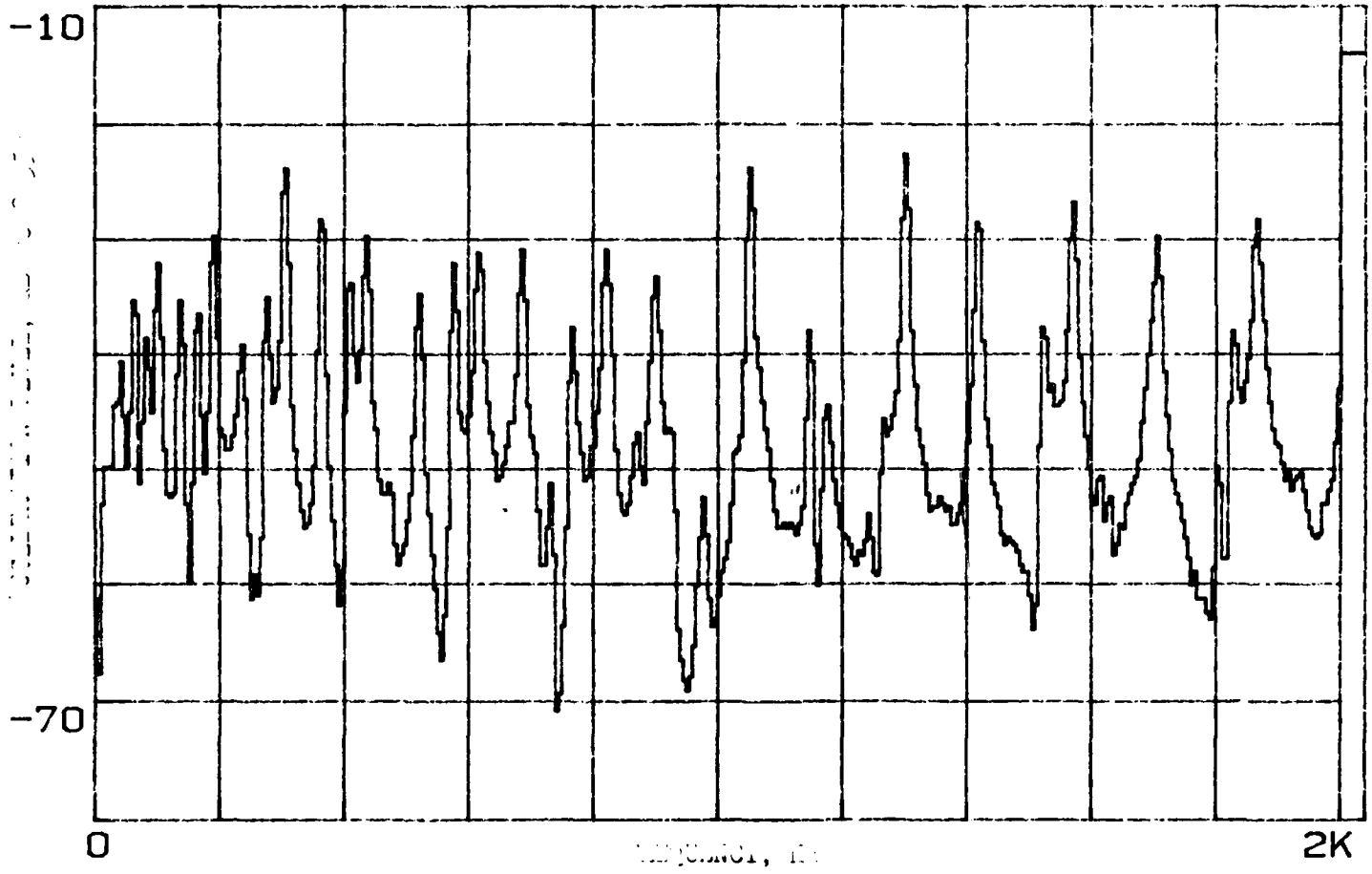

FIGURE 8

Response of the Driven Beam with Ends Free

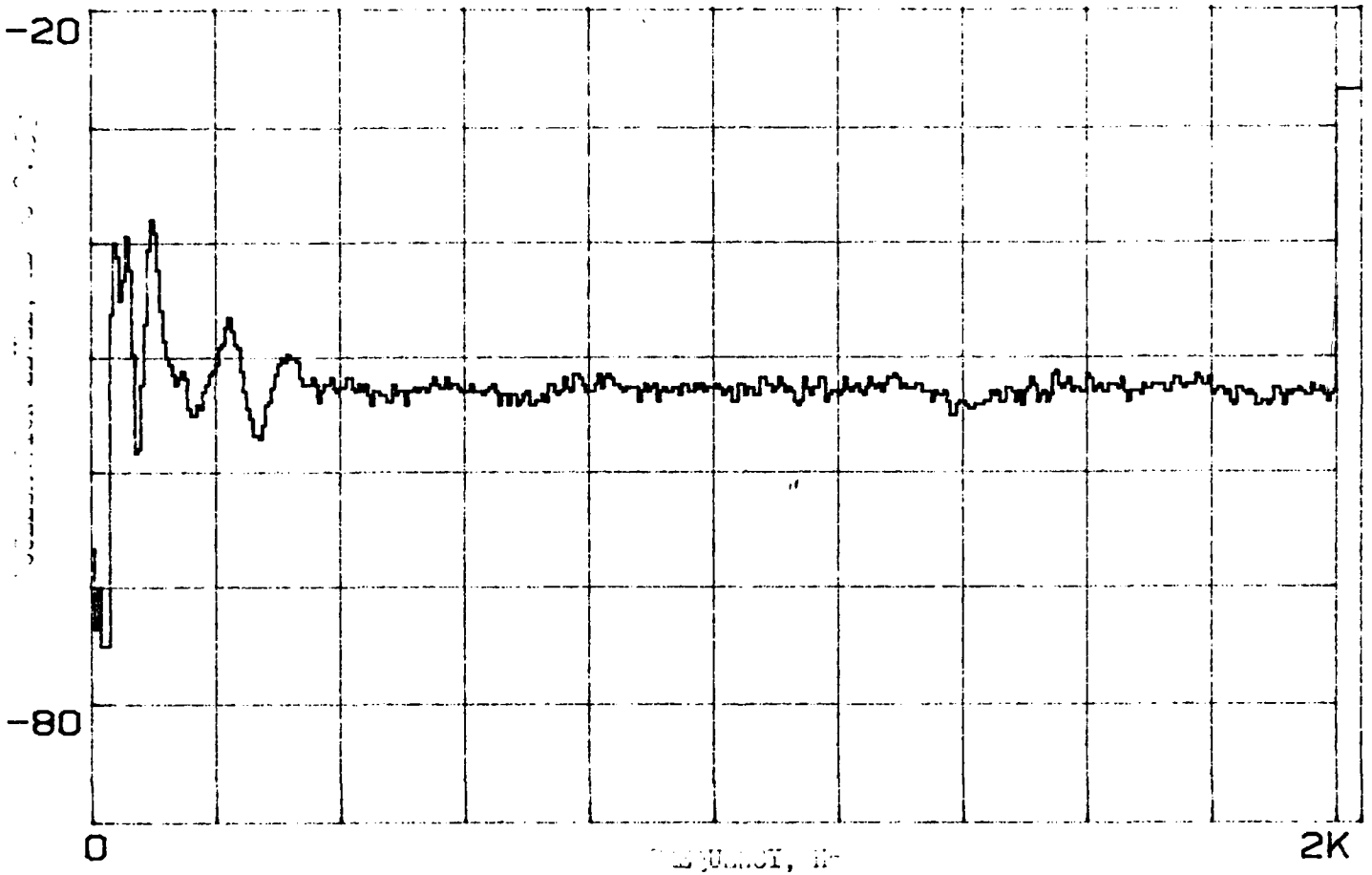

FIGURE 9

Response of the Driven Beam with Both Ends in Sand

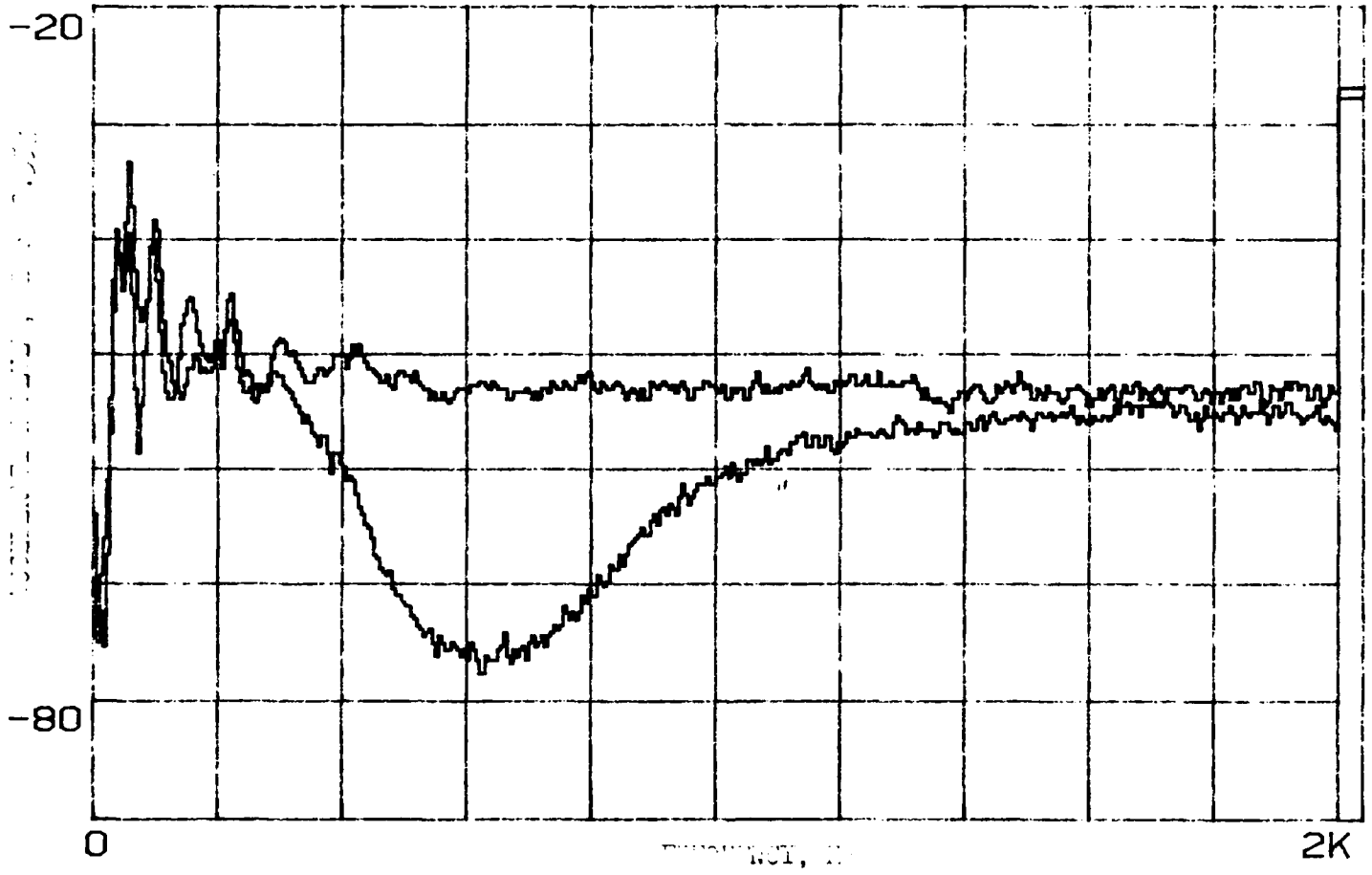

FIGURE 10

Typical Treated Beam Input and Output Data

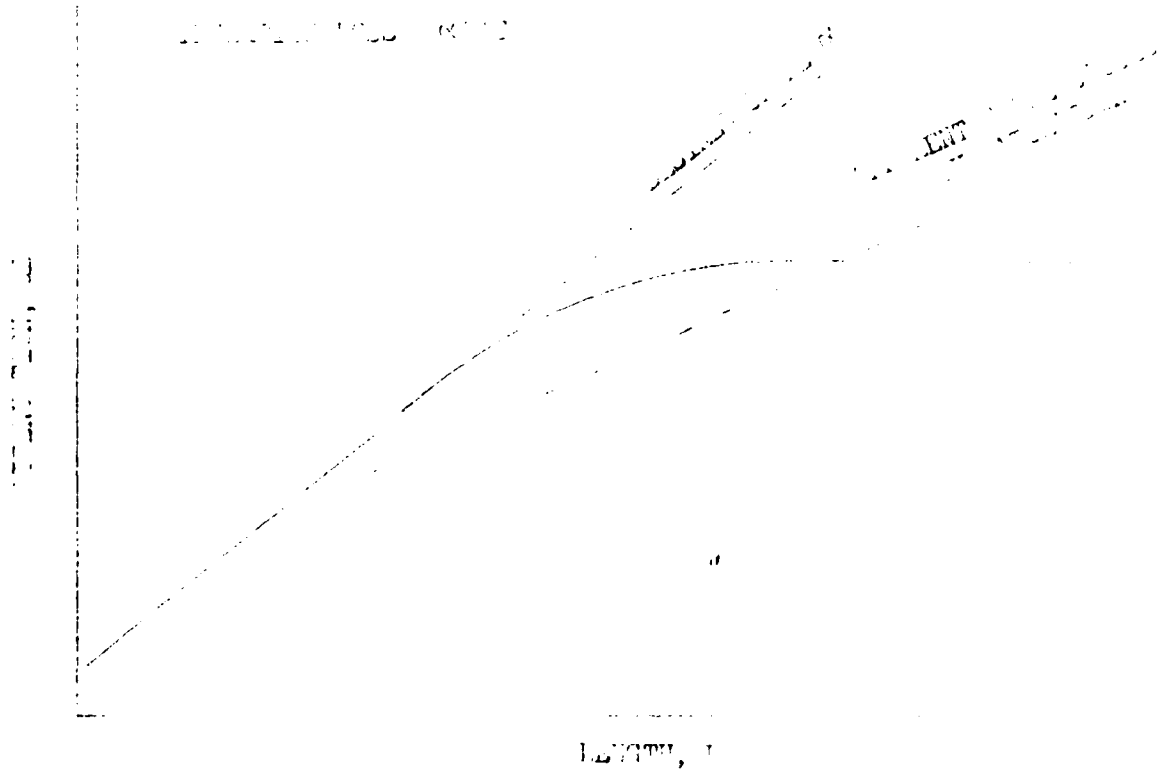

FIGURE 11

Example of Saturated Insertion Loss
Curve (Schematic)

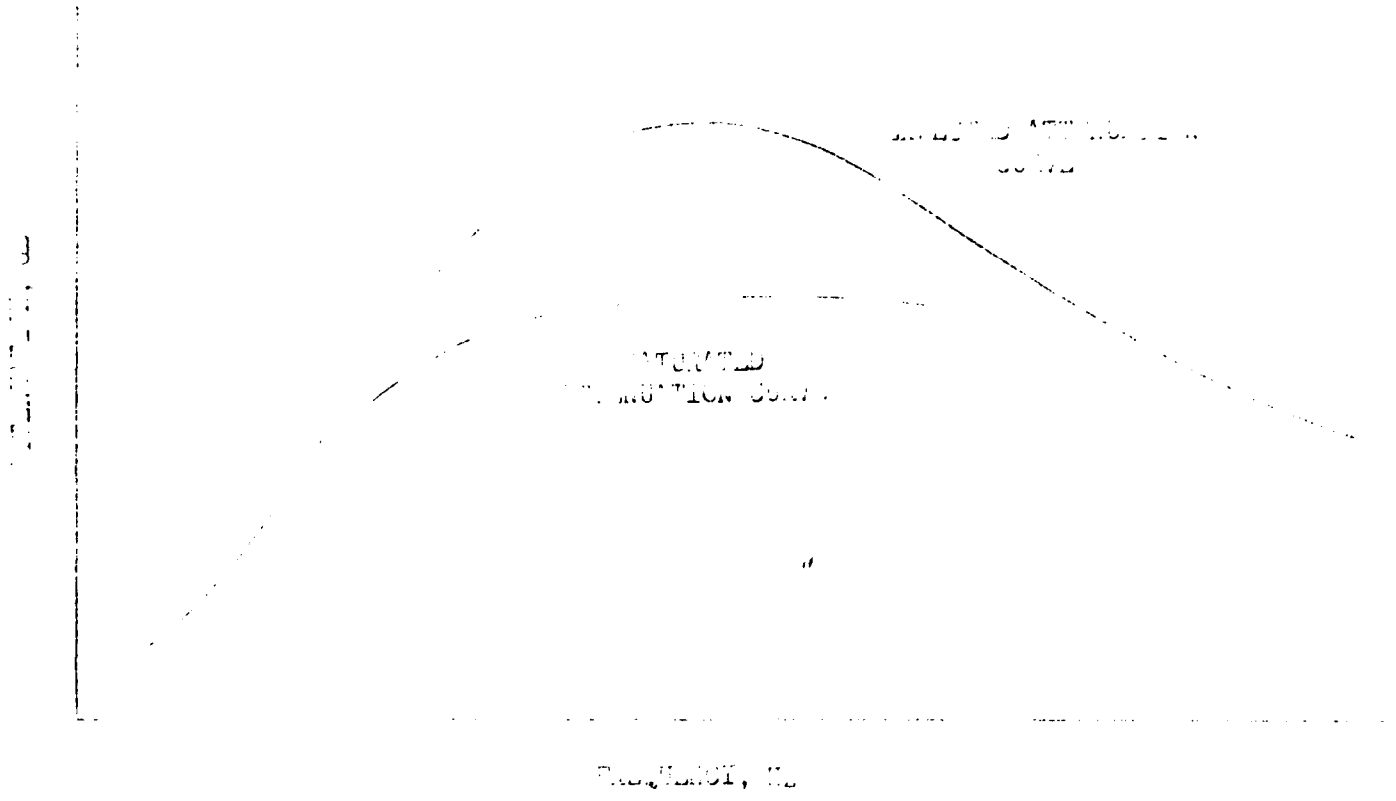

FIGURE 12

Effect of Saturation on Attenuation
Curve (Schematic)

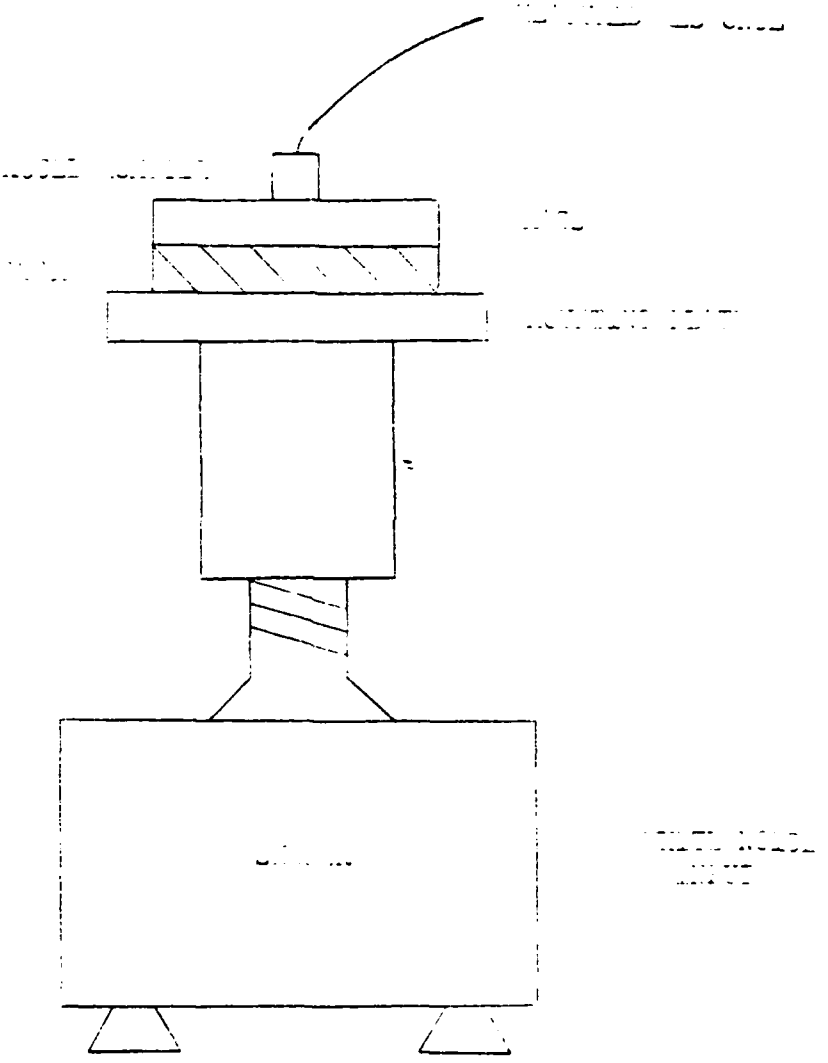

FIGURE 13

Apparatus for Experimentally
Determining R' and k

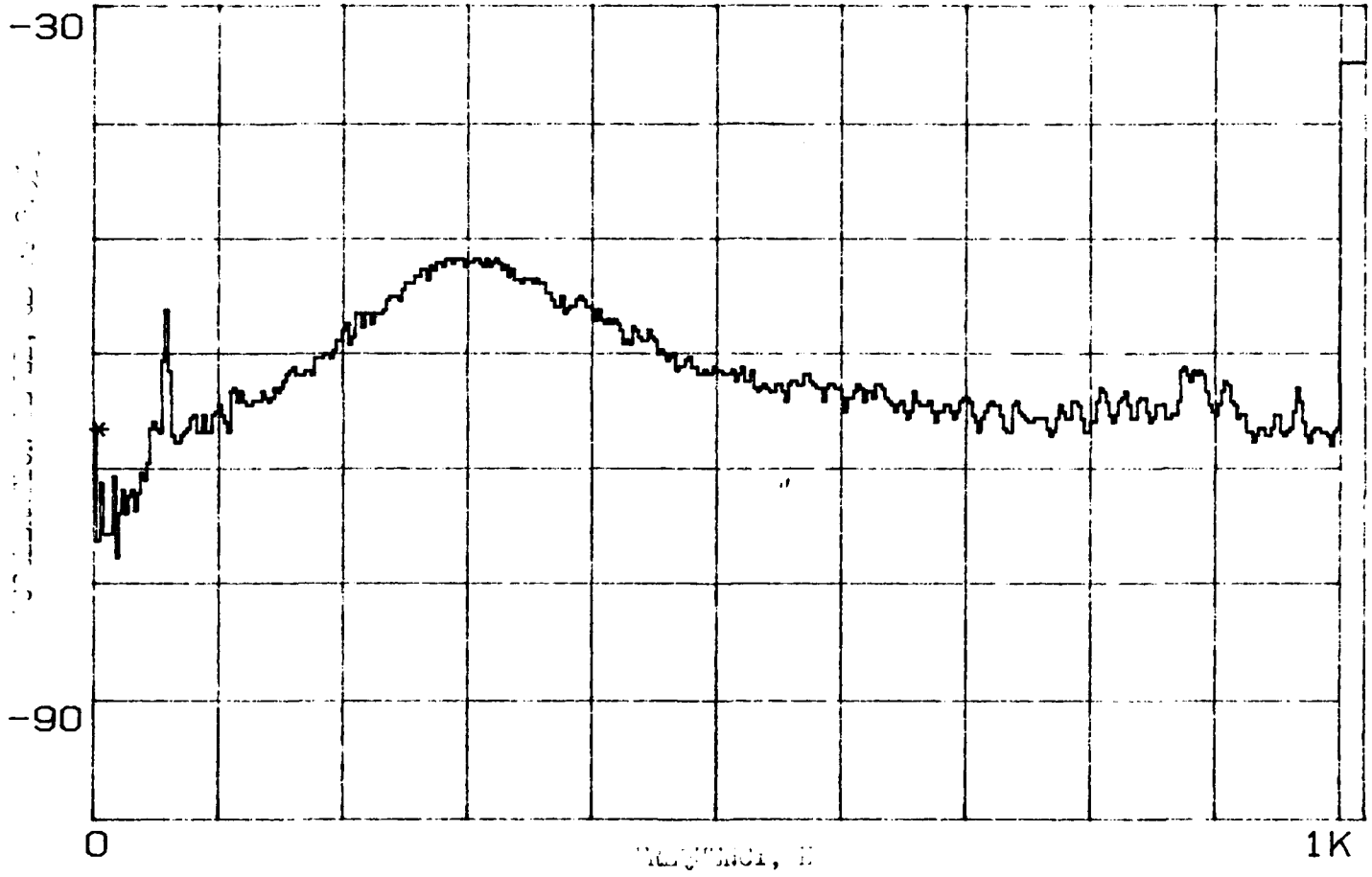

FIGURE 14

Typical Amplitude Versus Frequency
Response Used for Determining R' & k

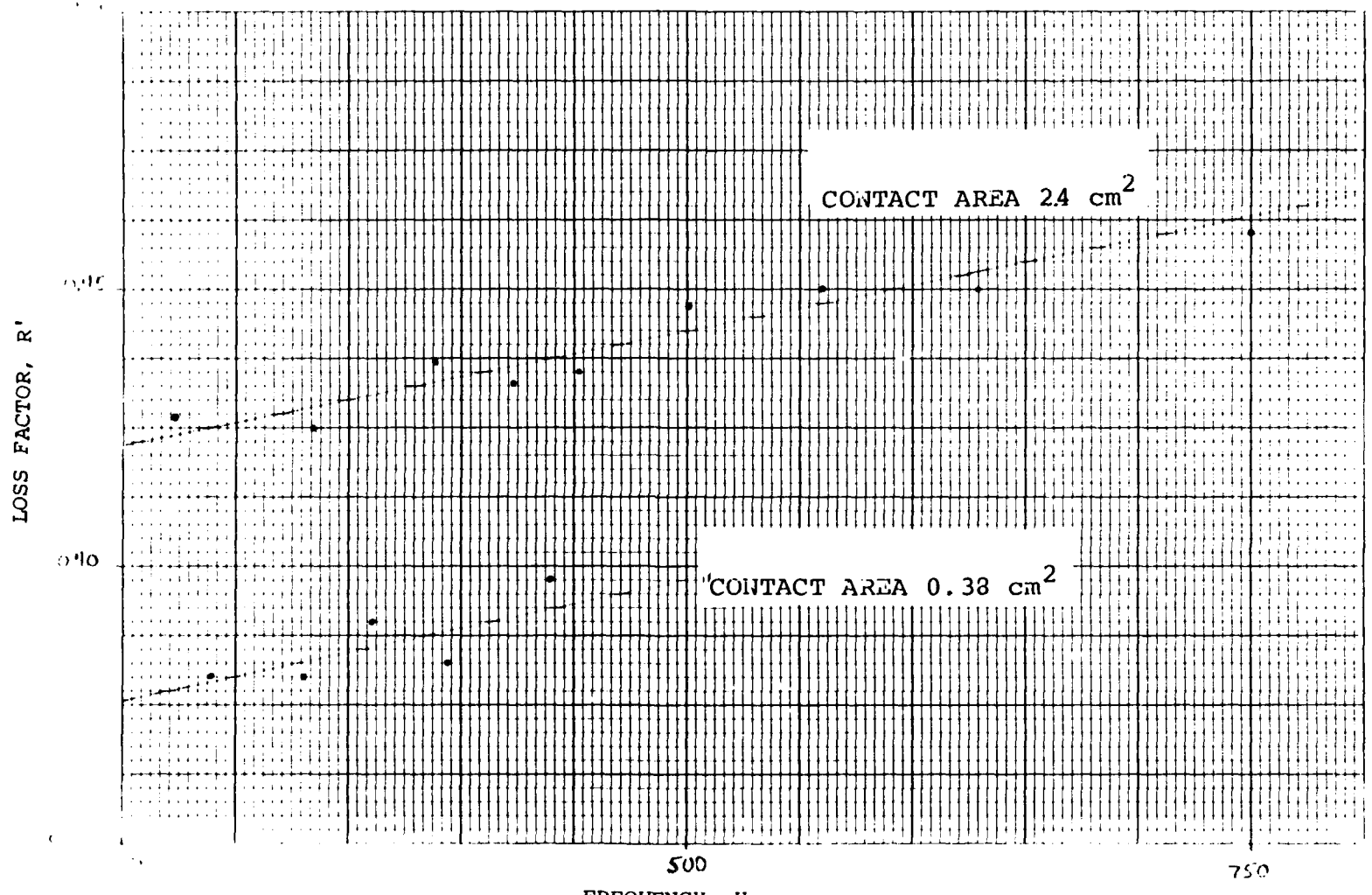

FIGURE 15

Experimentally Determined R' for
Closed Cell Foam

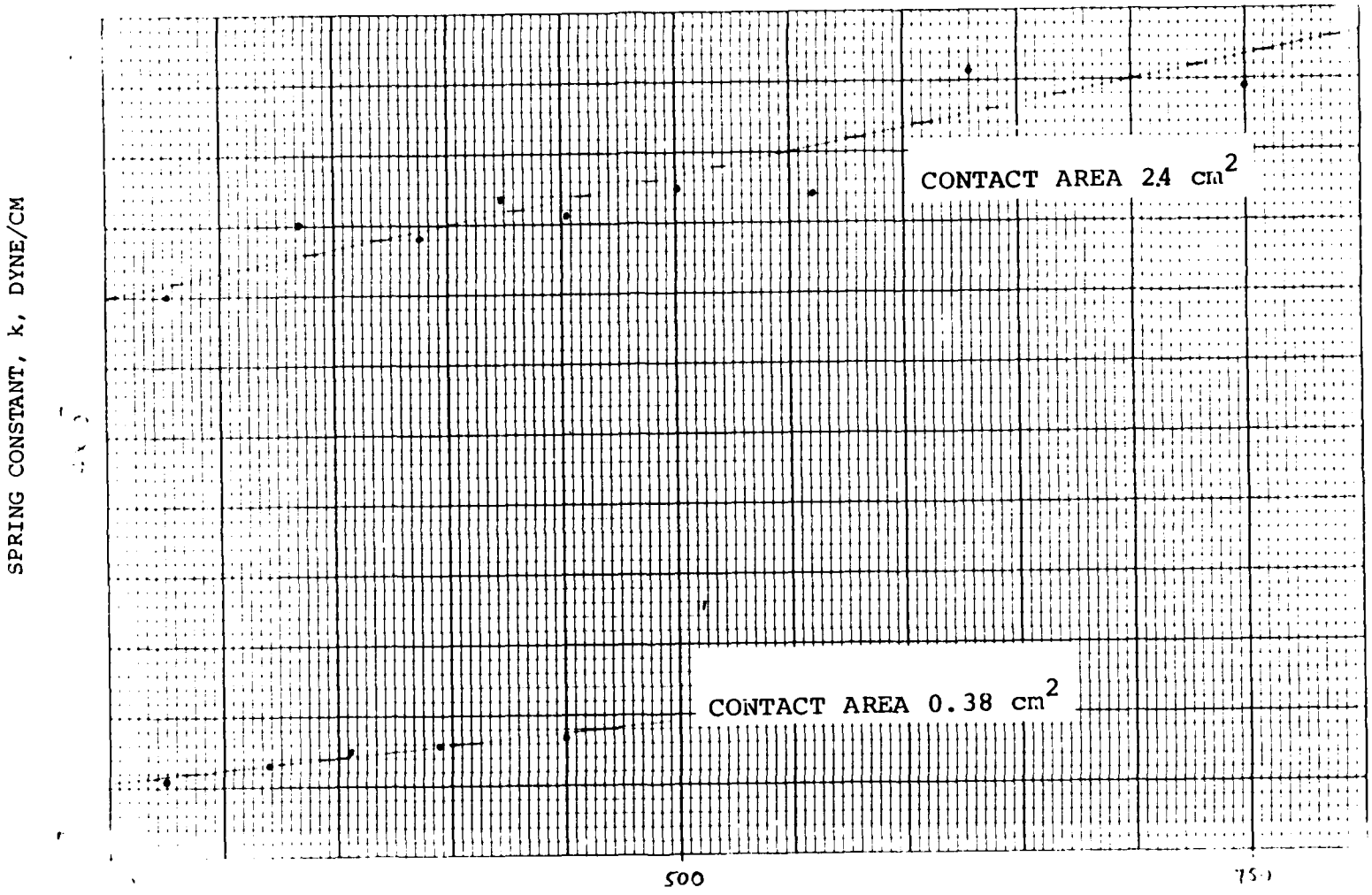

FIGURE 16

Experimentally Determined k for
Closed Cell Foam

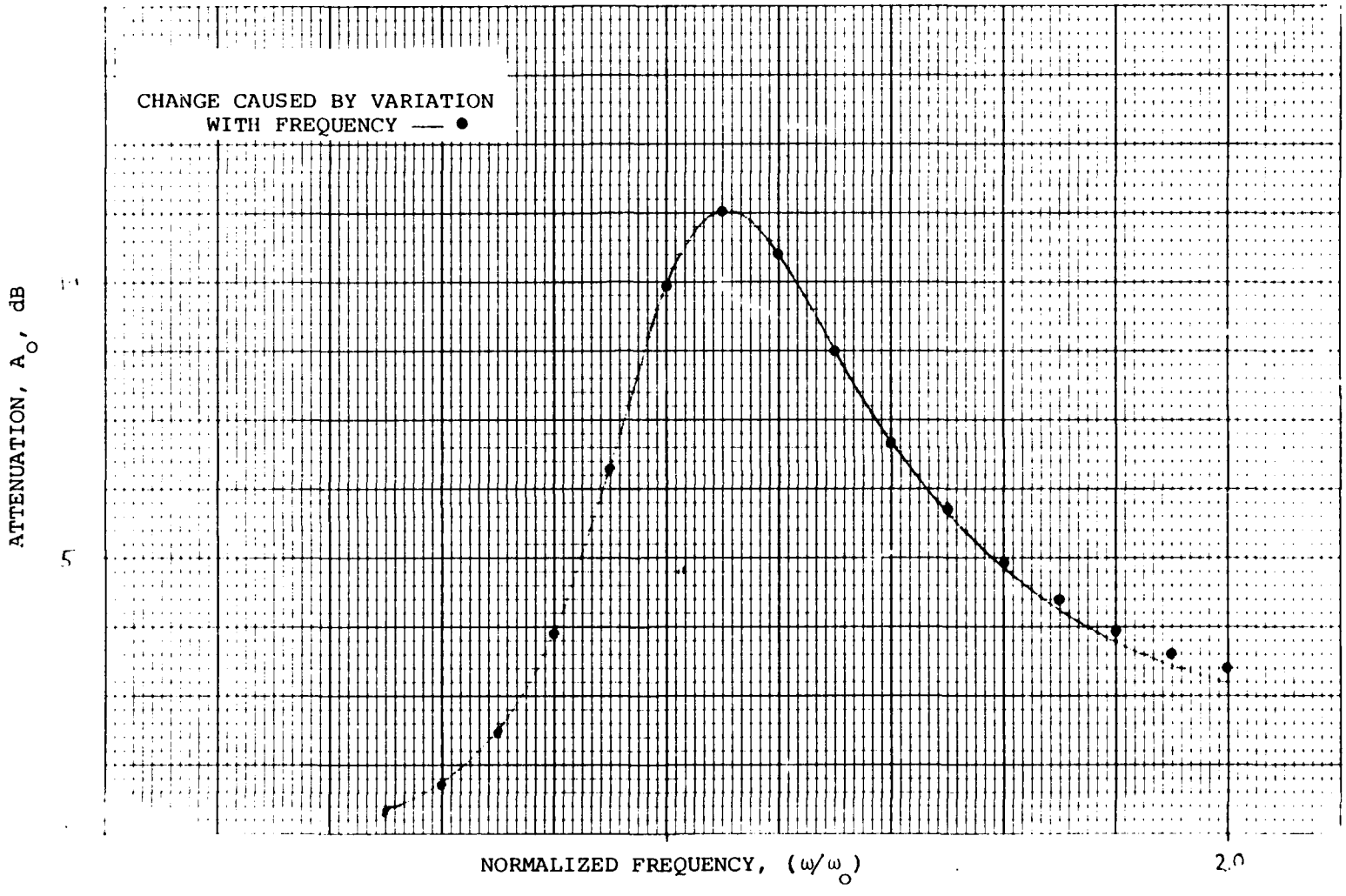

FIGURE 17

Effect of R' Variation with Frequency
on Attenuation Curve

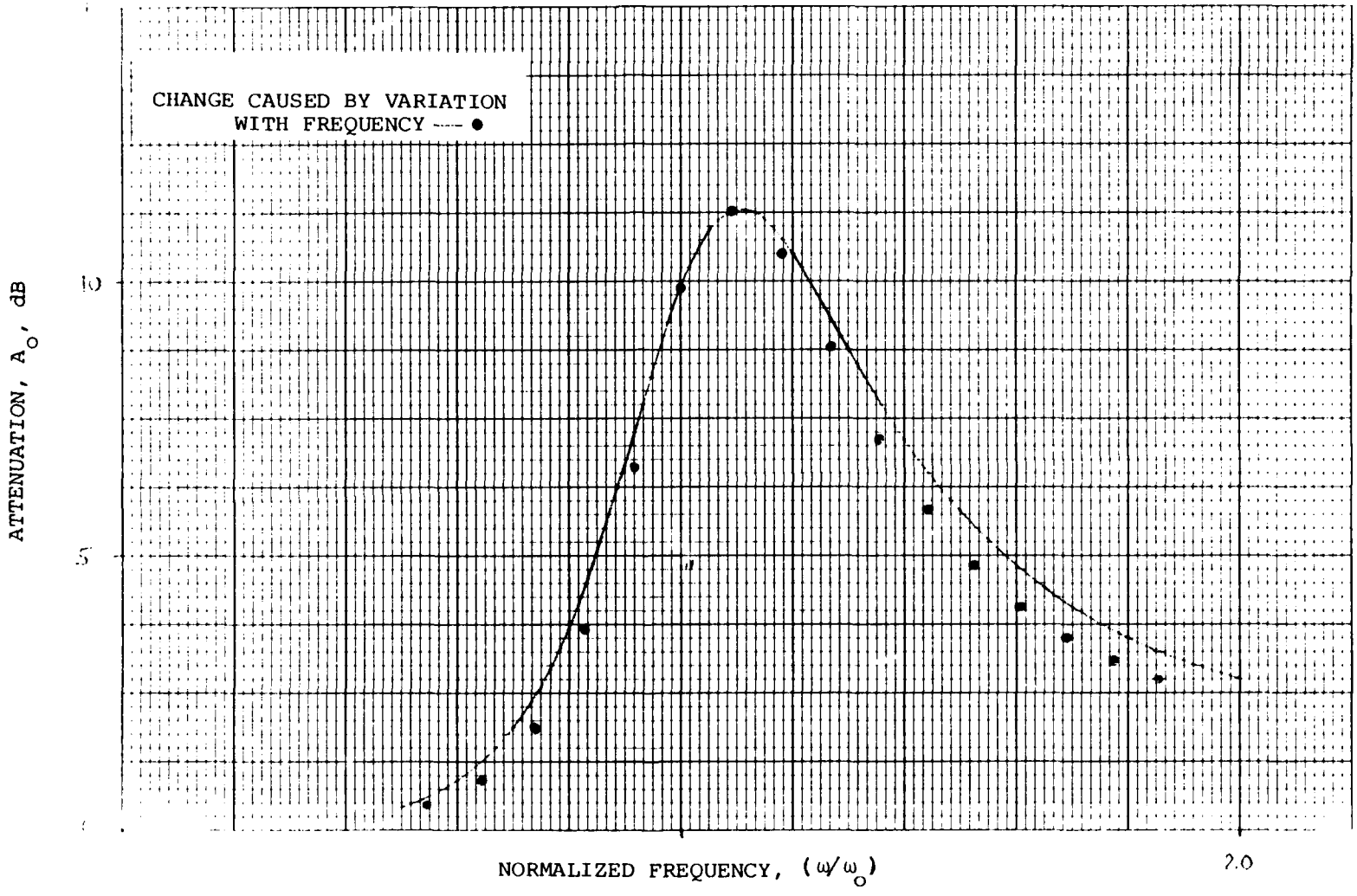

FIGURE 18

Effect of k Variation with Frequency
on Attenuation Curve

4. RESULTS

The experimental data compared quite well with the analytical predictions. Figures 19 through 26 show the comparisons graphically. Each figure is a plot of the attenuation A_o, measured in dB, versus normalized frequency, ω/ω_o. The solid curve shows the analytically determined attenuation for the given values of β and R'. The experimental data points are shown by circles (the raw data is compiled in Appendices B through I). Comparison of the data with the predicted attenuation in Figures 19 through 26 confirms the analytical model adopted.

As discussed in Section 3.3, values for k depend upon the geometry of the mass-foam contact. Hence, to determine ω_o more precisely for the experimental case, the experimental curves were form-fitted to the respective analytical curves. This was done by matching the peak of the analytical curve and the apparent peak of the experimental curve. From the fit, ω_o was determined and then used to check the value of k with that previously determined to ensure that it was reasonable.

Some of the figures show appreciable data scatter on the 'tails' of the attenuation curve. This was caused by experimental noise. The figures in the Appendices show that near the ends of the attenuation region, fluctuations in the measured spectrum level begin to be a significant

fraction of the level differences.

Figures 27 and 28 show results of experiments in which two different mass ratios were used simultaneously on the beam. The two masses were attached to the resilient material alternately such that the distribution remained pseudo continuous. The mass combinations were chosen such that the magnitude of their respective peak attenuations were similar and such that there was sufficient frequency separation between the peaks to allow both peaks to be detected if they were present.

Both peaks were observed as is shown in the figures (the raw data is compiled in Appendices J and K). In these two figures, the analytical curves were form-fitted to the experimental curves. This is the reverse of what had been done with the single mass ratio case, but was necessary due to the relative uncertainties in the spring constants.

The combination mass ratio curves confirm one of the major assumptions implicit in the analytical model. That is, each mass acts independently of its neighbors, or, that there is no appreciable coupling between masses. This is true because if there was mass coupling, the two attenuations peaks would tend to merge to an average value. This result is interesting because it implies that a very broad attenuation band could be created by a combination of many different mass-spring-damper systems.

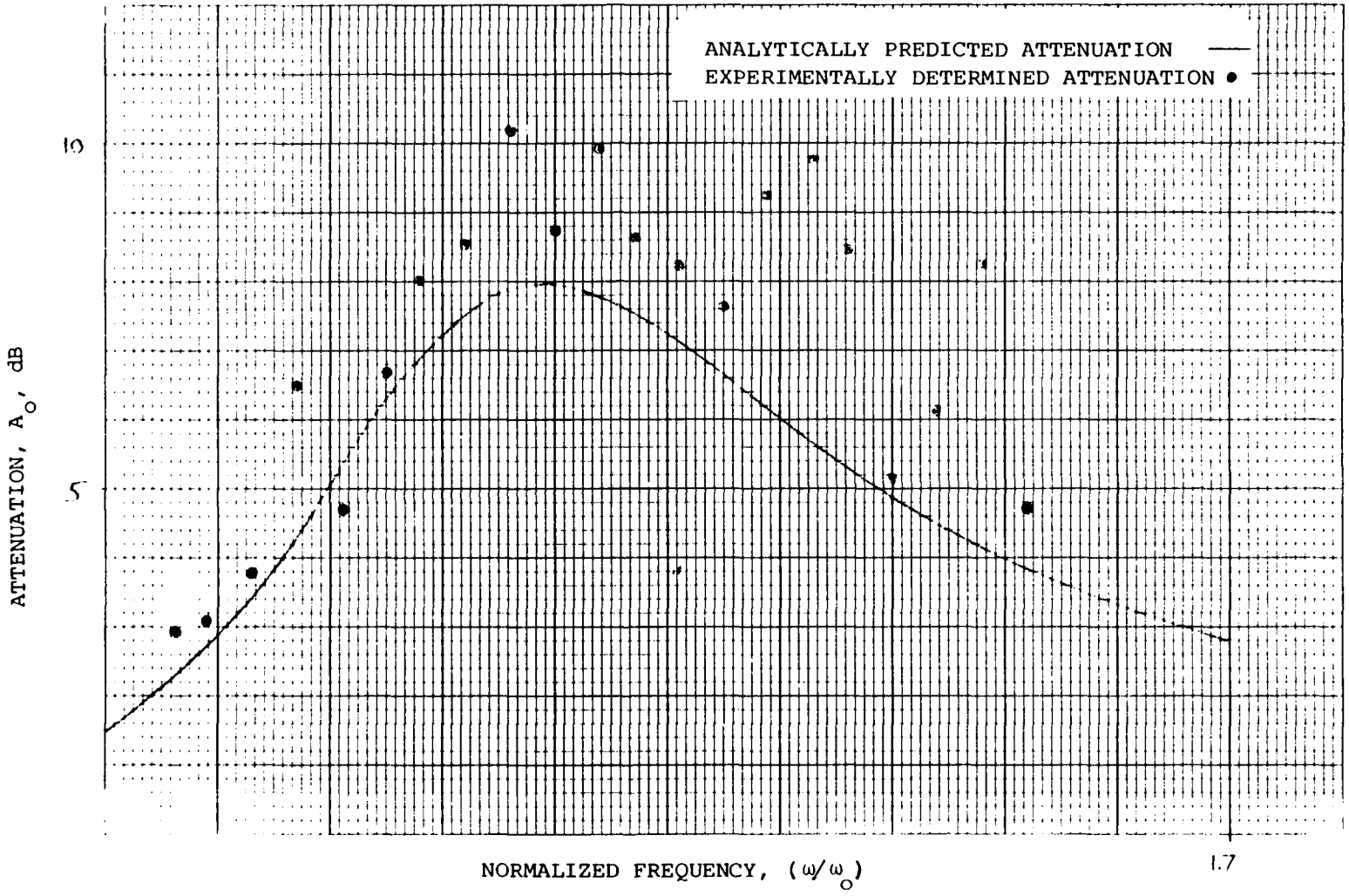

FIGURE 19

Attenuation vs. Normalized Frequency
$\beta = 0.35$, $R' = 0.50$

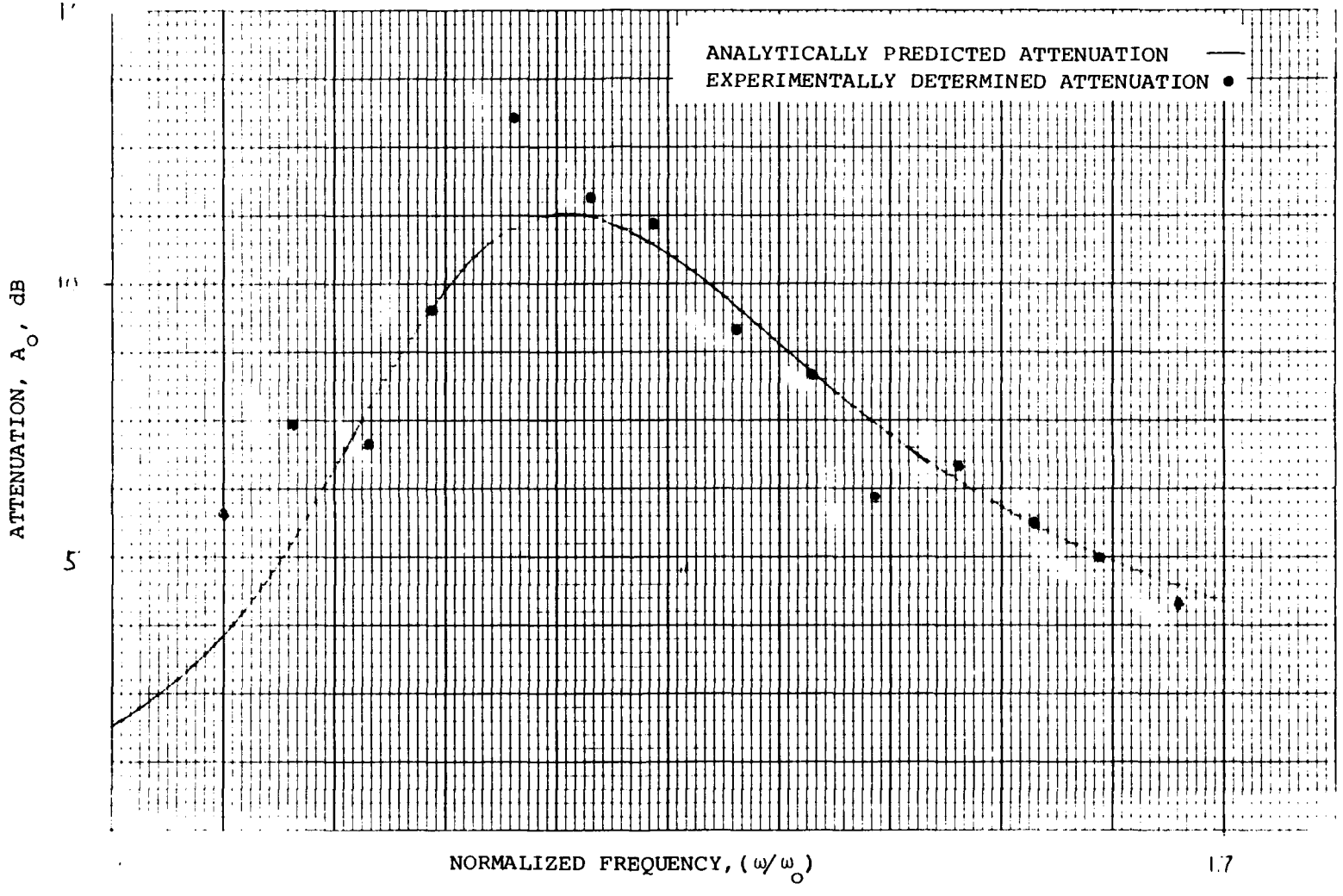

FIGURE 20

Attenuation vs. Normalized Frequency
$\beta = 0.51$, $R' = 0.47$

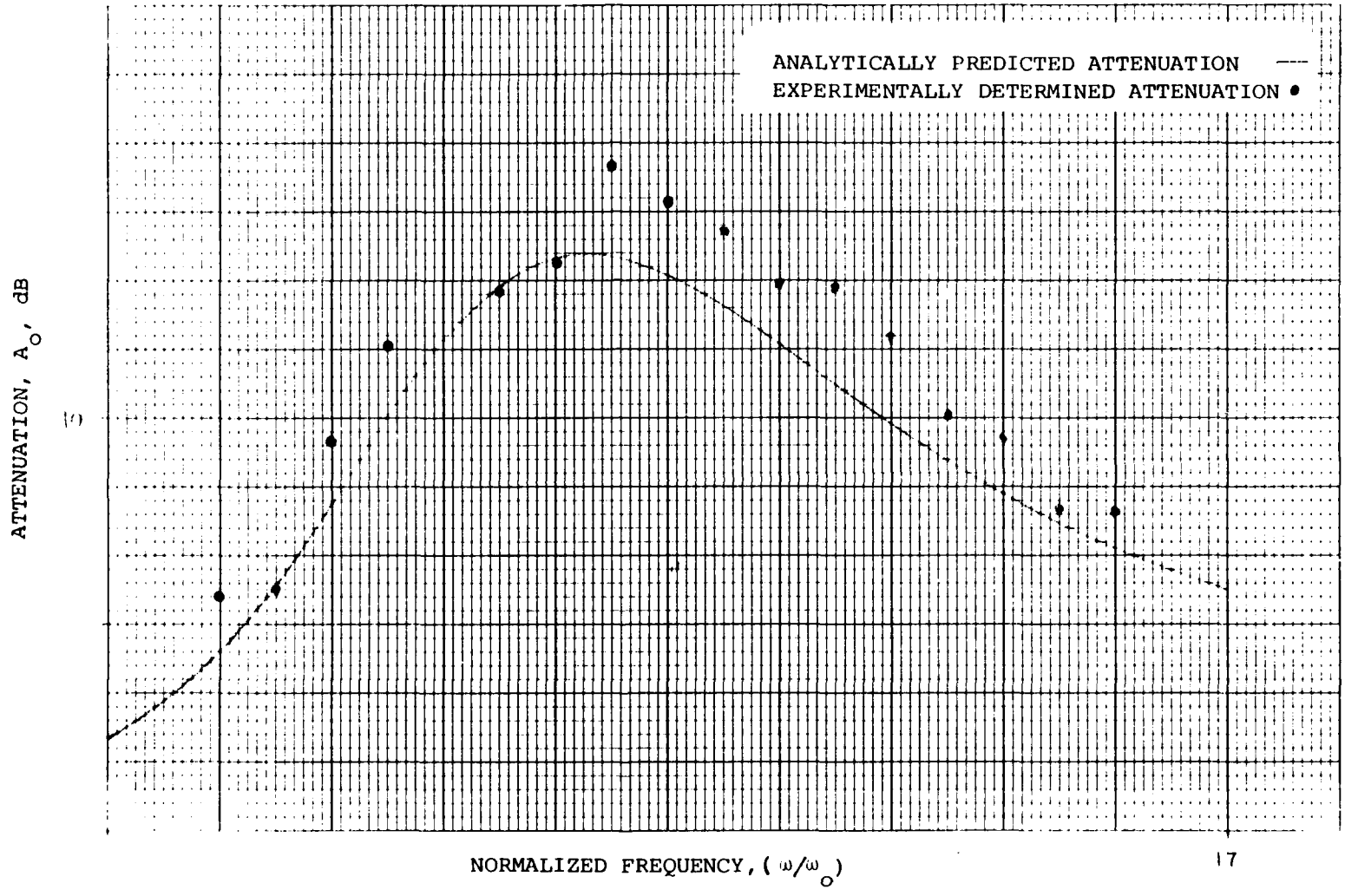

FIGURE 21

Attenuation vs. Normalized Frequency
$\beta = 0.69$, $R' = 0.47$

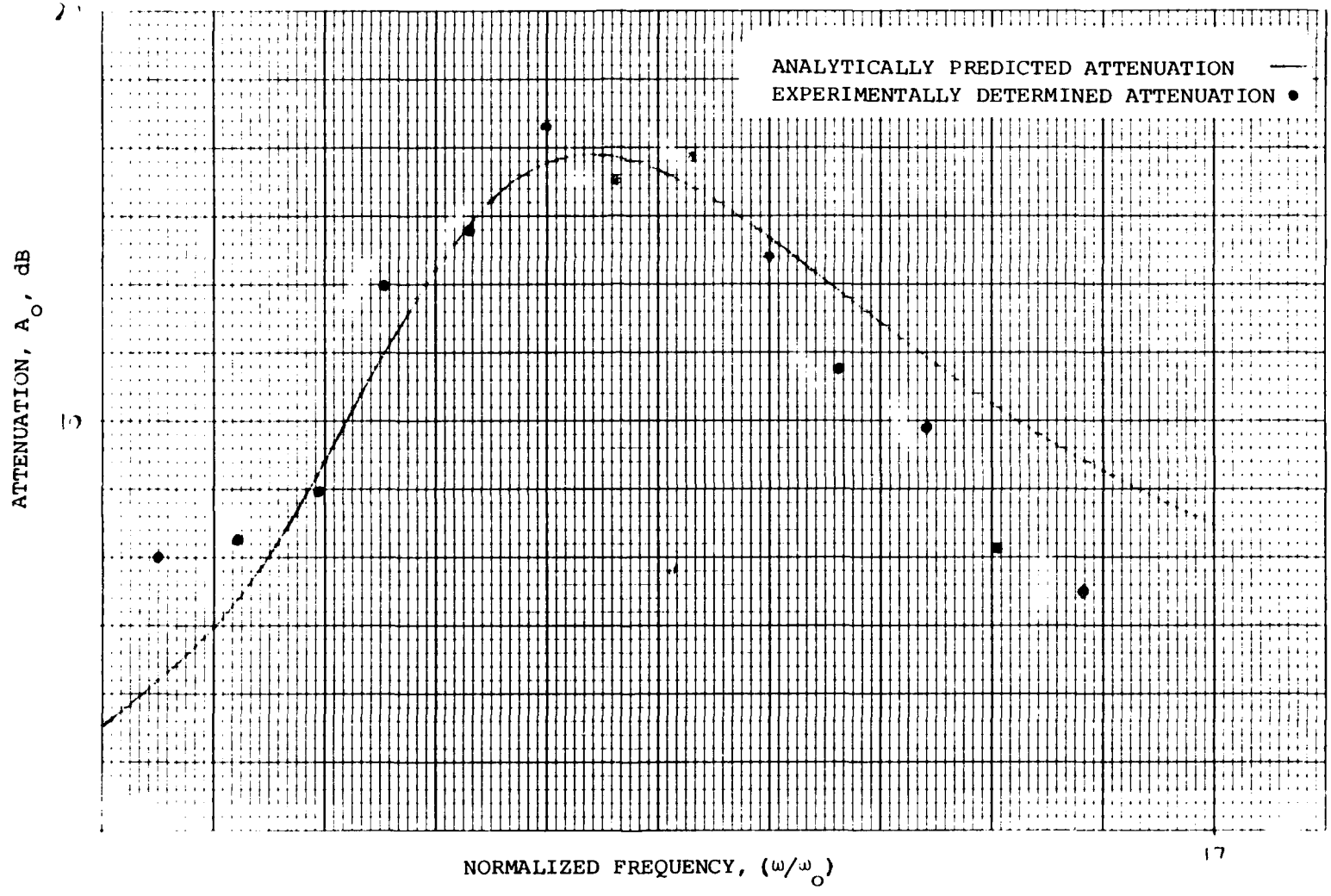

FIGURE 22

Attenuation vs. Normalized Frequency
$\beta = 0.87$, $R' = 0.46$

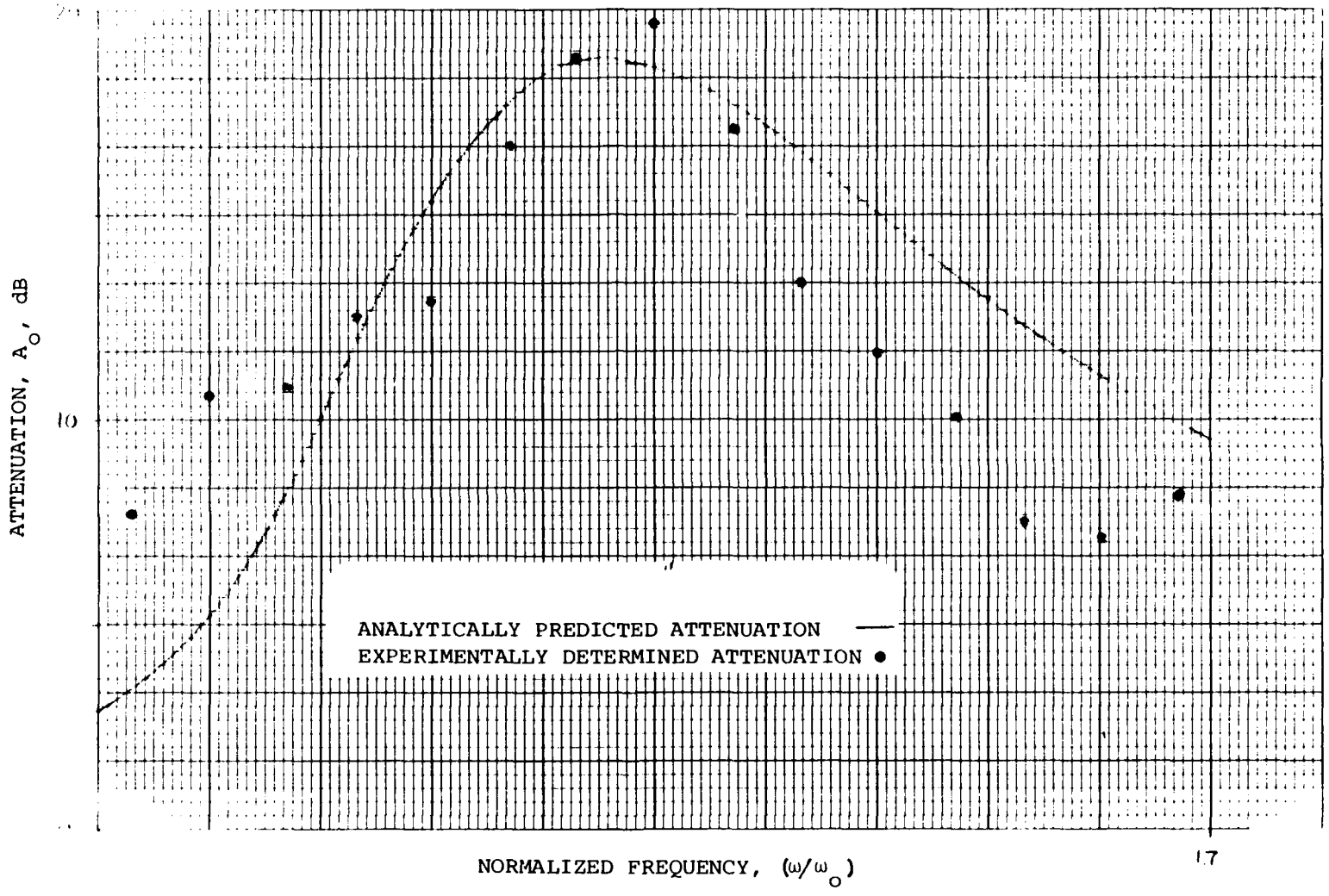

FIGURE 23

Attenuation vs. Normalized Frequency
$\beta = 1.12$, $R' = 0.46$

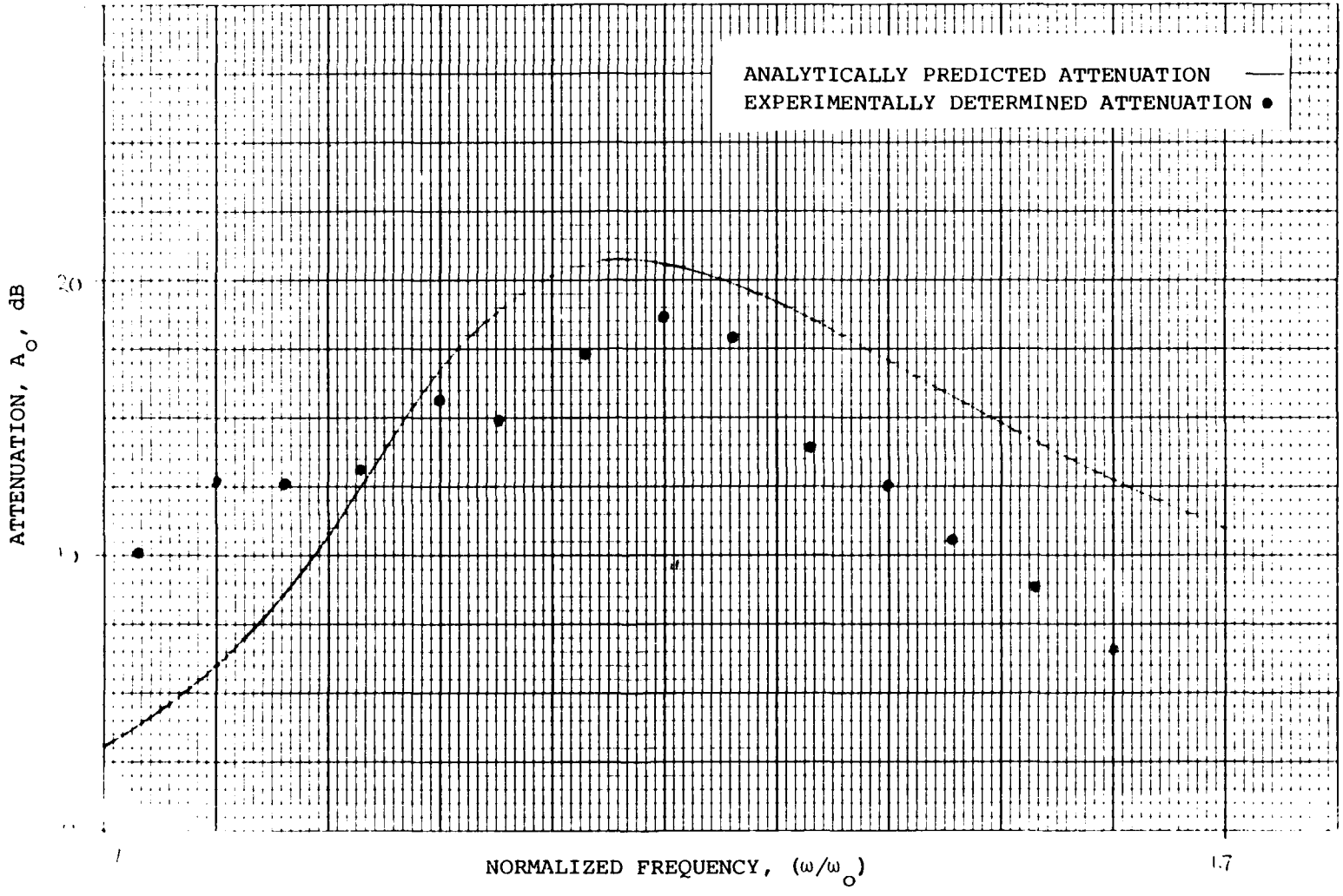

FIGURE 24

Attenuation vs. Normalized Frequency
$\beta = 1.26$, $R' = 0.45$

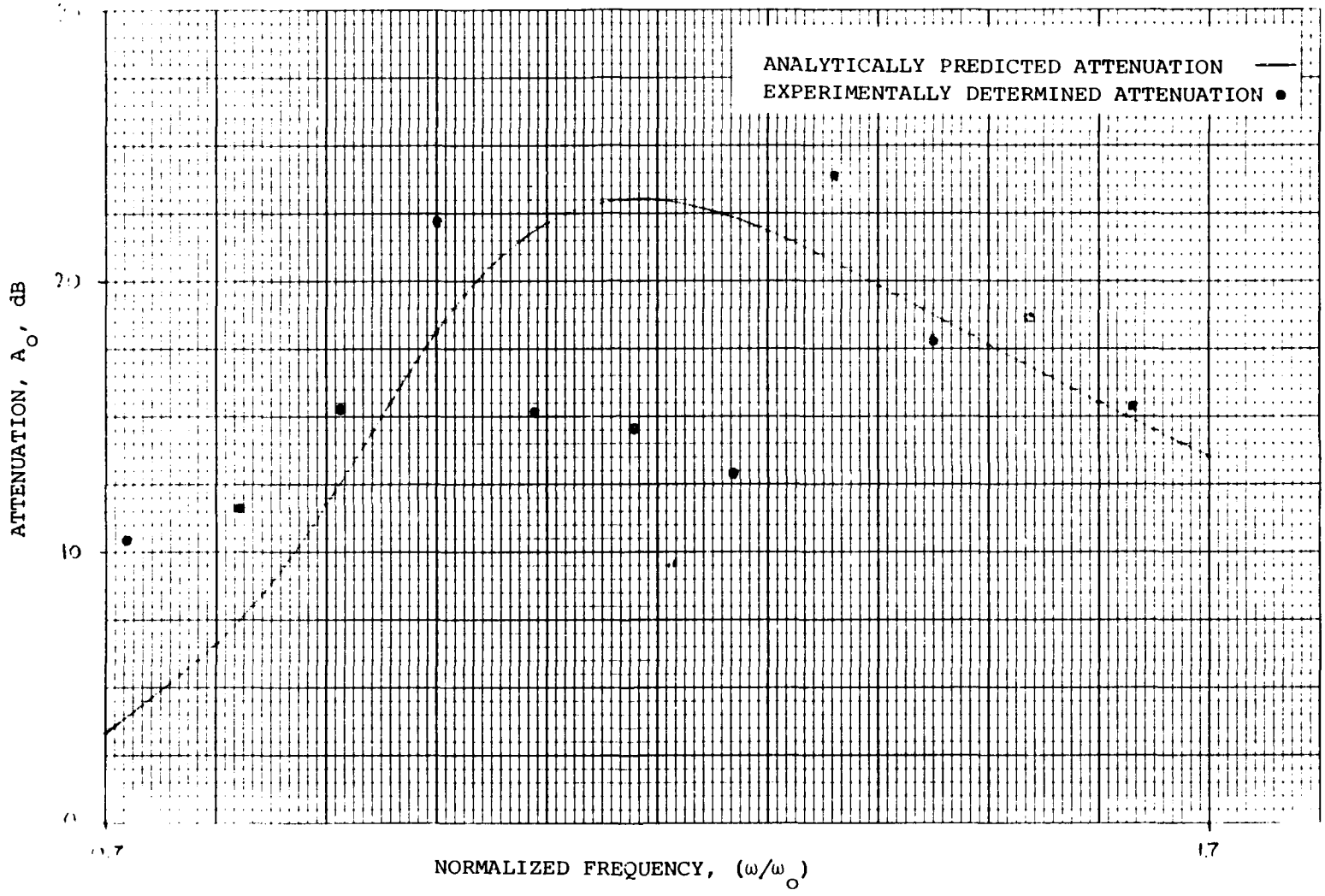

FIGURE 25

Attenuation vs. Normalized Frequency
$\beta = 1.55$, $R' = 0.45$

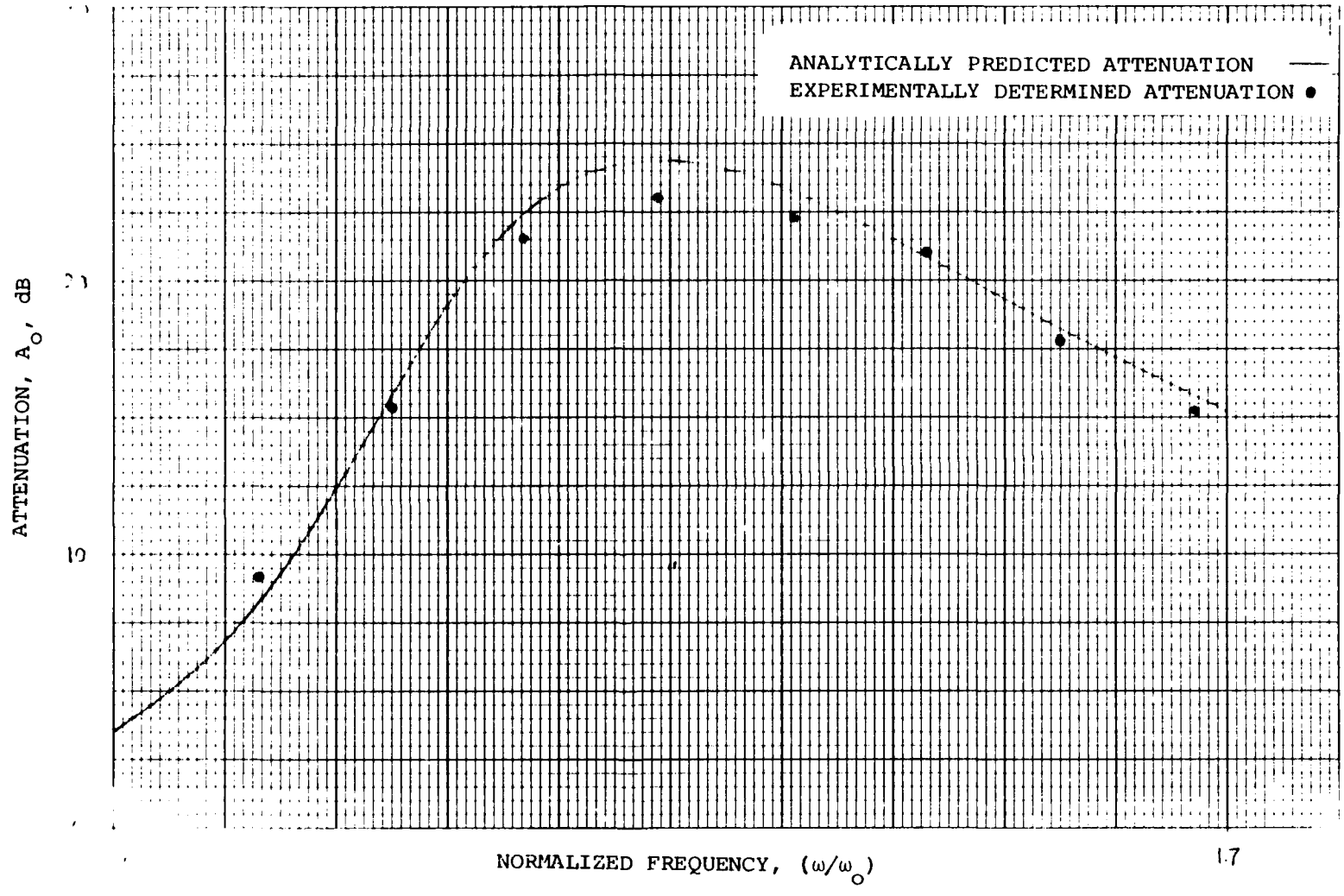

FIGURE 26

Attenuation vs. Normalized Frequency
$\beta = 1.75$, $R' = 0.45$

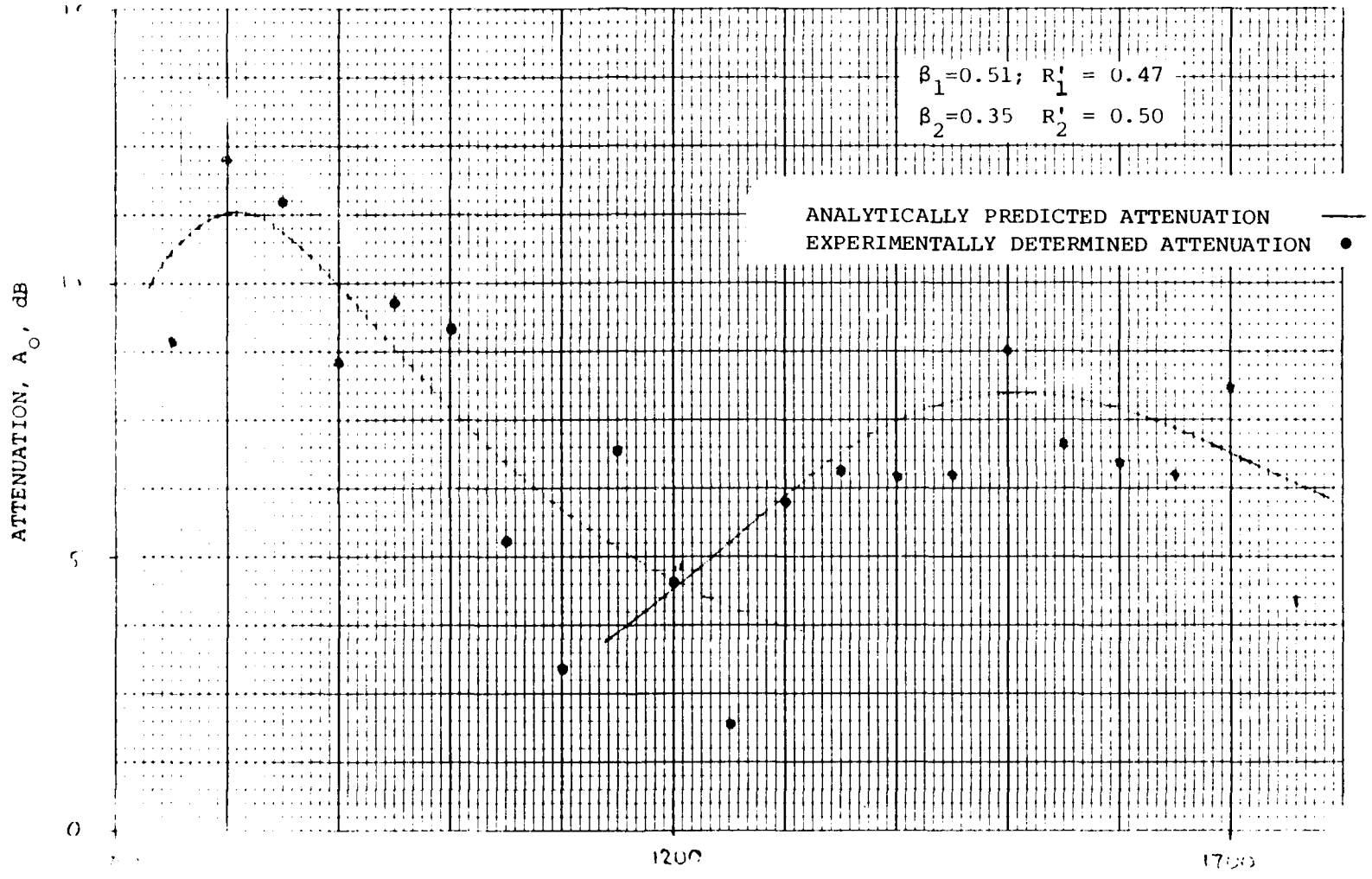

FIGURE 27

ATTENUATION VS. FREQUENCY

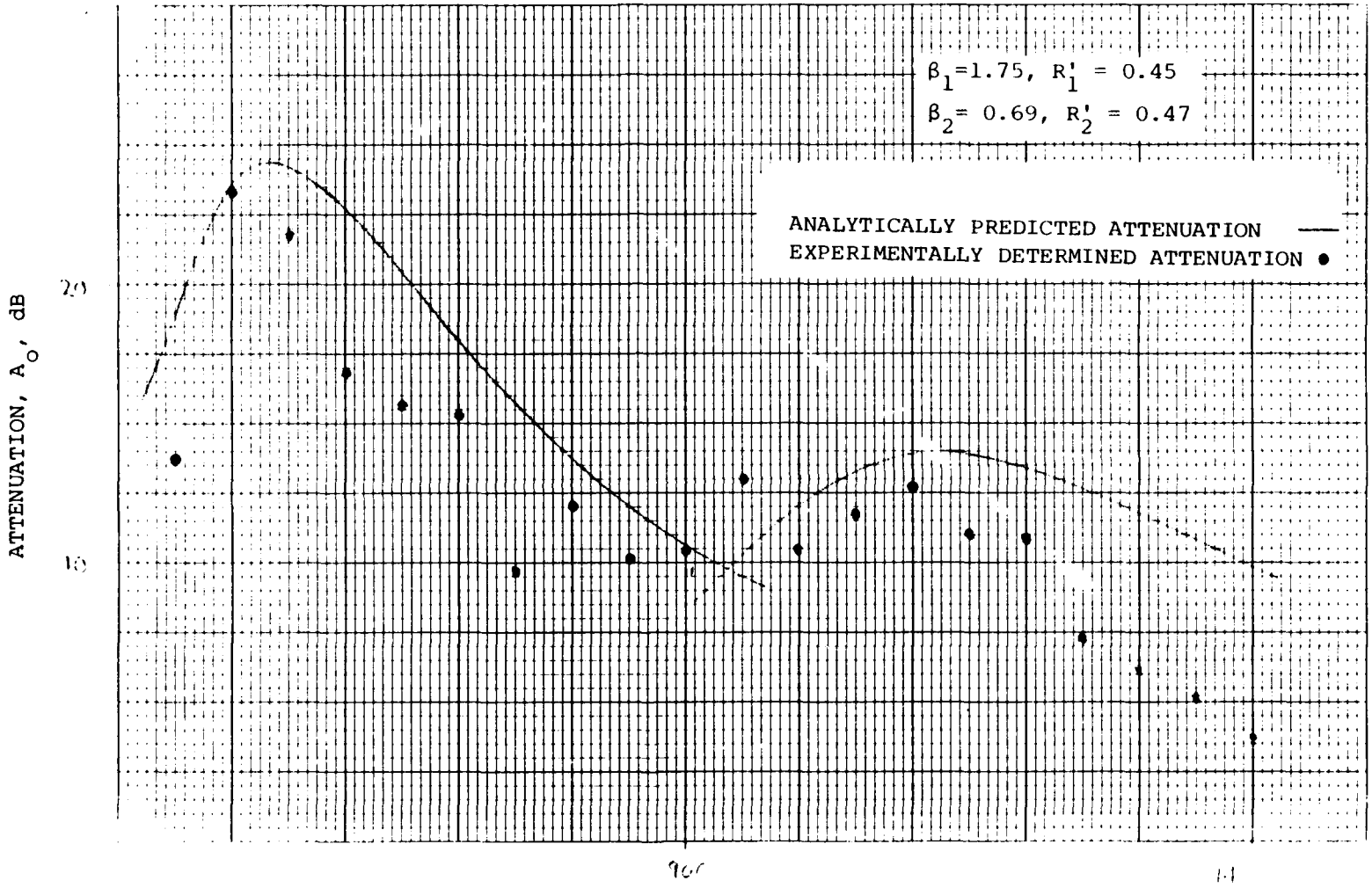

FIGURE 28

ATTENUATION VS. FREQUENCY

5. CONCLUSIONS

The experiments carried out in this thesis show that resiliently mounted masses attached to a beam do indeed act as dynamic absorbers. The extension of this is that the internally mounted equipment of a ship or submarine hull also act as dynamic absorbers with respect to hull vibrations. And while the internal equipment and mountings are more complex, they can be a significant factor in hull vibrations.

The experiments also confirm the analytical model adopted. The experimental results agrees quite well with the analytically predicted attenuation over a frequency band of about 0.7 ω_o to 1.7 ω_o. This range was limited by noise in the experiment. The data fit was good for all mass ratios used; from β=0.35, typical of hull structures, to a quite severe loading of β=1.75.

Another important point is that the attached masses acted independently. This is shown by the experiments using a combination of two mass ratios. The independence was achieved by using a foam as the resilient material. The foam deformed locally during vibration and did not cause coupling between the masses. This result allows attenuation over a much broader frequency range through the use of a varied mass distribution.

There are some immediate extensions of this thesis.

One is an investigation of the importance of mass rotations. The assumption used here was that no mass rotation took place and for the geometries of this experiment, this was apparently a good assumption. A similar experiment could be made using masses with greatly varied geometries or moments of inertia. Another would be to make a similar study on a cylindrical shell instead of a beam. The shell and probable mass distributions would complicate the modelling and measurements, but would more closely approximate a submarine hull. Finally, the importance of beam-mass asymmetry, not addressed in this thesis, should be assessed.

There are recommendations to improve the results obtained in these experiments. One is to use a much larger beam, both in length and cross section. This would permit the attachment of larger masses to the beam and would make some measurements easier, particularly those of R' and k. In the present experiment the mass of the accelerometer was about the same as the attached masses. Second, one could use a resilient material with a smaller loss factor and a spring constant large enough to keep the attenuation frequency range well into the smooth part of the beam spectrum. The smaller loss factor would make the attenuation peaks higher and sharper and also make the determination of R' and k easier.

APPENDICES

APPENDIX A

BEAM DATA

BEAM DATA

Material - Rolled Aluminum

Properties - $\rho = 2.7$ gm/cm^3 $E = 6.9 \times 10^{11}$ dyne/cm^2

Dimensions - 305 cm x 127 cm x 0.64 cm (10' x 1/2" x 1/4")

Cross Sectional Area - $A = 0.81$ cm^2

Area Moment of Inertia - $I = 2.7 \times 10^{-2}$ cm^4

Dispersion Relation - $\lambda_o^2 = 5.8 \times 10^5 f^{-1}$ λ(cm); f(Hz)

Computed Free-Free Natural Frequencies:

$$\omega = \left(\frac{\alpha}{\ell^2}\right) \sqrt{\frac{EI}{\rho A}} = 2\pi f$$

MODE	1	2	3	4	5
$\alpha^{(4)}$	22.4	61.7	121	200	299
f	3.5	9.7	19.0	31.4	46.9

APPENDIX B

ATTENUATION DATA

$\beta = 0.35$, $R^{4} = 0.50$

TABLE B2

$m = 0.38$ gm $f_o = 1320$ Hz $\beta = 0.35$ $R' = 0.50$

RESULTS:

f(Hz)	SLOPE (dB/cm)	ATTEN (dB)	f/f_o
1000	0.124	2.9	0.76
1050	0.131	3.0	0.79
1100	0.165	3.7	0.83
1150	0.289	6.4	0.87
1200	0.214	4.7	0.91
1250	0.311	6.6	0.95
1300	0.380	8.0	0.98
1350	0.406	8.5	1.02
1400	0.501	10.1	1.06
1450	0.443	8.8	1.10
1500	0.506	9.9	1.14
1550	0.446	8.6	1.17
1600	0.434	8.2	1.21
1650	0.408	7.6	1.25
1700	0.495	9.1	1.29
1750	0.532	9.6	1.33
1800	0.472	8.4	1.36
1850	0.292	5.1	1.40
1900	0.350	6.1	1.44
1950	0.479	8.2	1.48
2000	0.280	4.7	1.52

TABLE B2

m = 0.38 gm f_o = 1320 Hz ζ = 0.35 R'= 0.50

ATTENUATION DATA:

ℓ(cm)	26	28	30	32	34	36	38	40
f(Hz)	ATTENUATION (dB)							
1000	1.2	2.7	2.8	2.0	3.7	2.0	2.8	4.2
1050	2.7	3.1	3.4	3.2	3.1	3.6	3.9	5.2
1100	3.9	3.2	2.7	3.1	4.8	3.0	6.0	5.5
1150	4.7	5.7	4.8	4.2	7.9	6.8	8.0	8.6
1200	6.8	5.8	5.0	6.5	7.1	8.0	9.1	8.2
1250	6.9	6.9	5.6	8.0	10.6	8.6	10.4	10.2
1300	8.2	8.3	7.3	9.9	9.2	10.4	12.9	12.8
1350	9.7	10.1	9.3	10.6	12.3	11.5	14.8	14.9
1400	9.7	12.3	12.5	11.4	15.2	13.8	17.1	17.2
1450	11.4	13.2	12.4	14.5	15.7	15.2	16.5	18.3
1500	12.8	12.6	13.5	14.4	15.7	16.7	17.9	19.6
1550	12.2	13.9	13.4	14.5	15.5	15.9	17.8	18.9
1600	12.5	14.4	14.0	13.4	15.8	16.6	18.4	18.6
1650	10.0	12.6	13.4	13.4	16.0	14.8	16.4	16.1
1700	9.9	10.2	11.7	11.8	14.9	14.8	16.1	15.8
1750	8.3	10.0	10.4	12.0	13.8	13.9	14.9	15.8
1800	6.6	7.5	10.0	11.9	11.8	12.5	13.9	12.3
1850	7.9	8.0	8.7	8.8	11.1	11.9	10.4	11.5
1900	6.2	7.1	8.2	9.2	9.1	10.9	11.5	10.1
1950	5.0	6.9	7.2	9.1	8.6	10.6	11.1	12.1
2000	6.3	5.2	5.1	7.8	8.4	9.7	8.5	8.6

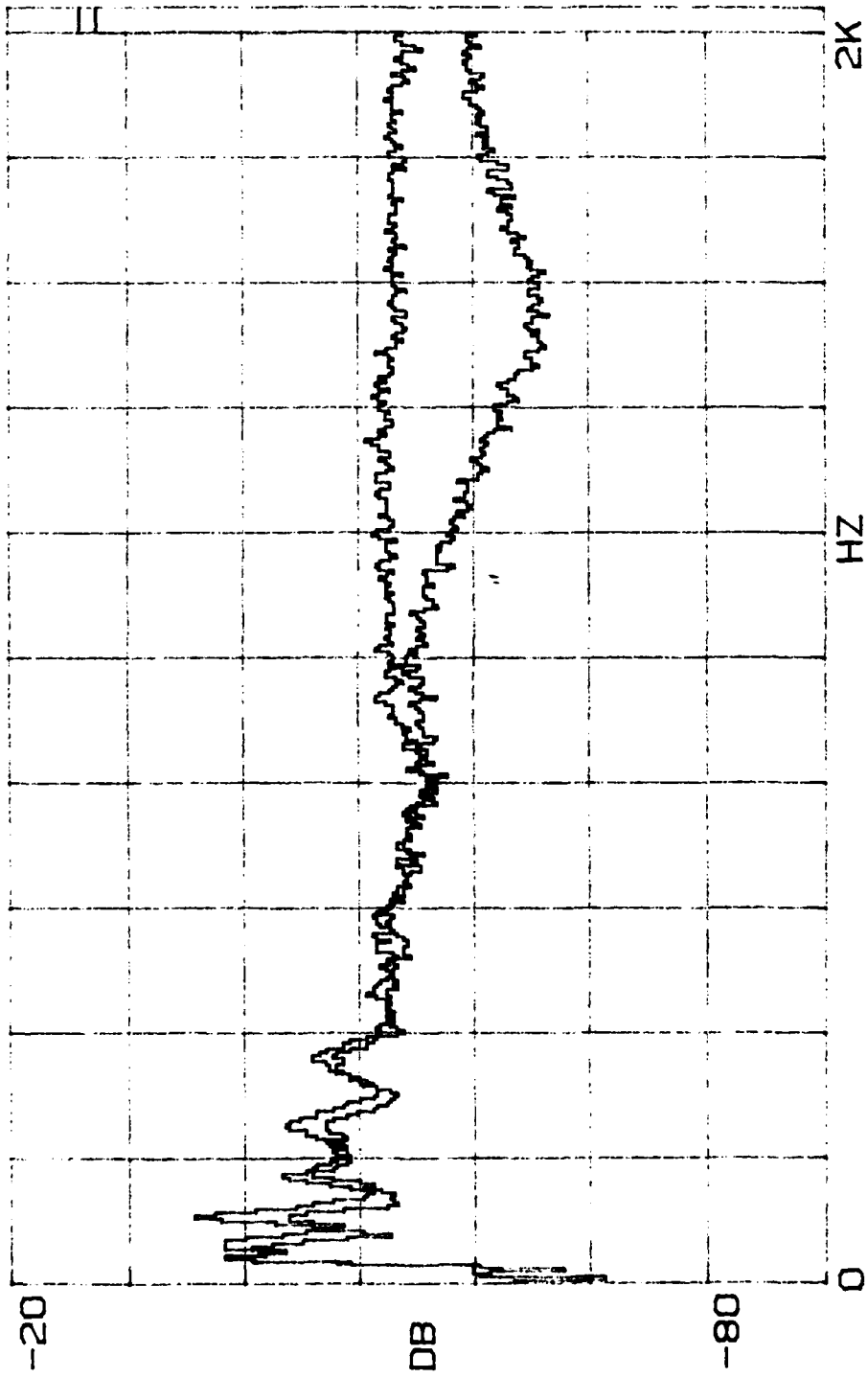

FIGURE B1

β = 0.35, R' = 0.50, l = 26 cm

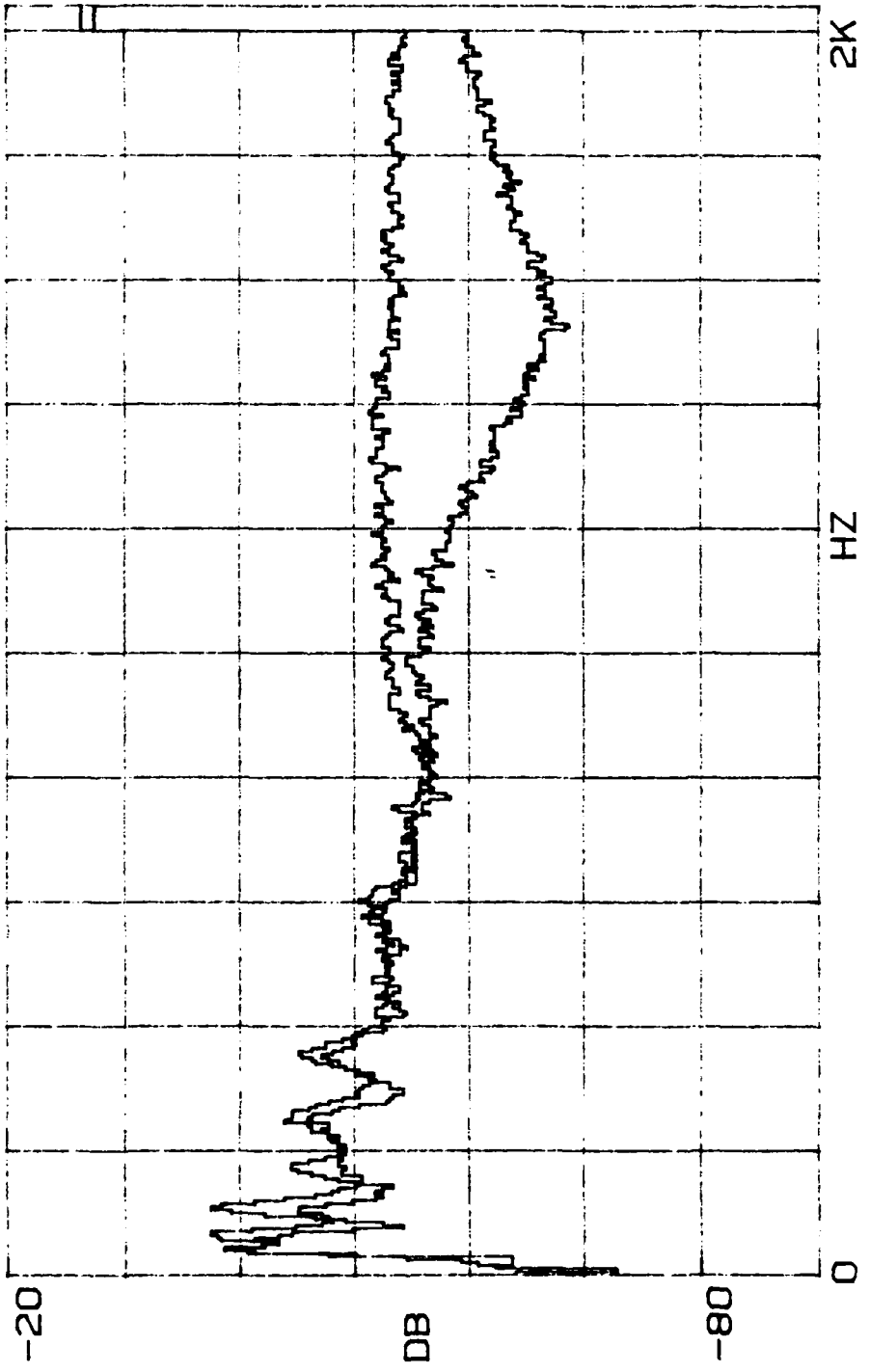

FIGURE B2

β = 0.35, R' = 0.50, l = 28 cm

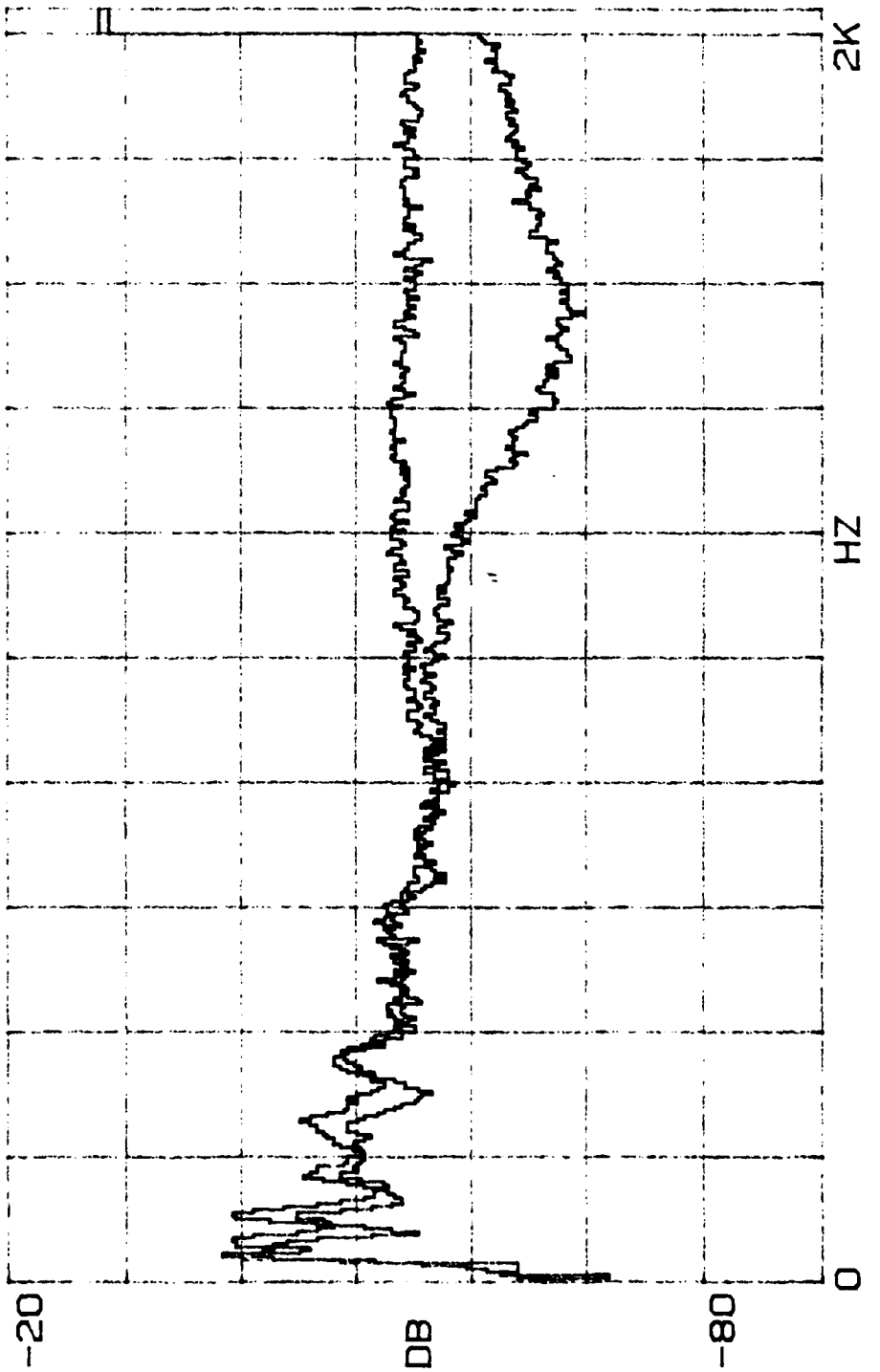

FIGURE B3

β = 0.35, R' = 0.50, l = 30 cm

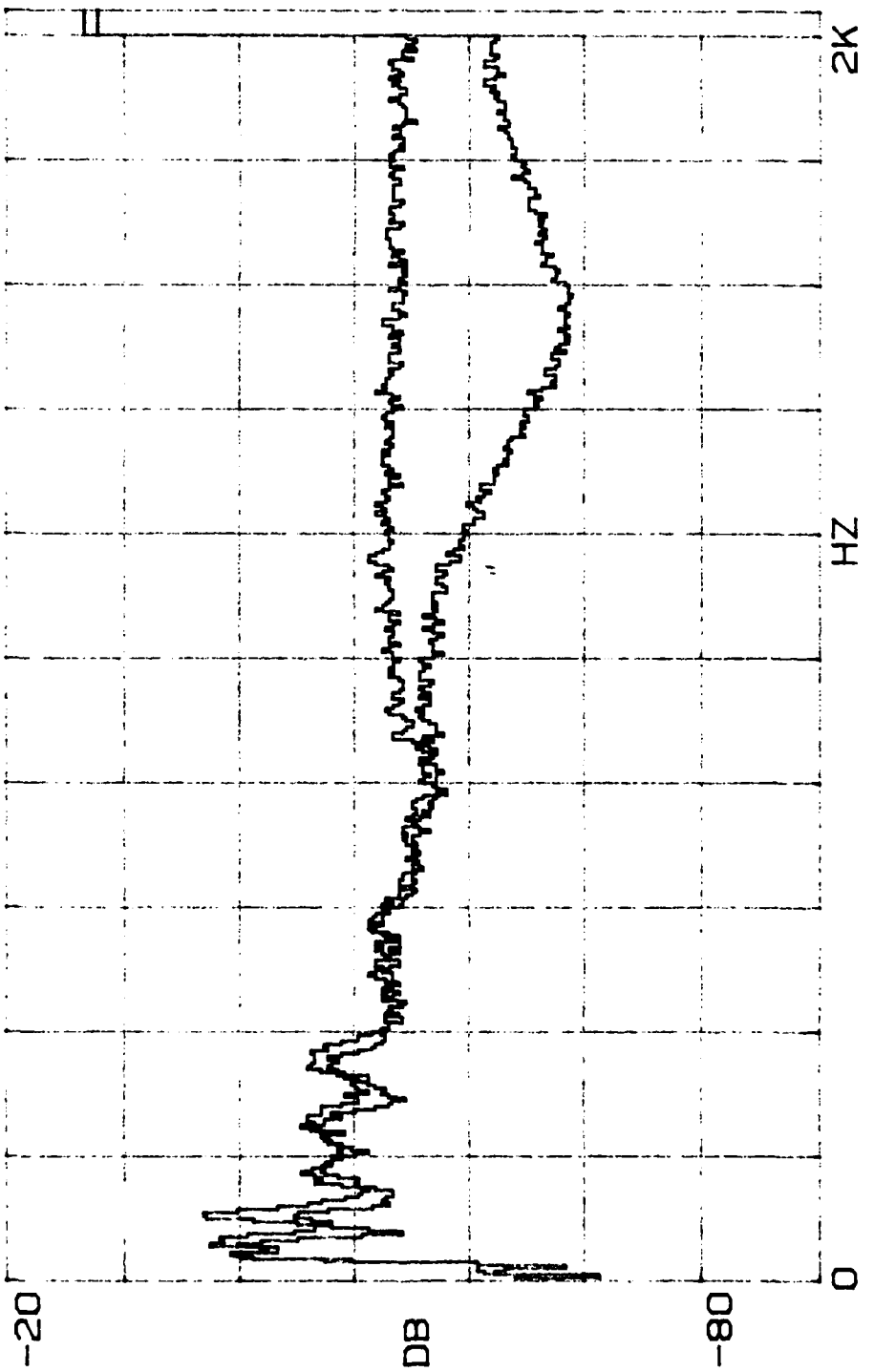

FIGURE B4

β = 0.35, R' = 0.50, l = 32 cm

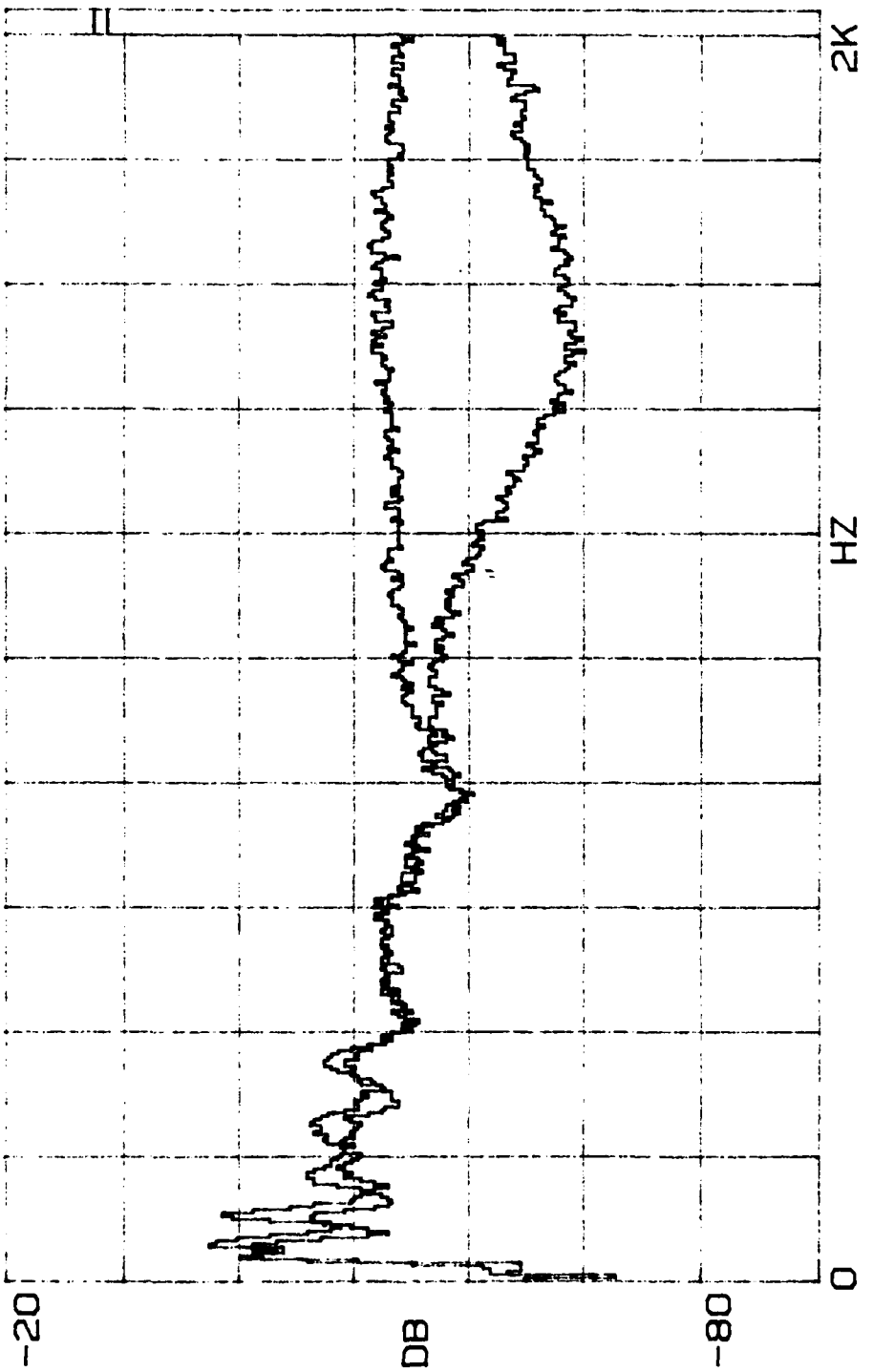

FIGURE B5

$\beta = 0.35$, $R' = 0.50$, $l = 34$ cm

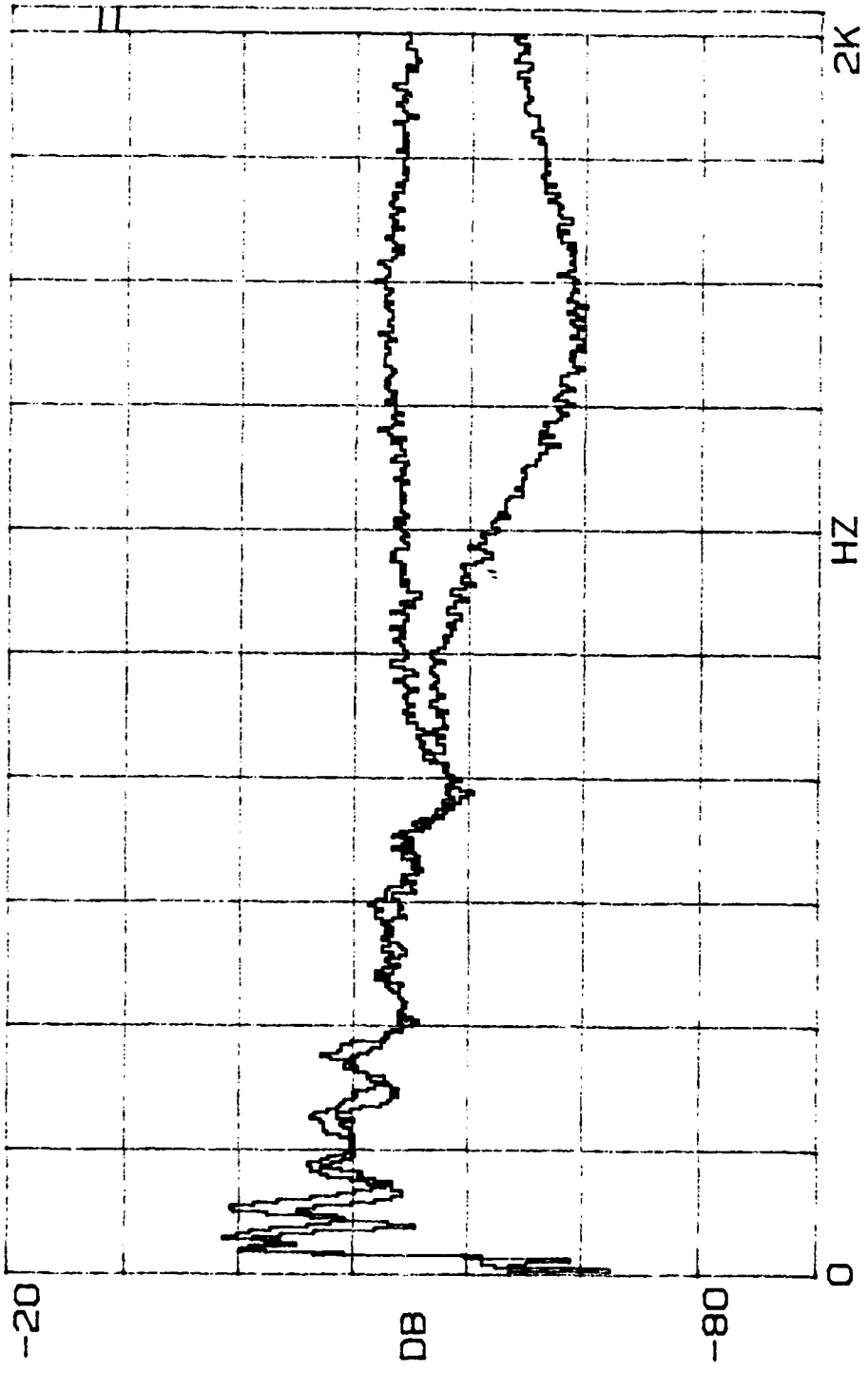

FIGURE B6

β = 0.35, R' = 0.50, l = 36 cm

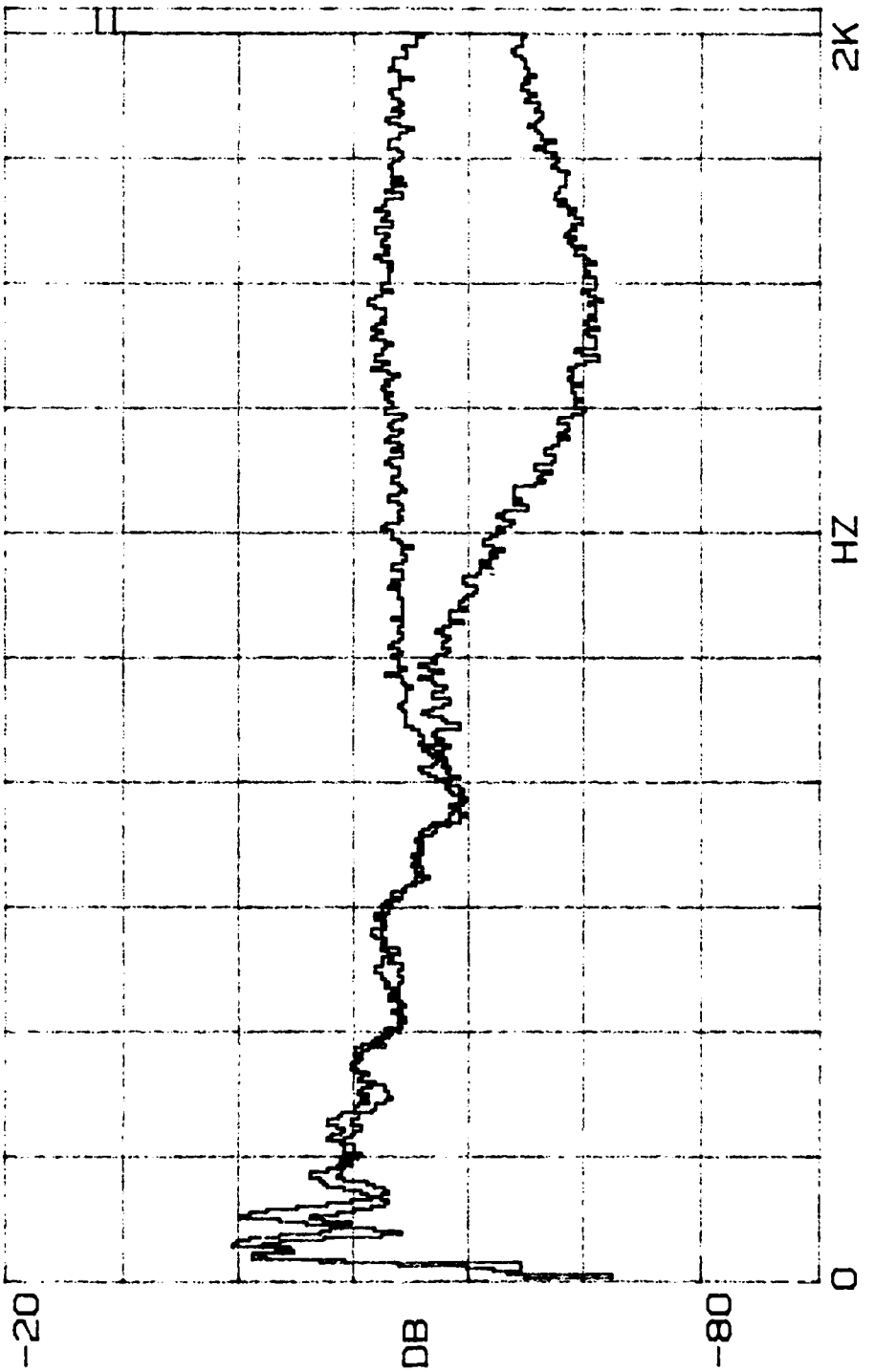

FIGURE B7

β = 0.35, R' = 0.50, l = 38 cm

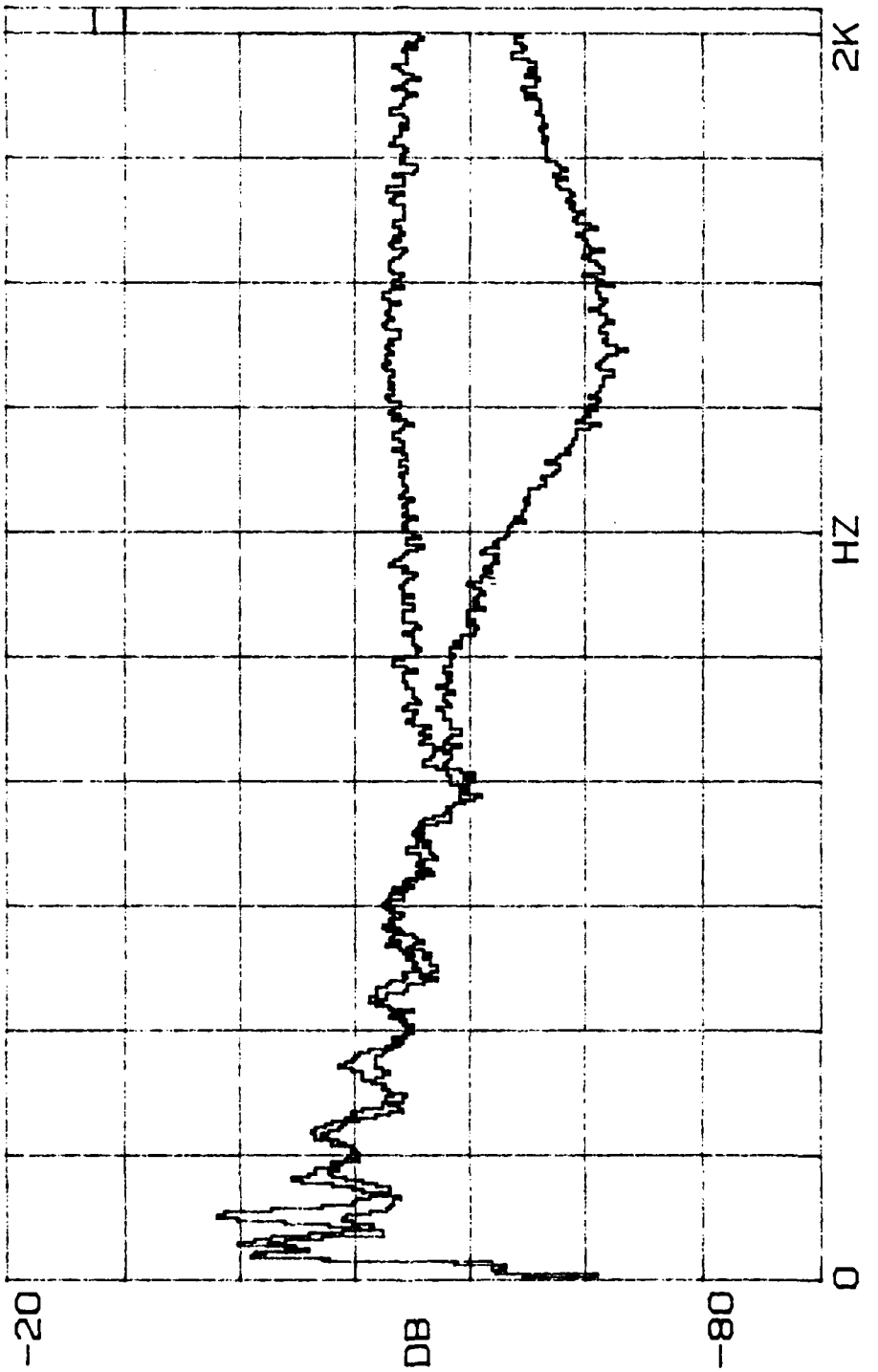

FIGURE B8

$\beta = 0.35$, $R' = 0.50$, $l = 40$ cm

APPENDIX C

ATTENUATION DATA

$\beta = 0.51$, $R^4 = 0.47$

TABLE 21

m = 0.55 gm f_o = 750 Hz ζ = 0.51 R' = 0.47

ATTENUATION DATA:

ℓ(cm)	22	24	26	28	30	32	34	36	38	40
f(Hz)	ATTENUATION (dB)									
600	0.9	1.0	2.3	1.6	2.3	4.2	3.2	3.7	3.8	5.0
650	2.2	3.0	3.9	3.1	3.7	4.7	4.5	4.8	5.1	7.1
700	4.5	5.5	3.6	4.4	6.1	7.1	7.2	7.3	8.4	3.9
750	6.7	7.1	7.1	7.0	8.3	9.9	11.3	10.9	12.8	6.2
800	9.0	10.9	8.0	10.4	11.8	13.9	13.5	16.9	16.3	8.1
850	10.1	13.0	11.7	13.2	15.6	15.5	15.2	16.5	19.3	11.1
900	13.6	12.2	12.7	14.0	16.5	16.2	18.5	18.1	19.9	16.4
950	13.0	11.4	12.4	13.4	14.9	15.3	16.8	15.9	18.9	18.2
1000	10.3	11.1	11.3	12.7	12.9	13.8	14.6	15.4	16.7	19.0
1050	8.3	10.5	9.5	9.6	11.5	12.7	11.7	13.3	12.7	17.4
1100	6.7	7.9	7.7	8.9	8.8	9.4	11.0	10.5	11.3	15.6
1150	5.5	6.9	6.2	5.8	5.9	9.9	8.1	9.3	9.5	13.2
1200	3.8	5.3	4.8	7.4	5.6	6.1	8.1	7.9	8.9	12.4
1250	3.1	4.3	4.3	6.0	6.4	5.2	5.2	6.3	6.9	9.8
1300	3.5	4.0	2.7	3.7	4.3	4.3	5.3	6.3	5.2	7.3
1350	2.6	3.5	3.4	4.2	4.1	5.2	5.6	5.1	5.1	7.3
1400	2.0	3.6	3.0	2.3	3.6	3.2	3.6	4.0	4.3	5.5
1450	2.6	3.7	2.9	2.9	3.6	4.0	4.3	4.5	4.4	5.3
1500	2.4	3.4	2.8	2.0	2.6	4.3	4.0	2.7	4.3	5.3

TABLE C2

$m = 0.55$ gm $f_o = 750$ Hz $\beta = 0.51$ $R' = 0.47$

RESULTS:

f(Hz)	SLOPE (dB/cm)	ATTEN (dB)	f/f_o
600	0.141	4.3	0.80
650	0.168	5.0	0.86
700	0.244	7.0	0.93
750	0.342	9.5	1.00
800	0.486	13.0	1.06
850	0.445	11.6	1.13
900	0.441	11.1	1.20
950	0.376	9.1	1.26
1000	0.345	8.3	1.33
1050	0.261	6.1	1.40
1100	0.291	6.6	1.46
1150	0.252	5.6	1.53
1200	0.227	4.9	1.60
1250	0.159	4.0	1.66
1300	0.149	3.1	1.73
1350	0.119	2.4	1.80
1400	0.120	2.4	1.86
1450	0.147	2.9	1.93
1500	0.140	2.7	2.00

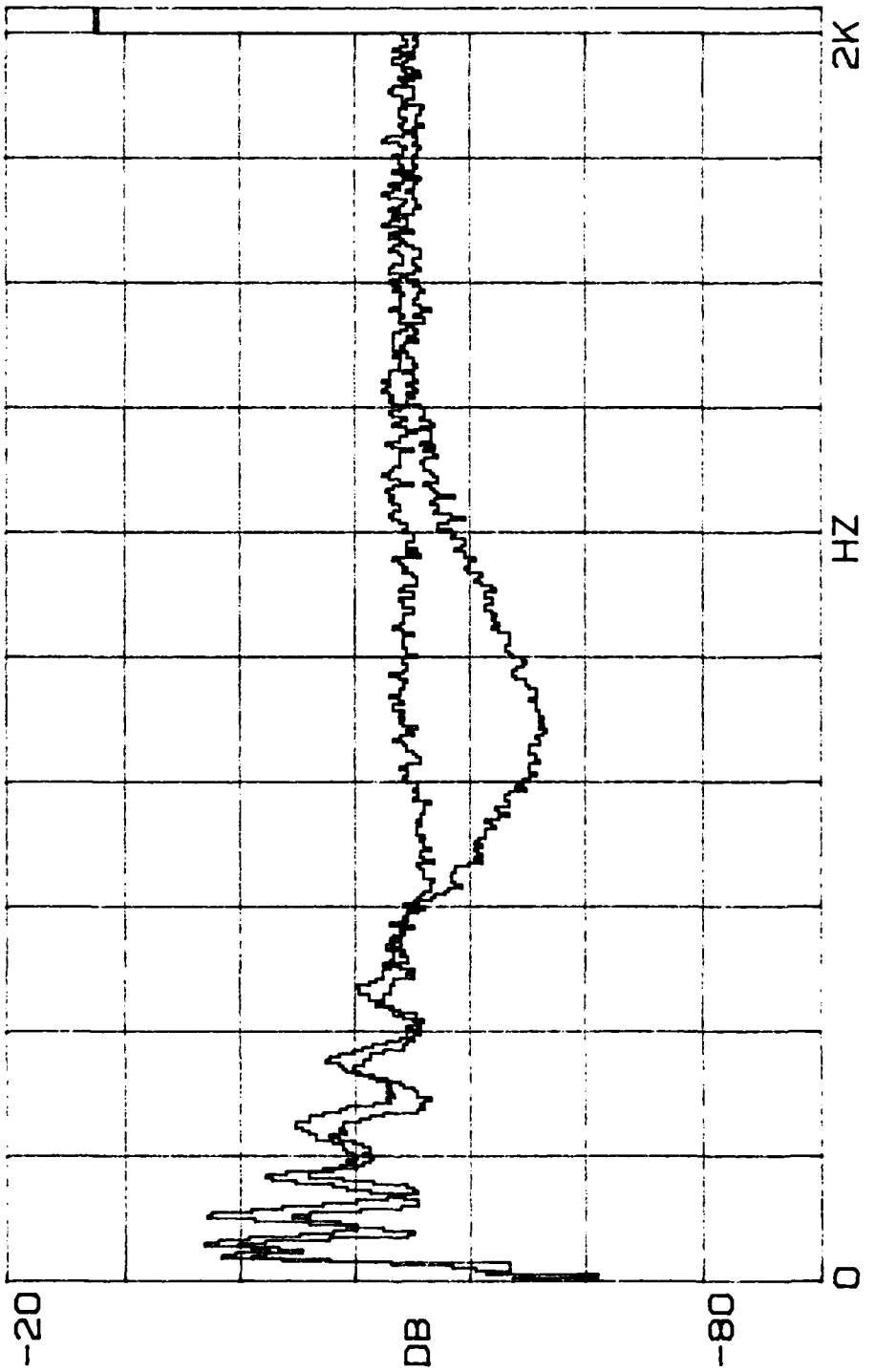

FIGURE C1

β = 0.51, R' = 0.47, l = 22 cm

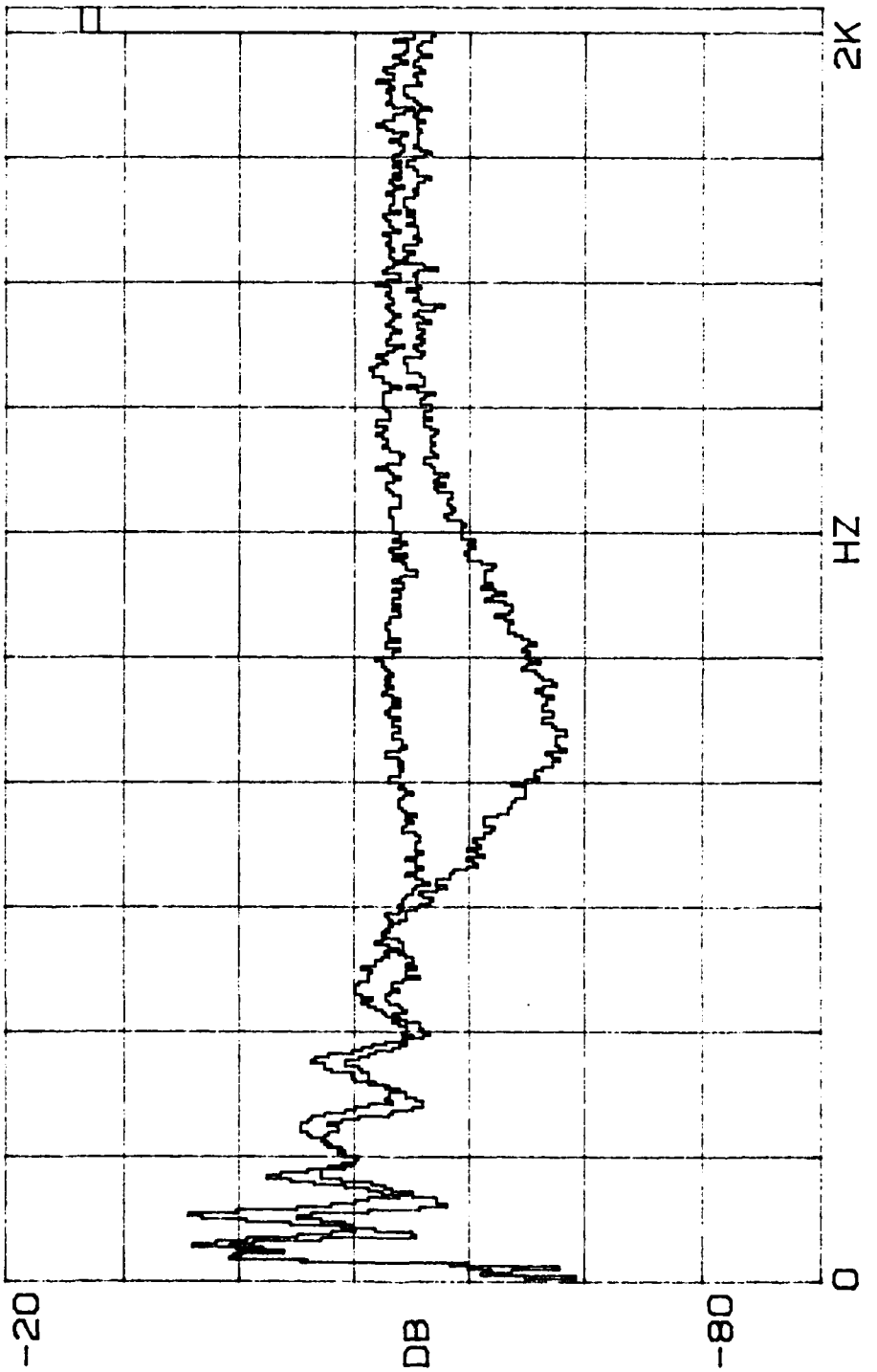

FIGURE C2

β = 0.51, R' = 0.47, l = 24 cm

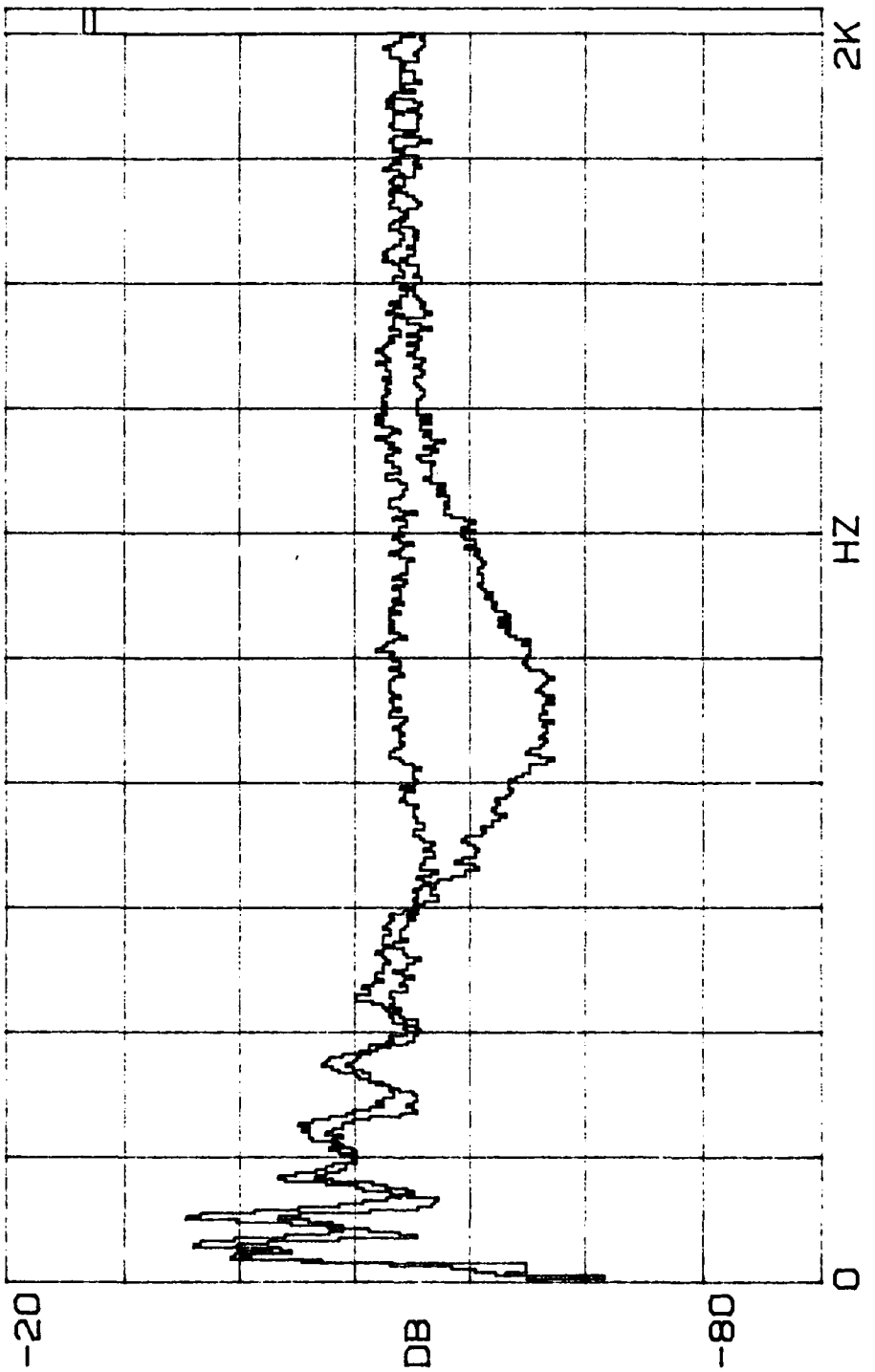

FIGURE C3

$\beta = 0.51$, $R' = 0.47$, $l = 26$ cm

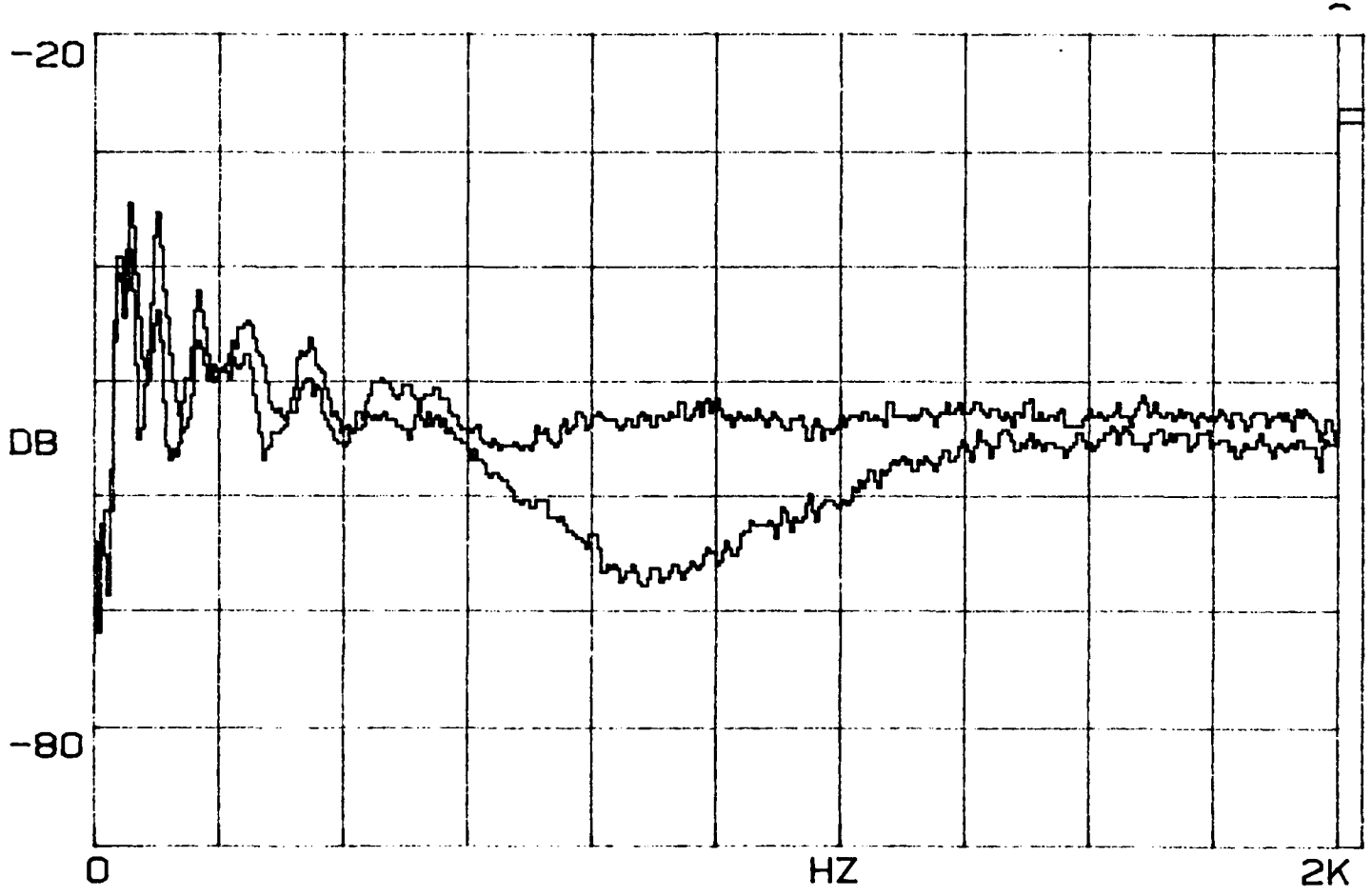

FIGURE C4

β = 0.51, R' = 0.47, l = 28 cm

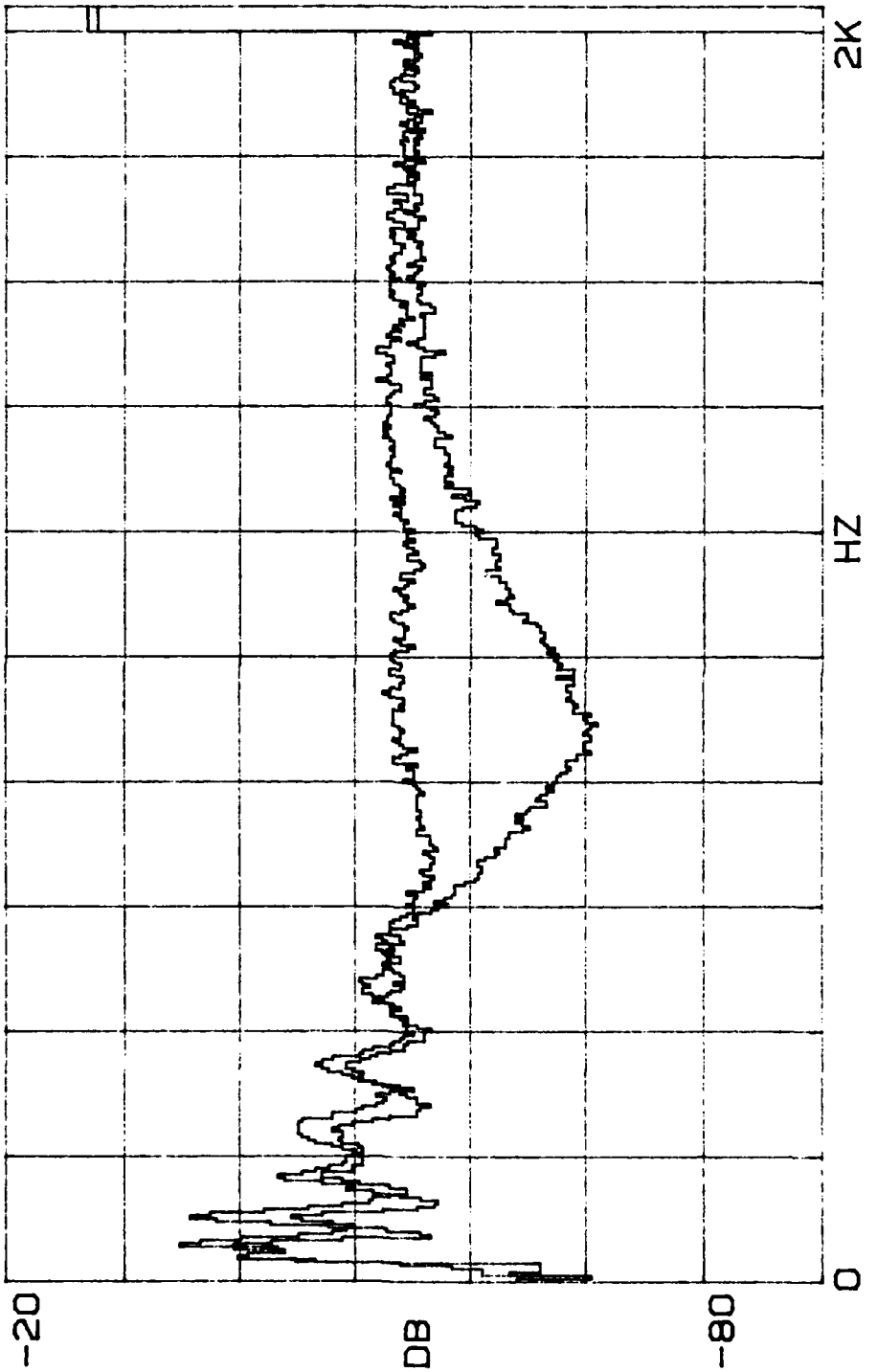

FIGURE C5

$\beta = 0.51$, $R' = 0.47$, $l = 30$ cm

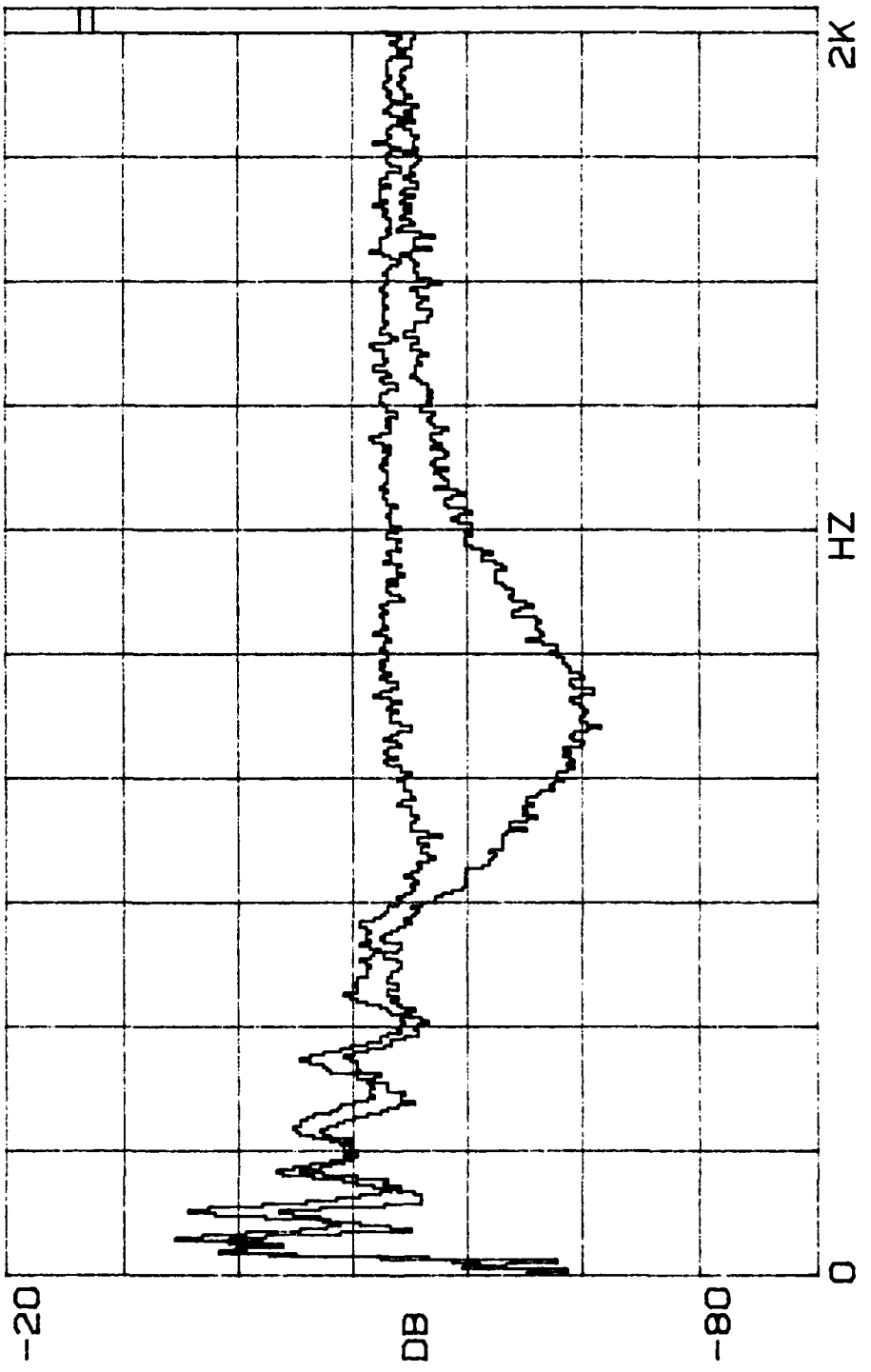

FIGURE C6

$\beta = 0.51$, $R' = 0.47$, $l = 32$ cm

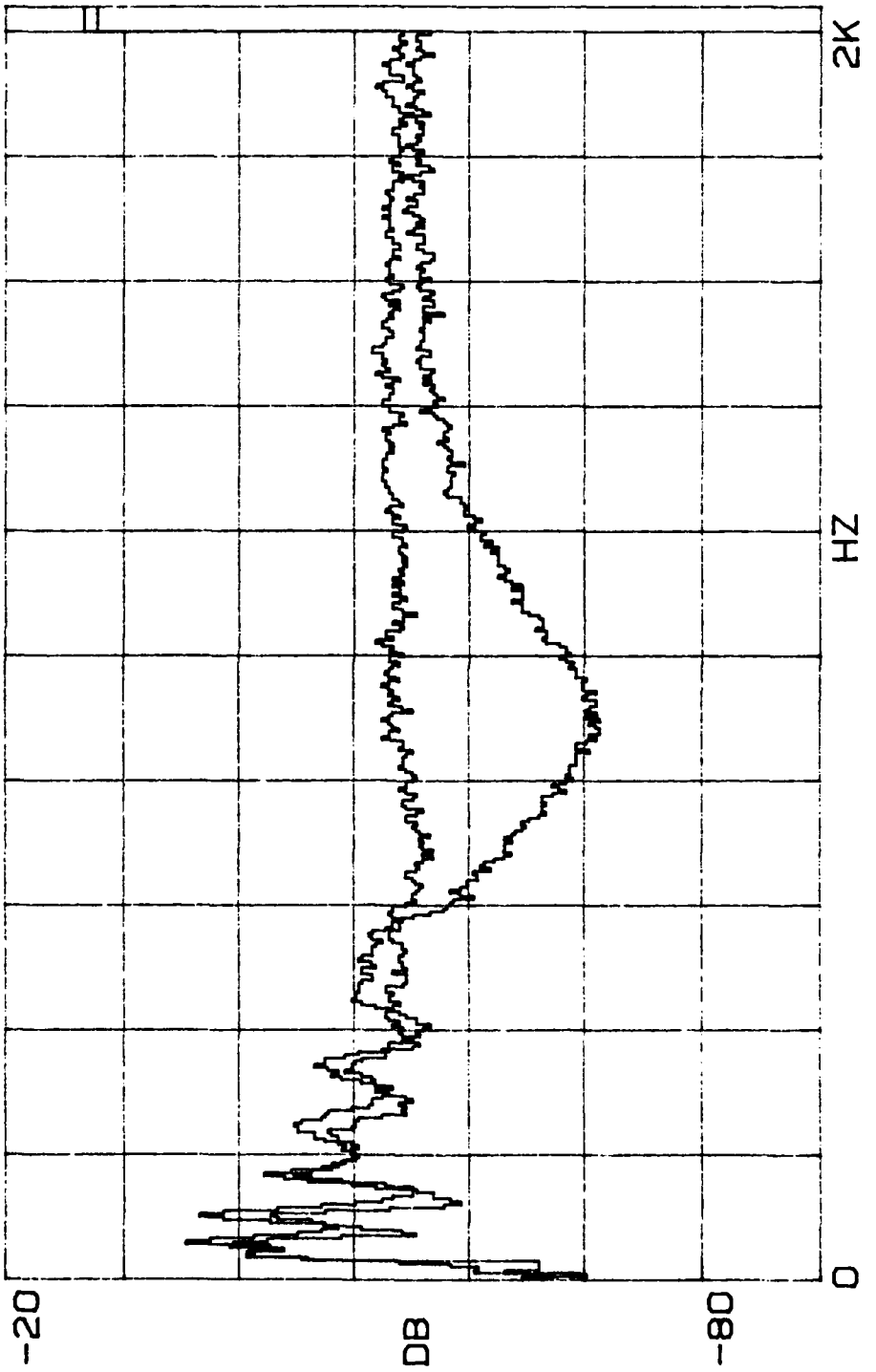

FIGURE C7

β = 0.51, R' = 0.47, l = 34 cm

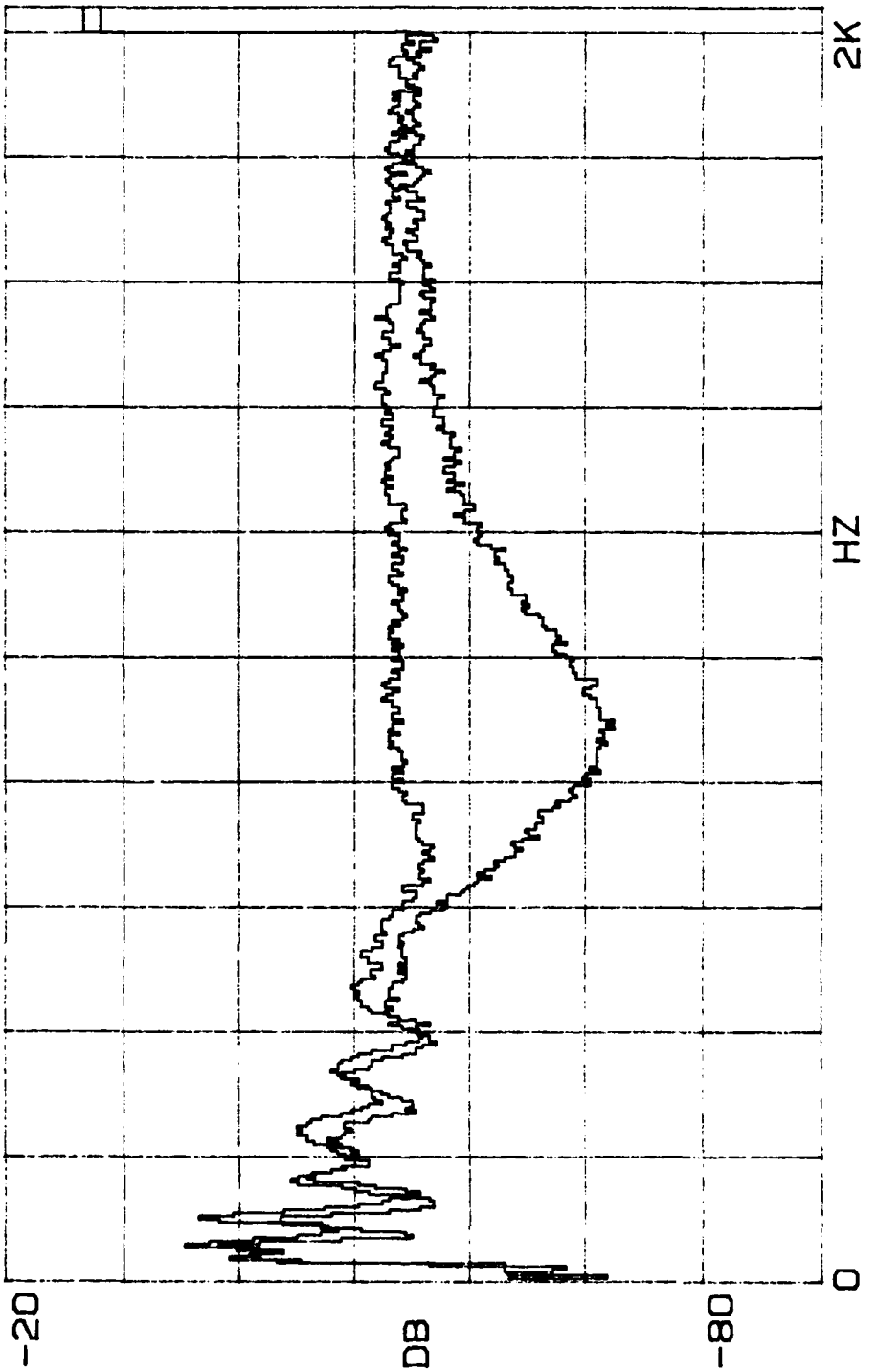

FIGURE C8

$\beta = 0.51$, $R' = 0.47$, $l = 36$ cm

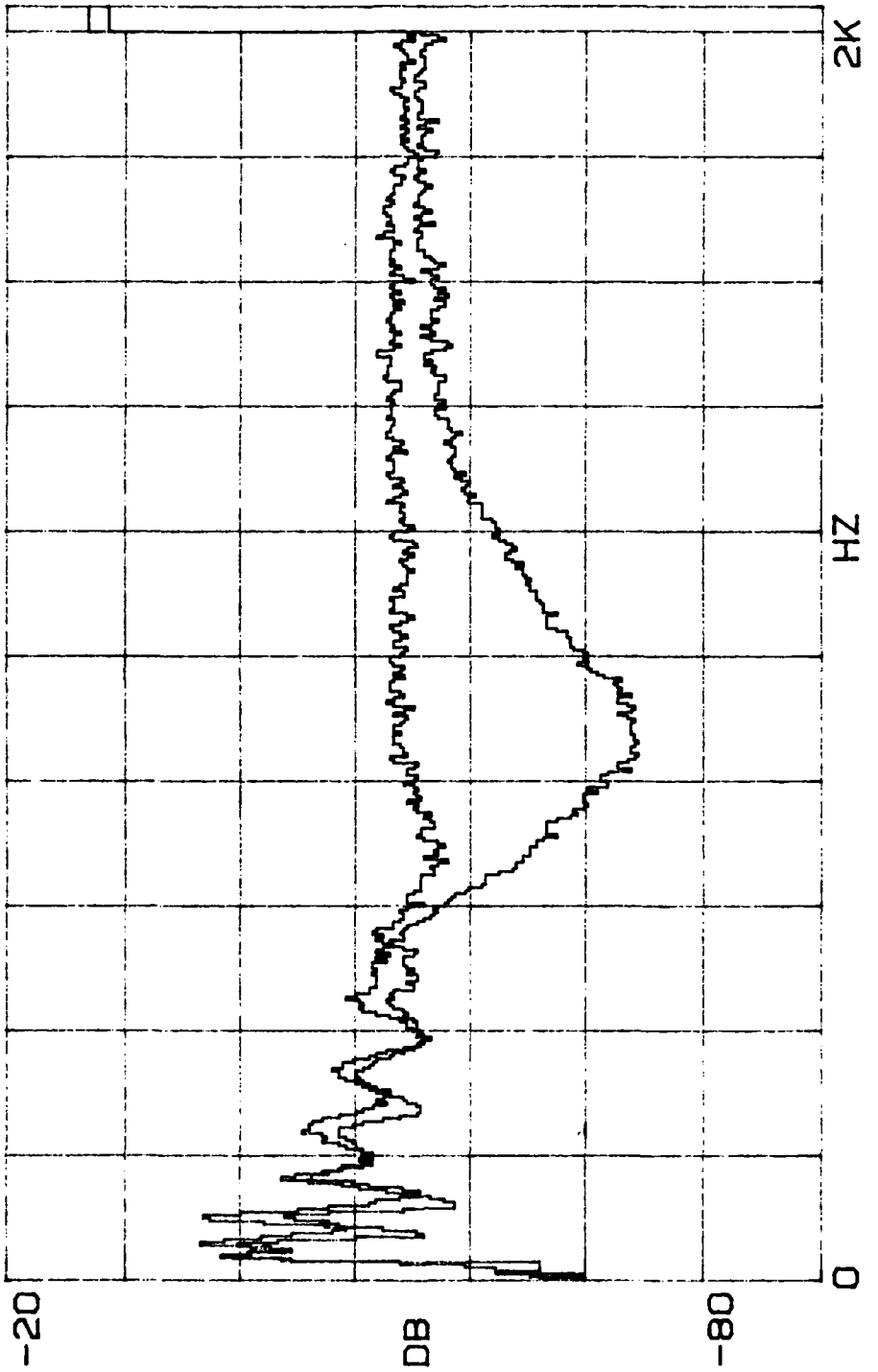

FIGURE C9

$\beta = 0.51$, $R' = 0.47$, $l = 38$ cm

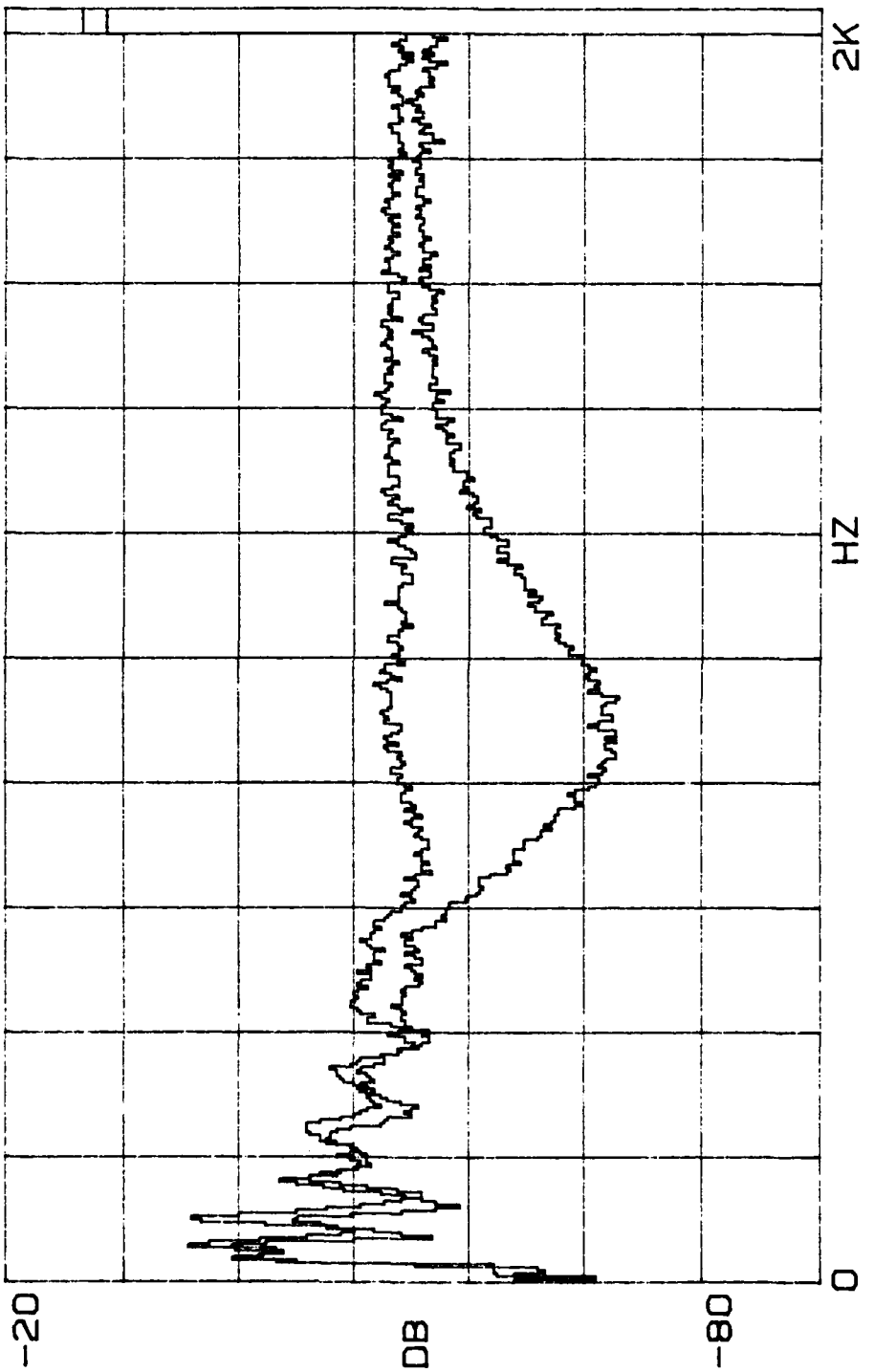

FIGURE C10

$\beta = 0.51$, $R' = 0.47$, $l = 40$ cm

APPENDIX D

ATTENUATION DATA

$\beta = 0.69$, $R' = 0.47$

m = 1.00 gm f_o = 1000 Hz β = 0.69 R'= 0.47

ATTENUATION DATA:

ℓ(cm)	12.0	14.6	17.4	20.0	22.7	25.2	28.0	30.6
f(Hz)	ATTENUATION (dB)							
700	2.4	2.7	3.1	4.7	3.5	3.6	5.1	4.8
750	4.4	2.8	6.0	5.1	4.4	6.6	5.2	6.4
800	4.0	5.0	6.4	5.6	6.2	7.0	8.2	8.1
850	7.3	6.5	7.4	7.4	8.5	10.2	10.3	10.4
900	5.7	7.5	7.5	9.8	9.0	13.0	12.2	12.0
950	7.5	8.7	9.0	10.9	11.9	13.3	15.4	15.9
1000	8.1	11.1	12.7	12.0	11.6	16.3	15.5	16.8
1050	7.8	10.8	11.9	12.1	14.5	16.3	17.7	18.4
1100	8.0	10.5	12.4	13.2	13.5	16.5	18.7	19.5
1150	6.8	9.7	10.4	12.5	16.1	15.0	18.5	20.9
1200	6.1	9.5	9.1	12.4	13.1	16.6	17.1	19.5
1250	6.7	8.0	9.4	10.6	12 1	14.9	16.9	19.3
1300	5.4	8.6	8.6	9.3	12.1	14.4	17.4	16.3
1350	4.0	6.9	6.5	9.1	9.8	12.5	15.9	15.2
1400	3.8	6.3	6.3	7.7	8.3	12.0	12.8	15.3
1450	4.2	4.5	4.7	8.0	8.4	10.6	11.2	12.9
1500	4.5	3.4	3.8	6.5	7.1	8.9	10.9	12.3
1550	3.2	3.8	6.1	6.0	5.6	7.4	9.1	11.7
1600	3.1	3.3	3.7	4.8	6.5	6.4	8.5	10.9
1650	2.5	2.2	3.2	3.8	5.8	6.3	6.0	10.2
1700	1.2	2.8	2.1	3.4	5.6	5.3	6.5	7.6

TABLE D2

m = 1.00 gm f_o = 1000 Hz β = 0.69 R'= 0.47

RESULTS:

f(Hz)	SLOPE (dB/cm)	ATTEN (dB)	f/f_o
700	0.131	3.7	0.70
750	0.121	3.3	0.75
800	0.211	5.6	0.80
850	0.225	5.8	0.85
900	0.372	9.4	0.90
950	0.475	11.7	0.95
1000	0.417	10.0	1.00
1050	0.556	13.0	1.05
1100	0.600	13.7	1.10
1150	0.717	16.0	1.15
1200	0.693	15.2	1.20
1250	0.674	14.5	1.25
1300	0.629	13.2	1.30
1350	0.636	13.1	1.35
1400	0.586	11.9	1.40
1450	0.503	10.0	1.45
1500	0.483	9.4	1.50
1550	0.401	7.7	1.55
1600	0.405	7.7	1.60
1650	0.377	7.0	1.65
1700	0.336	6.2	1.70

AD-A159 039 THE ATTENUATION OF FLEXURAL WAVES IN MASS LOADED BEAMS 2/2
(U) MASSACHUSETTS INST OF TECH CAMBRIDGE DEPT OF OCEAN
ENGINEERING T L SMITH MAY 85 N66314-78-A-0073
UNCLASSIFIED F/G 20/11 NL

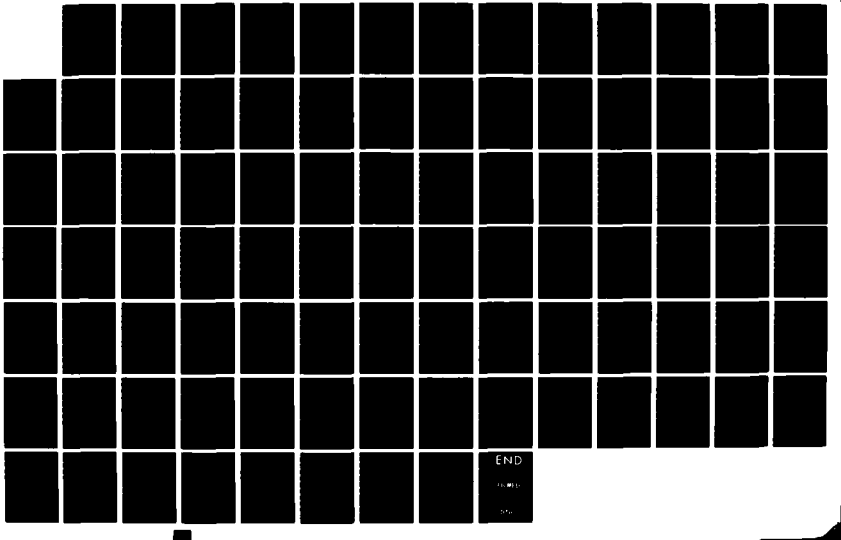

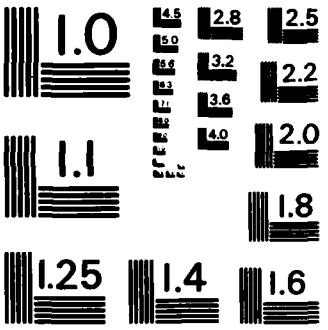

MICROCOPY RESOLUTION TEST CHART
NATIONAL BUREAU OF STANDARDS - 1963 - A

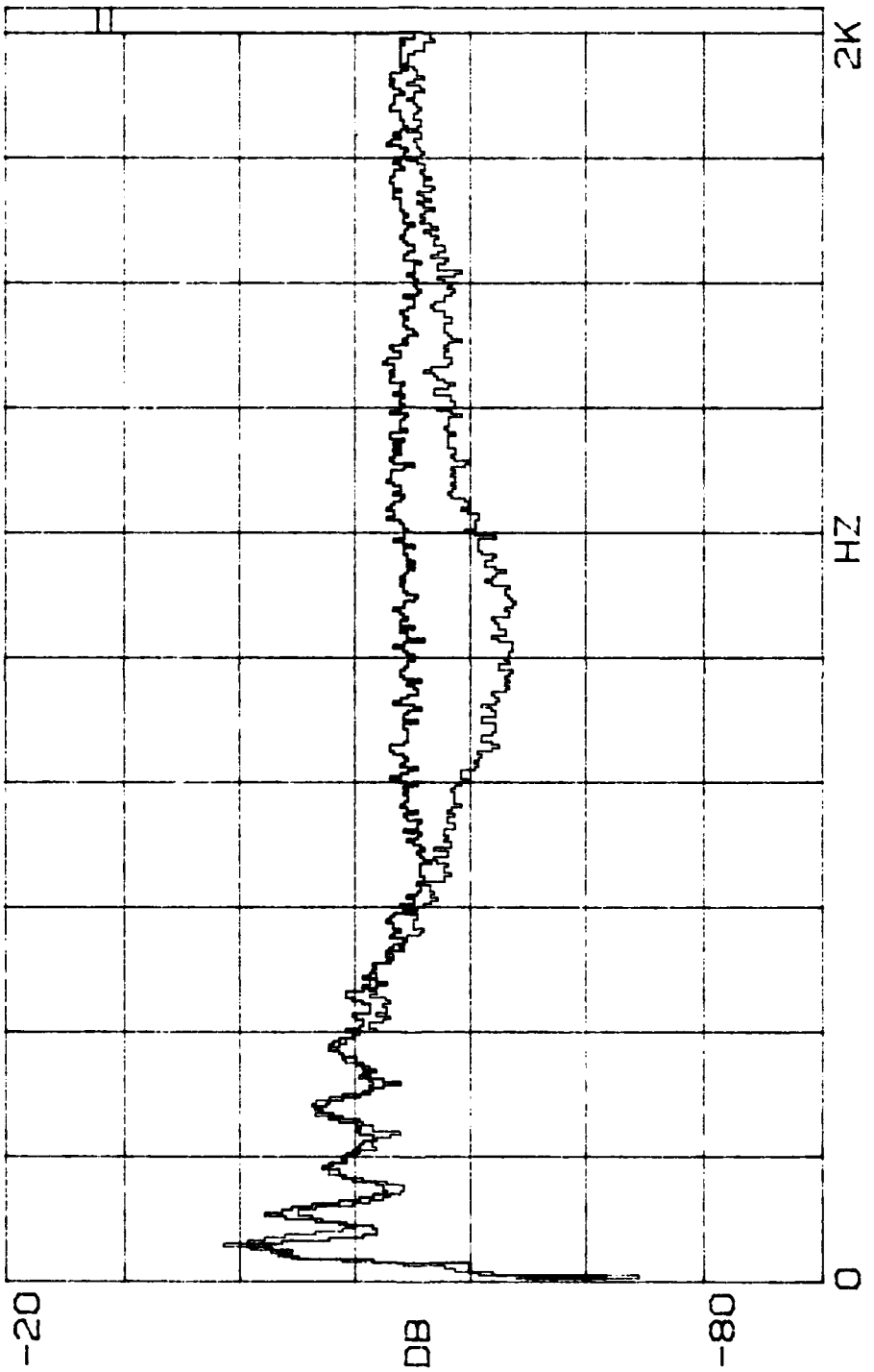

FIGURE D1

β = 0.69, R' = 0.47, l = 12.0 cm

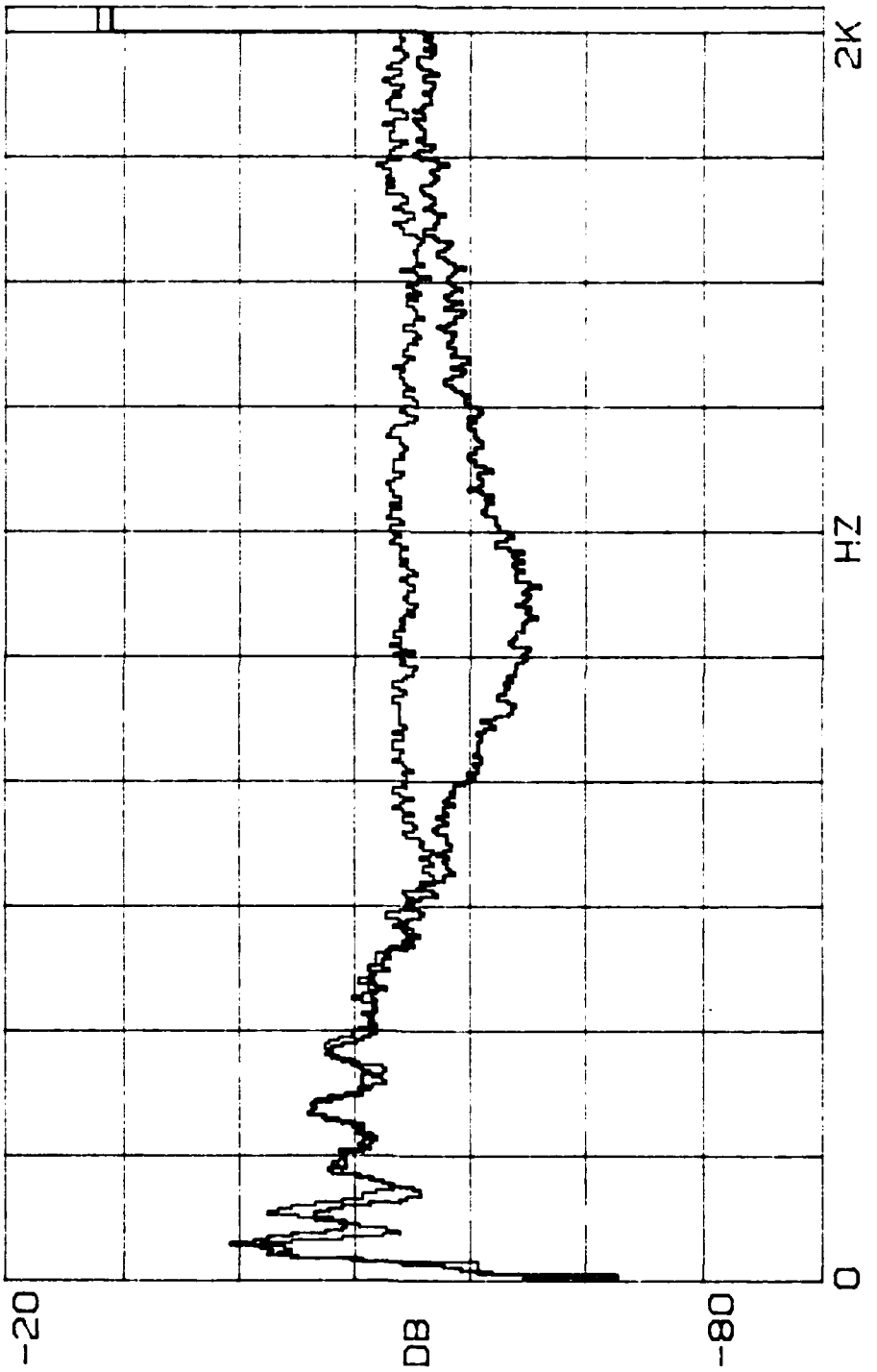

FIGURE D2

β = 0.69, R' = 0.47, l = 14.6 cm

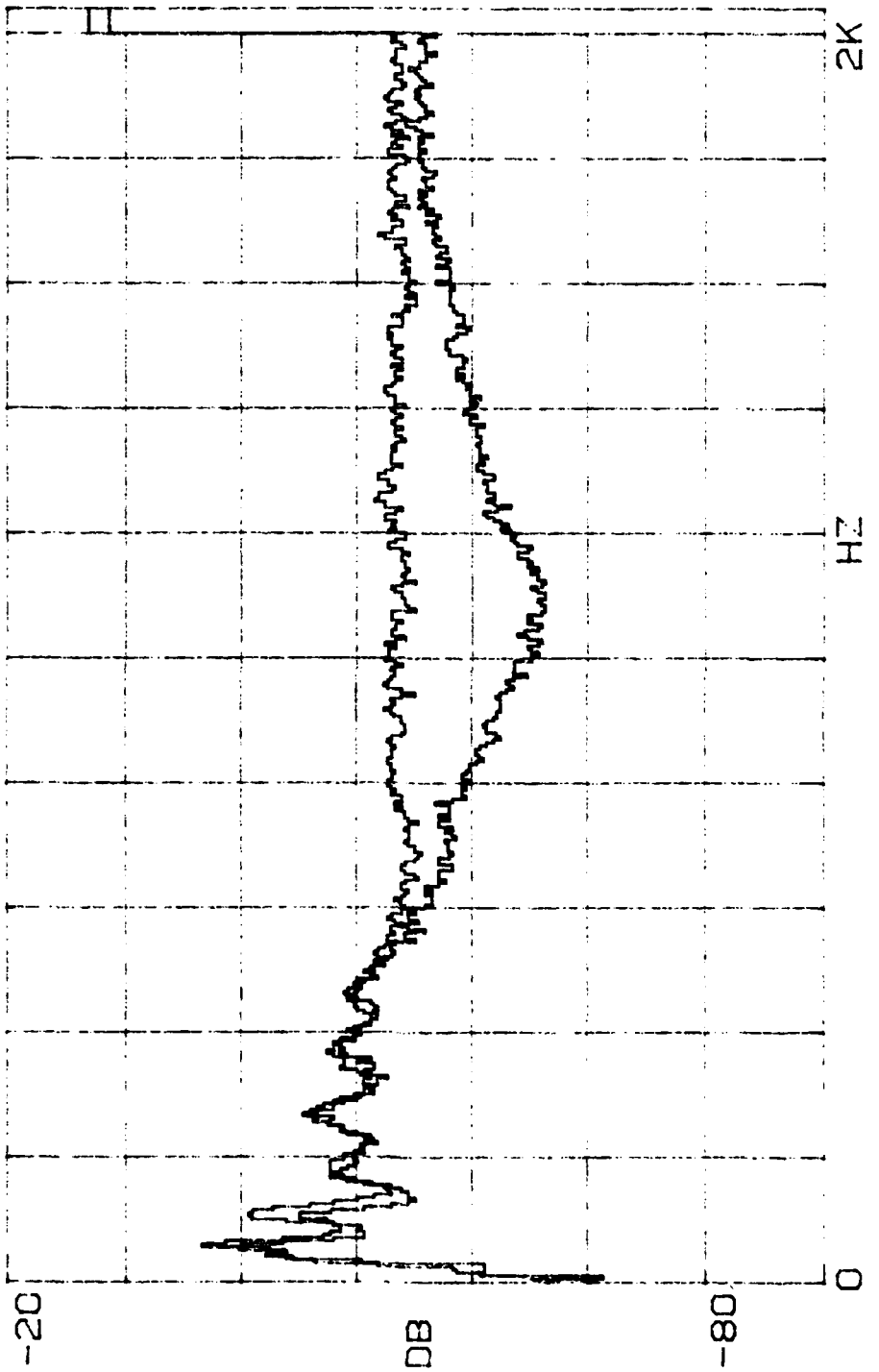

FIGURE D3

β = 0.69, R' = 0.47, l = 17.4 cm

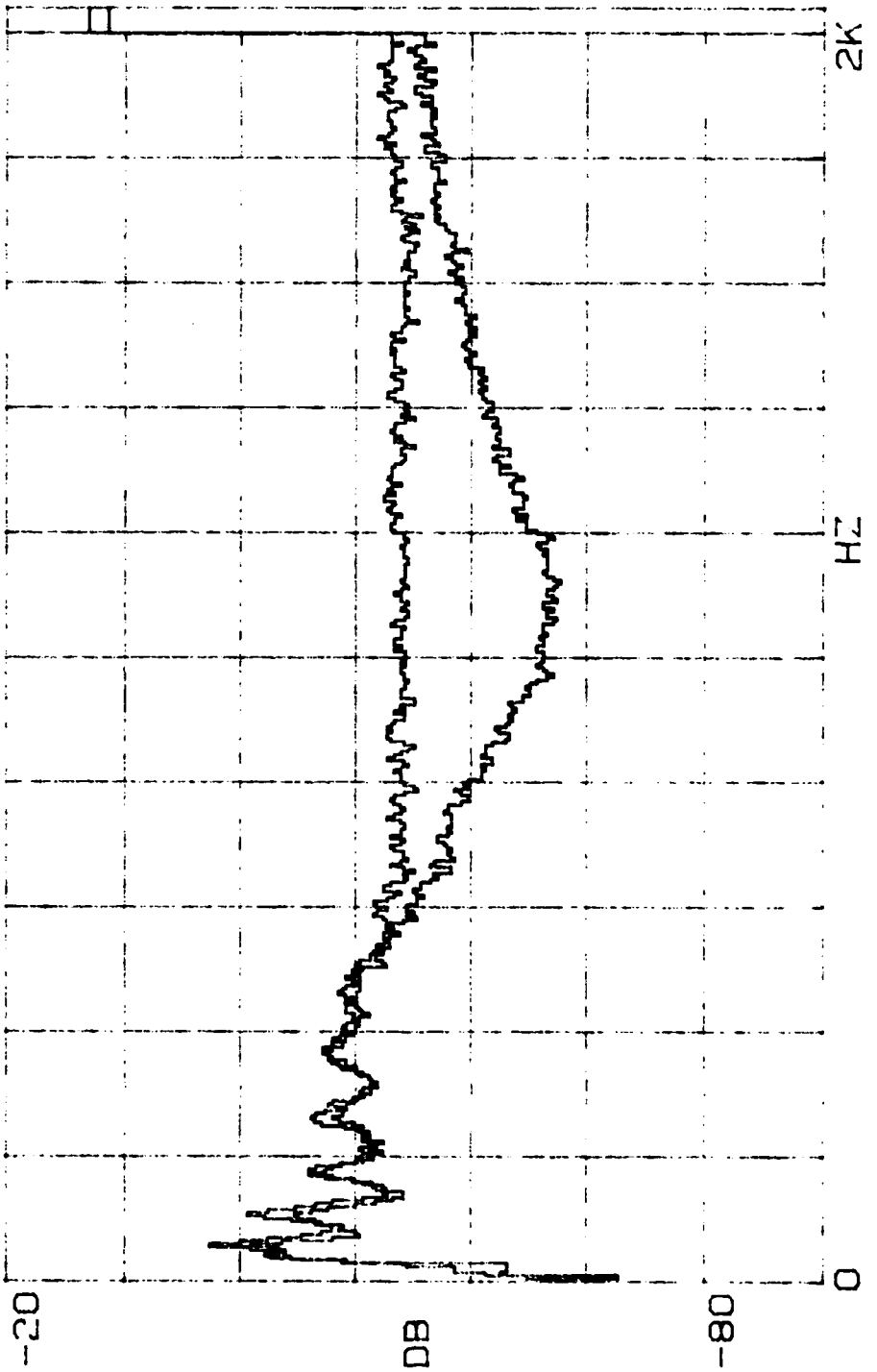

FIGURE D4

δ = 0.69, R' = 0.47, l = 20.0 cm

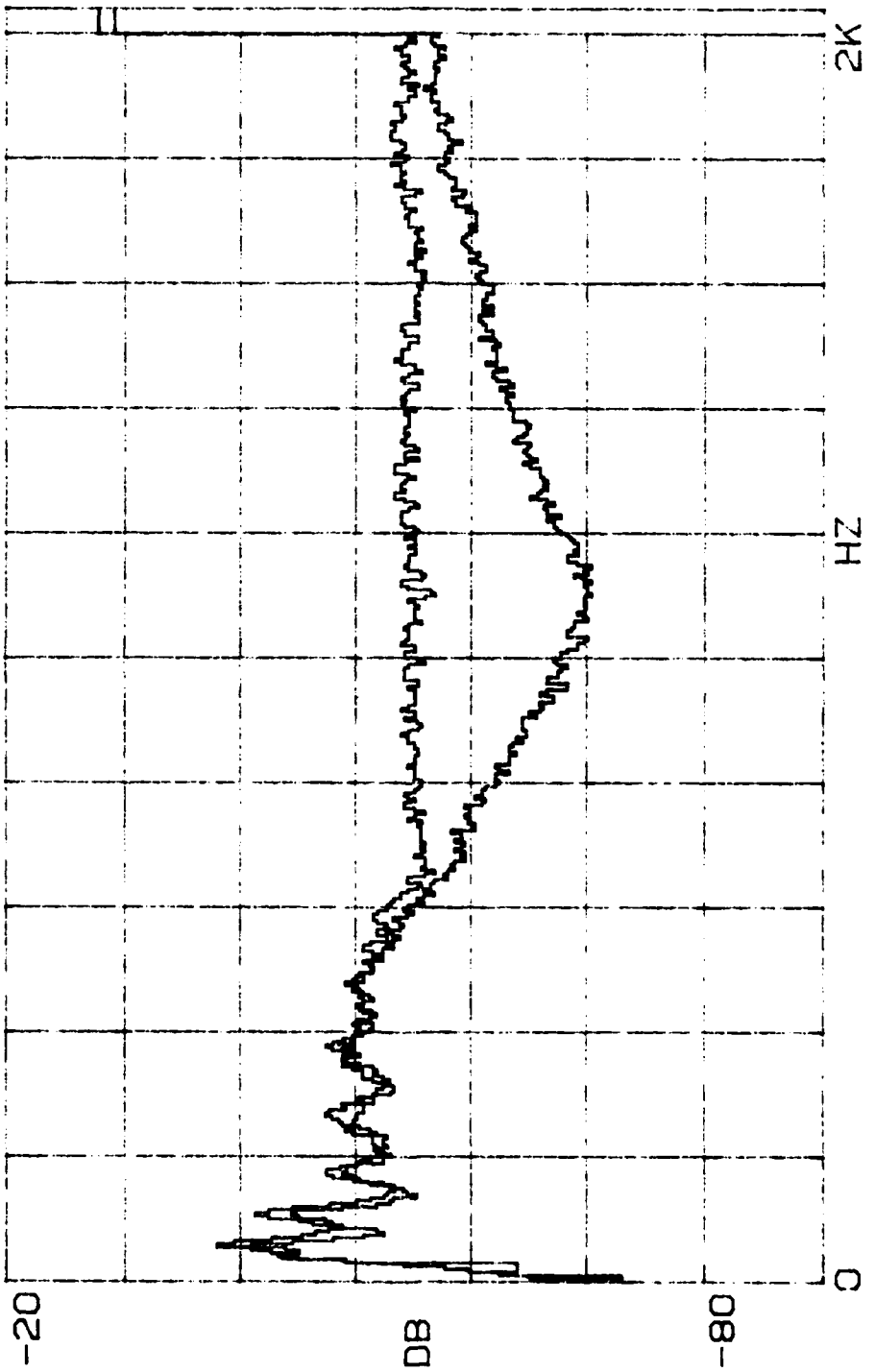

FIGURE D5

β = 0.69, R' = 0.47, l = 22.7 cm

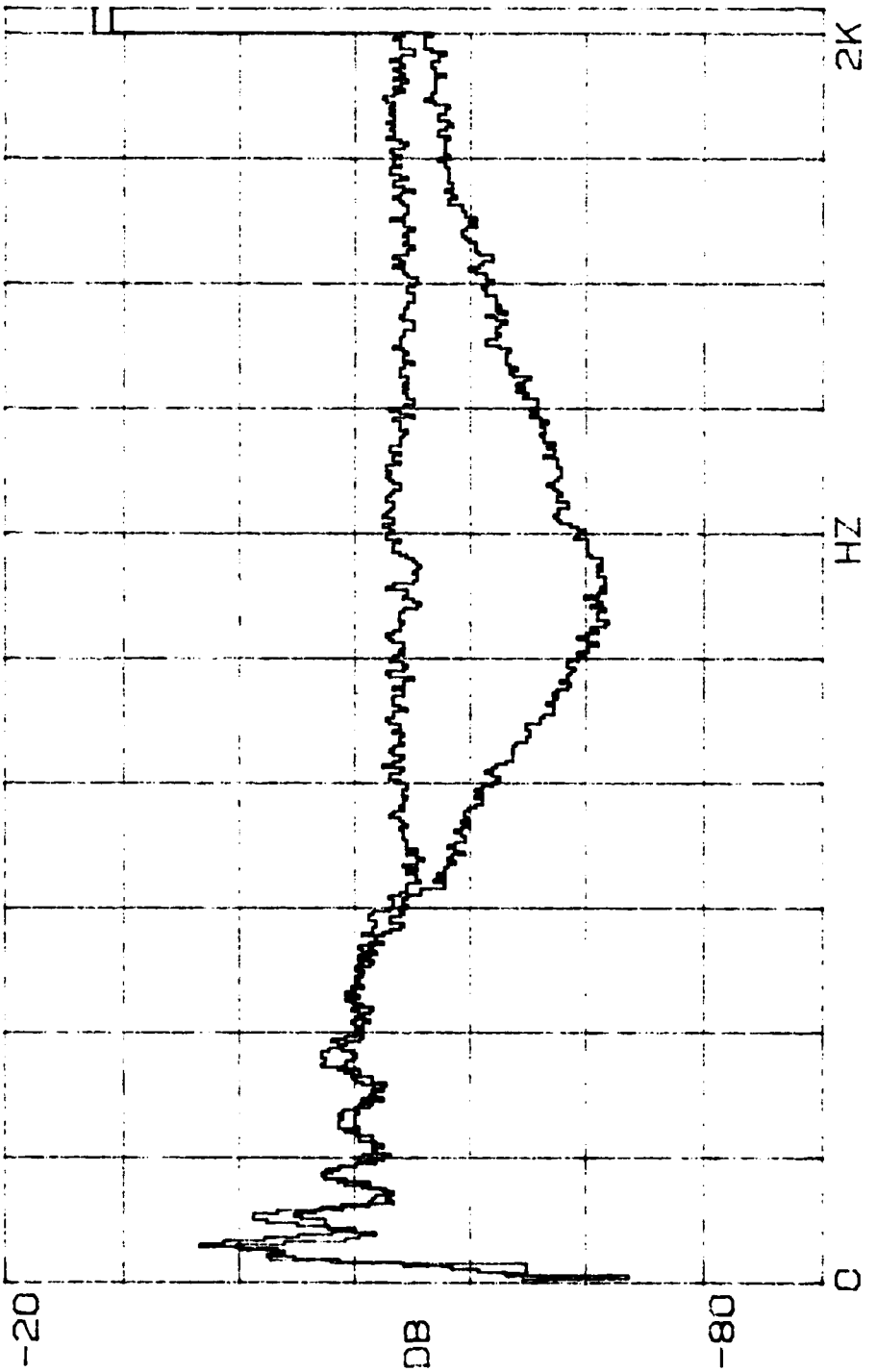

FIGURE D6

β = 0.69, R' = 0.47, l = 25.2 cm

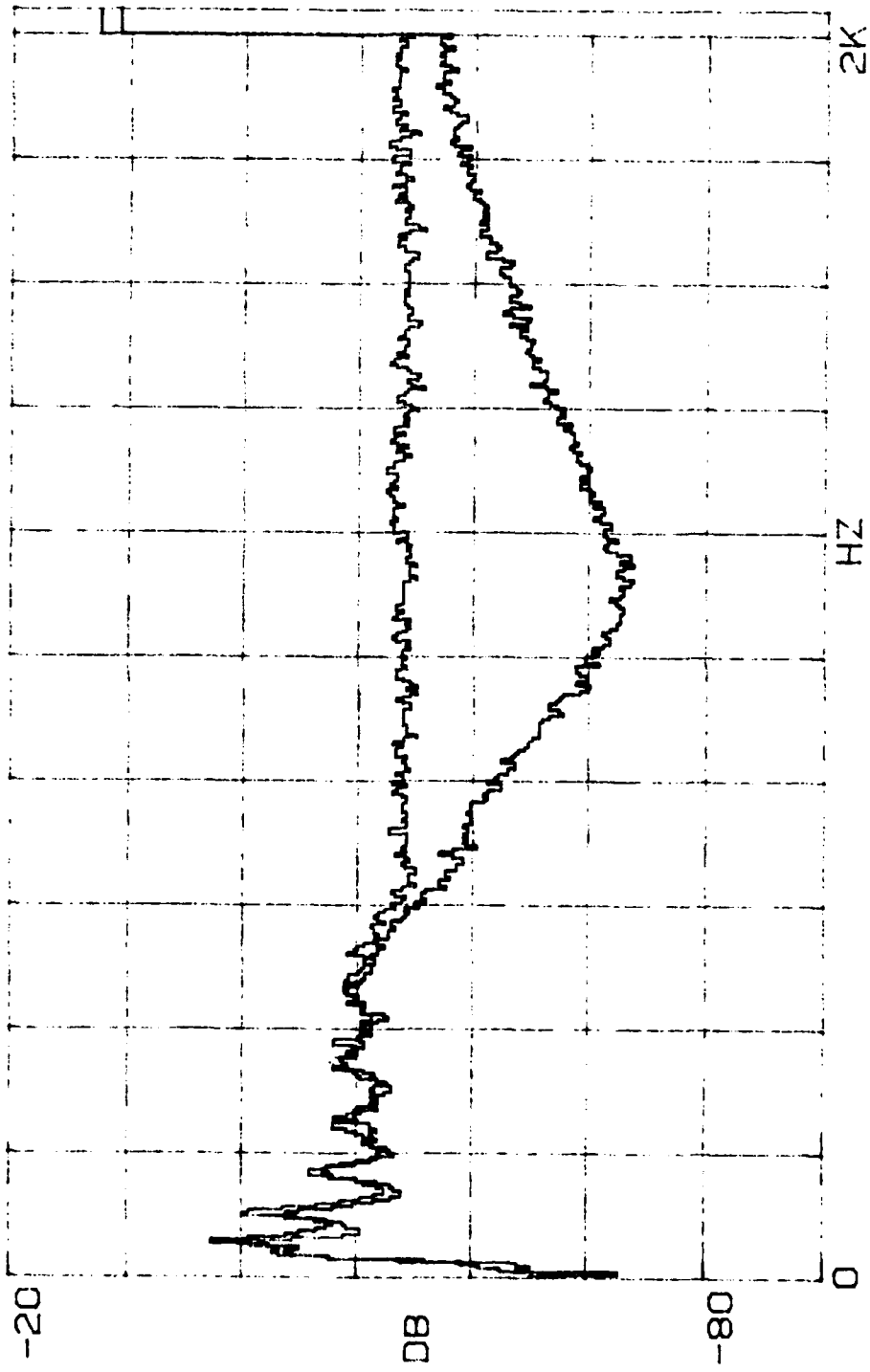

FIGURE D7

β = 0.69, R' = 0.47, l = 28.0 cm

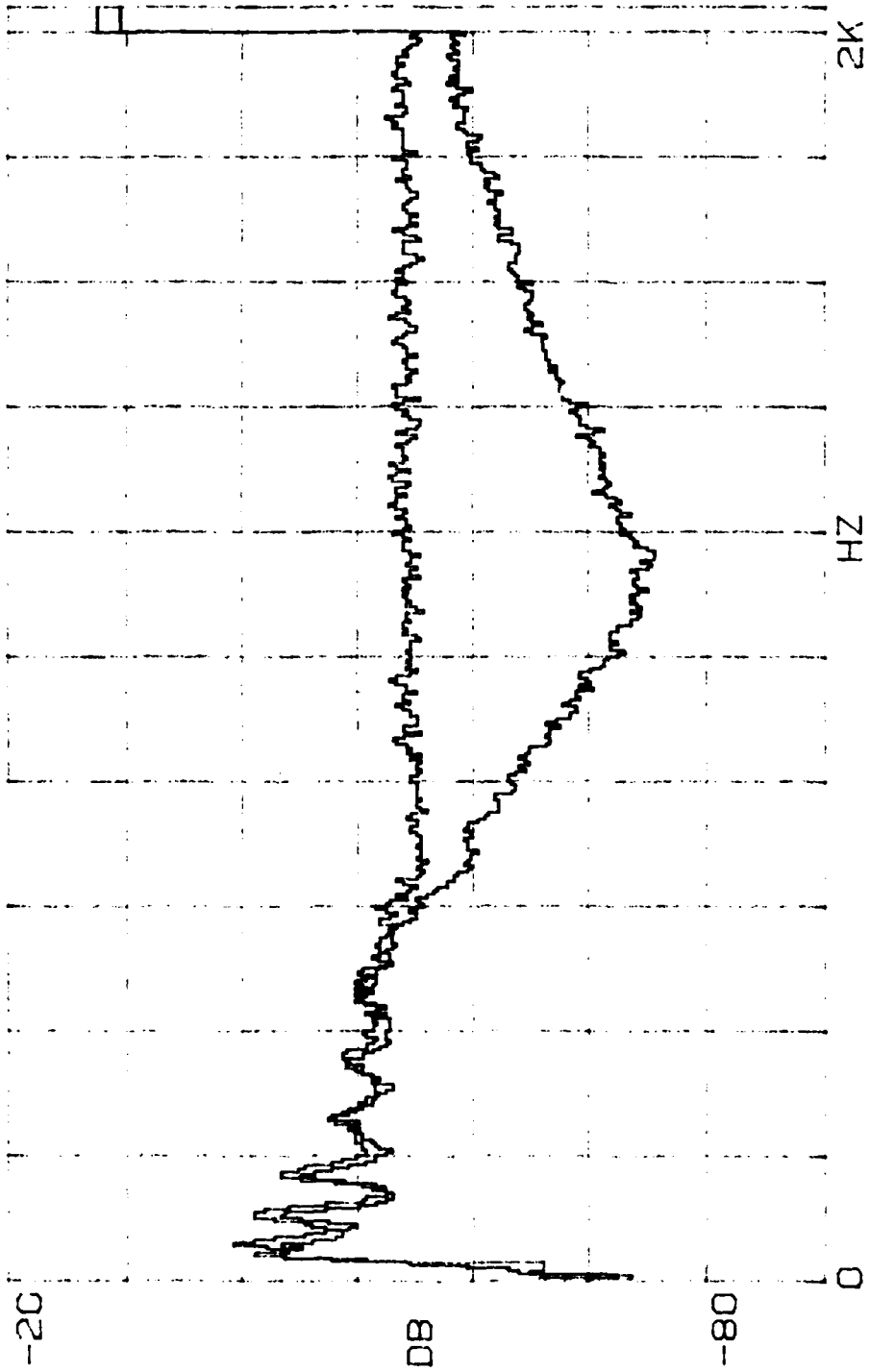

FIGURE D8

β = 0.69, R' = 0.47, l = 30.6 cm

APPENDIX E

ATTENUATION DATA

$\beta = 0.87$, $R' = 0.46$

TABLE 21

m = 0.95 gm f_o = 700 Hz ε = 0.87 R'= 0.46

ATTENUATION DATA:

ℓ(cm)	16	18	20	22	24	26	28	30	32	34
f(Hz)	ATTENUATION (dB)									
500	1.2	2.1	3.0	2.7	3.5	5.2	3.9	4.5	4.8	5.0
550	3.7	2.3	3.5	4.7	4.0	5.1	5.0	6.5	6.2	7.0
600	6.1	5.9	5.4	6.3	6.3	7.4	7.7	8.7	7.9	8.0
650	10.9	11.4	9.2	9.7	11.7	11.6	13.0	14.8	14.6	14.5
700	11.3	12.7	10.1	9.8	11.3	12.1	12.2	13.3	13.6	13.8
750	11.5	14.5	16.6	14.7	17.8	17.8	18.5	21.1	21.7	21.5
800	10.6	11.9	14.8	13.3	15.4	16.6	17.5	22.4	21.0	21.2
850	8.9	10.4	12.1	13.7	13.3	15.6	17.4	20.1	19.3	18.4
900	7.3	8.7	10.5	10.6	13.4	12.3	15.1	18.0	17.9	18.4
950	6.5	7.6	8.7	8.7	9.7	11.4	14.0	13.8	16.1	15.9
1000	5.6	5.7	4.9	6.8	6.8	9.4	9.7	10.8	12.6	12.9
1050	3.4	3.4	5.8	6.2	6.1	7.4	8.7	8.5	10.1	11.1
1100	3.8	3.2	5.3	5.0	7.6	7.7	7.2	7.9	9.5	10.2
1150	2.3	2.6	3.8	4.1	3.8	4.3	4.7	5.8	5.9	7.4
1200	2.0	4.0	3.0	3.6	3.6	5.1	5.2	4.9	5.0	5.7
1250	2.9	2.0	1.7	2.4	3.9	3.6	3.9	3.8	5.5	5.1
1300	0.6	3.5	2.5	3.6	3.4	3.8	4.0	3.4	4.8	4.2
1350	1.8	2.1	2.0	1.6	2.5	3.6	2.7	2.3	3.0	4.3
1400	1.7	3.1	3.3	1.6	2.4	2.9	3.3	2.2	3.9	4.9

TABLE E2

m = 0.95 gm f_o = 700 Hz β = 0.87 R' = 0.46

RESULTS:

f(Hz)	SLOPE (dB/cm)	ATTEN (dB)	f/f_o
500	0.124	4.2	0.71
550	0.206	6.6	0.79
600	0.230	7.1	0.86
650	0.278	8.3	0.93
700	0.323	9.2	1.00
750	0.528	14.6	1.07
800	0.639	17.1	1.14
850	0.610	15.9	1.21
900	0.649	16.4	1.29
950	0.567 (0.665)*	14.0 (16.4)*	1.36
1000	0.469 (0.610)	11.2 (14.6)	1.43
1050	0.420 (0.350)	9.8 (8.2)	1.50
1100	0.298 (0.325)	6.8 (7.4)	1.57
1150	0.255 (0.100)	5.7 (2.2)	1.64
1200	0.170 (0.295)	3.7 (6.4)	1.71
1250	0.179 (0.280)	3.8 (6.0)	1.79
1300	0.144 (0.160)	3.0 (3.3)	1.86
1350	0.127 (0.170)	2.6 (3.5)	1.93
1400	0.168 (0.065)	3.4 (1.3)	2.00

* slope through first five data points

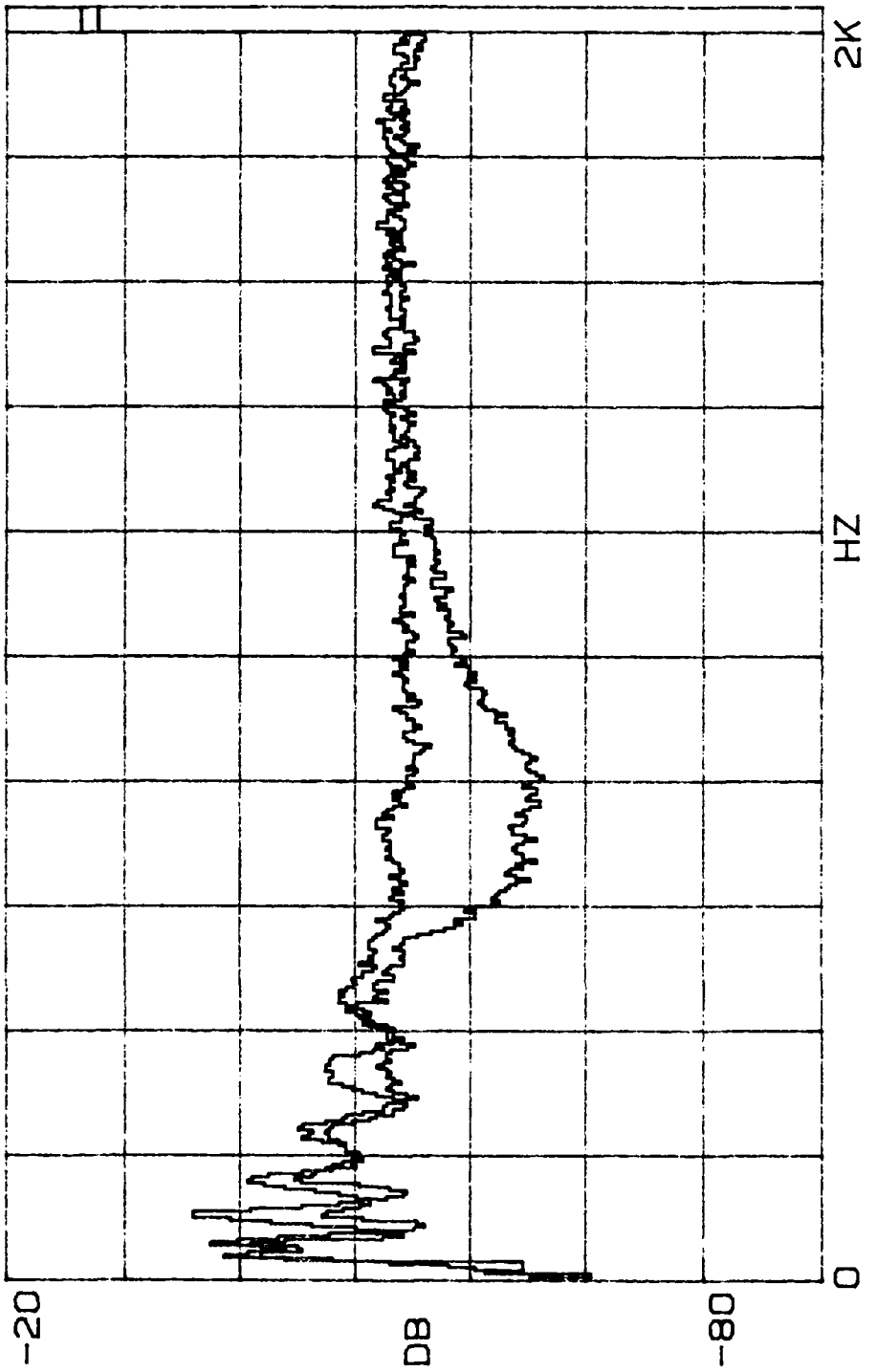

FIGURE E1

β = 0.87, R' = 0.46, l = 16 cm

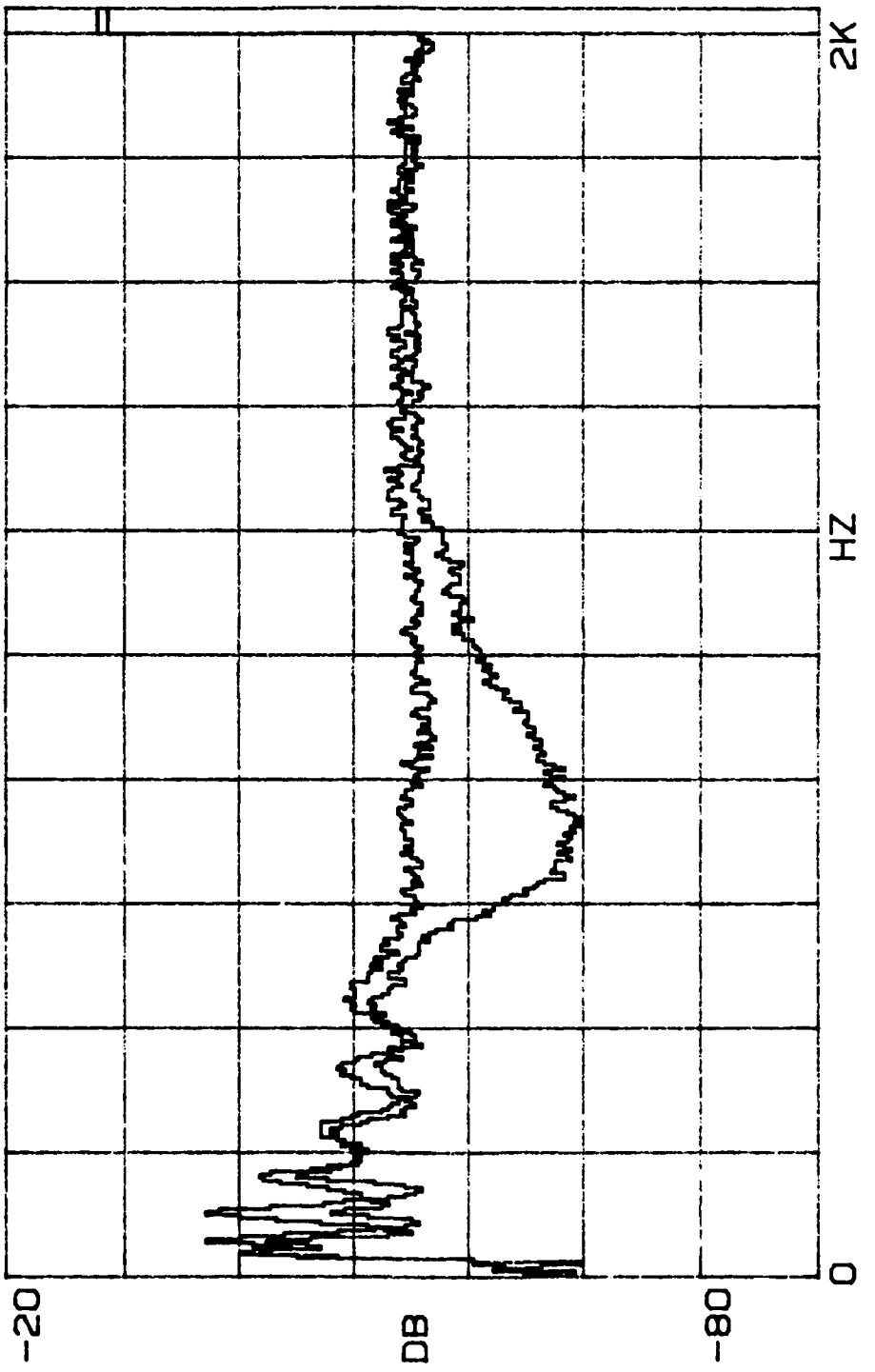

FIGURE E2

β = 0.87, R' = 0.46, l = 18 cm

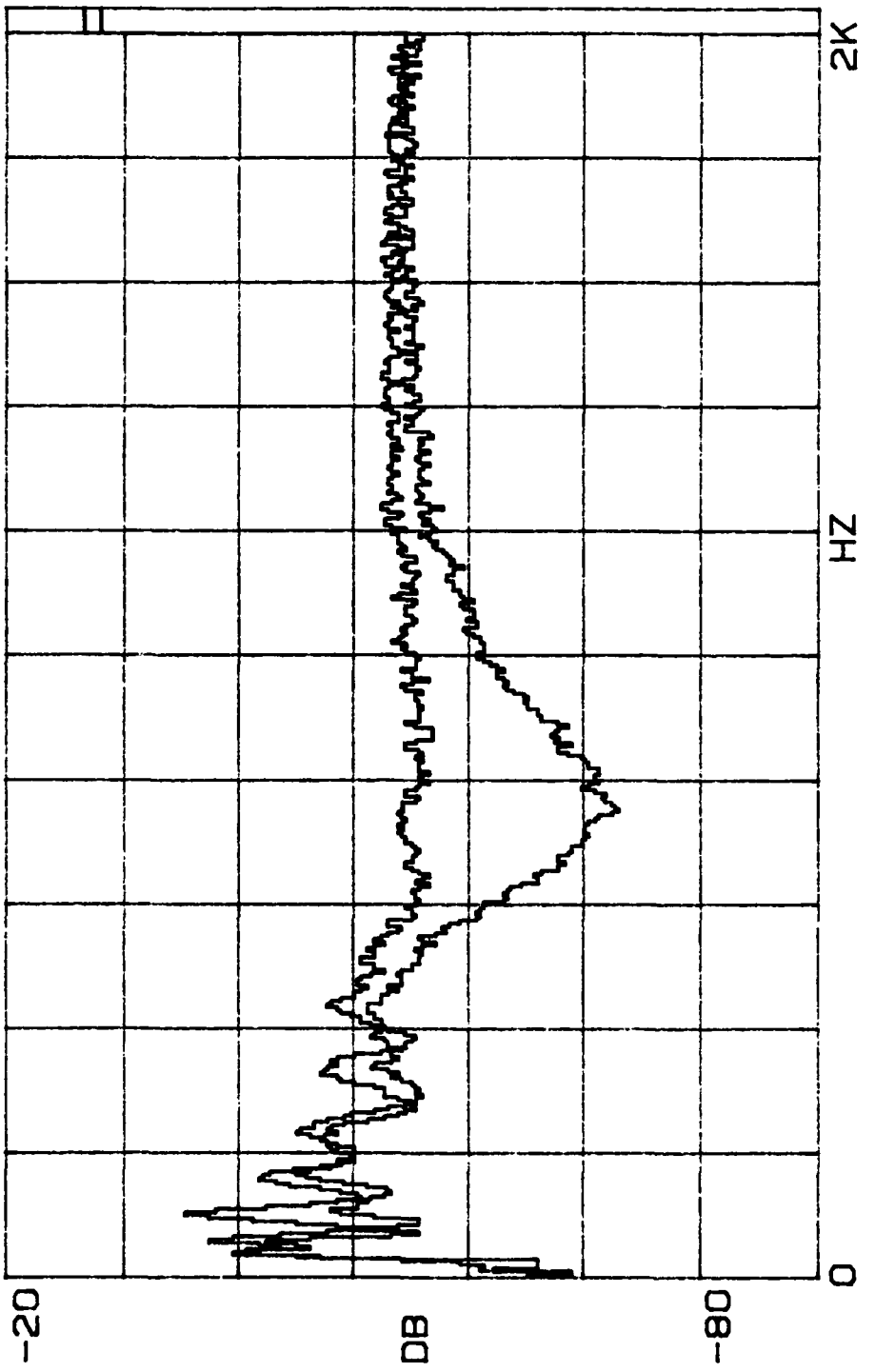

FIGURE E3

β = 0.87, R' = 0.46, l = 20 cm

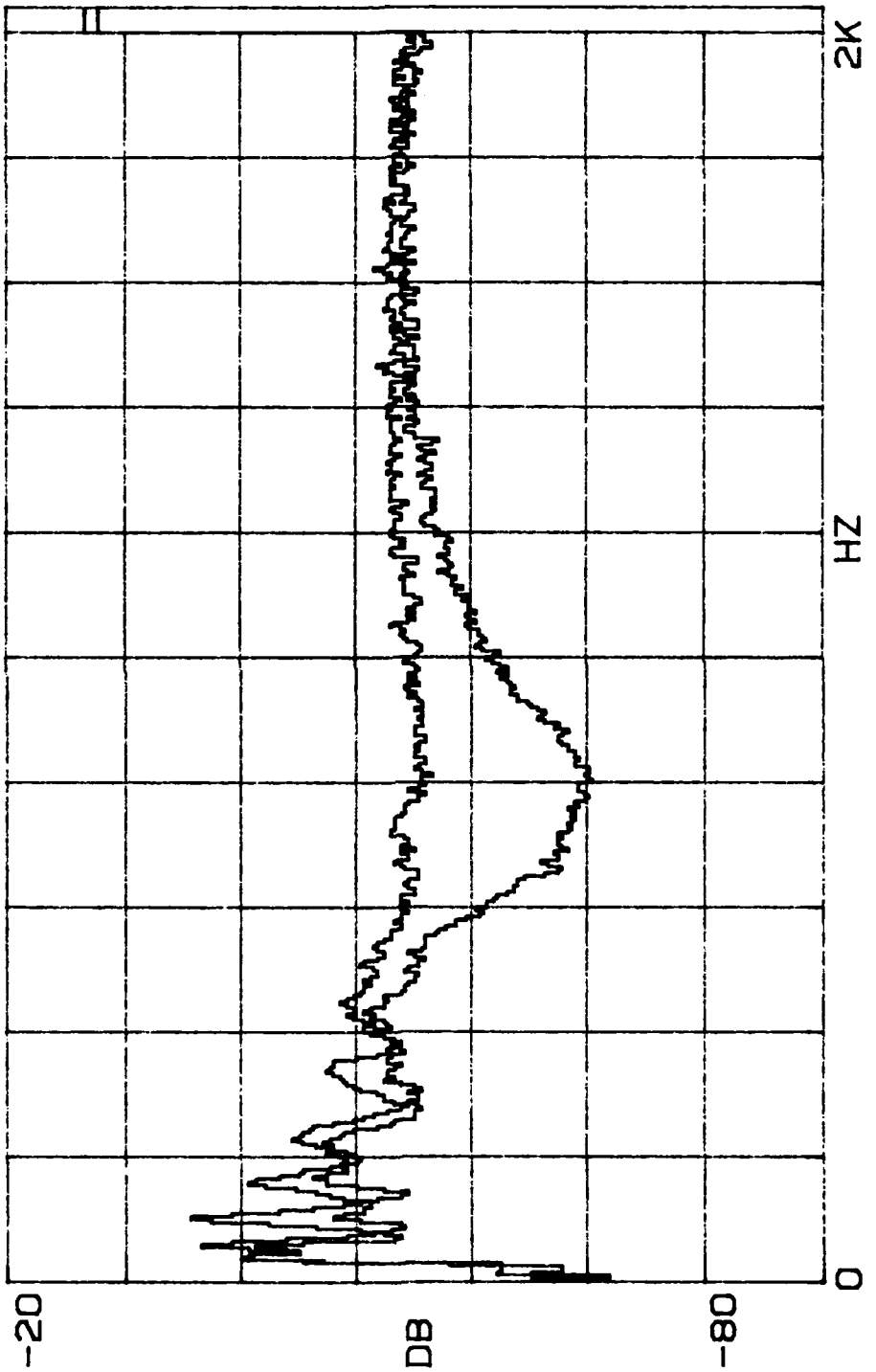

FIGURE E4

β = 0.87, R' = 0.46, l = 22 cm

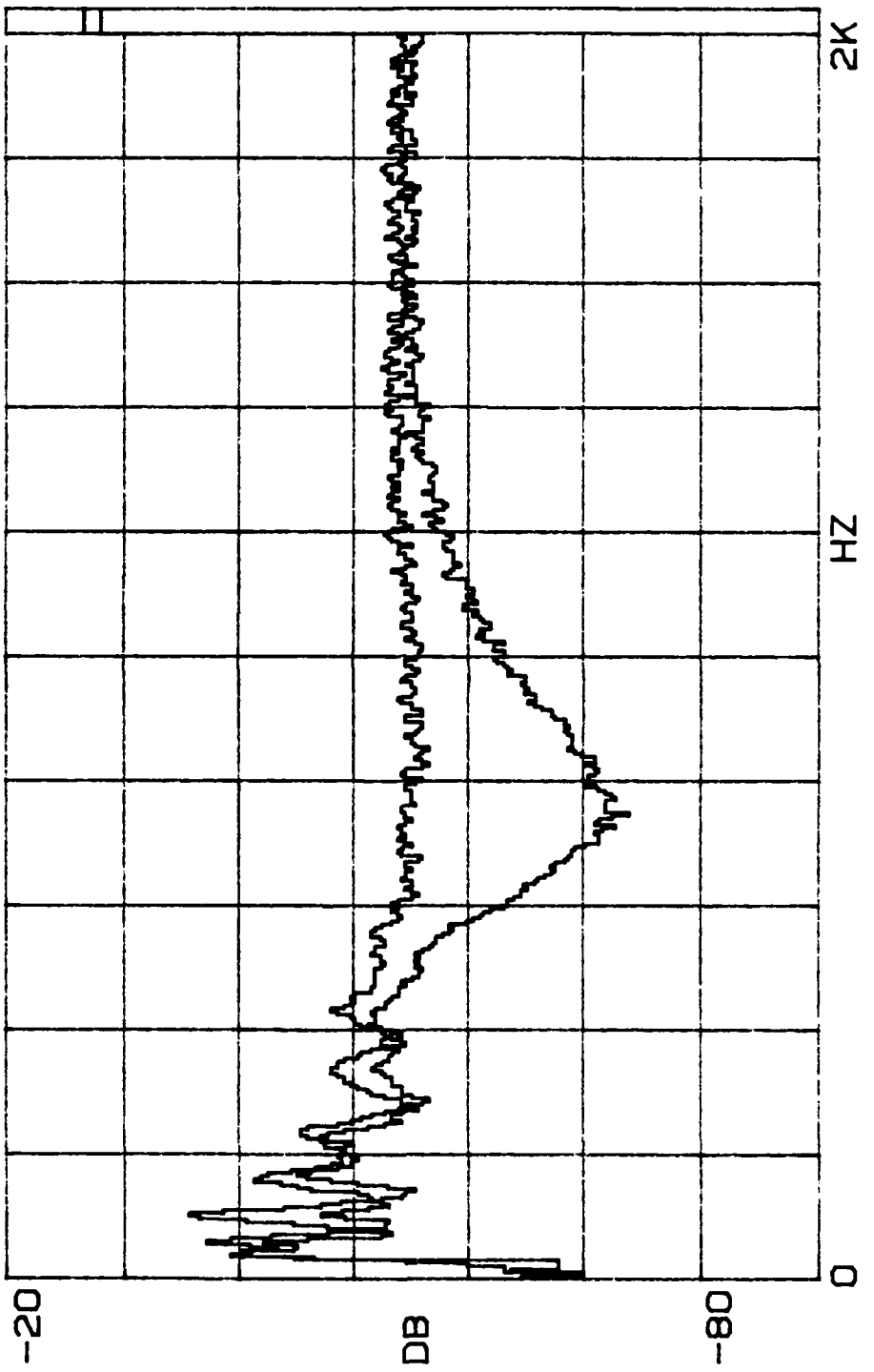

FIGURE E5

$\beta = 0.87$, $R' = 0.46$, $l = 24$ cm

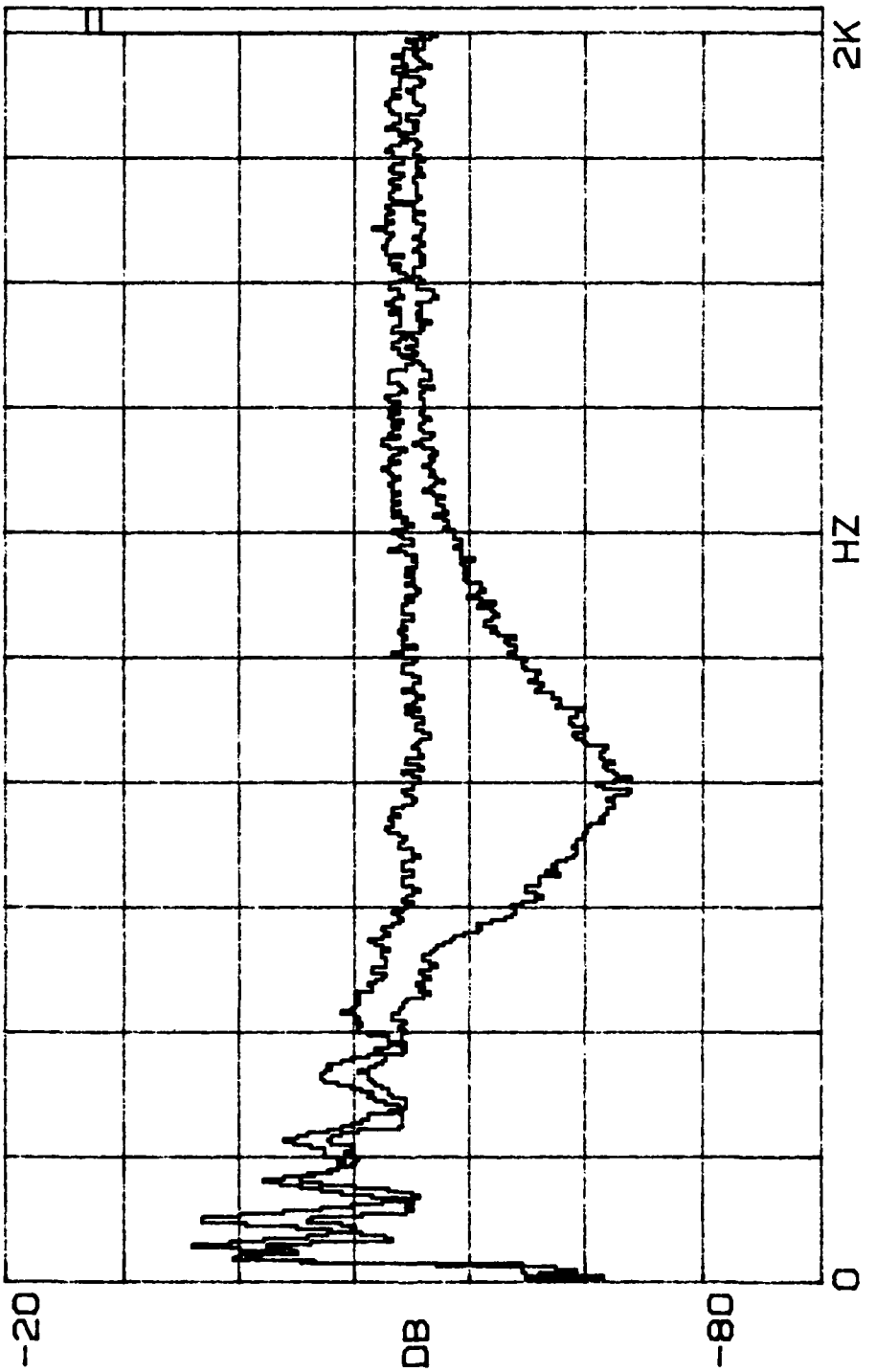

FIGURE E6

$\beta = 0.87$, $R' = 0.46$, $l = 26$ cm

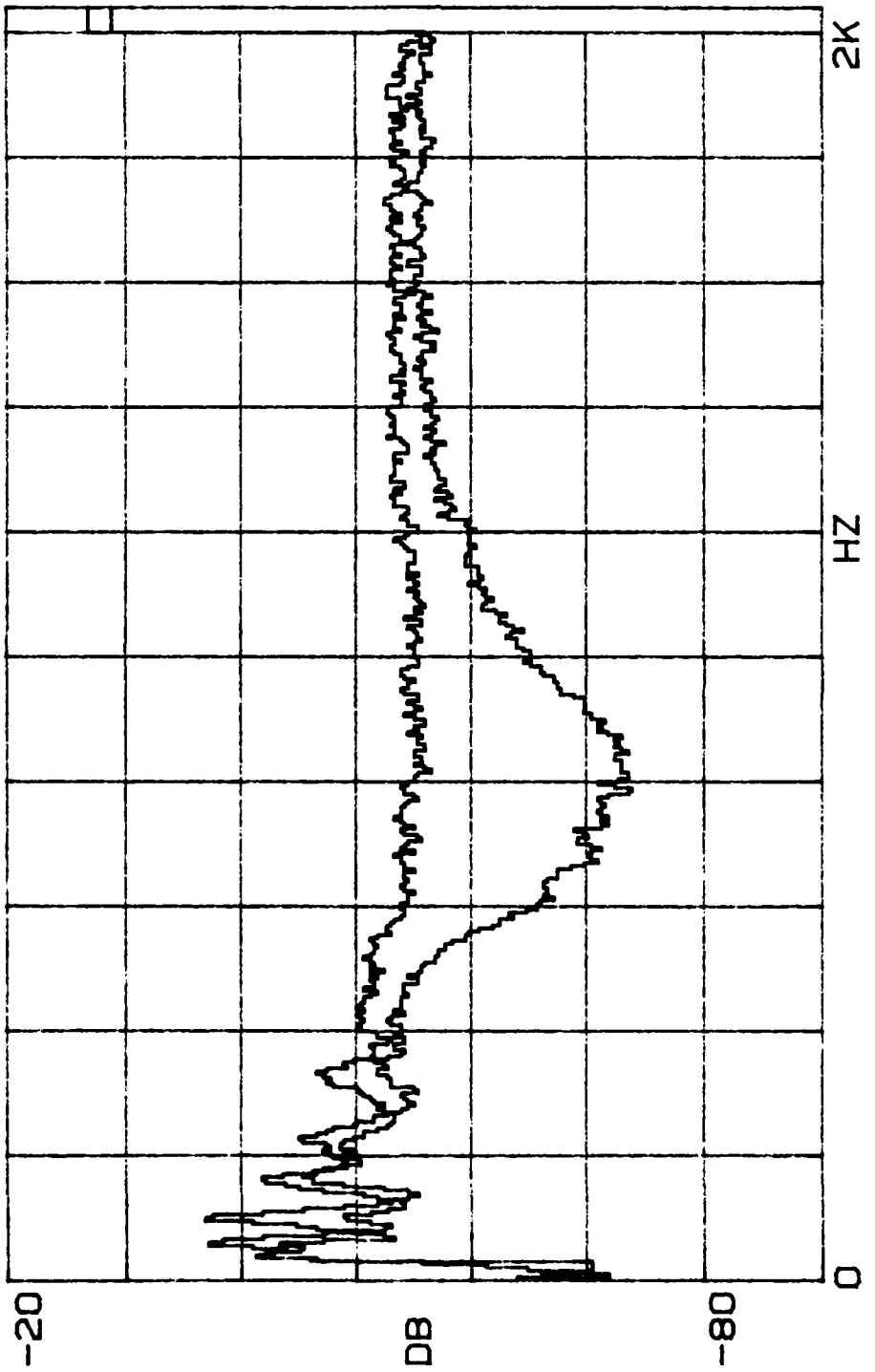

FIGURE E7

β = 0.87, R' = 0.46, l = 28 cm

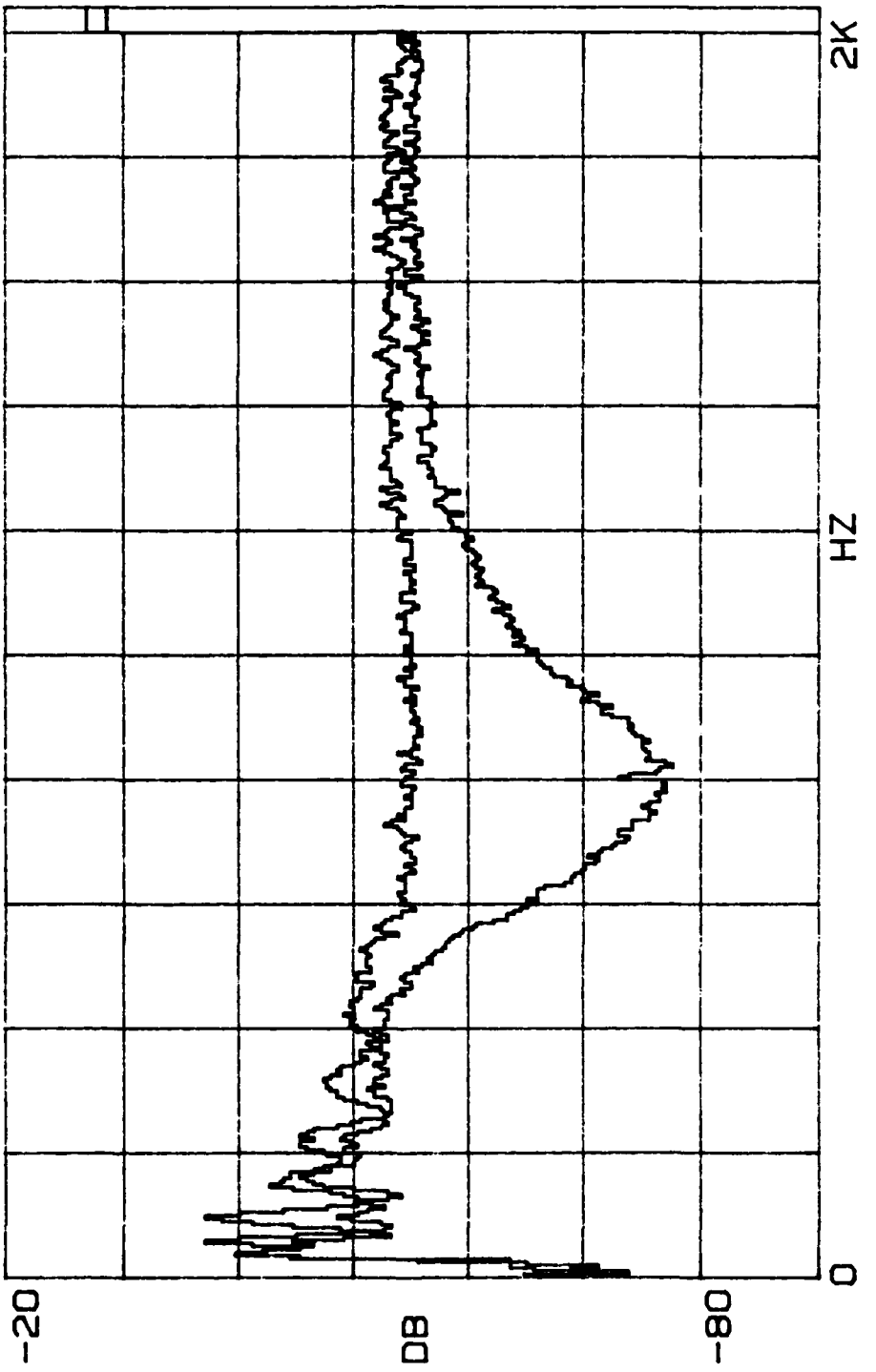

FIGURE E8

$\beta = 0.87$, $R' = 0.46$, $l = 30$ cm

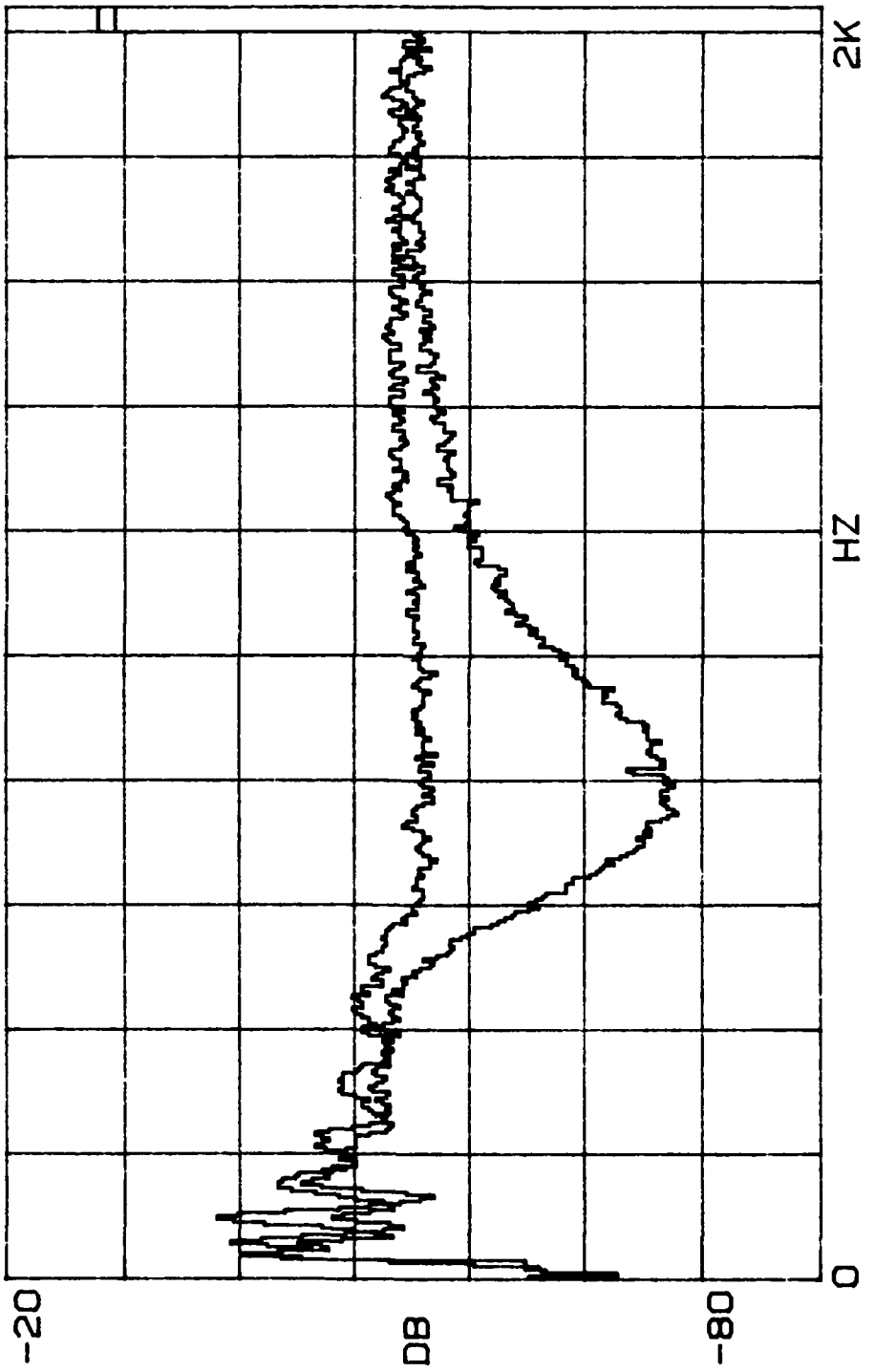

FIGURE E9

β = 0.87, R' = 0.46, l = 32 cm

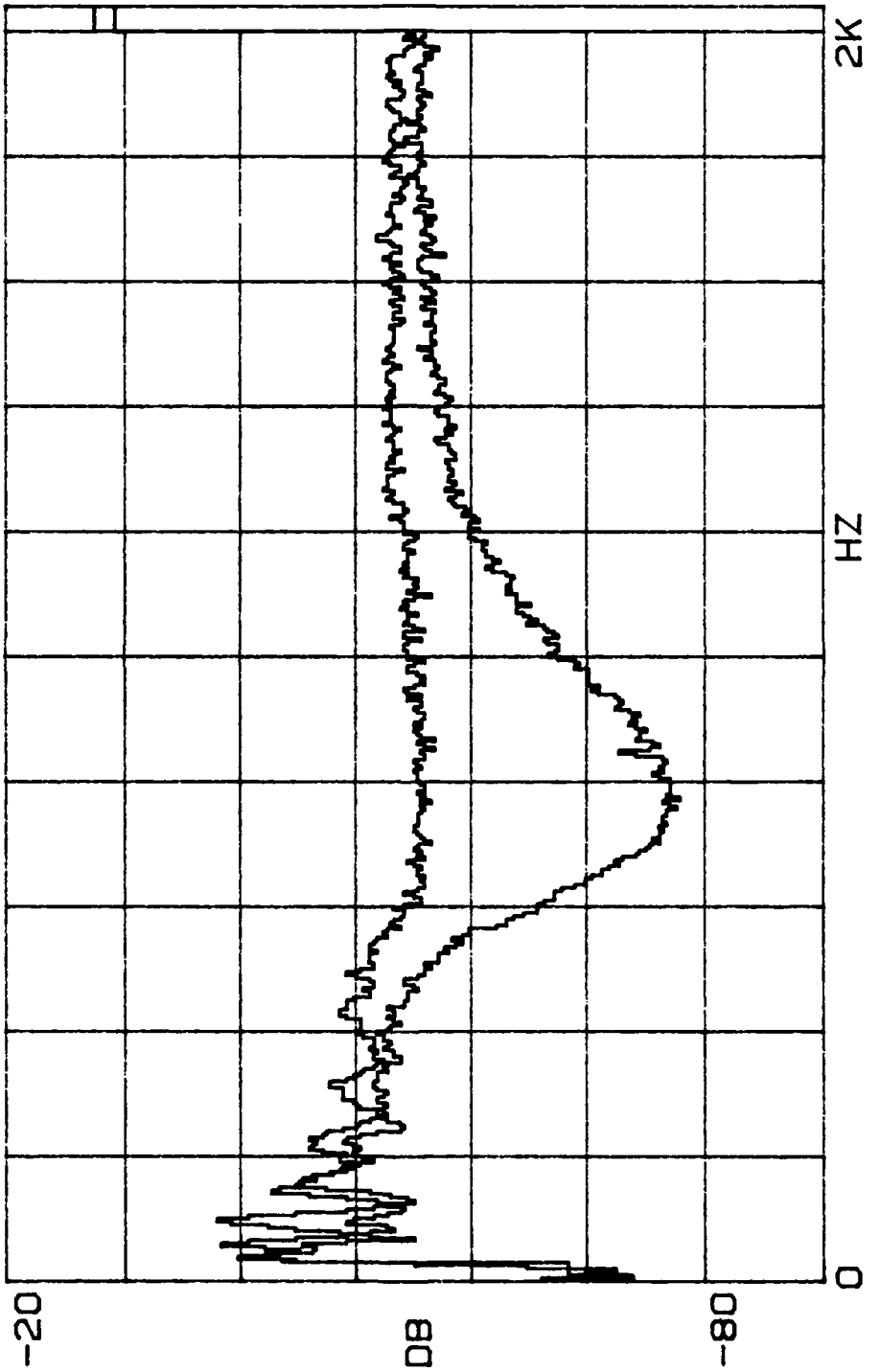

FIGURE E10

β = 0.87, R' = 0.46, l = 34 cm

APPENDIX F

ATTENUATION DATA

$\beta = 1.09$, $R' = 0.46$

TABLE F1

m = 1.19 gm f_o = 750 Hz ζ = 1.09 R'= 0.46

ATTENUATION DATA:

ℓ(cm)	12	14	16	18	20	22	24	26	28	30
f(Hz)	ATTENUATION (dB)									
500	2.4	1.9	3.0	4.1	4.1	4.8	4.8	3.9	4.0	5.3
550	5.4	2.4	5.7	6.2	5.6	7.0	7.8	7.1	6.0	9.8
600	8.5	7.1	6.6	7.5	8.1	10.4	9.5	12.0	11.2	13.7
650	12.5	11.3	11.0	11.2	11.9	13.3	15.8	15.8	14.5	18.7
700	14.0	14.5	15.7	14.6	15.0	14.5	17.4	20.8	20.0	22.0
750	13.7	15.4	15.8	16.6	18.1	16.8	18.0	20.7	21.8	22.7
800	13.5	14.2	14.0	15.1	16.4	19.0	19.3	21.9	24.9	21.8
850	10.9	12.8	13.2	15.2	16.3	17.9	18.4	22.0	24.6	22.0
900	8.5	11.8	11.7	12.3	14.0	14.9	17.6	19.3	23.1	22.1
950	6.8	9.1	9.2	10.2	11.6	11.6	13.2	17.3	18.6	19.4
1000	5.5	6.7	7.3	10.5	11.4	10.9	11.8	13.1	15.1	15.2
1050	3.5	5.3	6.4	6.4	7.4	8.7	9.1	11.4	11.7	12.8
1100	3.4	5.3	5.7	5.6	6.4	7.0	9.5	9.8	11.2	11.1
1150	2.9	4.3	5.9	5.0	6.4	6.1	7.8	8.3	8.1	9.9
1200	2.6	3.3	3.8	3.8	6.3	4.8	7.6	5.9	6.9	9.3
1250	1.9	2.1	2.4	3.3	4.8	5.1	6.5	6.2	7.1	8.6
1300	2.1	3.5	4.6	3.4	3.9	4.5	4.9	4.9	5.7	5.6
1350	1.2	2.5	3.4	1.3	4.1	4.2	4.4	3.8	4.8	4.8
1400	1.2	2.5	2.2	2.4	3.5	3.3	4.9	3.4	3.8	5.6

TABLE F2

m = 1.19 gm f_o = 750 Hz β = 1.09 R'= 0.46

RESULTS:

f(Hz)	SLOPE (dB/cm)	ATTEN (dB)	f/f_o
500	0.146	4.9	0.66
550	0.236	7.6	0.73
600	0.341	10.5	0.80
650	0.362	10.8	0.86
700	0.436	12.5	0.93
750	0.464	12.8	1.00
800	0.619	16.6	1.06
850	0.720	18.7	1.13
900	0.777	19.7	1.20
950	0.695	17.1	1.26
1000	0.541 (0.470)*	13.0 (11.3)*	1.33
1050	0.494 (0.385)	11.6 (9.0)	1.40
1100	0.435 (0.450)	9.9 (10.3)	1.46
1150	0.332 (0.245)	7.4 (5.5)	1.53
1200	0.321 (0.430)	7.0 (9.4)	1.60
1250	0.376 (0.500)	8.0 (10.7)	1.66
1300	0.160 (0.446)	3.3 (9.4)	1.73
1350	0.181 (0.245)	3.7 (5.0)	1.80
1400	0.188 (0.315)	3.8 (6.4)	1.86

* slope through first five data points only

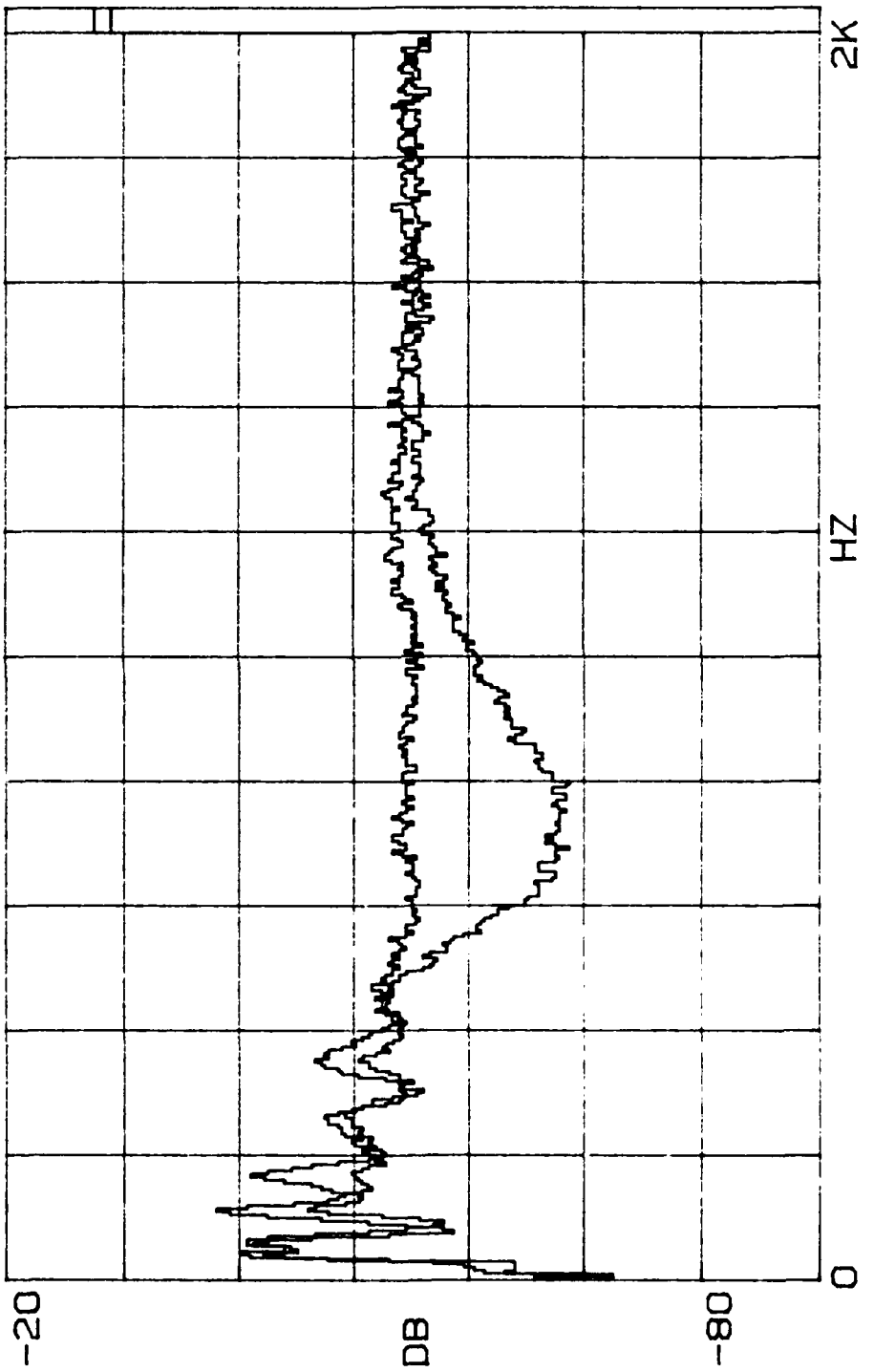

FIGURE F1

β = 1.09, R' = 0.46, l = 12 cm

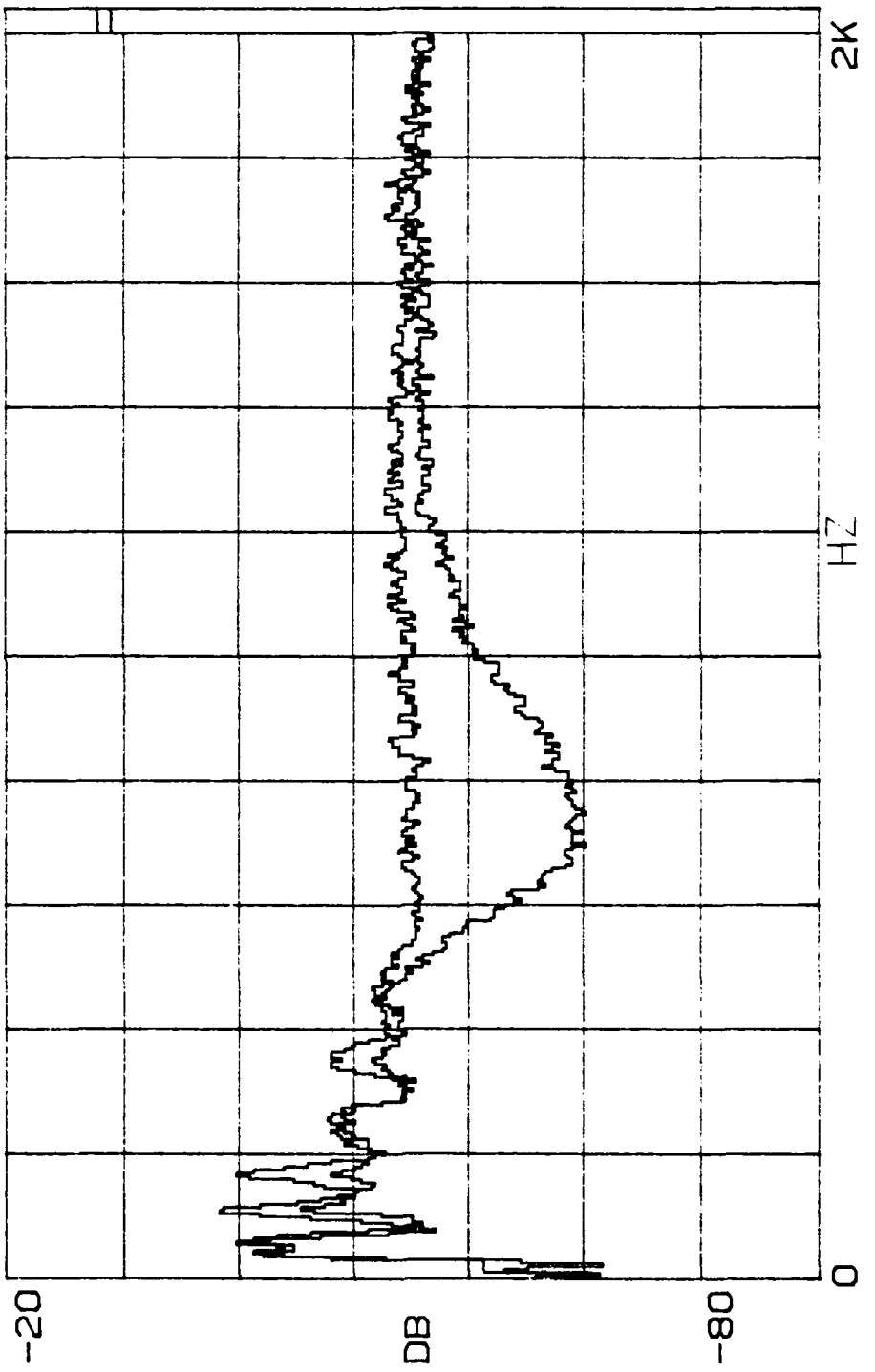

FIGURE F2

β = 1.09, R' = 0.46, l = 14 cm

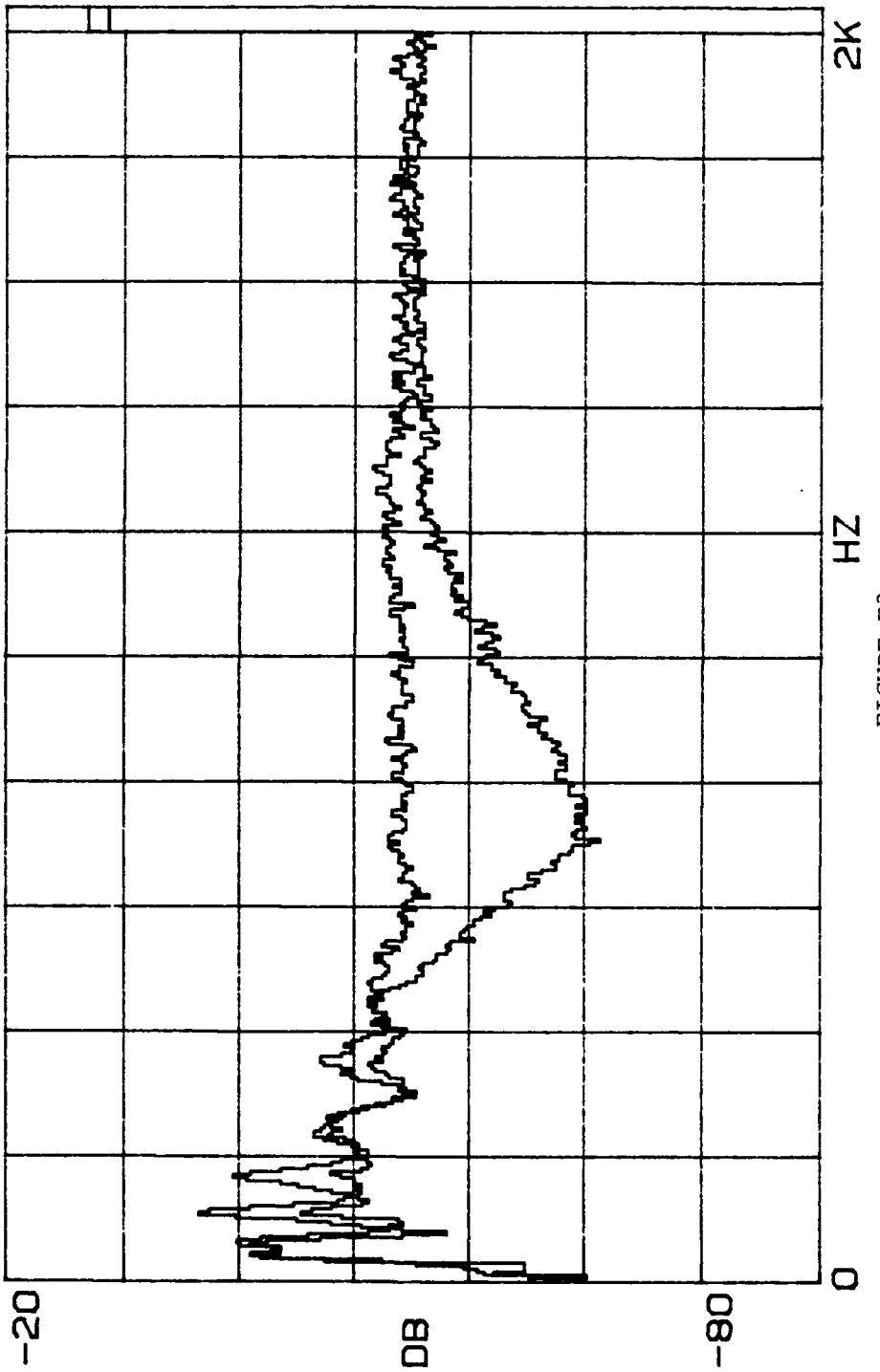

FIGURE F3

$\beta = 1.09$, $R' = 0.46$, $l = 16$ cm

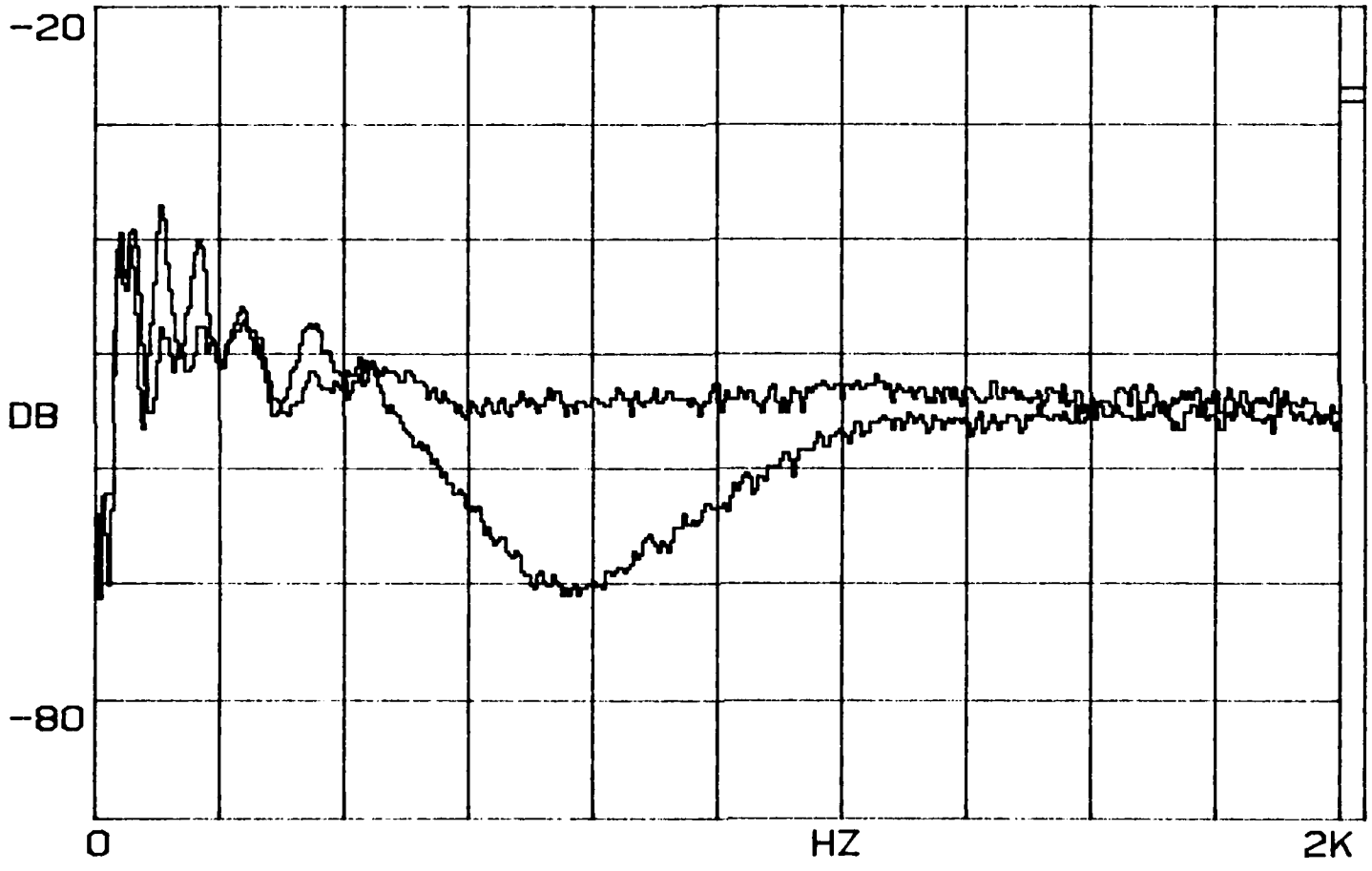

FIGURE F4

β = 1.09, R' = 0.46, l = 18 cm

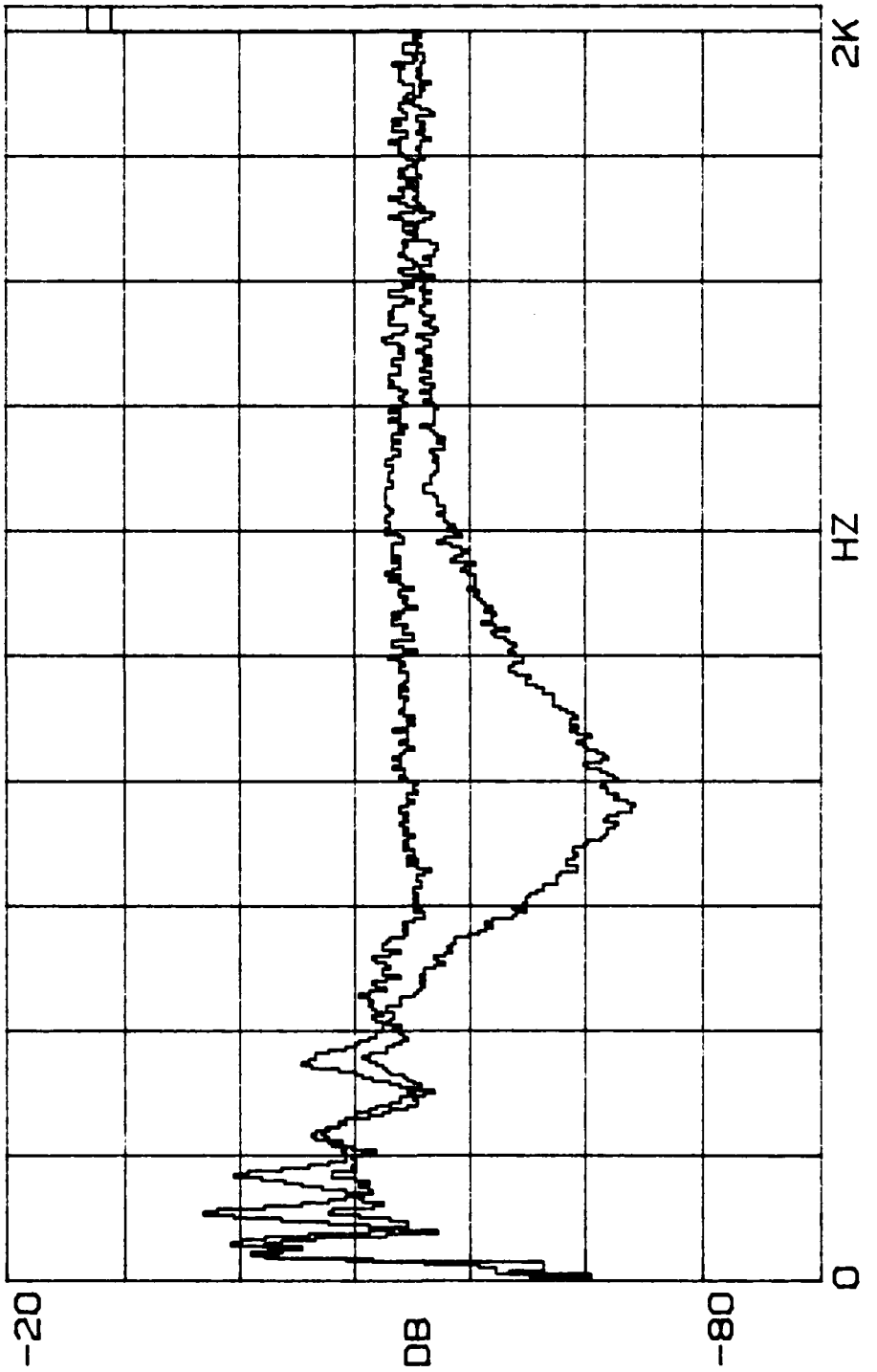

FIGURE F5

β = 1.09, R' = 0.46, l = 20 cm

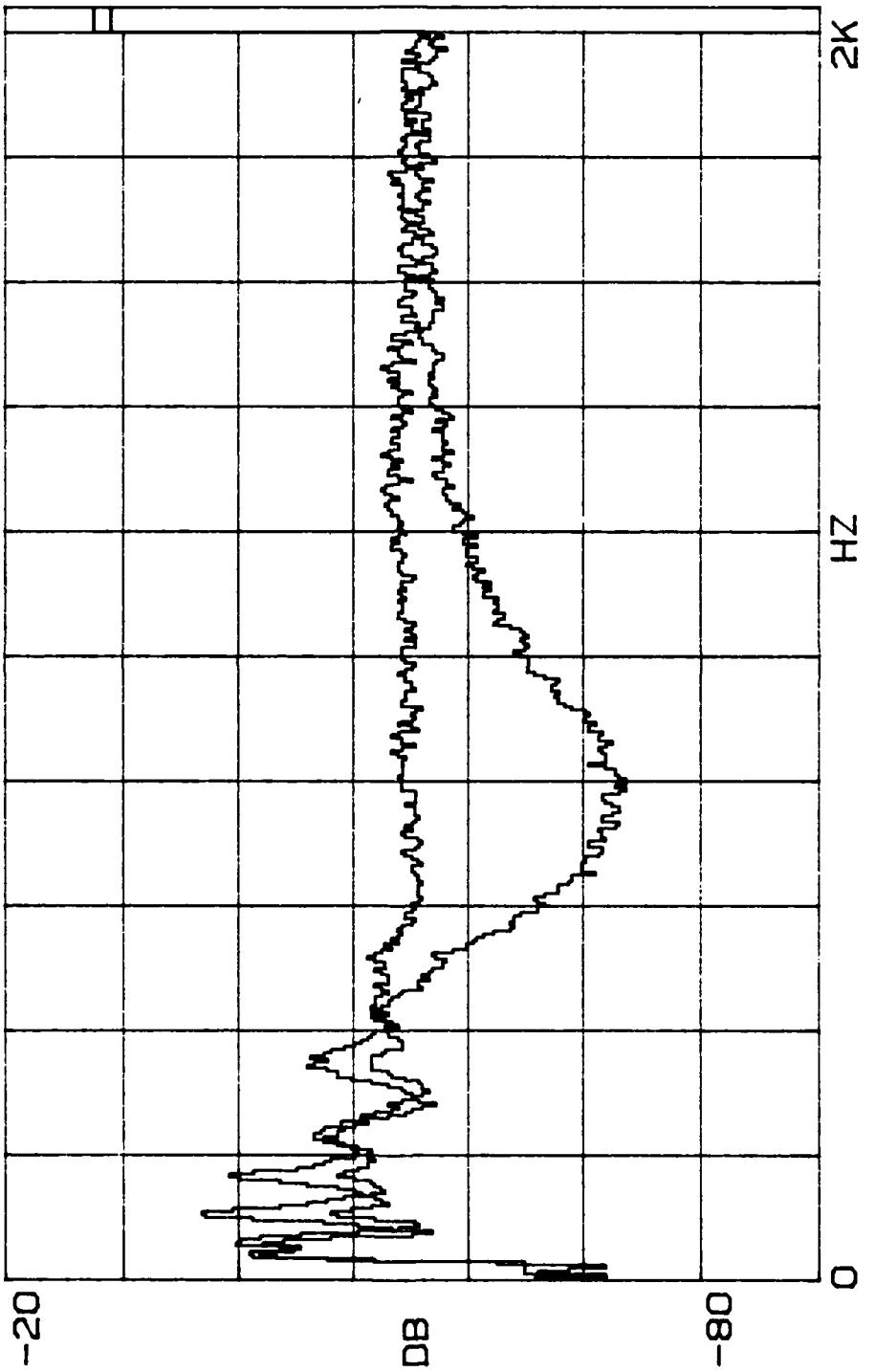

FIGURE F6

β = 1.09, R' = 0.46, l = 22 cm

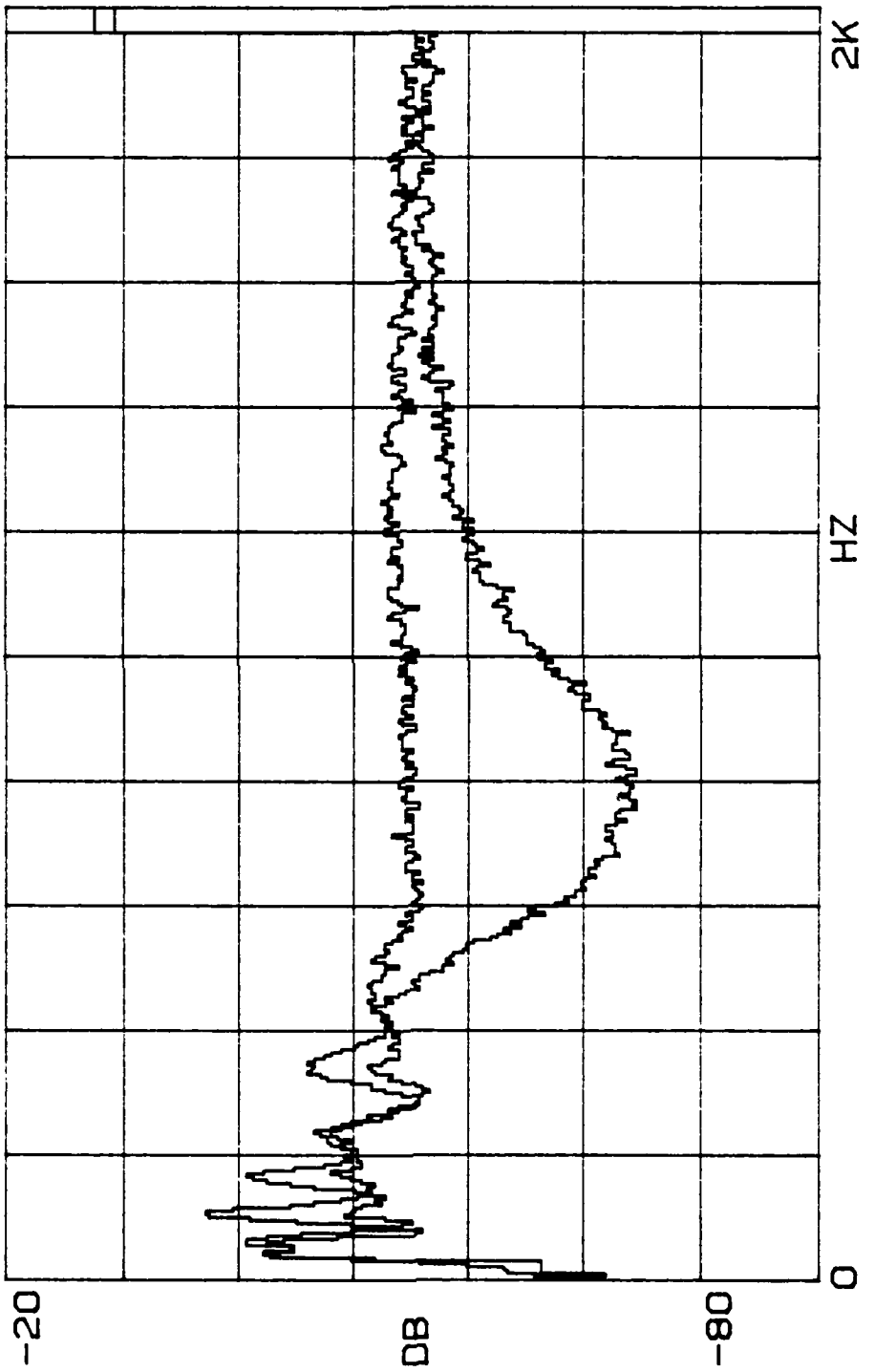

FIGURE F7

β = 1.09, R' = 0.46, l = 24 cm

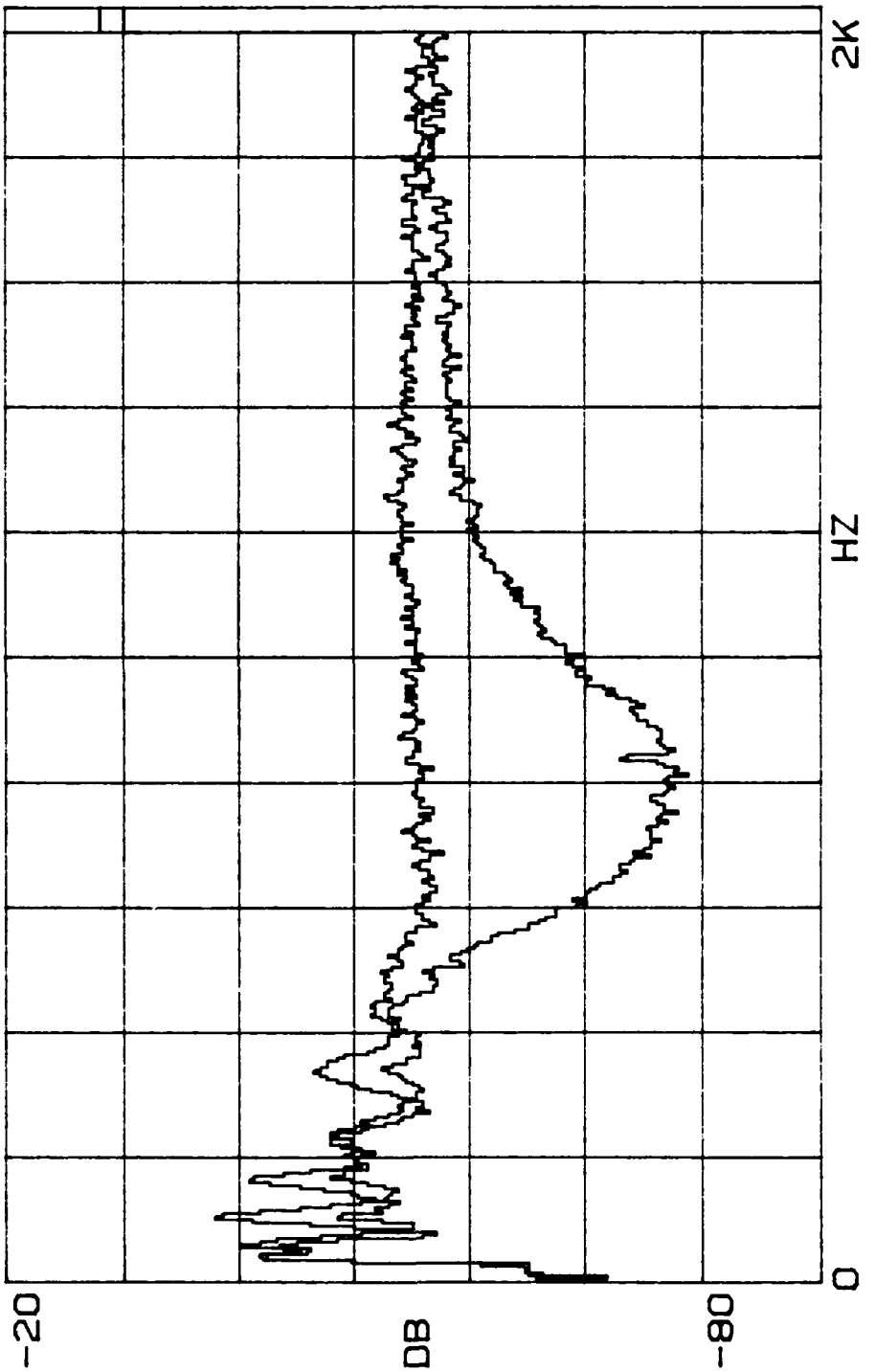

FIGURE F8

β = 1.09, R' = 0.46, l = 26 cm

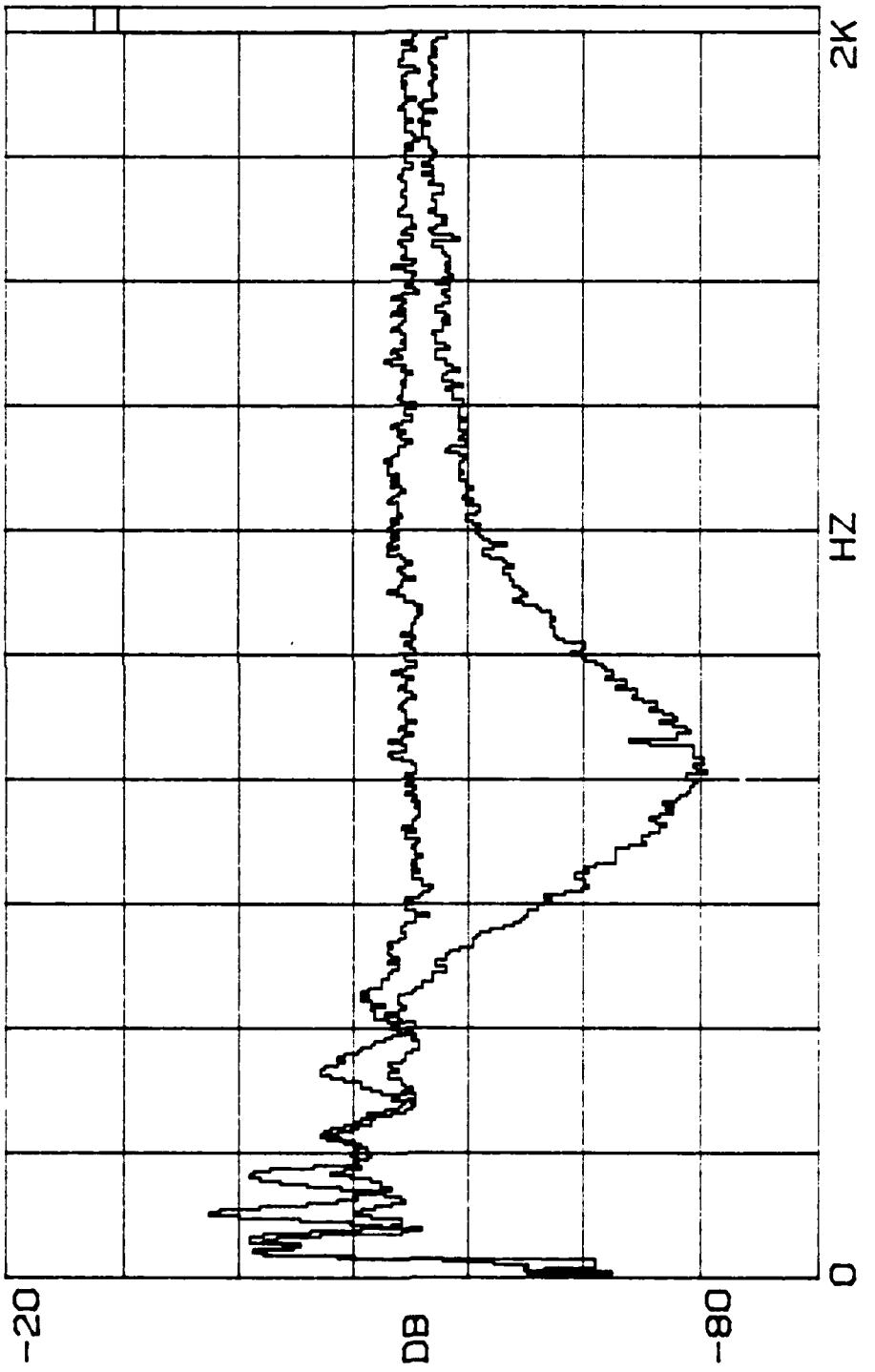

FIGURE F9

β = 1.09, R' = 0.46, l = 28 cm

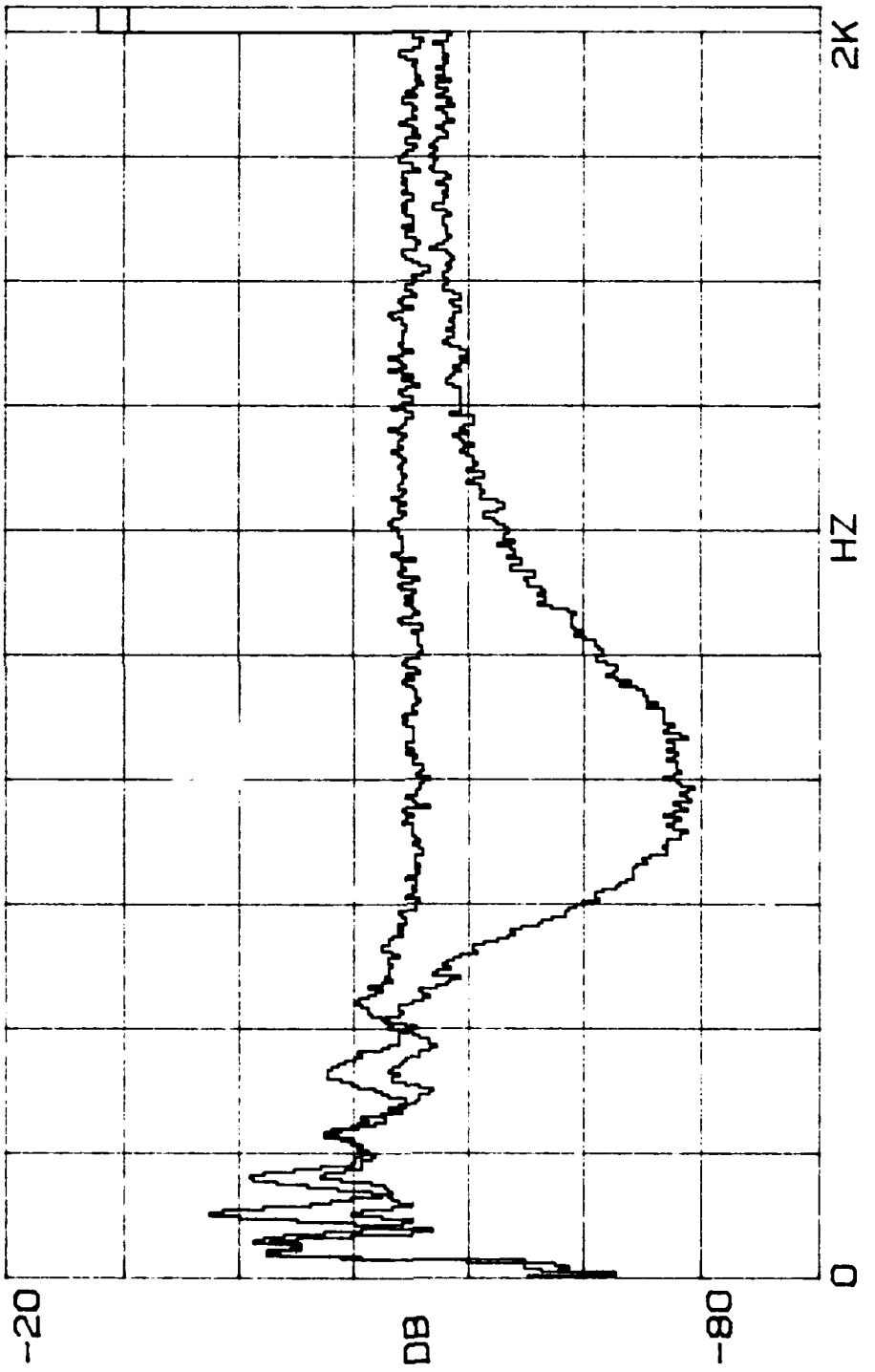

FIGURE F10

$\beta = 1.09$, $R' = 0.46$, $l = 30$ cm

APPENDIX G

ATTENUATION DATA

$\beta = 1.26,\ R' = 0.45$

TABLE II

m = 1.37 gm f_o = 750 Hz β = 1.26 R'= 0.45

ATTENUATION DATA:

ℓ(cm)	12	14	16	18	20	22	24	26	28	30
f(Hz)	ATTENUATION (dB)									
400	3.5	2.5	2.9	-0.1	0.8	0.0	2.3	2.3	-0.7	3.2
450	2.3	2.2	2.6	2.9	5.4	2.7	3.2	5.0	5.1	5.7
500	3.1	3.9	5.6	4.0	4.9	6.8	6.3	5.7	7.5	6.1
550	5.4	5.4	4.7	5.8	5.8	6.9	6.3	7.6	8.9	9.9
600	9.4	6.5	6.3	7.0	9.9	9.5	7.5	10.7	10.7	14.2
650	10.1	10.2	11.7	10.4	12.1	11.2	14.5	14.9	15.7	17.4
700	11.1	13.0	14.8	18.9	17.1	18.1	19.6	20.5	21.5	18.1
750	13.4	14.8	14.7	13.8	16.8	16.4	16.6	18.9	21.3	23.0
800	12.2	14.3	14.2	15.4	17.5	18.2	17.4	22.4	22.4	22.1
850	11.0	12.4	12.3	14.3	16.1	16.9	17.1	21.0	22.3	22.2
900	9.4	10.0	10.0	12.4	13.5	14.2	15.1	19.5	19.7	21.6
950	7.6	8.3	8.5	9.7	11.8	10.9	13.2	15.8	17.1	20.2
1000	5.9	5.4	7.2	8.6	8.8	9.9	10.9	12.7	14.9	16.1
1050	5.0	3.4	4.8	8.0	8.8	8.0	9.8	10.6	12.1	14.0
1100	4.3	4.1	4.7	6.1	6.4	6.9	7.9	10.3	10.8	12.1
1150	4.1	2.9	3.3	4.9	5.4	6.0	7.9	8.7	9.0	9.7
1200	2.4	3.9	4.4	4.3	4.2	4.8	5.4	8.6	8.4	7.0
1250	2.2	2.4	3.7	4.8	3.5	5.2	5.3	4.4	6.7	6.2
1300	0.9	2.4	3.0	4.2	2.8	5.2	4.2	5.6	5.5	5.7
1350	2.1	2.3	2.6	2.4	3.2	4.2	3.8	4.0	5.7	5.8
1400	1.9	0.8	3.4	3.4	1.8	3.8	3.2	3.9	2.6	5.3

TABLE G2

m = 1.37 gm f_o = 750 Hz β = 1.26 R'= 0.45

RESULTS:

f(Hz)	SLOPE (dB/cm)	ATTEN (dB)	f/f_o
400	---	---	0.53
450	0.185	6.6	0.60
500	0.186	6.3	0.66
550	0.311	10.0	0.73
600	0.408	12.6	0.80
650	0.421	12.5	0.86
700	0.454	13.0	0.93
750	0.560	15.5	1.00
800	0.553 (0.460)*	14.8 (12.3)*	1.06
850	0.663 (0.610)	17.0 (15.9)	1.13
900	0.742 (0.900)	18.8 (22.8)	1.20
950	0.724 (0.530)	17.8 (13.0)	1.26
1000	0.579 (0.435)	13.9 (10.4)	1.33
1050	0.532 (0.500)	12.4 (11.7)	1.40
1100	0.458 (0.360)	10.5 (8.2)	1.46
1150	0.393 (0.515)	8.8 (11.5)	1.53
1200	0.296 (0.125)	6.5 (2.7)	1.60
1250	0.221 (0.180)	4.7 (3.8)	1.66
1300	0.243 (0.170)	5.1 (3.5)	1.73
1350	0.210 (0.210)	4.3 (4.3)	1.80
1400	0.143 (0.000)	2.9 (0.0)	1.86

* slope through first five data points only

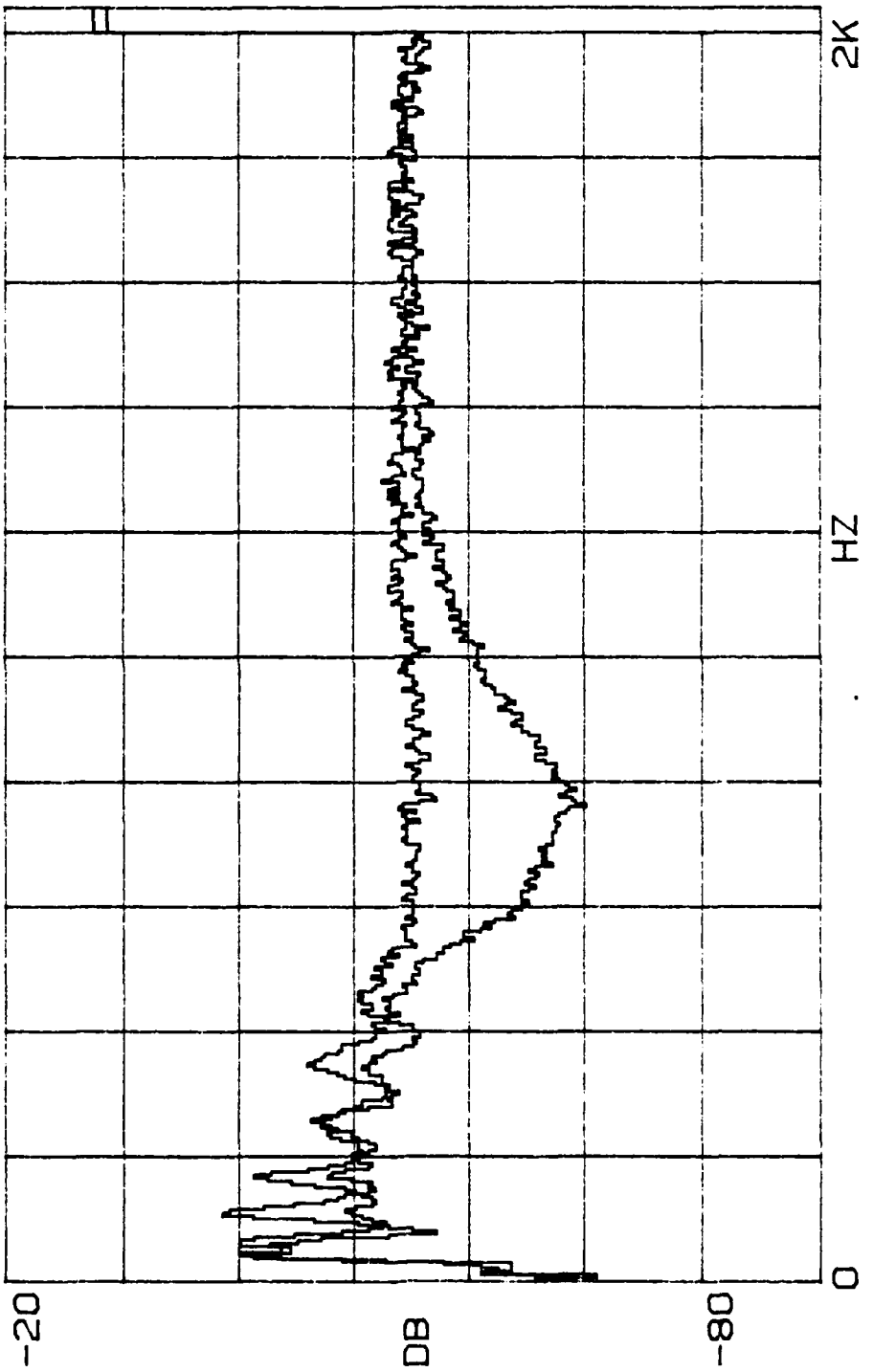

FIGURE G1

$\beta = 1.26$, $R' = 0.45$, $l = 12$ cm

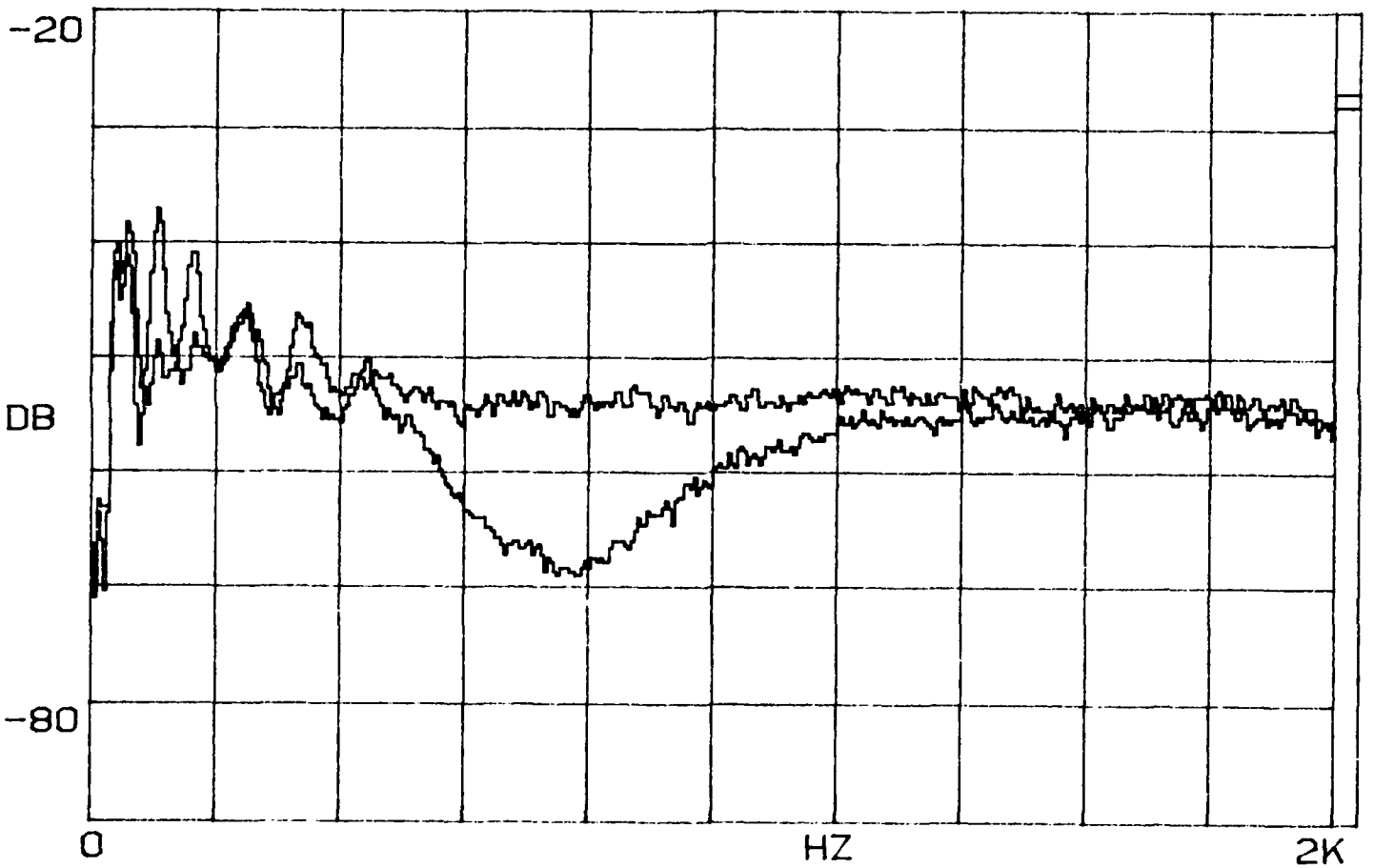

FIGURE G2

β = 1.26, R' = 0.45, l = 14 cm

-20
DB
0

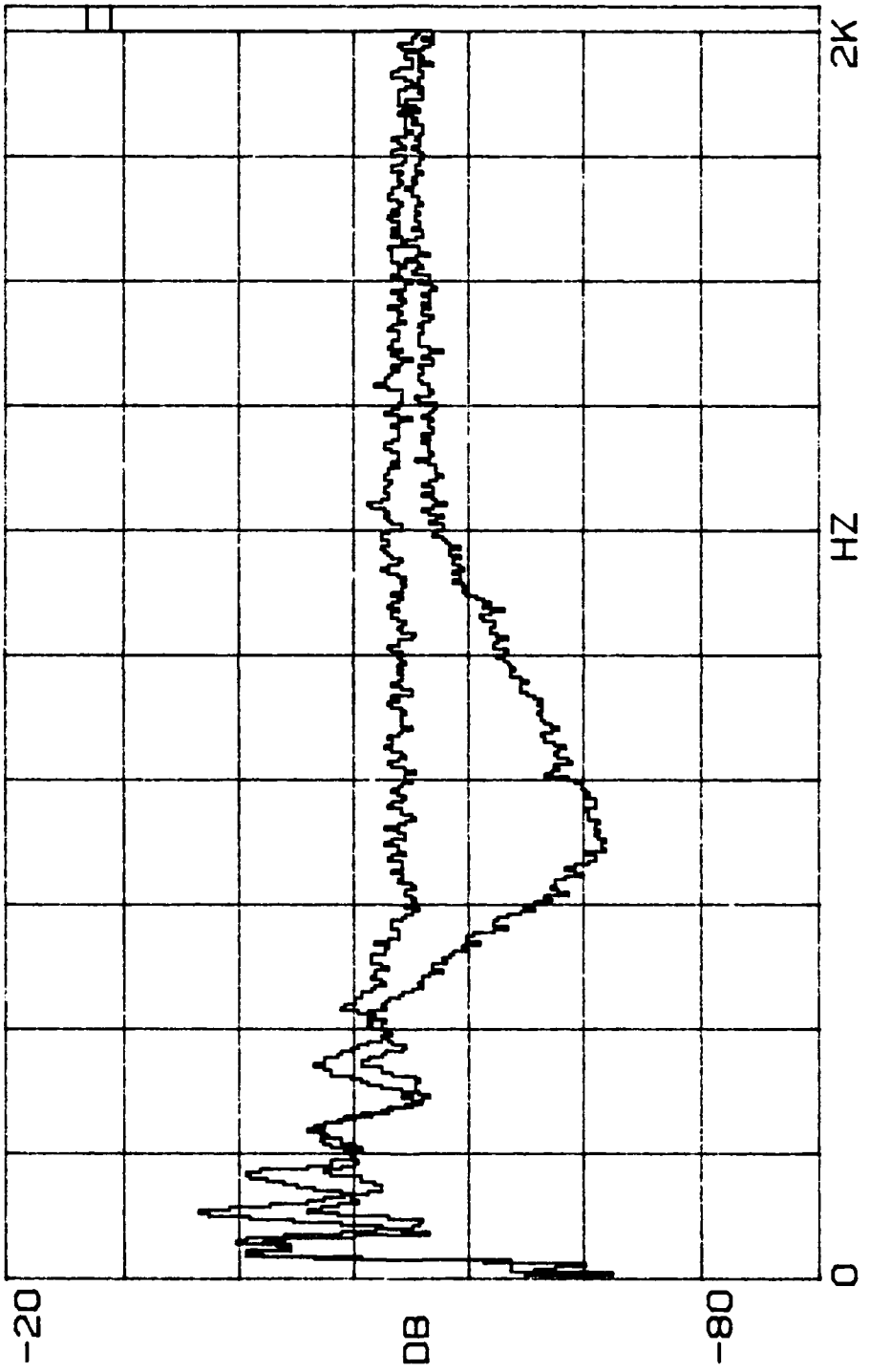

FIGURE G4

β = 1.26, R' = 0.45, l = 18 cm

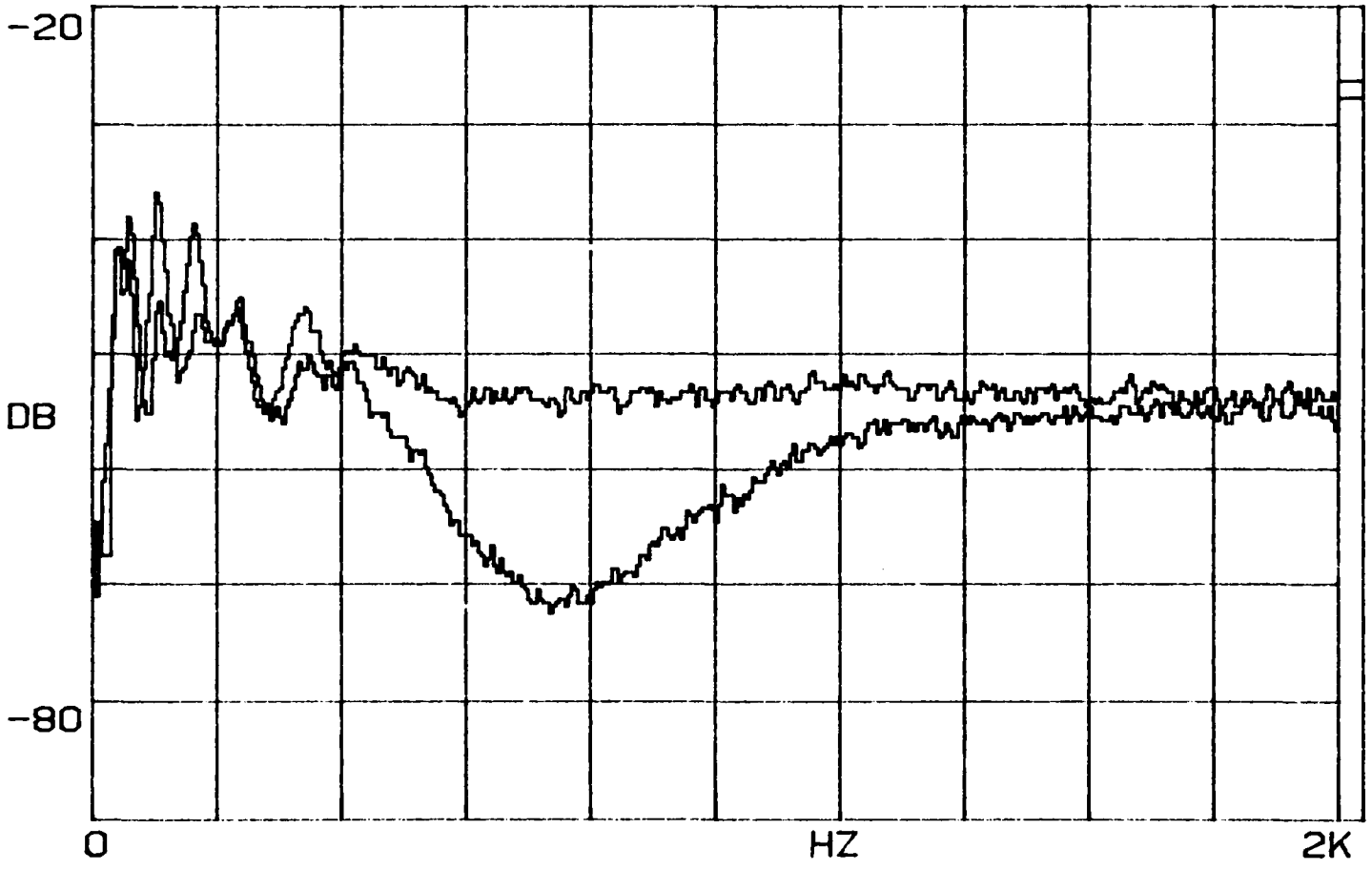

FIGURE G5

β = 1.26, R' = 0.45, l = 20 cm

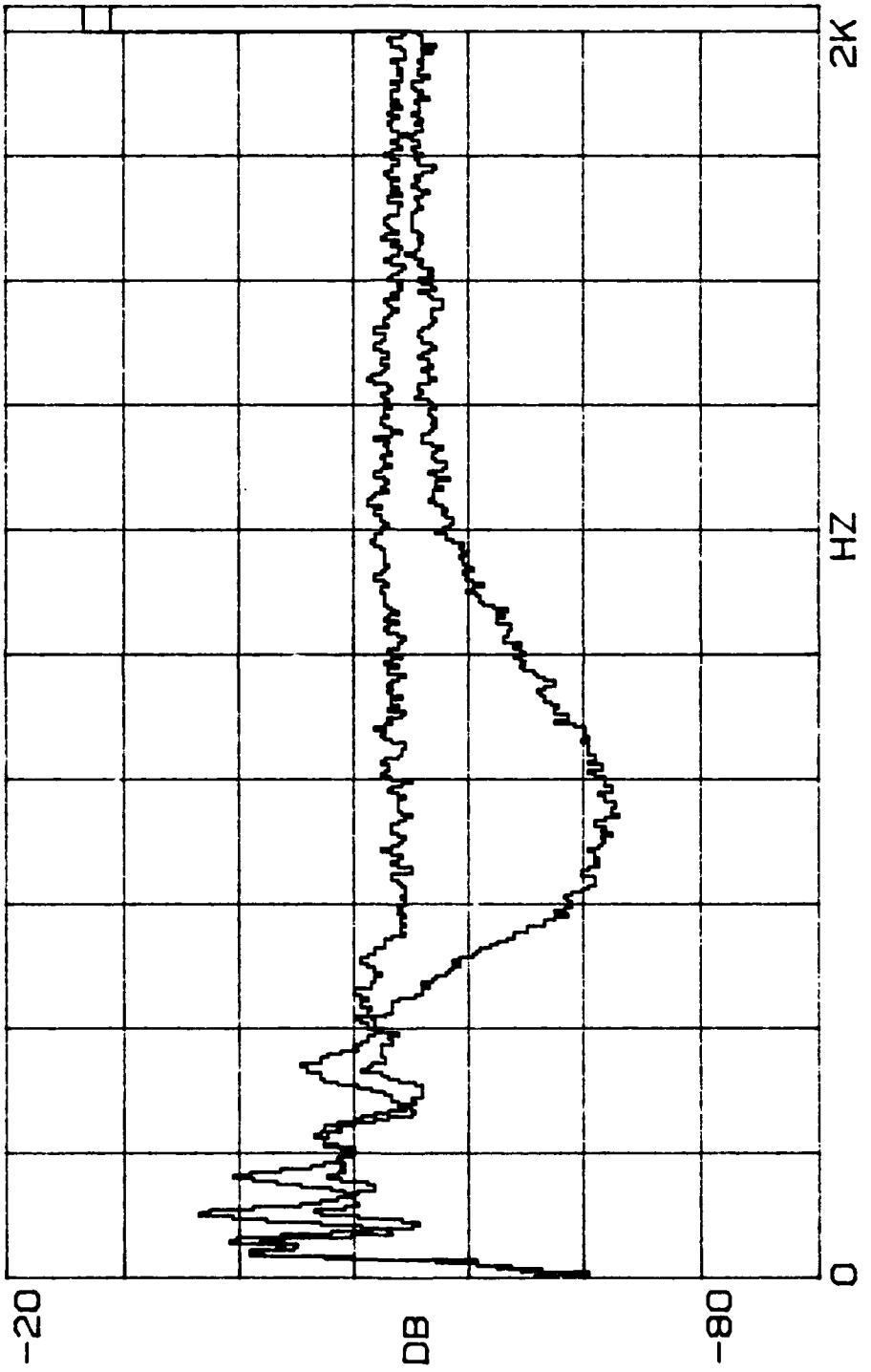

FIGURE G6

β 1.26, R' = 0.45, l = 22 cm

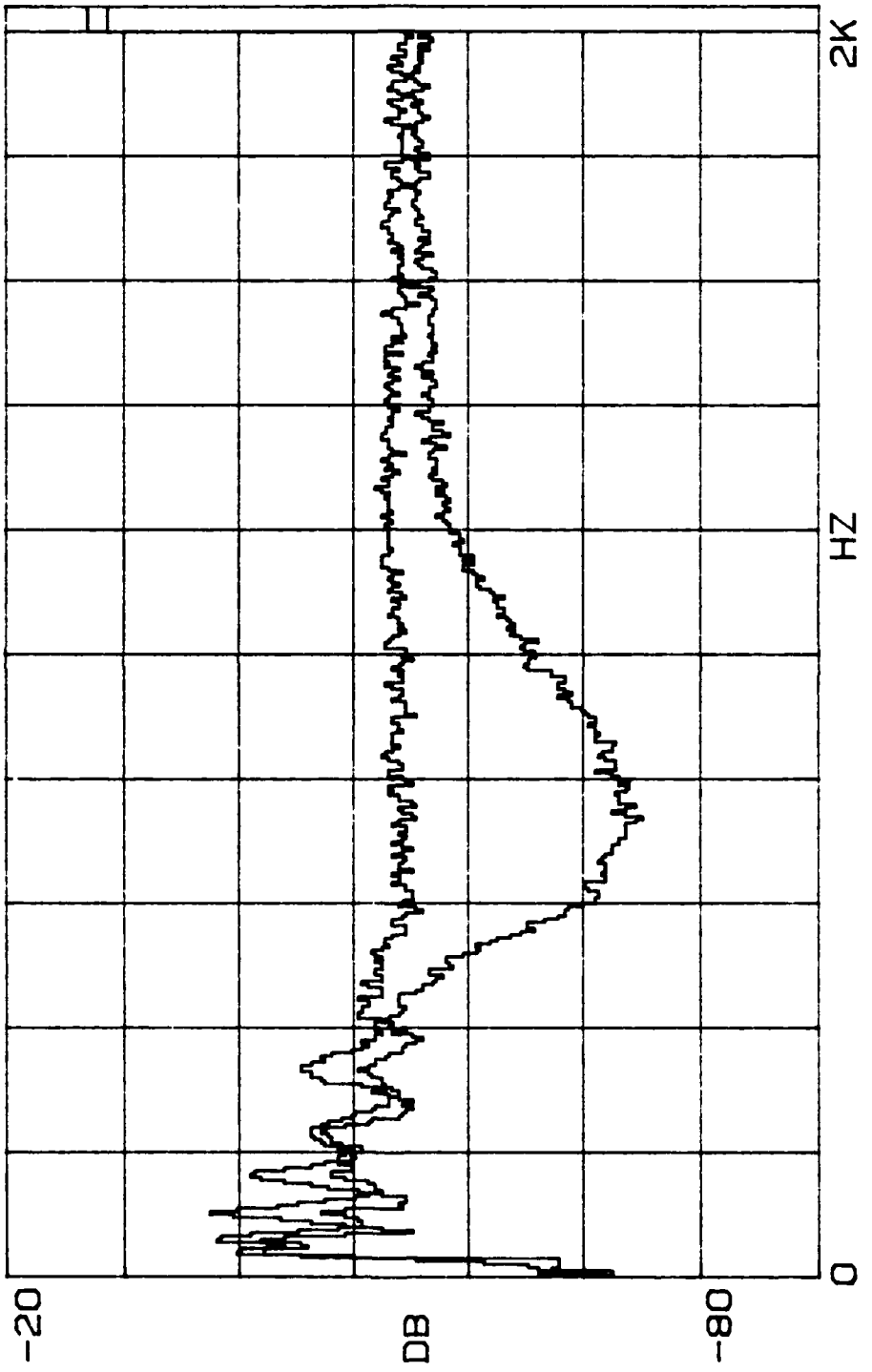

FIGURE G7

β = 1.26, R' = 0.45, l = 24 cm

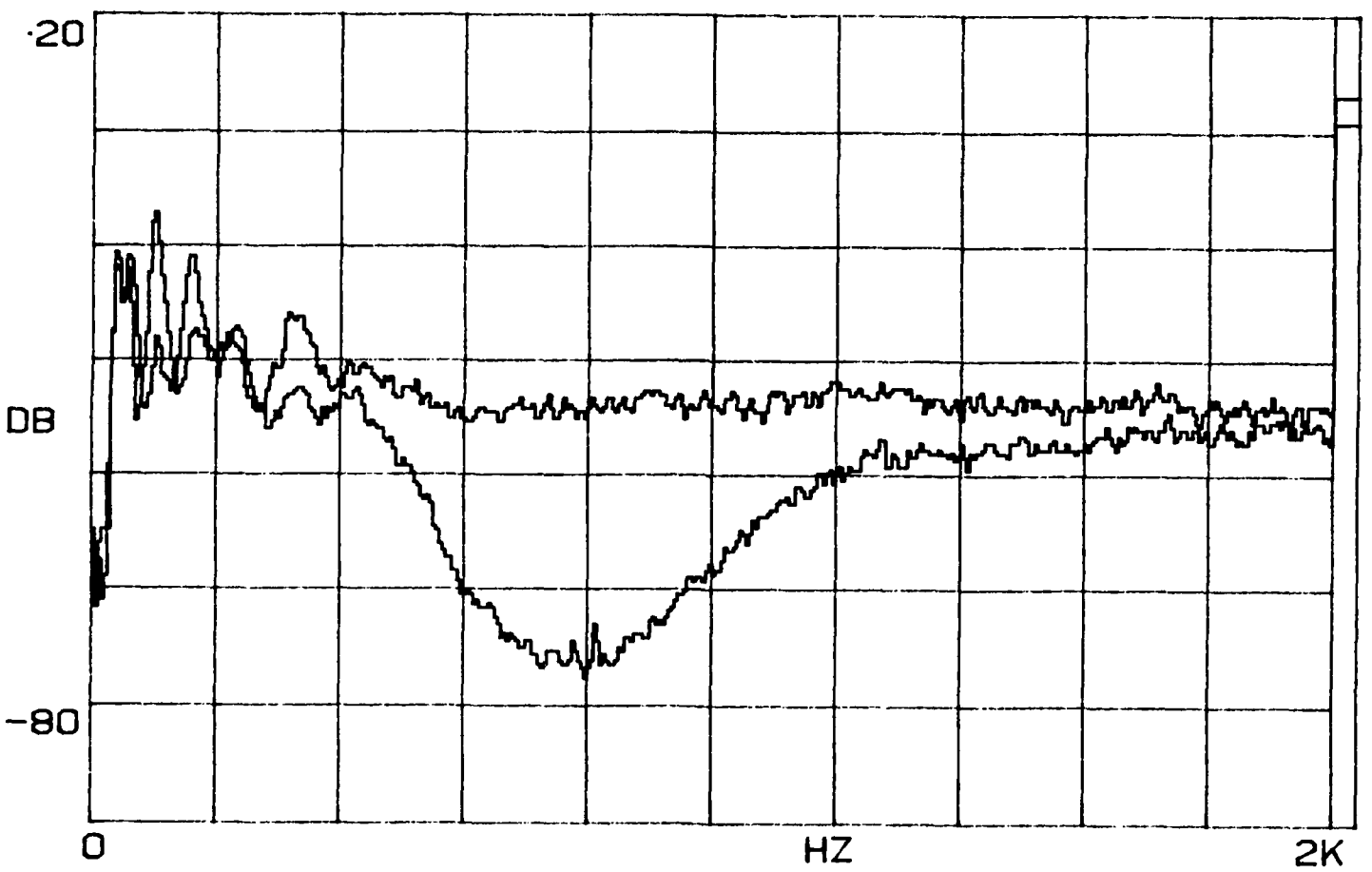

FIGURE G8

$\beta = 1.26$, $R' = 0.45$, $l = 26$ cm

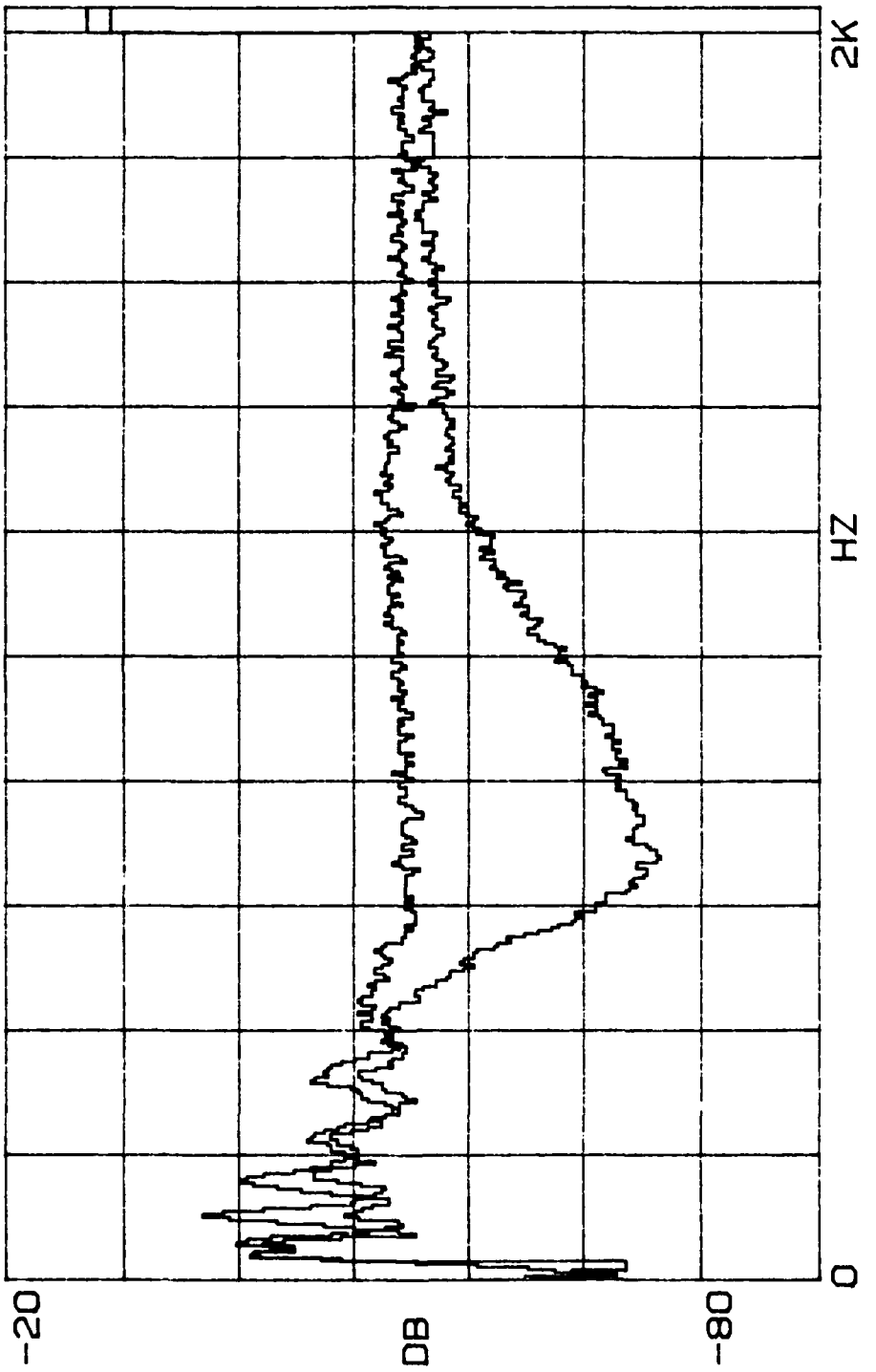

FIGURE G9

β = 1.26, R' = 0.45, l = 28 cm

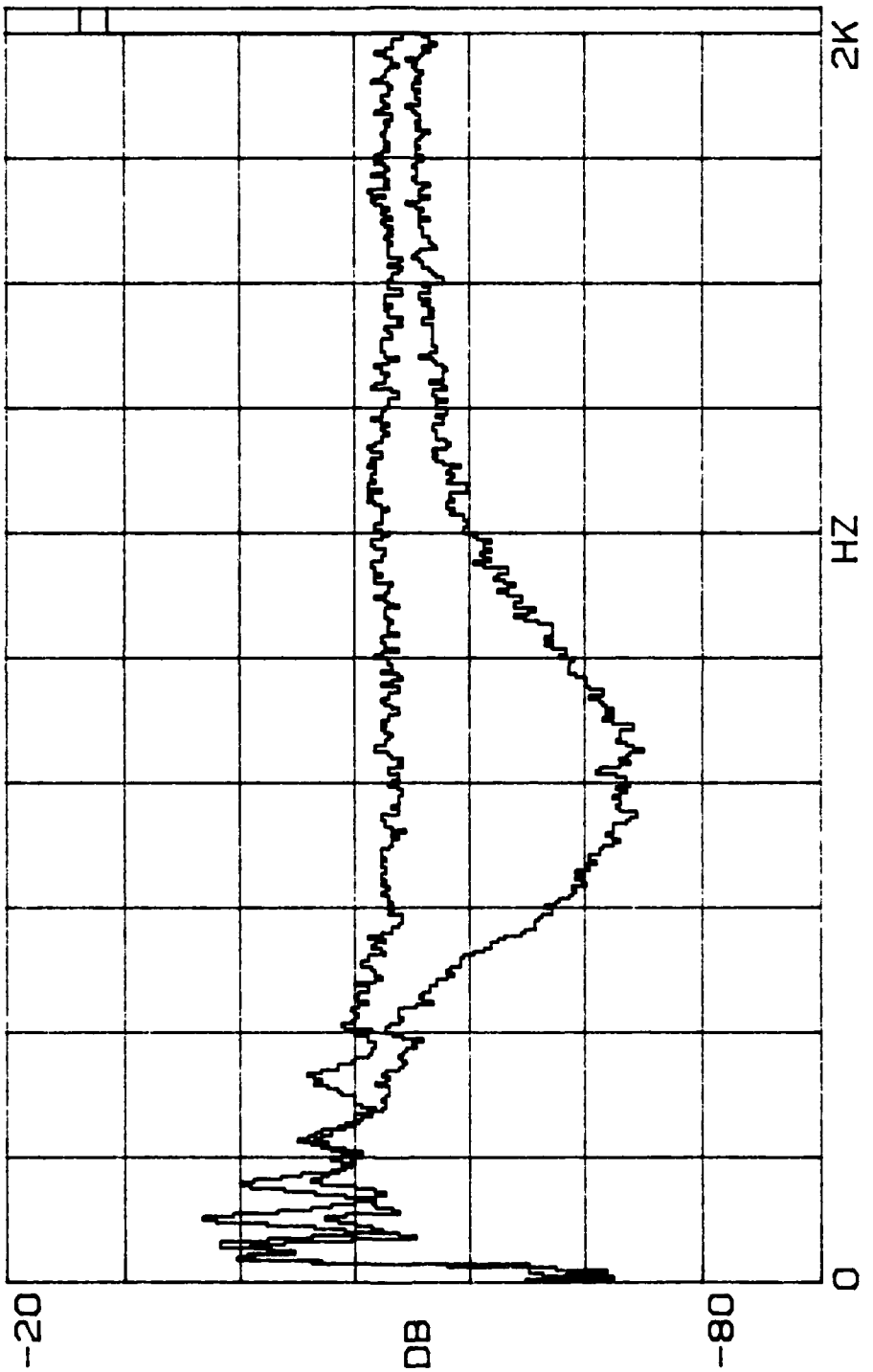

FIGURE G10

β = 1.26, R' = 0.45, l = 30 cm

APPENDIX H

ATTENUATION DATA

$\beta = 1.55$, $R' = 0.45$

TABLE H1

m = 1.69 gm f_o = 550 Hz s = 1.55 R'= 0.45

ATTENUATION DATA:

ℓ(cm)	12	14	16	18	20	22	24	26
f(Hz)	ATTENUATION (dB)							
400	2.1	2.4	2.6	3.3	3.6	3.2	3.5	3.8
450	3.7	3.5	5.6	6.7	6.1	5.6	5.9	7.0
500	5.3	6.0	9.7	10.0	9.2	10.6	10.4	11.5
550	8.3	9.8	11.5	14.0	14.0	15.1	17.5	19.2
600	13.7	13.9	14.8	13.9	16.0	19.3	19.5	20.5
650	16.0	18.1	17.7	16.9	18.4	19.9	22.9	25.4
700	14.4	17.6	16.5	18.8	17.9	18.9	22.7	21.5
750	12.4	13.9	15.8	18.9	18.5	19.1	21.8	20.7
800	11.0	12.5	13.8	16.3	15.7	16.4	20.5	19.4
850	8.5	9.3	10.7	15.1	12.6	15.9	18.6	17.5
900	6.9	7.8	9.3	11.5	11.1	13.2	13.9	16.0
950	4.0	7.7	8.1	8.3	9.3	9.7	11.6	12.7
1000	3.4	4.5	5.7	6.8	7.7	8.8	7.8	10.9
1050	3.0	4.6	5.0	6.3	5.7	6.0	8.2	7.9
1100	3.4	2.5	3.3	3.2	5.0	4.0	6.7	6.7

TABLE H2

m = 1.69 gm f_o = 550 Hz β = 1.55 R'= 0.45

RESULTS:

f(Hz)	SLOPE (dB/cm)	ATTEN (dB)	f/f_o
400	0.277	10.5	0.73
450	0.325	11.6	0.82
500	0.449	15.2	0.91
550	0.680	22.0	1.00
600	0.487 (0.230)*	15.1 (7.1)*	1.09
650	0.468 (0.180)	13.9 (5.3)	1.18
700	0.449 (0.410)	12.9 (11.7)	1.27
750	0.548 (0.860)	15.2 (23.9)	1.36
800	0.517 (0.660)	13.9 (17.7)	1.45
850	0.575 (0.700)	15.0 (18.2)	1.54
900	0.469 (0.605)	11.9 (15.3)	1.64
950	0.385 (0.560)	9.5 (13.8)	1.73
1000	0.386 (0.545)	9.2 (13.1)	1.82
1050	0.303 (0.355)	7.1 (8.3)	1.91
1100	0.304 (0.195)	6.9 (4.4)	2.00

* slope through first five points only

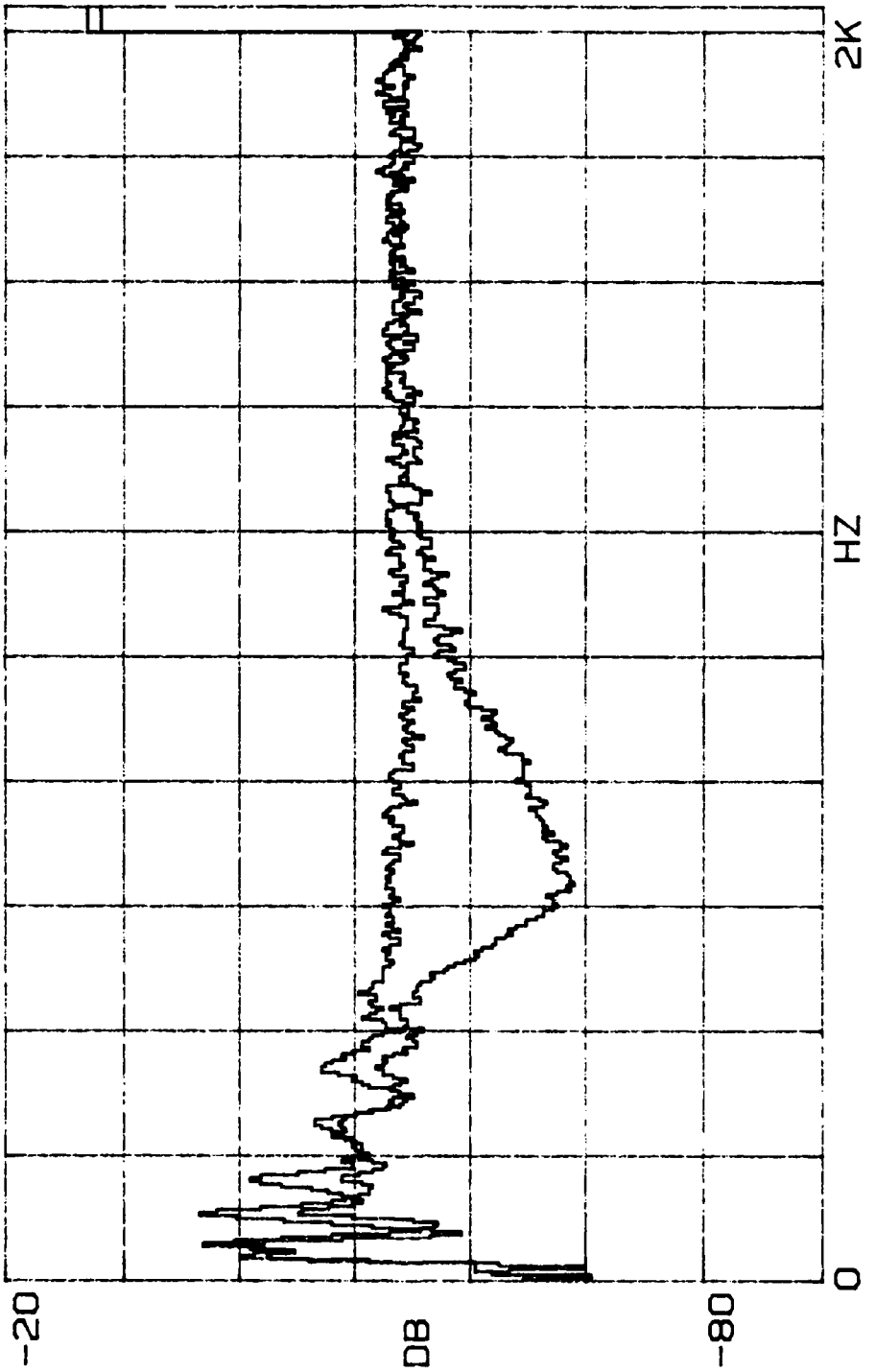

FIGURE H1

$\beta = 1.55$, $R' = 0.45$, $l = 12$ cm

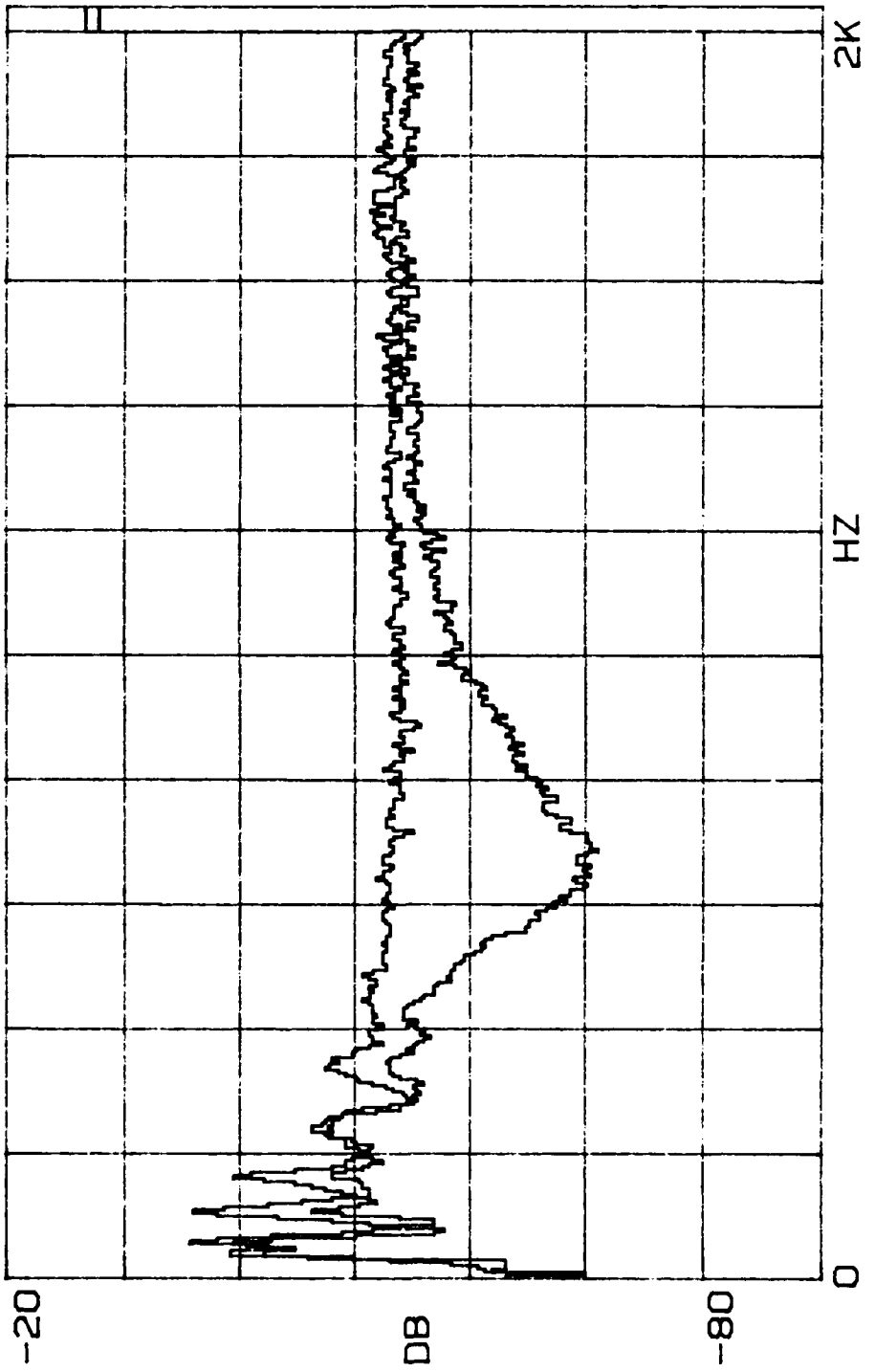

FIGURE H2

β = 1.55, R' = 0.45, l = 14 cm

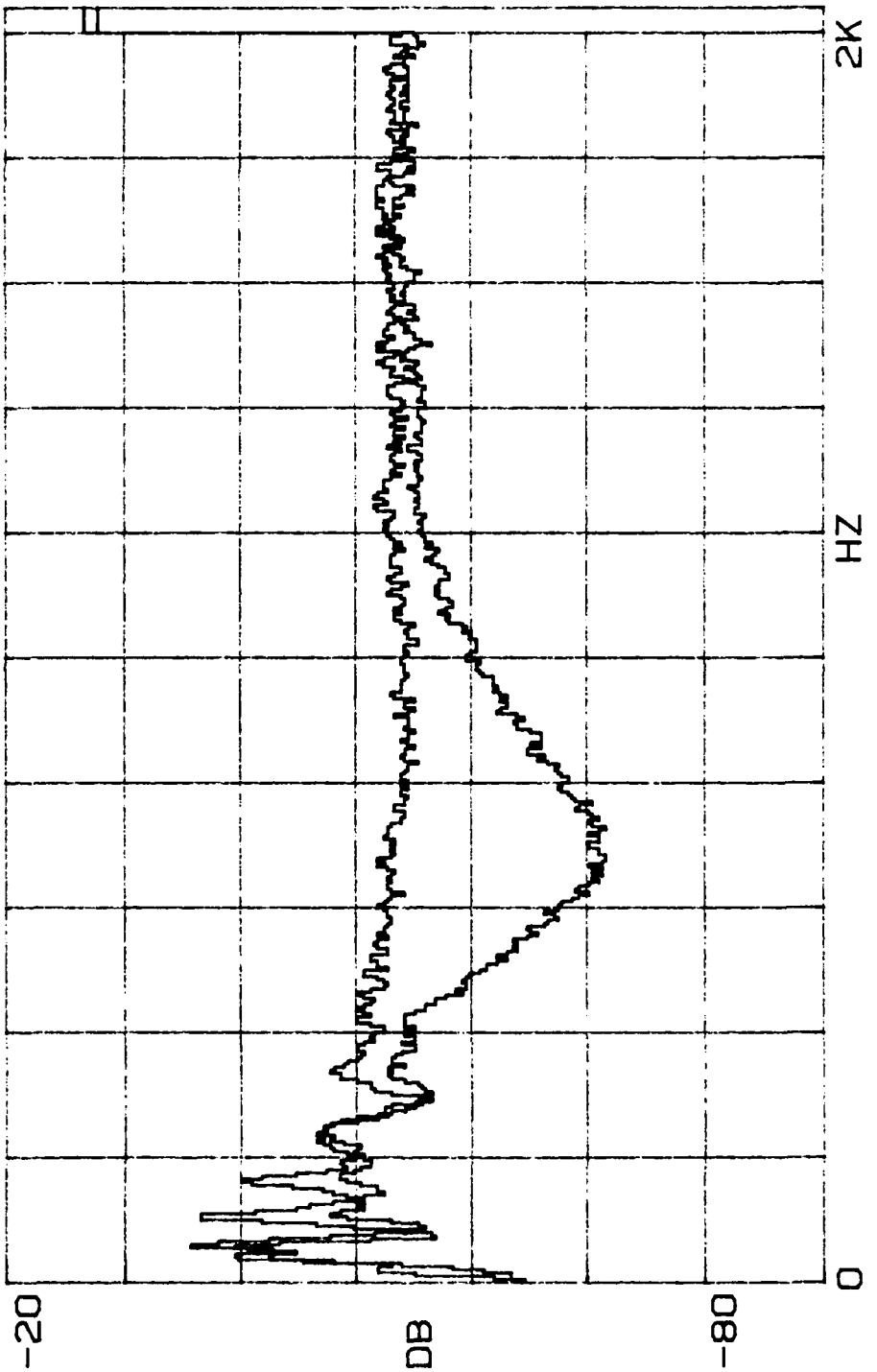

FIGURE H3

β = 1.55, R' = 0.45, l = 16 cm

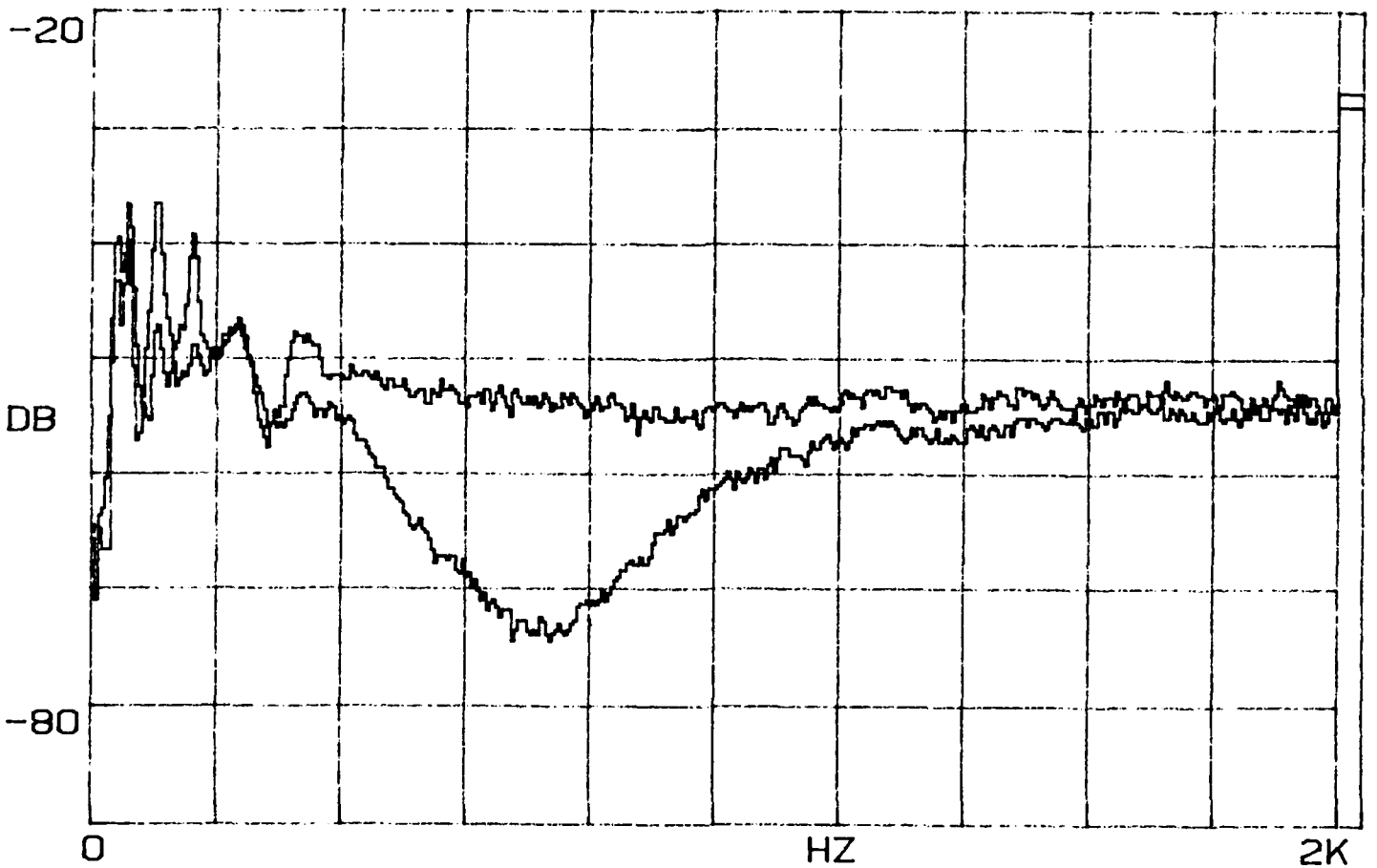

FIGURE H4

β = 1.55, R' = 0.45, l = 18 cm

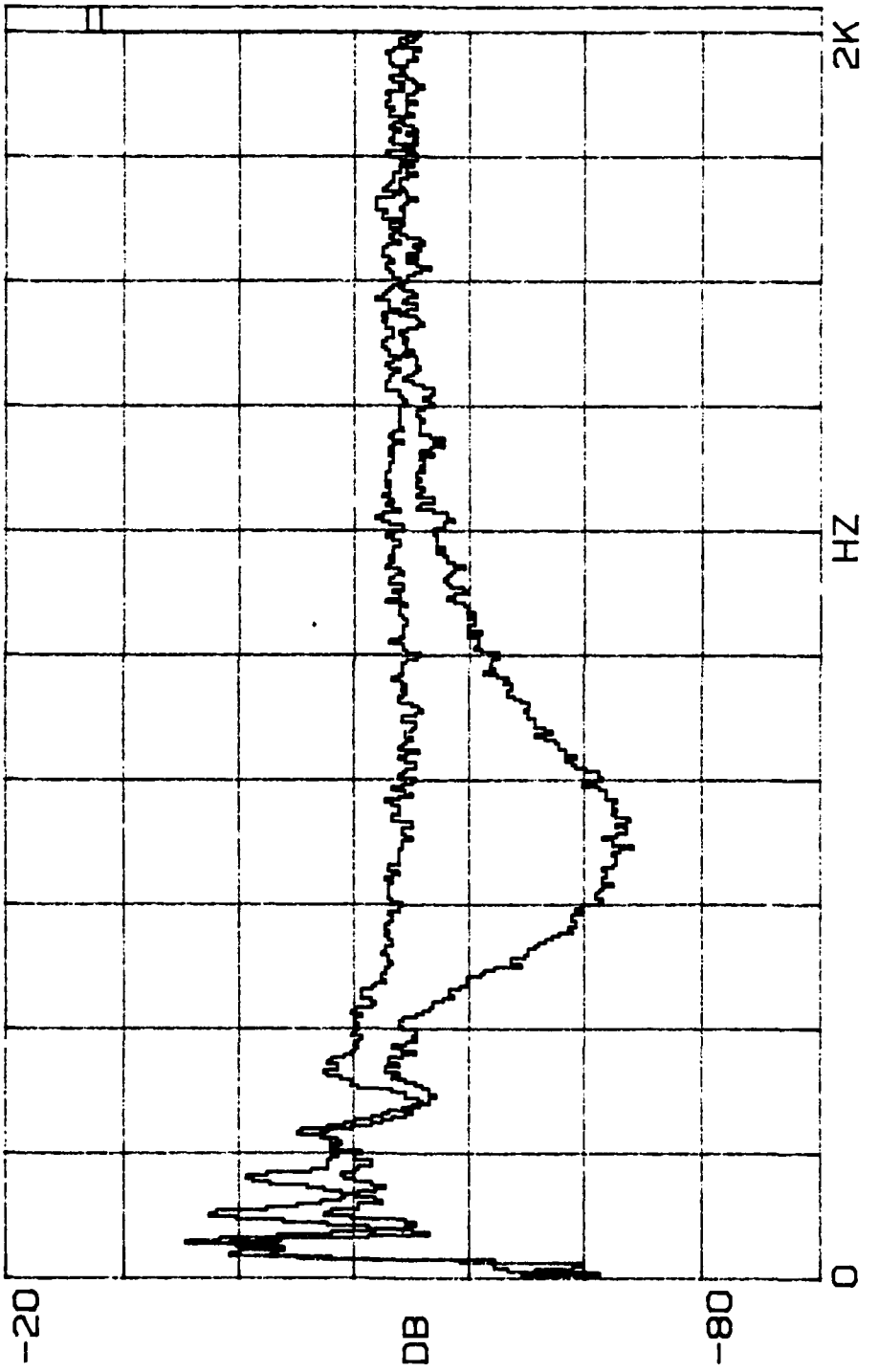

FIGURE H5

β = 1.55, R' = 0.45, l = 20 cm

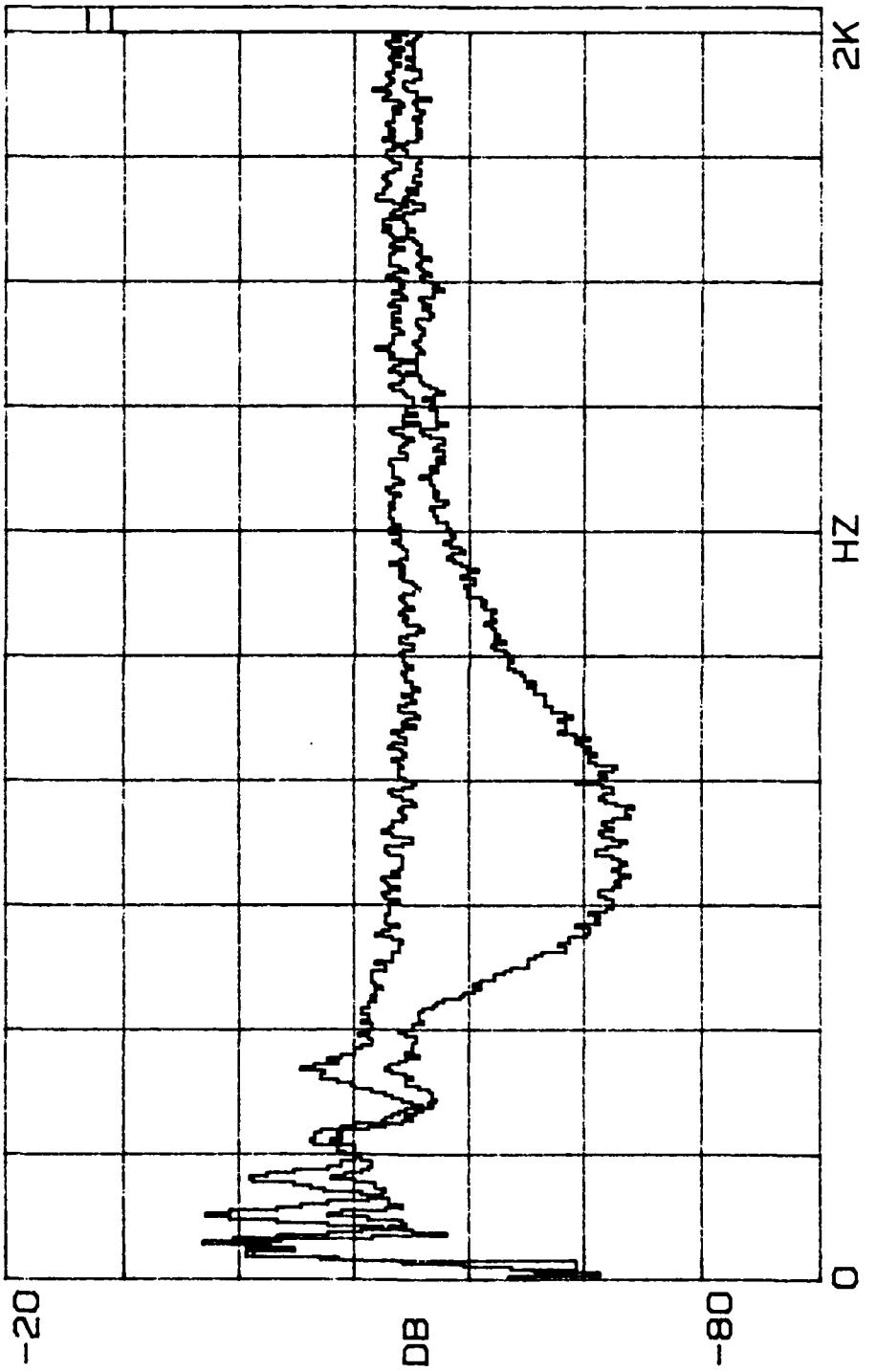

FIGURE H6

$\beta = 1.55$, $R' = 0.45$, $l = 22$ cm

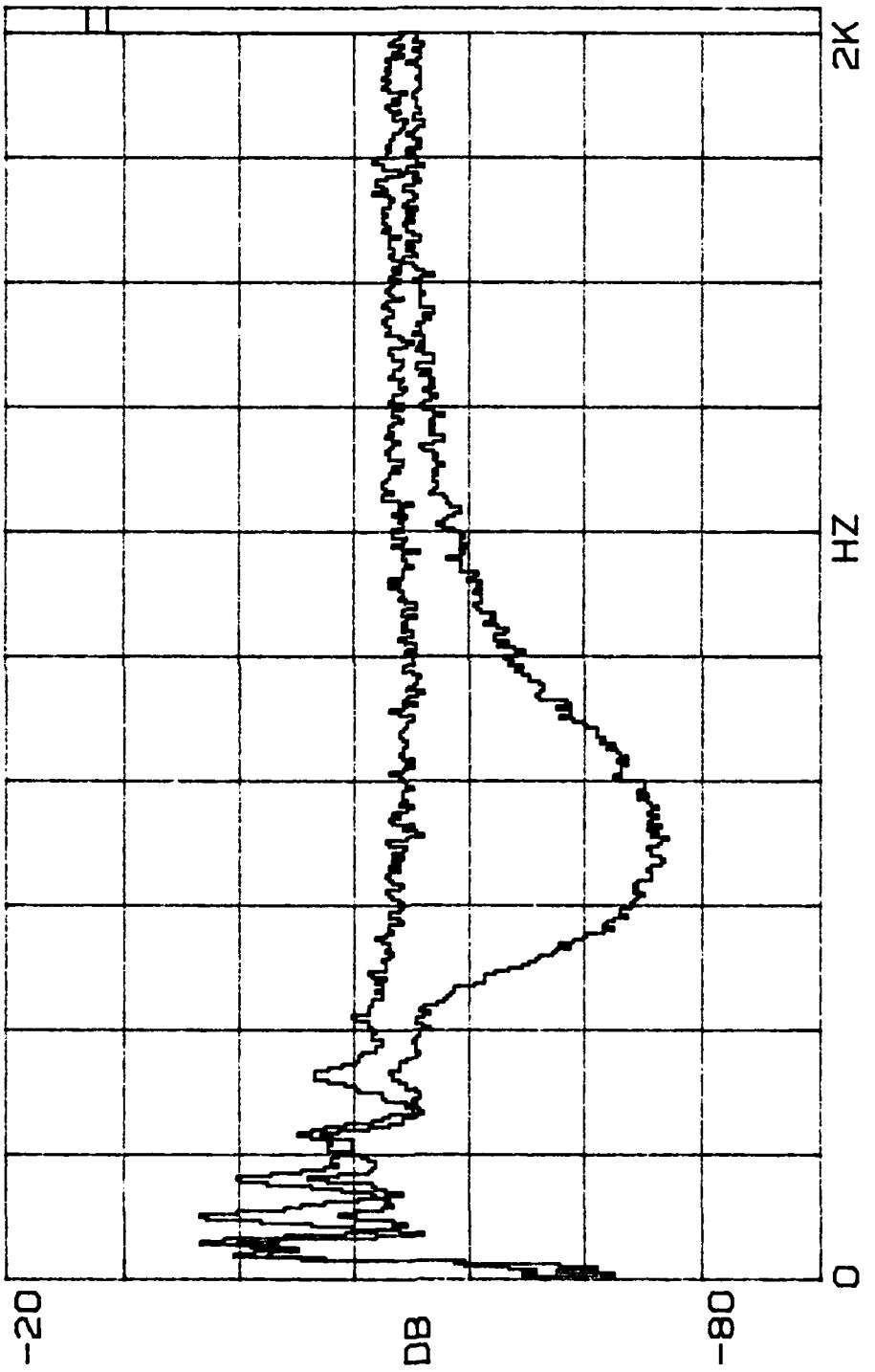

FIGURE H7

β = 1.55, R' = 0.45, l = 24 cm

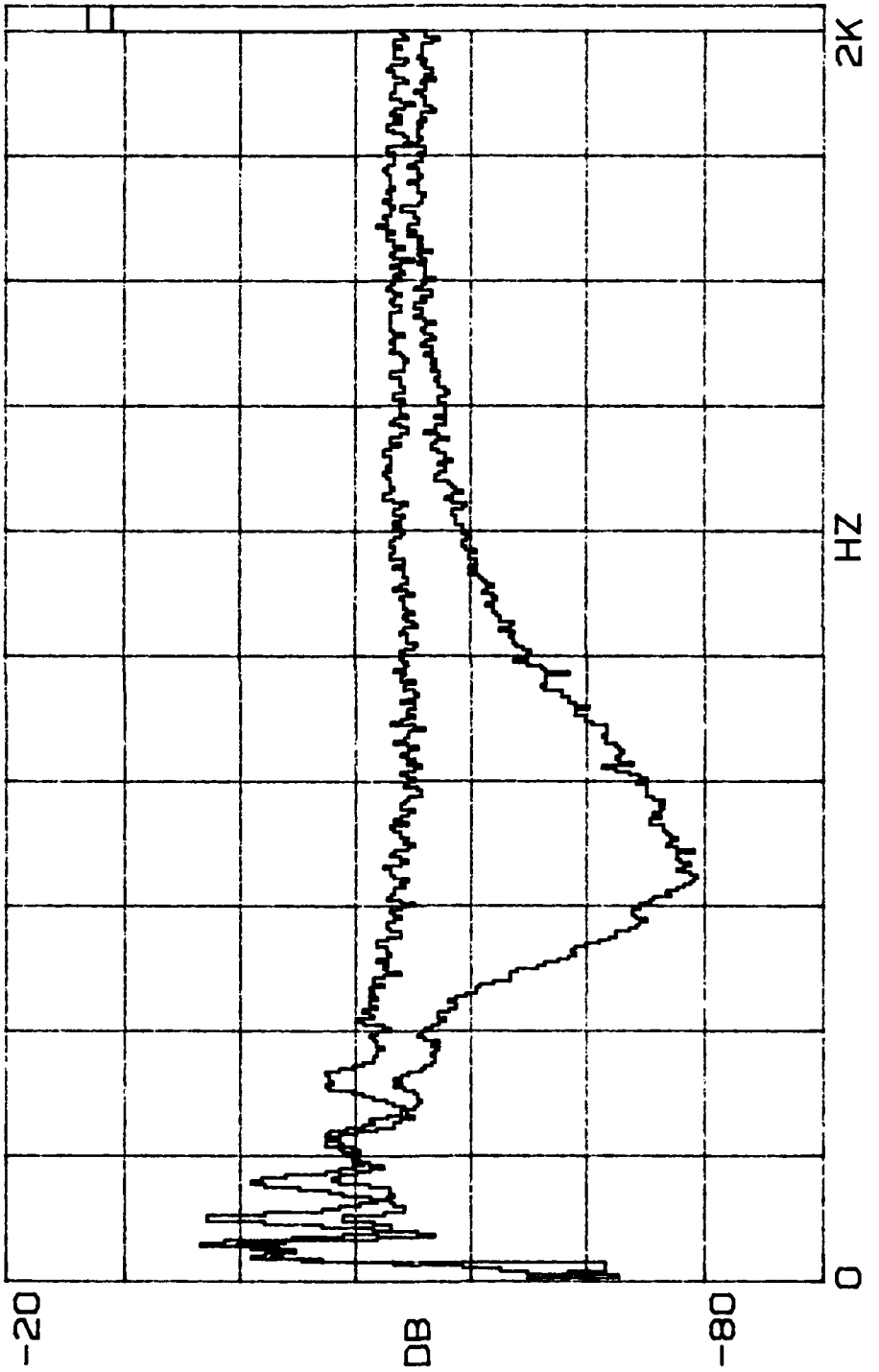

FIGURE H8

β = 1.55, R' = 0.45, l = 26 cm

APPENDIX I

ATTENUATION DATA

$\beta = 1.75$, $R' = 0.45$

m = 1.91 gm f_o = 420 Hz ζ = 1.75 R' = 0.45

ATTENUATION DATA:

ℓ(cm)	9.5	11.9	14.3	16.7	19.1	21.5	24.0	26.4
f(Hz)	ATTENUATION (dB)							
300	0.5	2.4	0.7	1.6	3.0	5.3	7.1	6.6
350	6.4	6.3	6.0	6.0	6.9	7.1	7.2	8.3
400	6.3	7.6	8.1	6.7	9.0	8.3	9.0	13.0
450	8.0	9.1	11.3	12.5	13.5	12.6	14.6	15.0
500	8.9	10.7	12.3	14.1	15.3	15.4	19.9	17.1
550	11.8	14.6	14.4	17.7	18.5	17.7	23.7	19.4
600	10.9	13.8	14.2	17.7	16.0	19.5	23.8	19.9
650	7.7	12.3	11.6	17.2	15.1	18.7	23.4	17.7
700	6.9	9.0	11.7	14.7	12.6	15.5	20.5	16.0
750	5.3	6.6	8.3	11.0	11.7	12.9	17.2	14.0
800	5.8	7.3	6.4	10.1	9.4	10.5	15.2	10.8

TABLE I2

m = 1.91 gm f_o = 420 Hz β = 1.75 R'= 0.45

RESULTS:

f(Hz)	SLOPE (dB/cm)	ATTEN (dB)	f/f_o
300	0.346	15.2	0.71
350	0.225	9.1	0.83
400	0.404	15.3	0.95
450	0.482 (0.600)*	17.2 (21.5)*	1.07
500	0.489 (0.675)	16.6 (22.9)	1.19
550	0.524 (0.688)	17.0 (22.3)	1.31
600	0.536 (0.675)	16.6 (20.9)	1.43
650	0.592 (0.821)	17.6 (24.5)	1.55
700	0.525 (0.713)	15.1 (20.5)	1.66
750	0.534 (0.717)	14.8 (19.9)	1.79
800	0.347 (0.458)	9.3 (12.3)	1.90

* slope through first five points only

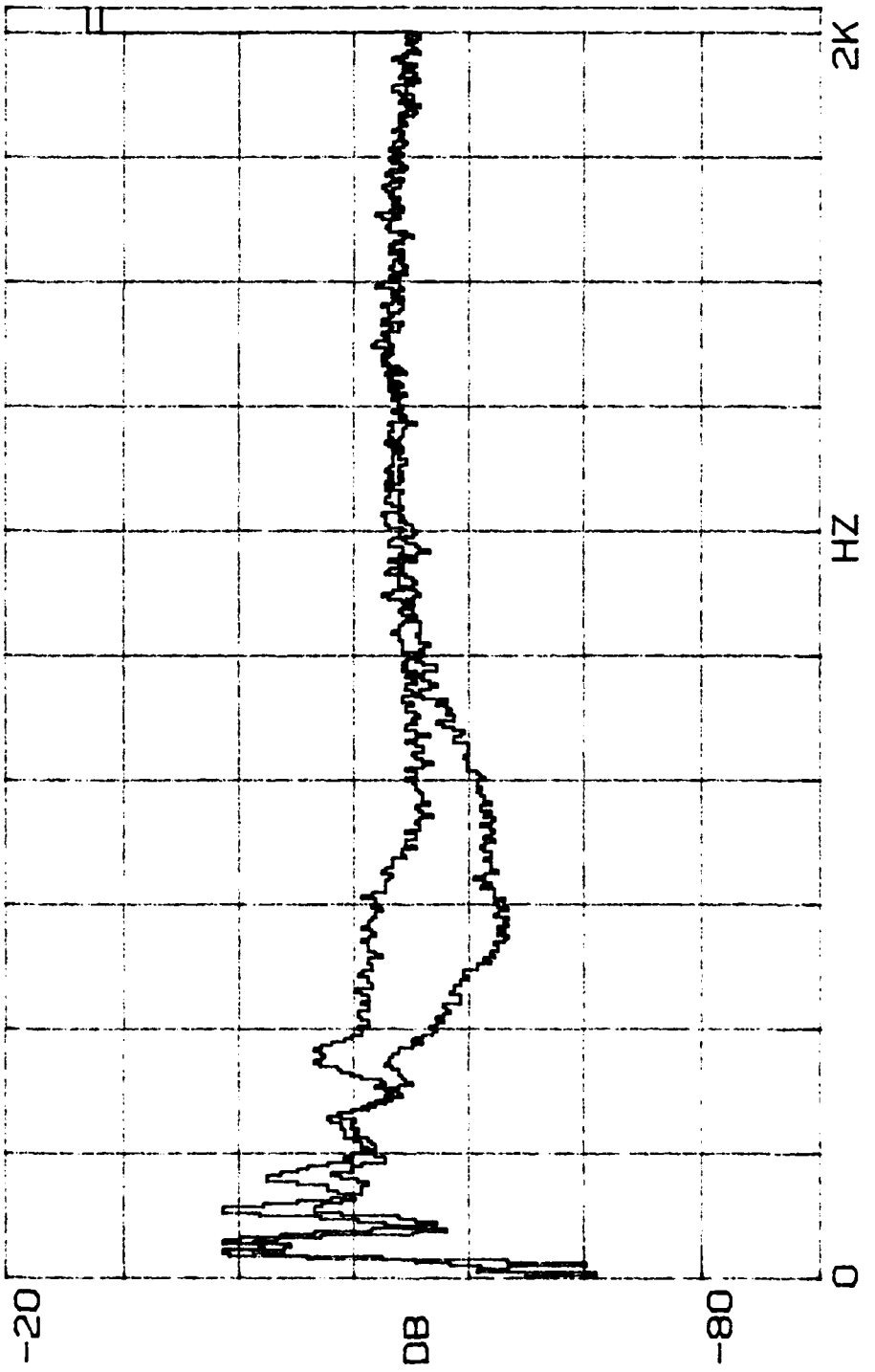

FIGURE 11

$\beta = 1.75$, $R' = 0.45$, $l = 9.5$ cm

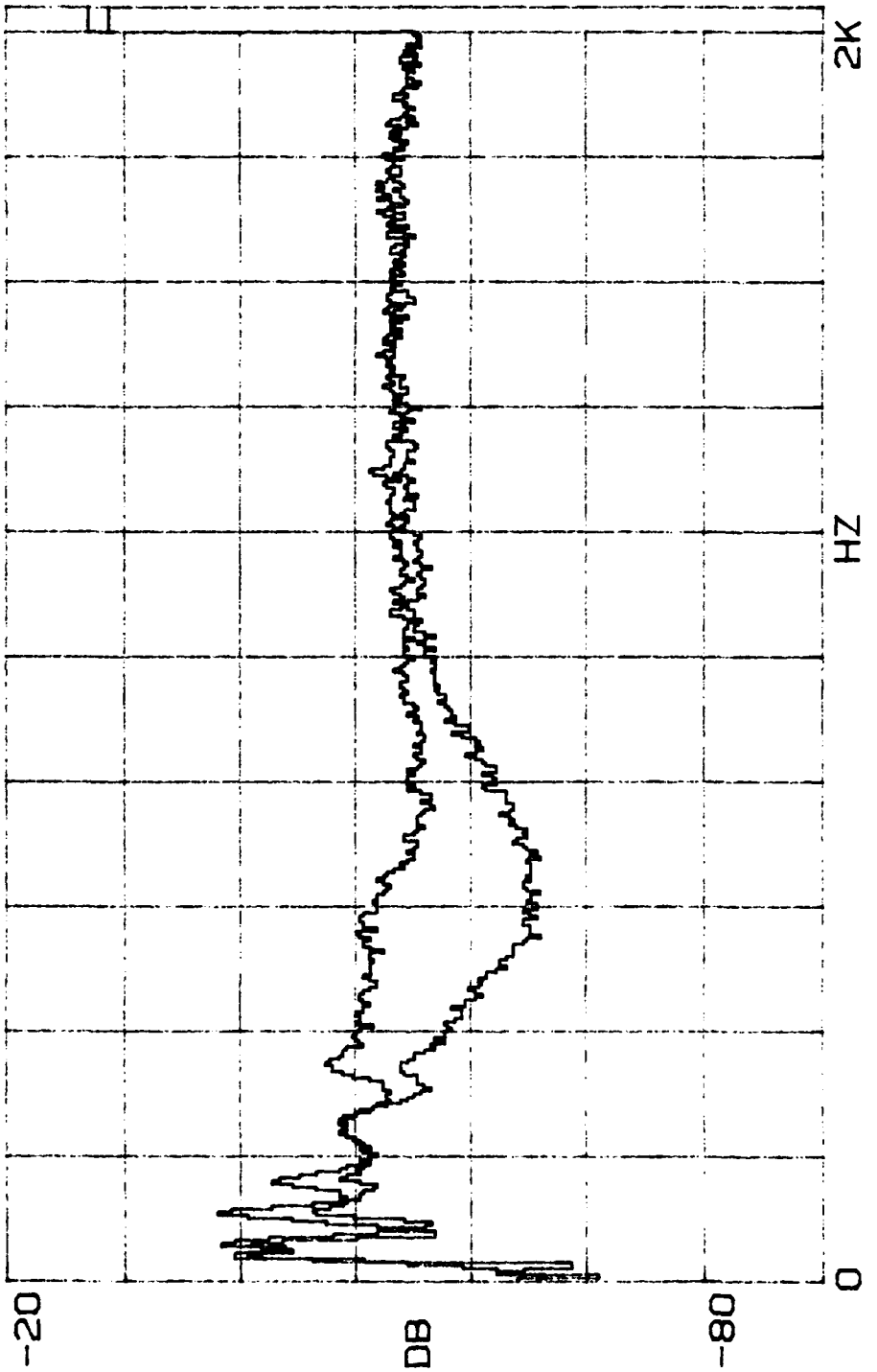

FIGURE I2

β = 1.75, R' = 0.45, l = 11.9 cm

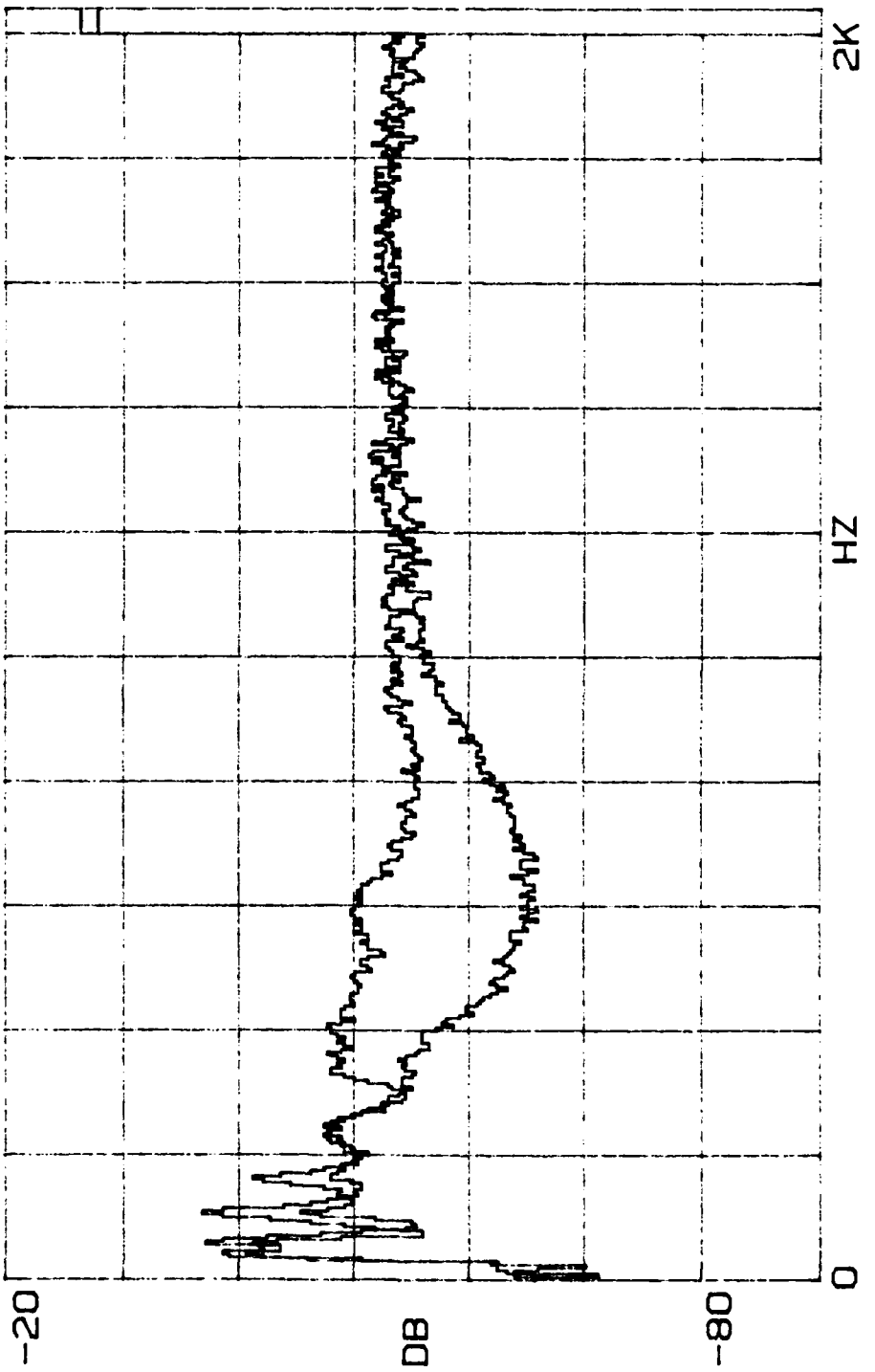

FIGURE I3

β = 1.75, R' = 0.45, l = 14.3 cm

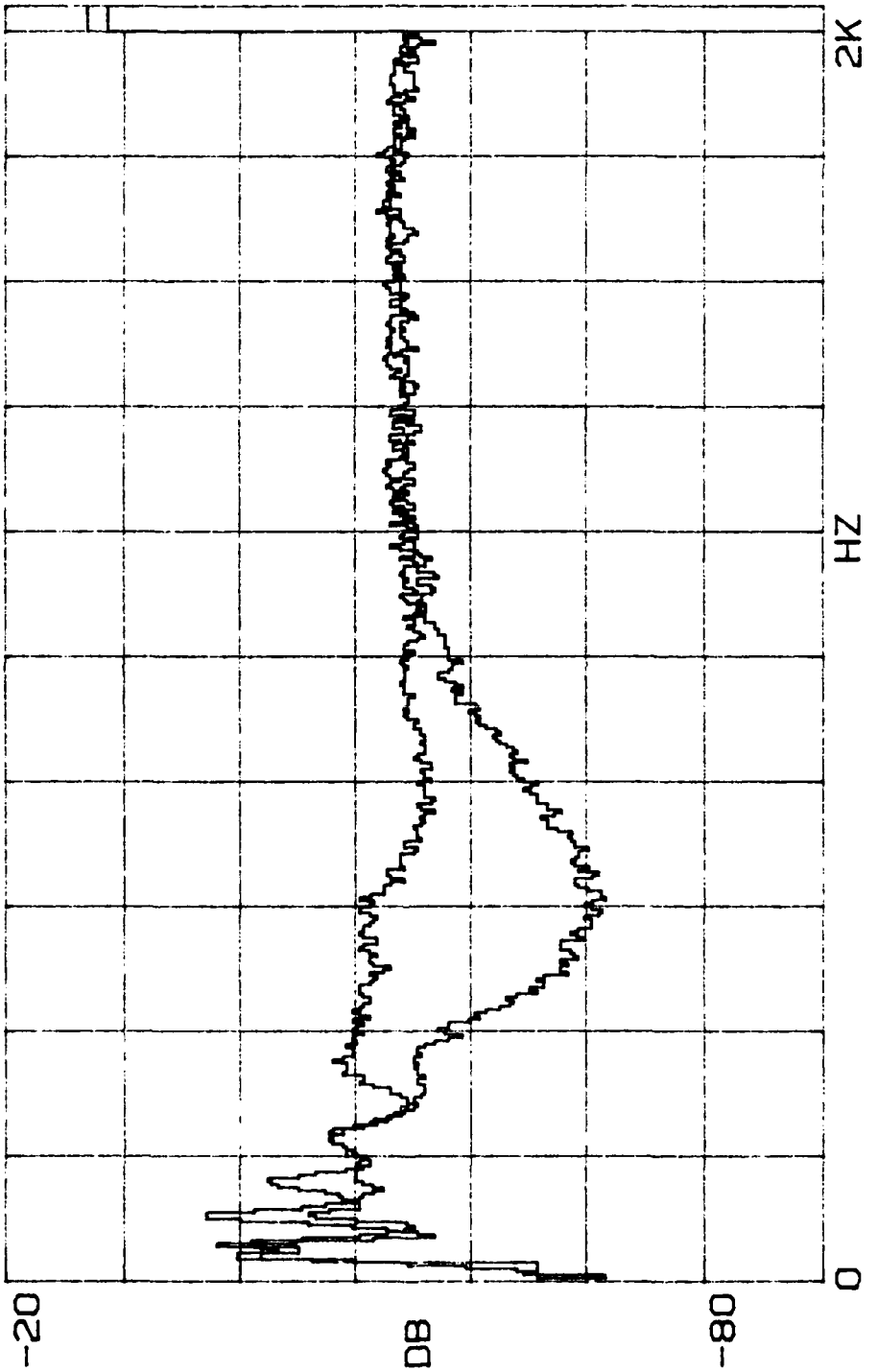

FIGURE I4

$\beta = 1.75$, $R' = 0.45$, $l = 16.7$ cm

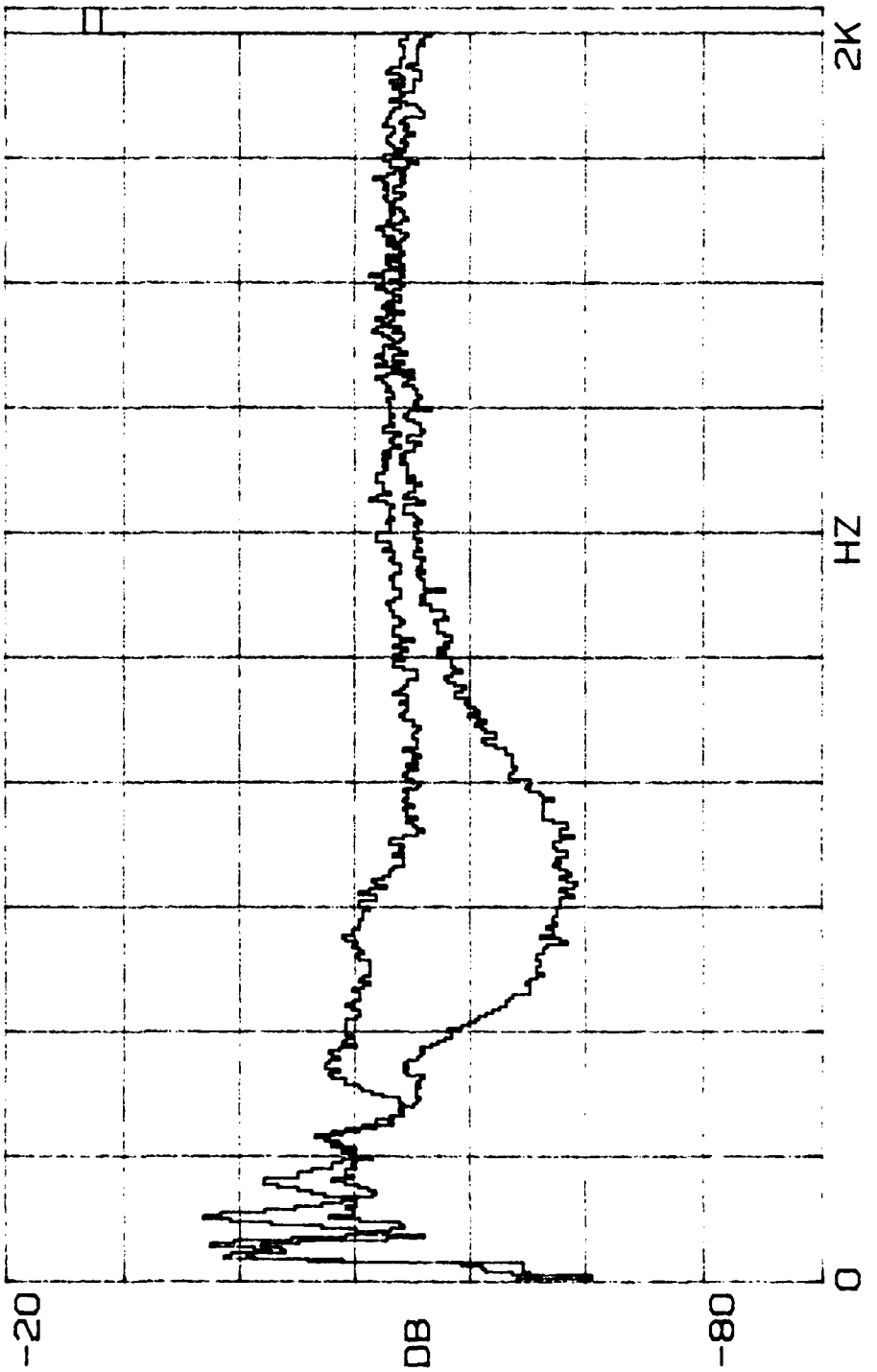

FIGURE I5

β = 1.75, R' = 0.45, l = 19.1 cm

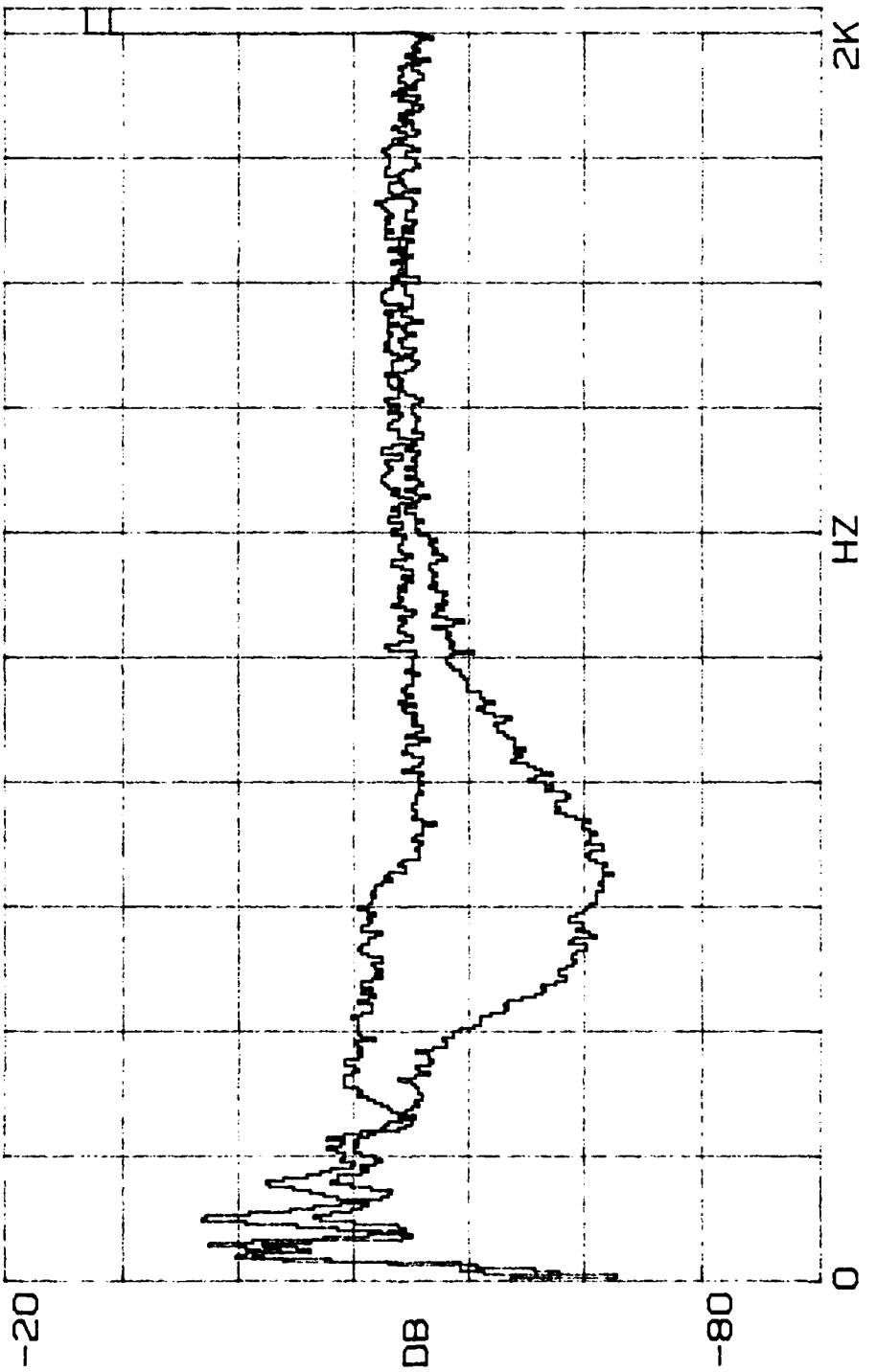

FIGURE I6

$\beta = 1.75$, $R' = 0.45$, $l = 21.5$

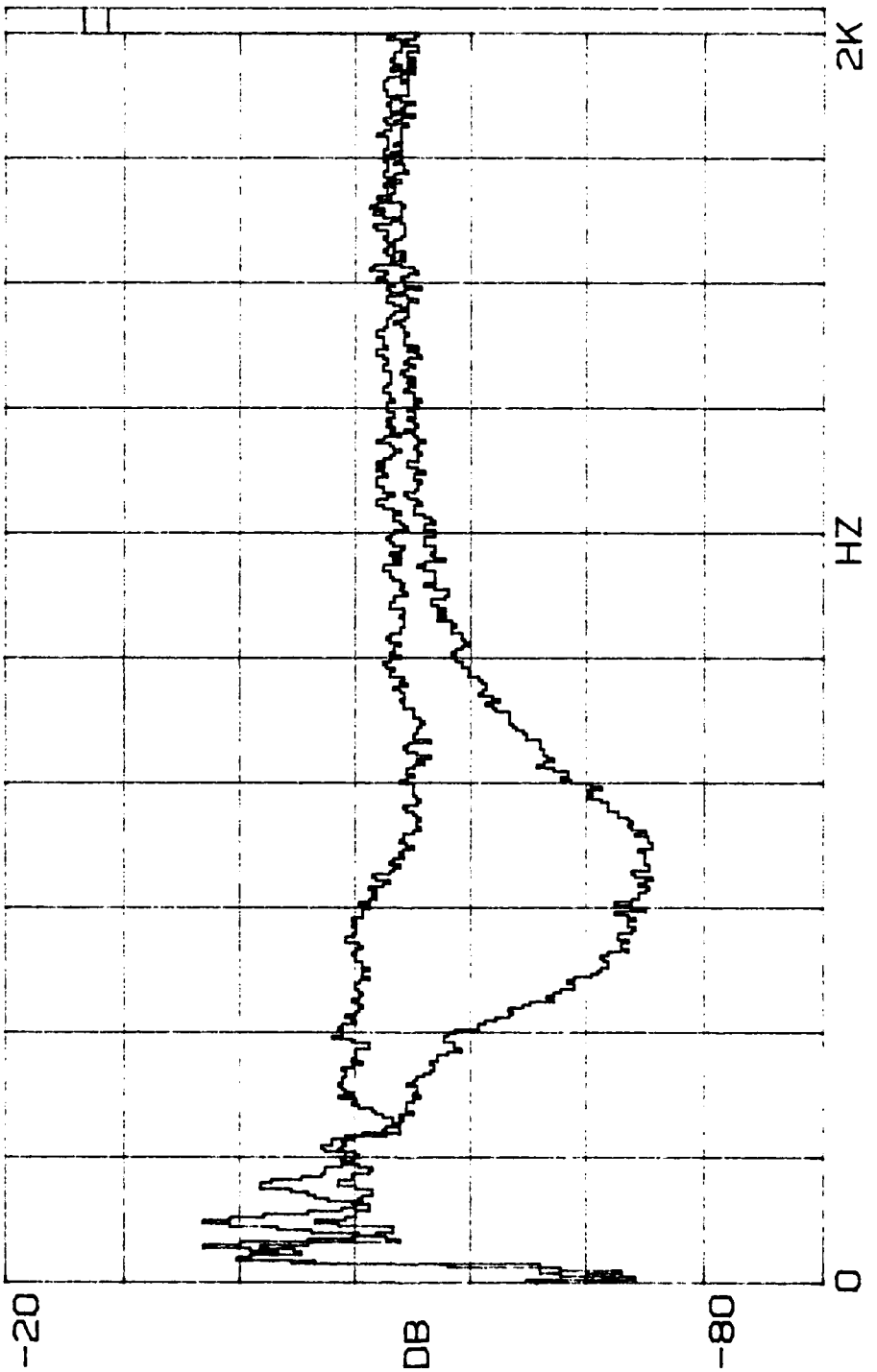

FIGURE I7

$\beta = 1.75$, $R' = 0.45$, $l = 24.0$ cm

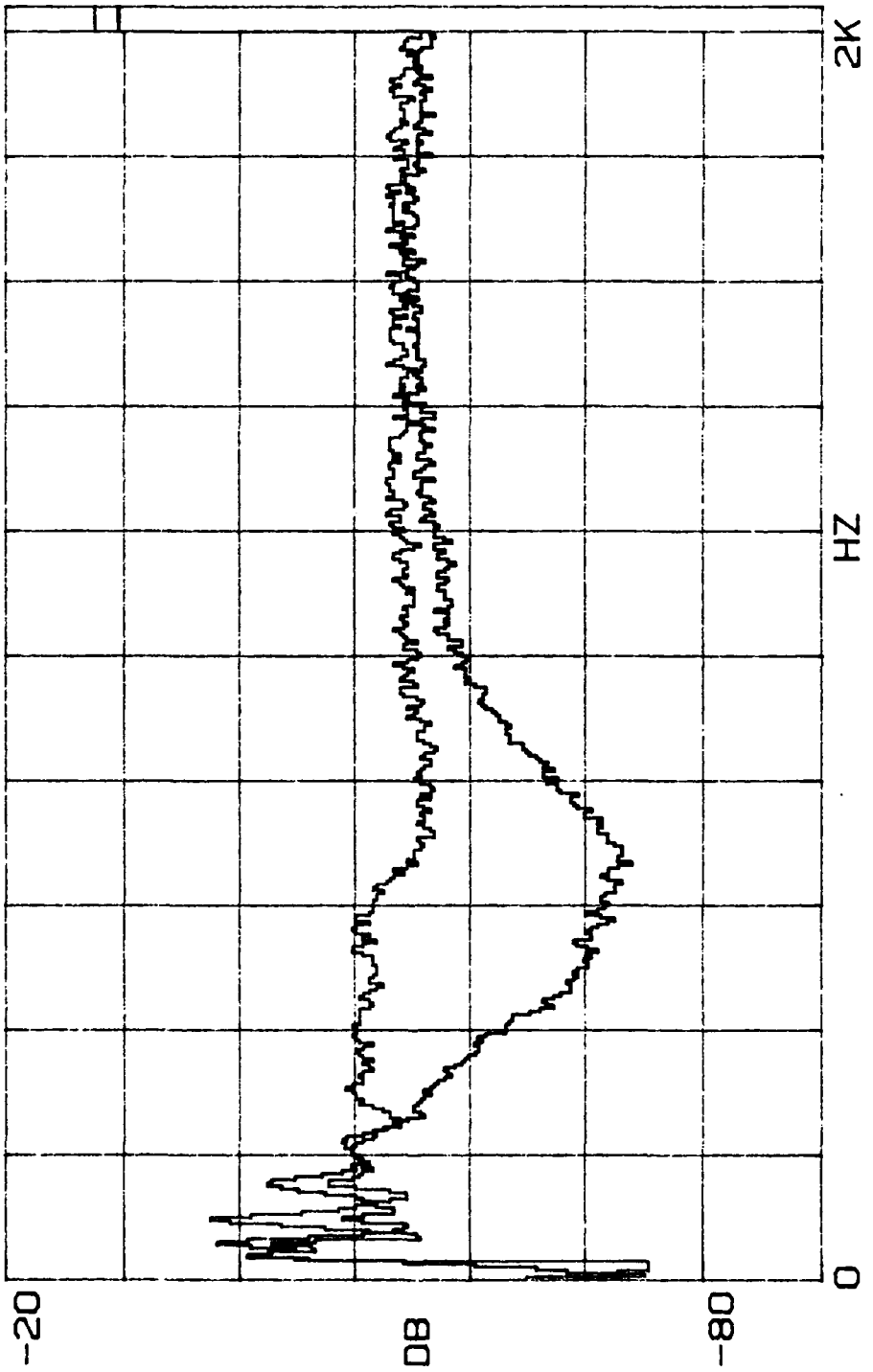

FIGURE I8

β = 1.75, R' = 0.45, l = 26.4 cm

APPENDIX J

ATTENUATION DATA

$\beta_1 = 0.35, \; R_1' = 0.50$

$\beta_2 = 0.51, \; R_2' = 0.47$

TABLE II

m_1 = 0.38 gm f_{o_1} = 1320 Hz ζ_1 = 0.35 R_1' = 0.50

m_2 = 0.55 gm f_{o_2} = 750 Hz ζ_2 = 0.51 R_2' = 0.47

ATTENUATION DATA:

ℓ(cm)	29	31	33	35	37	39
			ATTENUATION (dB)			
f(Hz)						
700	4.8	2.8	2.8	4.9	4.8	3.5
750	3.7	4.1	6.1	6.0	6.6	6.7
800	5.0	6.5	5.7	7.0	9.4	9.4
850	8.0	8.3	9.2	9.6	10.8	12.6
900	9.2	10.9	9.2	11.0	13.3	12.1
950	9.2	9.3	9.5	10.5	12.0	12.9
1000	6.9	7.9	9.0	9.0	11.4	10.1
1050	5.1	6.8	7.7	6.5	8.6	7.4
1100	5.7	5.5	5.5	7.5	6.3	6.6
1150	4.8	6.4	5.9	7.6	7.1	8.4
1200	4.3	5.9	6.0	6.3	5.5	7.4
1250	6.2	7.4	6.3	5.9	7.0	7.8
1300	6.5	5.4	7.1	6.6	8.2	8.9
1350	6.1	7.2	6.9	7.4	9.9	8.8
1400	7.0	7.0	7.9	8.6	9.0	10.1
1450	8.5	8.2	7.8	9.4	10.9	11.1
1500	6.8	7.6	8.4	8.3	11.4	10.8
1550	7.9	8.9	9.5	8.9	11.6	11.5
1600	7.6	9.1	9.2	10.1	10.6	11.4
1650	7.1	8.4	7.7	10.7	10.3	10.2
1700	4.1	6.6	7.4	7.8	9.3	9.5
1750	5.8	8.1	6.0	6.3	8.8	8.6
1800	4.7	7.1	5.8	6.9	8.0	7.9
1850	3.4	6.6	4.3	8.0	7.2	6.6
1900	4.0	5.9	4.1	4.4	5.8	5.2
1950	4.1	5.4	4.1	4.1	5.6	5.8
2000	3.5	3.9	3.6	4.8	4.5	5.2

TABLE J2

m_1 = 0.38 gm f_{o_1} = 1320 Hz $_1$ = 0.35 R_1' = 0.50

m_2 = 0.55 gm f_{o_2} = 750 Hz $_2$ = 0.51 R_2' = 0.47

RESULTS:

f(Hz)	SLOPE (dB/cm)	ATTEN (dB)
700	0.023	0.66
750	0.320	8.89
800	0.457	12.3
850	0.441	11.5
900	0.336	8.52
950	0.392	9.68
1000	0.379	9.12
1050	0.224	5.26
1100	0.127	2.91
1150	0.311	6.98
1200	0.208	4.53
1250	0.091	1.96
1300	0.284	5.99
1350	0.316	6.54
1400	0.317	6.44
1450	0.324	6.47
1500	0.447	8.78
1550	0.364	7.03
1600	0.349	6.64
1650	0.346	6.48
1700	0.507	9.36
1750	0.226	4.11
1800	0.283	5.08
1850	0.307	5.43
1900	0.086	1.50
1950	0.130	2.24
2000	0.164	2.79

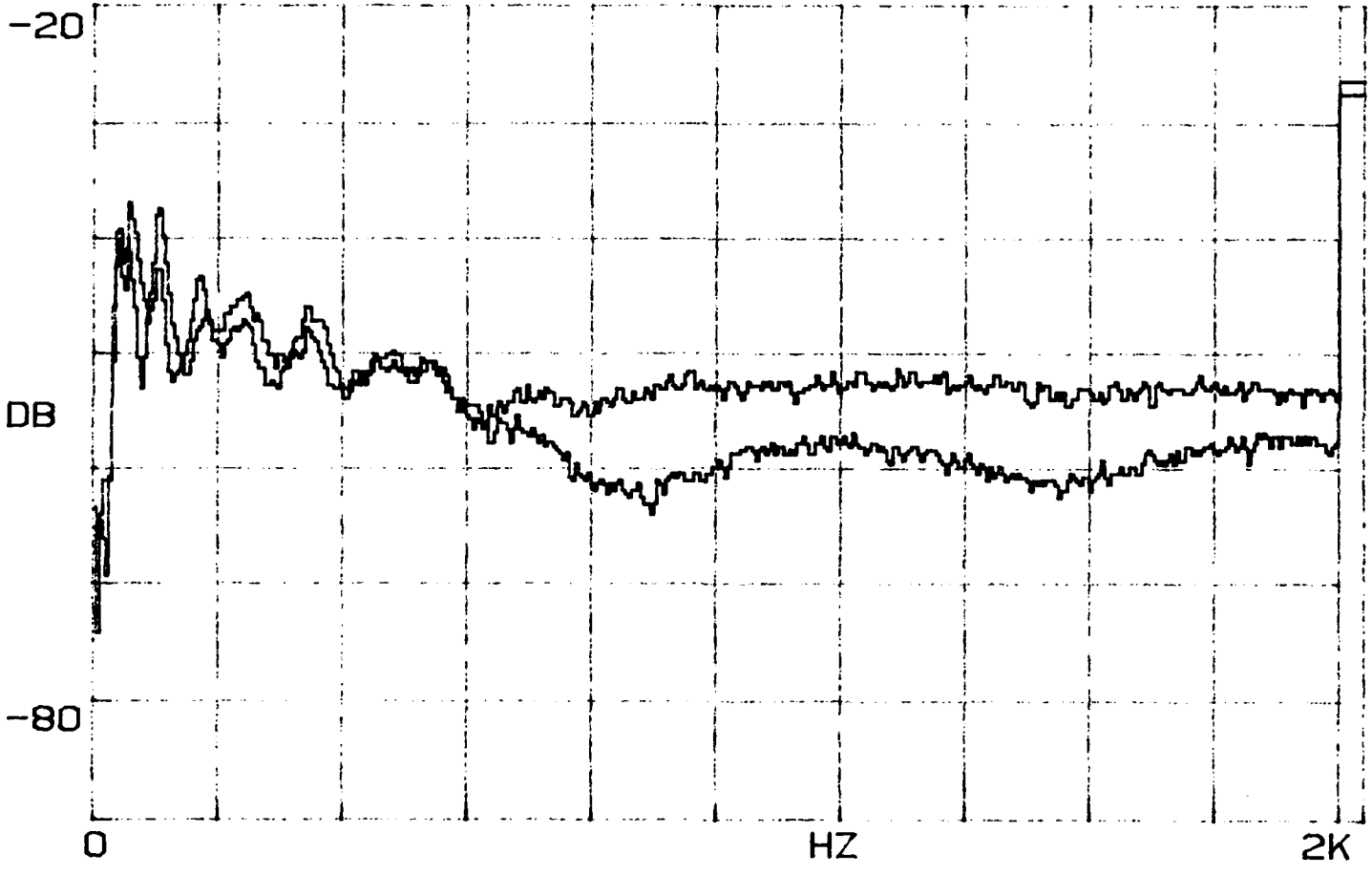

FIGURE J1

β_1=0.35, R'_1=0.50; β_2=0.51, R'_2=0.47

l = 29 cm

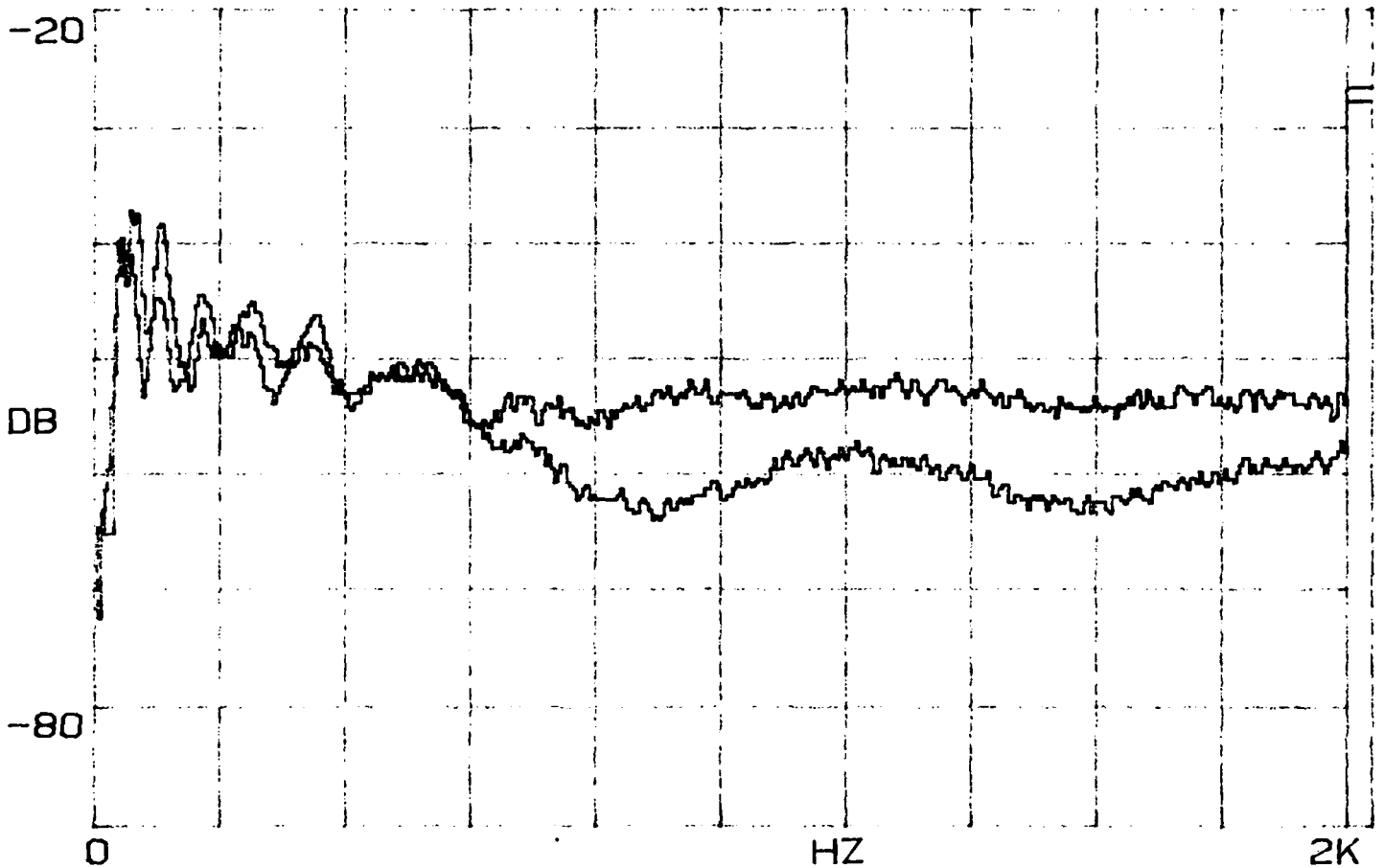

FIGURE J2

β_1=0.35, R'_1=0.50; β_2=0.51, R'_2=0.47

l = 31 cm

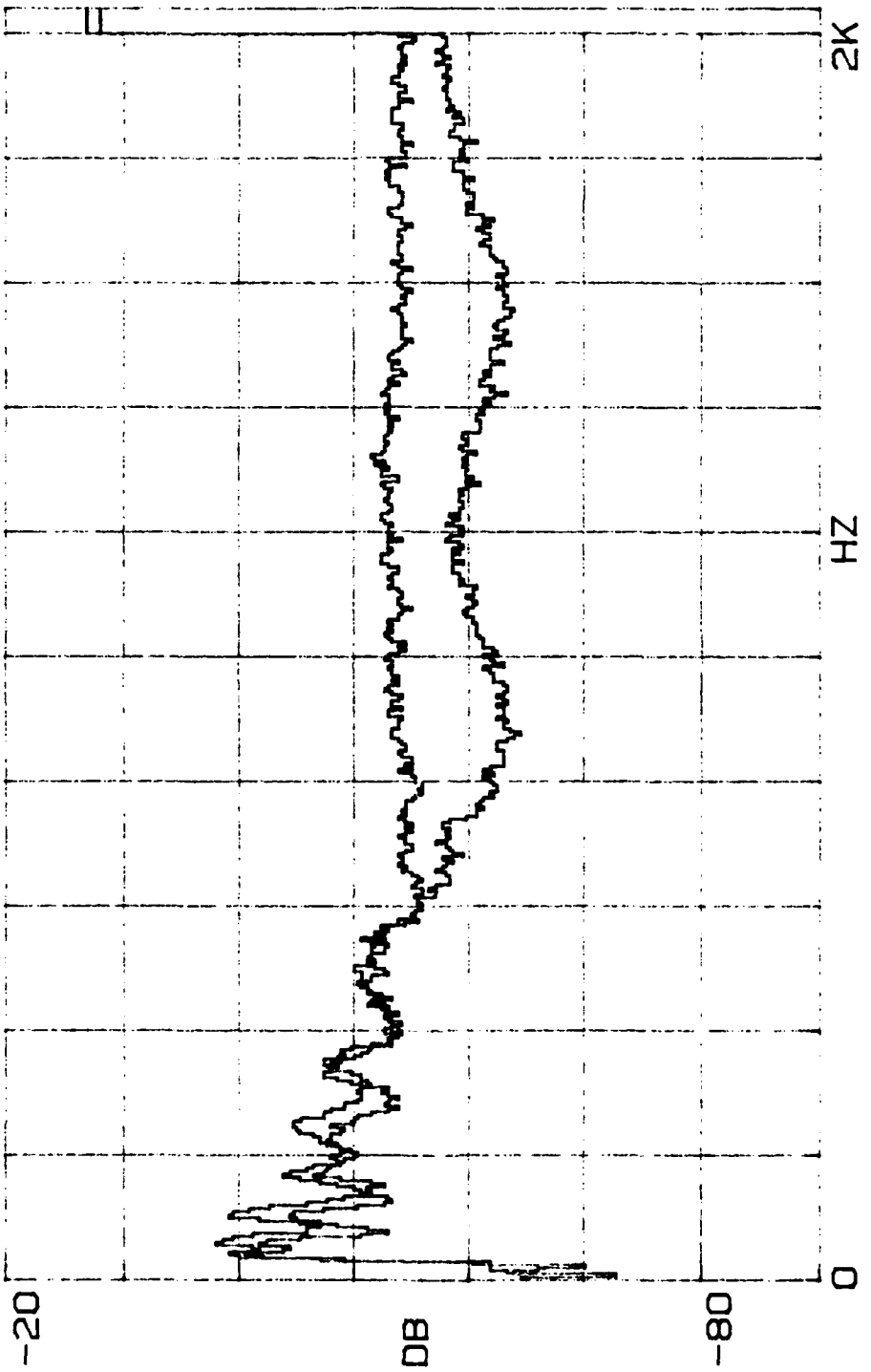

FIGURE J3

β_1=0.35, R'_1=0.50; β_2=0.51, R'_2=0.47

l = 33 cm

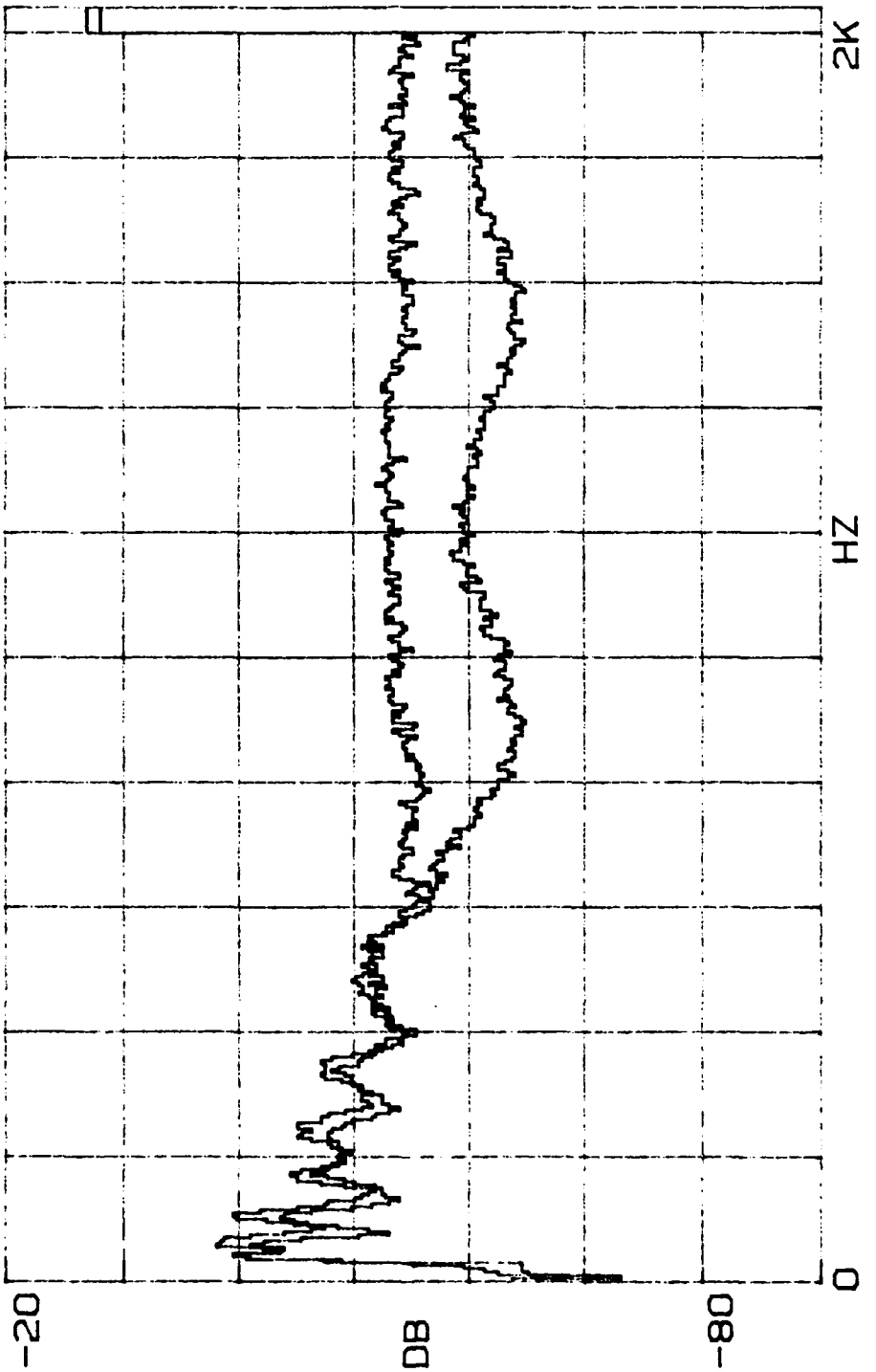

FIGURE J4

β_1=0.35, R'_1=0.50; β_2=0.51, R'_2=0.47

l = 35 cm

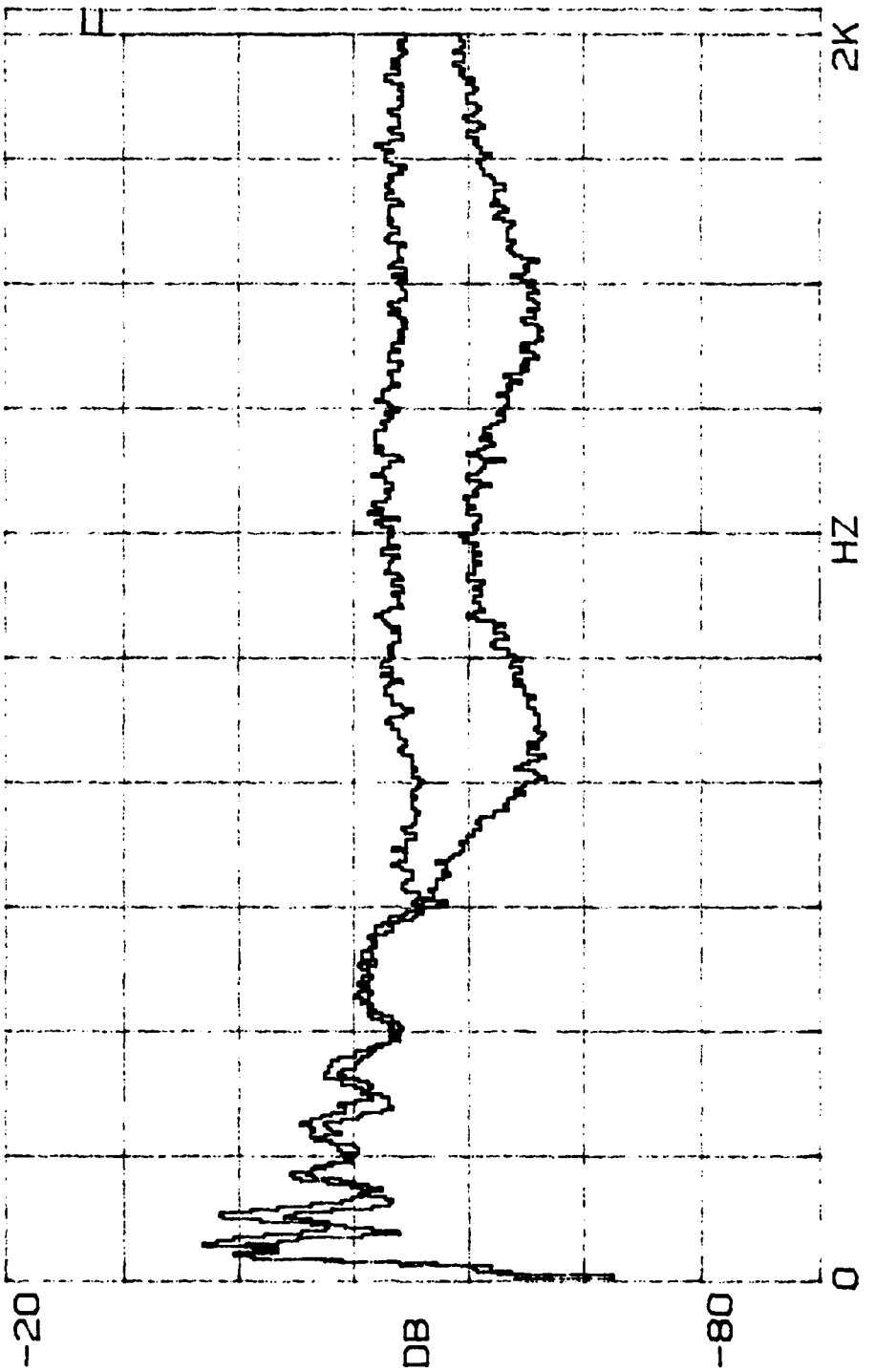

FIGURE J5

β_1=0.35, R'_1=0.50; β_2=0.51, R'_2=0.47

l = 37 cm

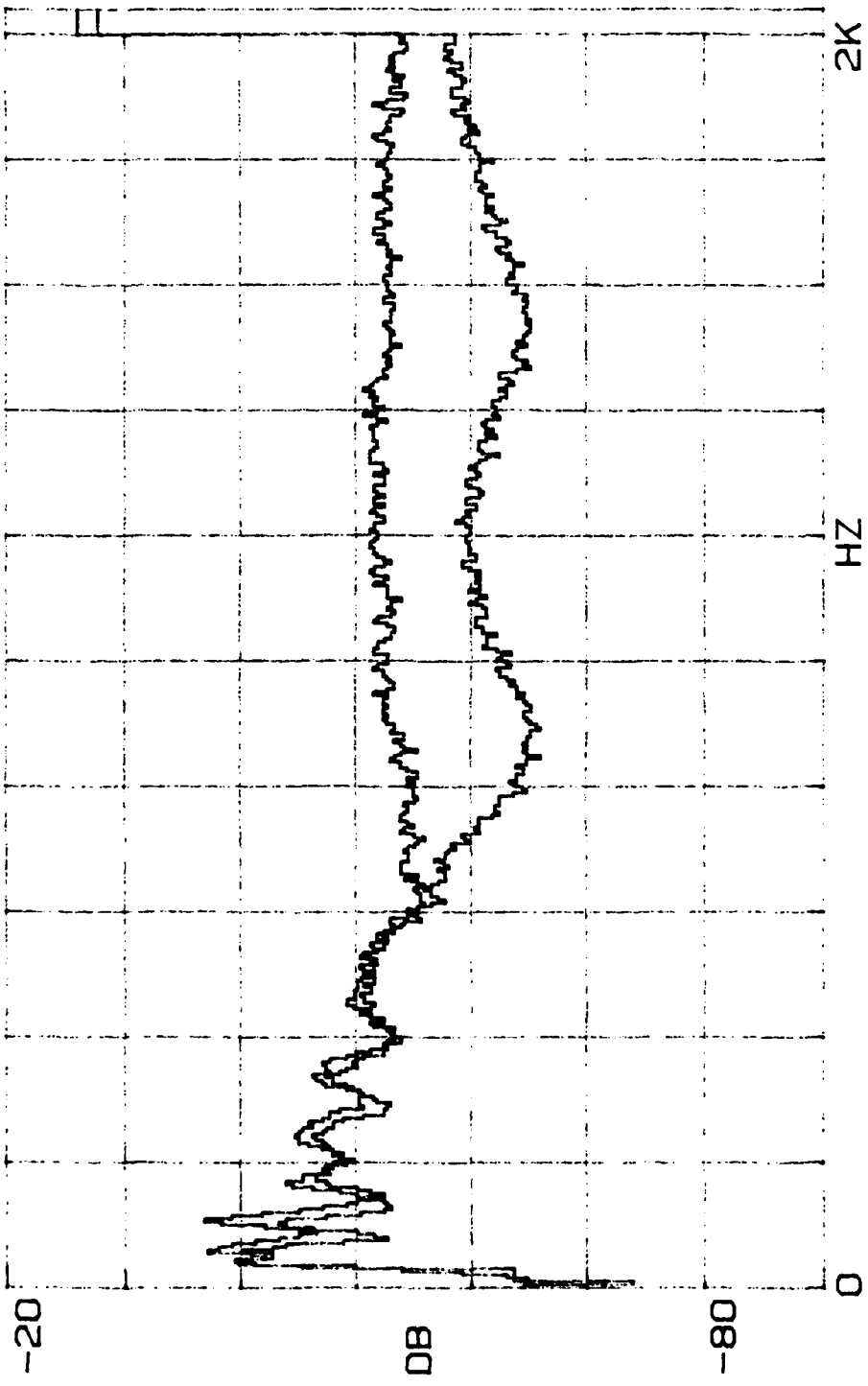

FIGURE J6

β_1=0.35, R'_1=0.50; β_2=0.51, R'_2=0.47

1 = 39 cm

APPENDIX K

ATTENUATION DATA

$\beta_1 = 0.69, \; R_1' = 0.47$

$\beta_2 = 1.75, \; R_2' = 0.45$

TABLE XI

m_1 = 1.00 gm f_{o_1} = 1000 Hz β_1 = 0.69 R_1' = 0.47

m_2 = 1.91 gm f_{o_2} = 420 Hz β_2 = 1.75 R_2' = 0.45

ATTENUATION DATA:

ℓ(cm)	15	17.5	20	22.5	25	27.5	30	32.5
f(Hz)	ATTENUATION (dB)							
400	1.5	0.8	4.4	3.6	3.2	4.4	6.7	7.3
450	4.2	4.7	6.2	6.9	6.7	7.3	10.0	12.1
500	6.5	6.8	9.6	11.3	11.3	12.0	14.2	16.3
550	9.2	11.7	10.0	14.1	16.4	17.0	17.6	19.6
600	12.2	14.4	14.1	15.4	16.6	18.4	21.7	21.2
650	11.0	14.0	13.6	15.5	13.8	18.8	19.2	20.9
700	8.3	11.4	11.8	12.6	12.8	14.8	16.1	18.2
750	9.4	7.4	9.7	11.4	10.0	11.7	14.1	14.5
800	6.3	6.3	9.0	8.7	9.7	11.3	13.9	13.2
850	6.8	6.5	7.0	8.2	9.0	10.3	12.5	12.6
900	5.6	6.9	7.5	8.0	10.1	10.1	13.6	13.1
950	6.2	6.4	8.4	8.9	11.2	12.2	14.3	14.4
1000	6.7	8.2	9.3	10.4	10.4	12.1	14.3	15.8
1050	7.2	6.8	9.0	9.4	10.6	13.4	15.5	16.5
1100	7.0	8.0	9.1	11.4	13.1	12.8	15.8	16.3
1150	7.3	6.9	9.7	10.0	11.9	11.4	12.6	15.1
1200	6.1	6.7	7.5	8.9	11.2	10.4	13.2	13.2
1250	5.5	6.9	7.1	8.6	8.9	8.6	9.4	11.8
1300	4.8	5.4	6.5	5.9	8.2	8.1	8.1	10.4
1350	4.4	5.4	4.7	6.1	6.7	7.2	7.8	8.9
1400	4.0	3.3	4.3	4.0	5.8	5.6	6.3	6.5

[illegible] K2

m_1 = 1.00 gm f_{o_1} = 1000 Hz ζ_1 = 0.69 R_1' = 0.47

m_2 = 1.91 gm f_{o_2} = 420 Hz ζ_2 = 1.75 R_2' = 0.45

RESULTS:

f(Hz)	SLOPE (dB/cm)	ATTEN (dB)
400	0.332 (0.396)*	12.6 (15.0)*
450	0.404 (0.384)	14.4 (13.7)
500	0.537 (0.688)	18.2 (23.4)
550	0.598 (0.672)	19.4 (21.8)
600	0.541 (0.392)	16.8 (12.1)
650	0.520 (0.524)	15.5 (15.6)
700	0.486 (0.532)	13.9 (15.3)
750	0.351 (0.332)	9.7 (9.2)
800	0.449	12.0
850	0.387	10.1
900	0.413	10.4
950	0.527	13.0
1000	0.489	11.7
1050	0.586	13.7
1100	0.557	12.7
1150	0.429 (0.492)**	9.6 (11.0)**
1200	0.444 (0.496)	9.7 (10.9)
1250	0.292 (0.340)	6.2 (7.3)
1300	0.285 (0.292)	6.0 (6.1)
1350	0.246 (0.212)	5.1 (4.3)
1400	0.182 (0.172)	3.7 (3.5)

* slope through first four data points only

** slope through first five data points only

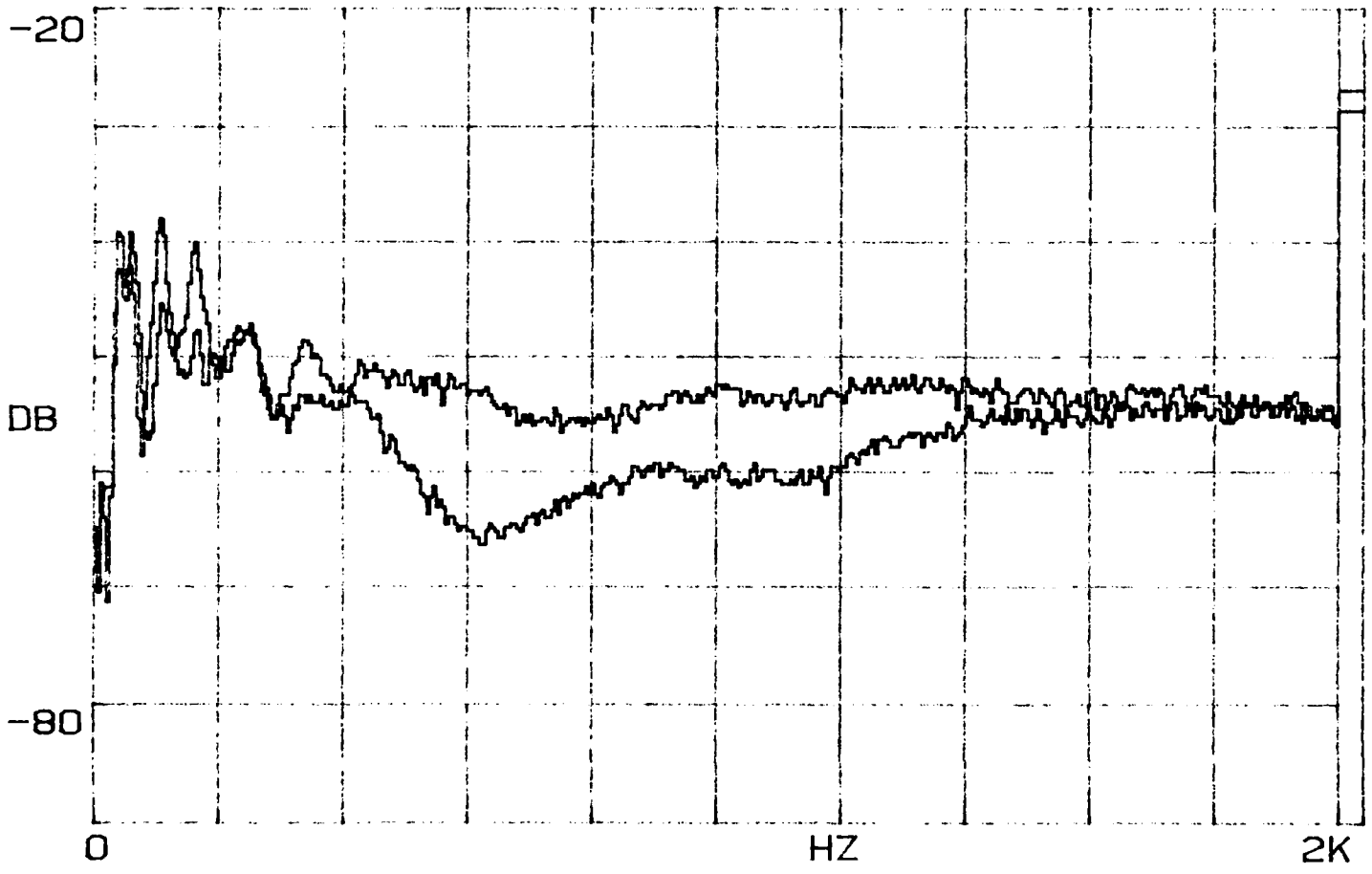

FIGURE K1

β_1=0.69, R'_1=0.47; β_2=1.75, R'_2=0.45

1 = 15 cm

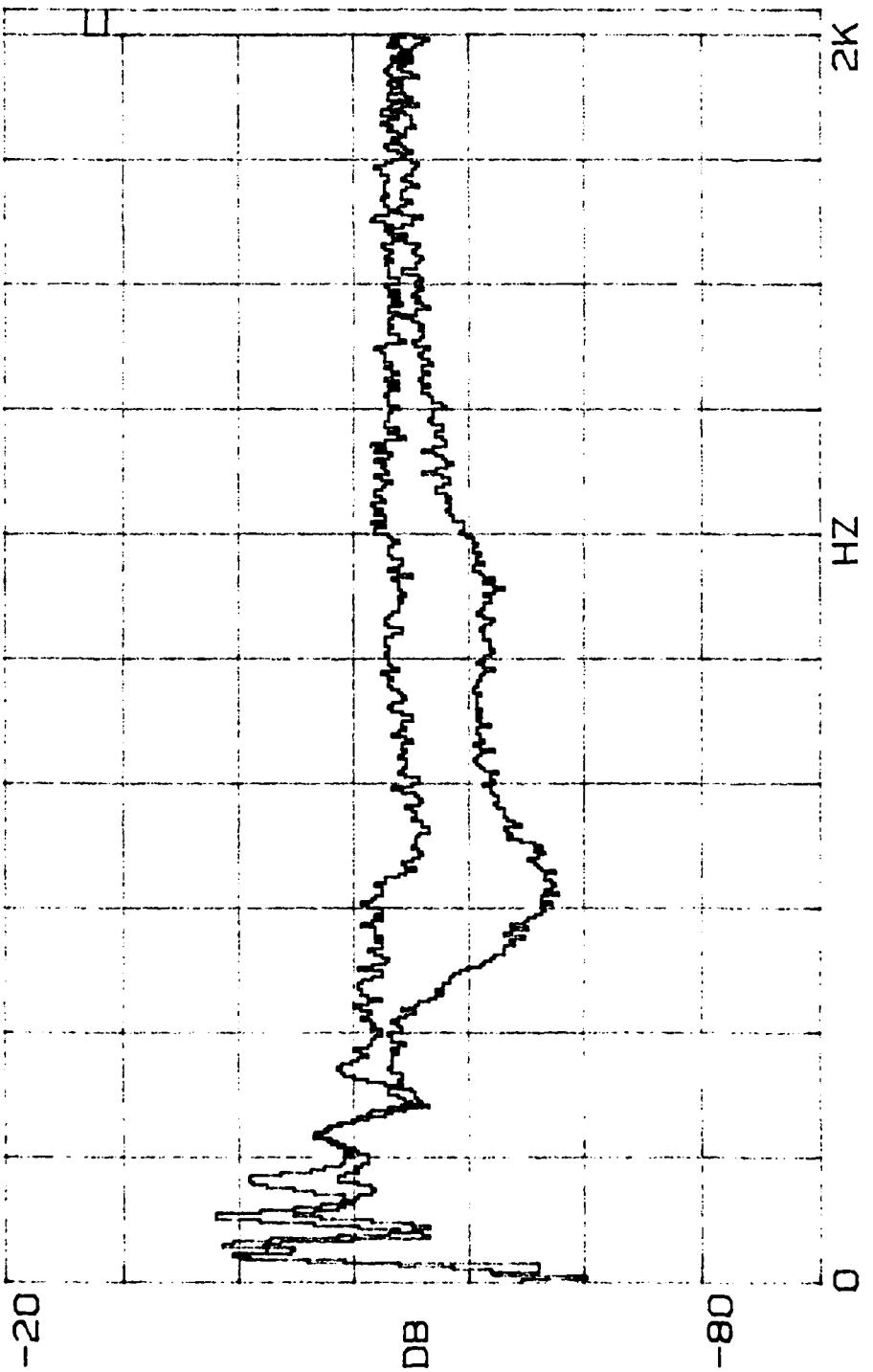

FIGURE K2

β_1=0.69, R'_1=0.47; β_2=1.75, R'_2=0.45
l = 17.5 cm

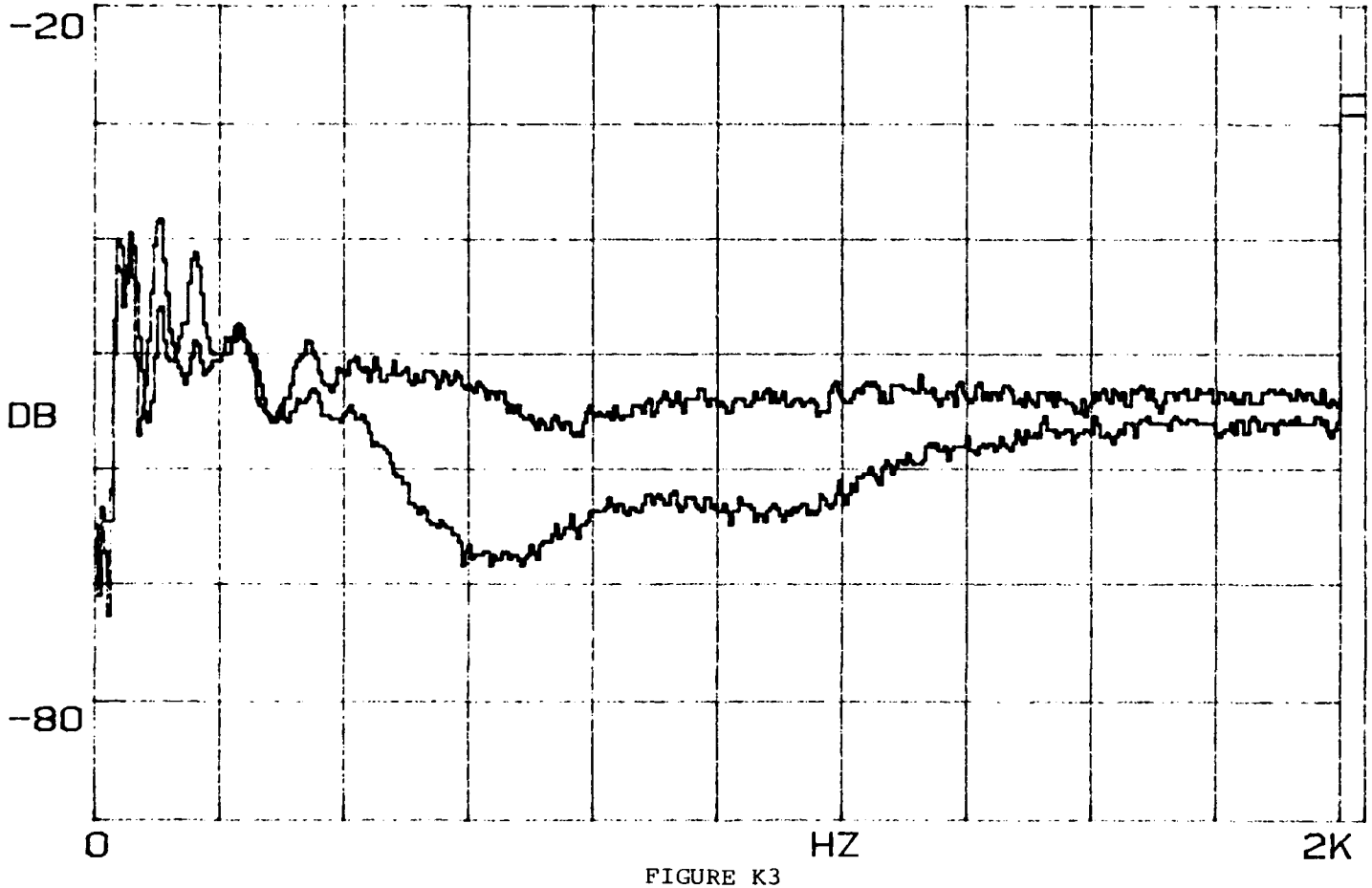

FIGURE K3

β_1=0.69, R'_1=0.47; β_2=1.75, R'_2=0.45

l = 20 cm

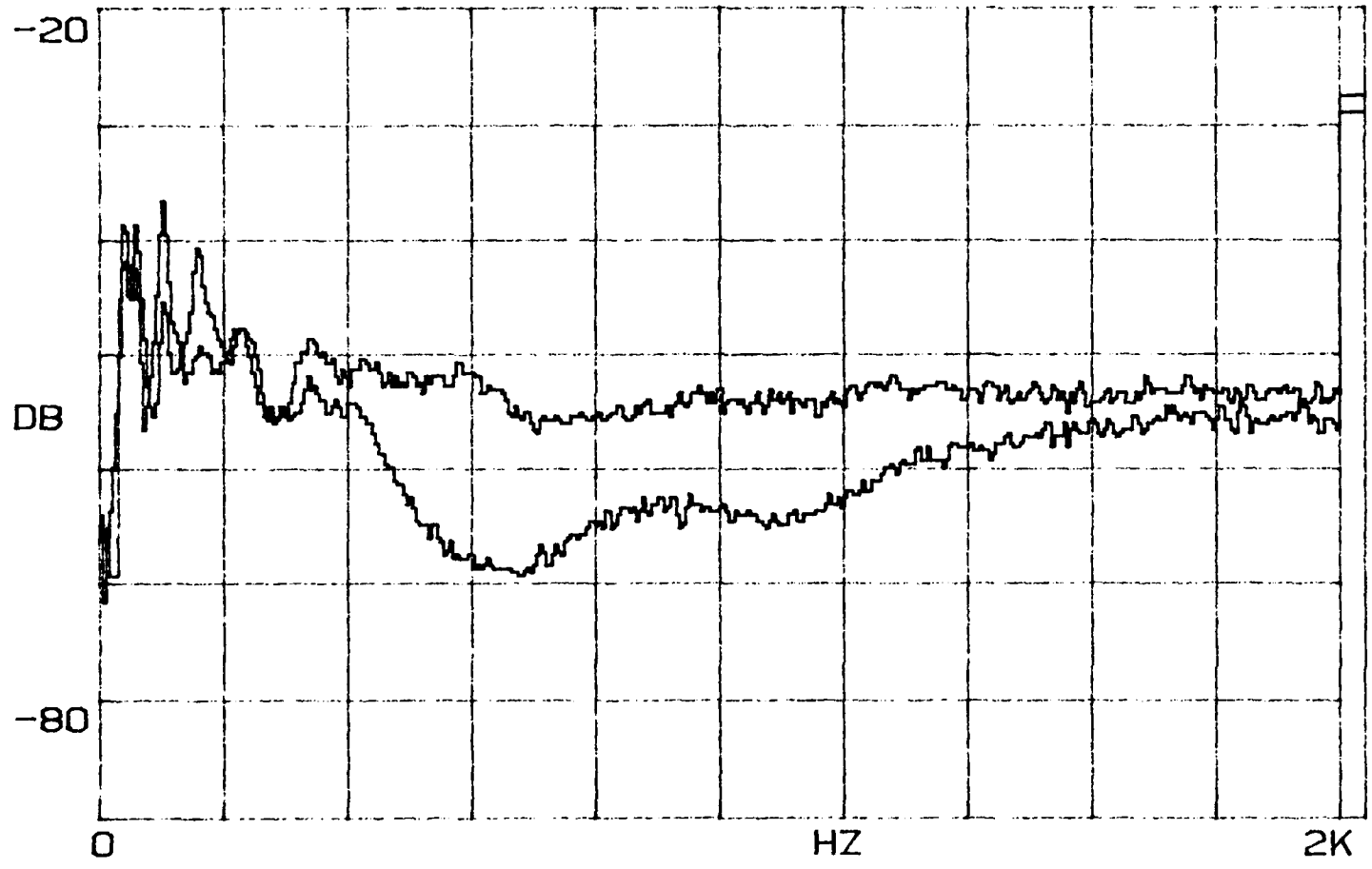

180

FIGURE K4

β_1=0.69, R_1'=0.47; β_2=1.75, R_2'=0.45

l = 22.5 cm

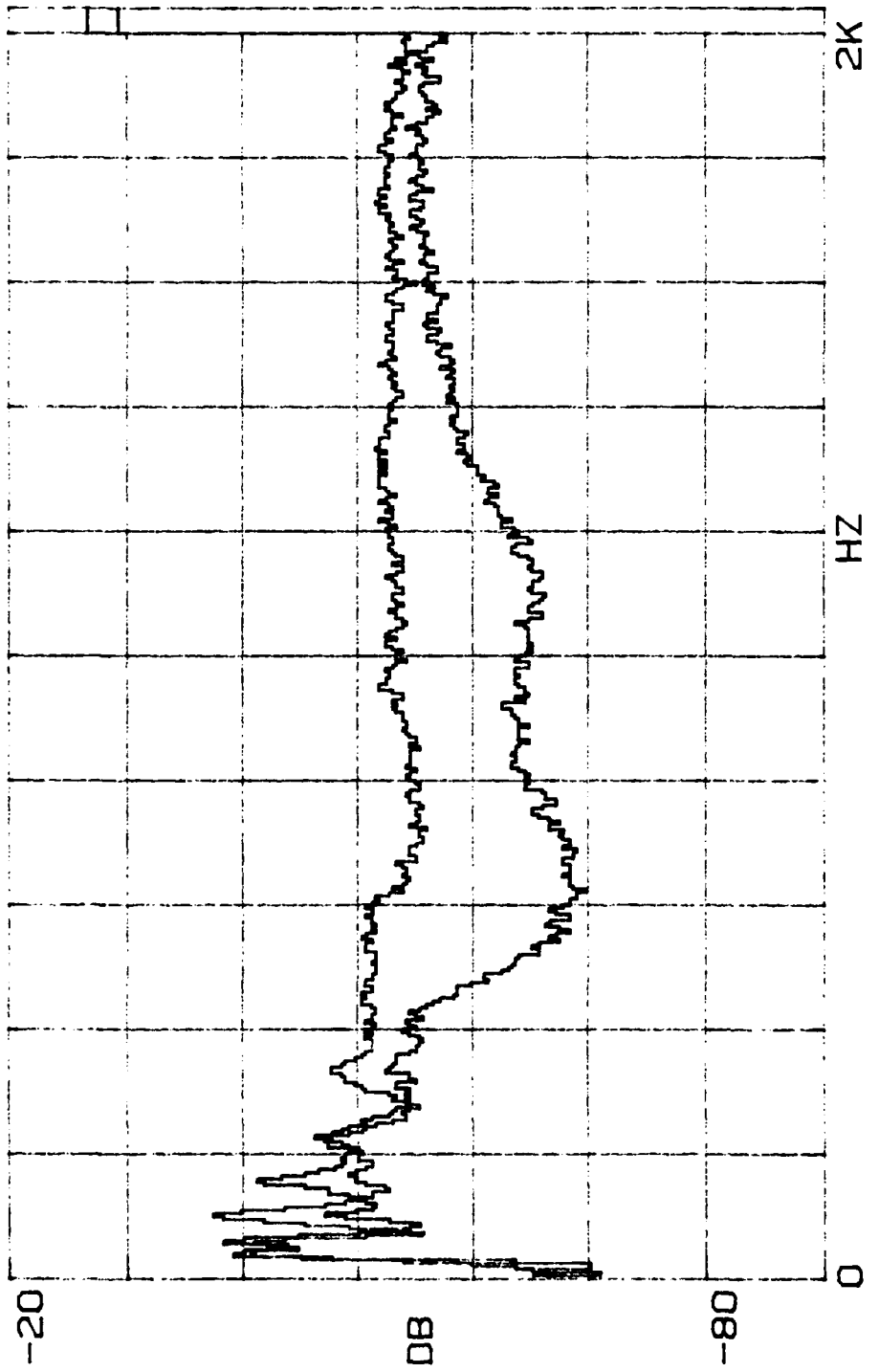

FIGURE K5

β_1=0.69, R'_1=0.47; β_2=1.75, R'_2=0.45

l = 25 cm

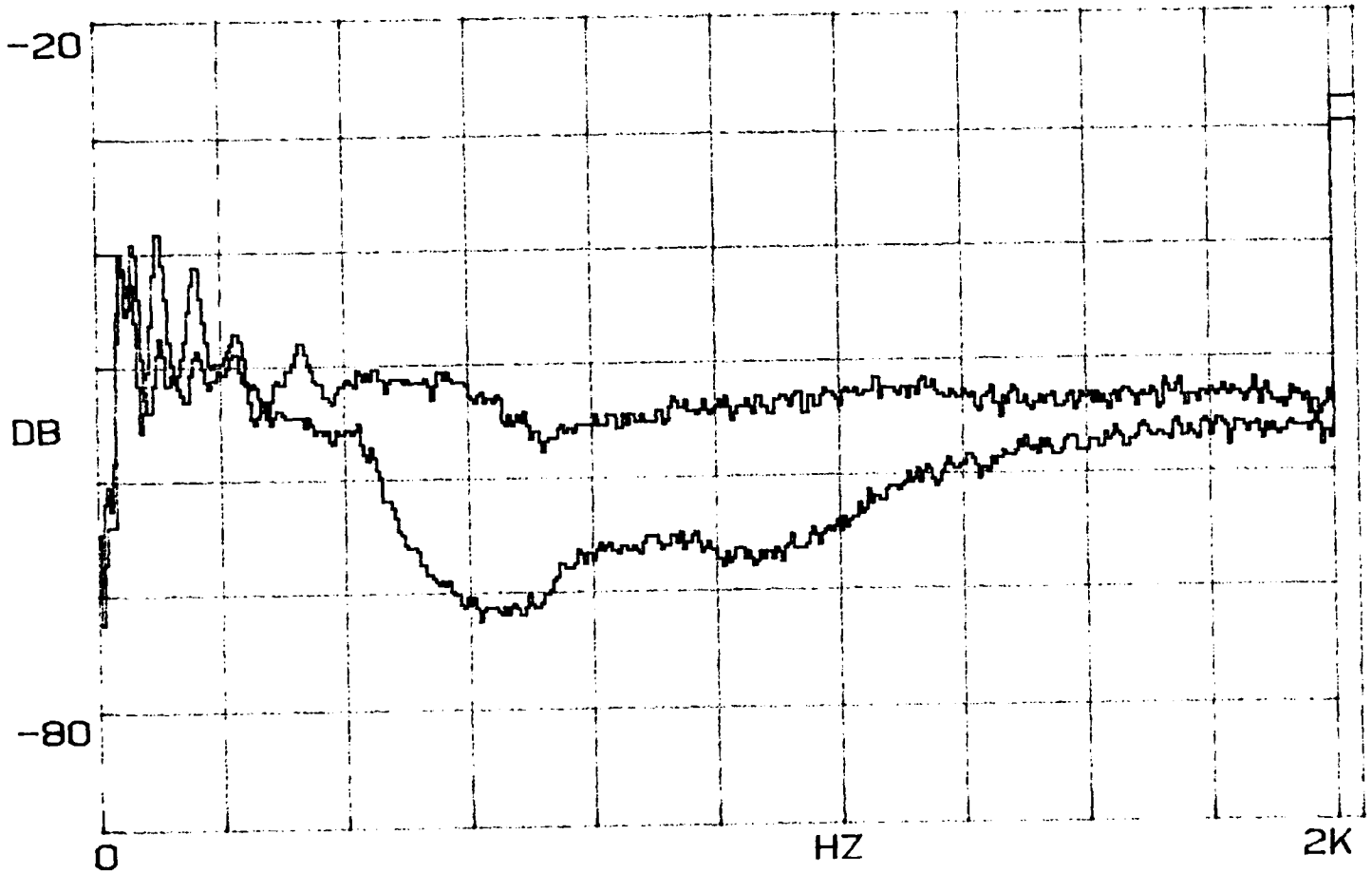

FIGURE K6

β_1=0.69, R_1'=0.47; β_2=1.75, R_2'=0.45

1 = 27.5 cm

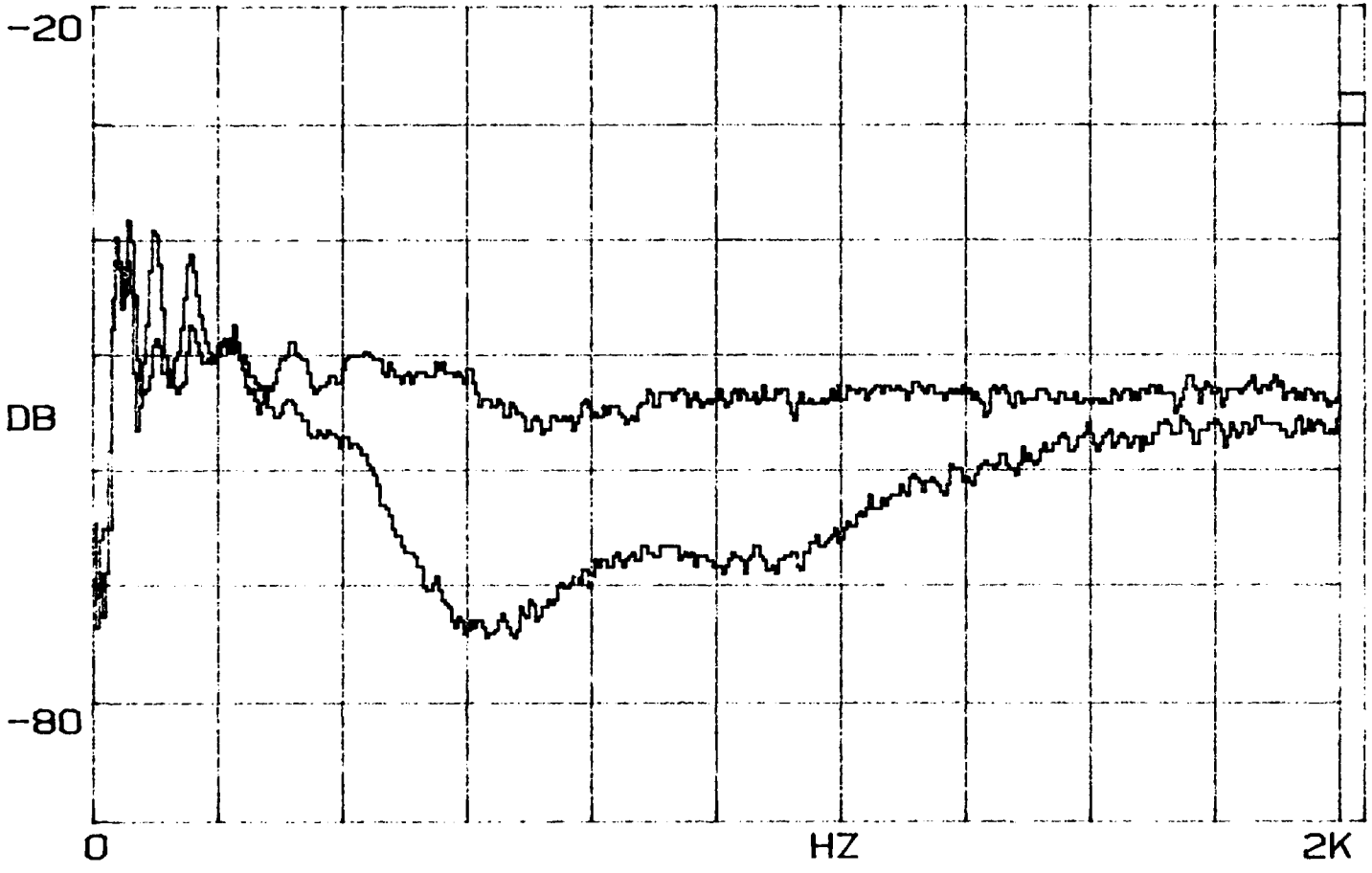

FIGURE K7

β_1=0.69, R_1'=0.47; $\beta_2$1.75, R_2'=0.45

l = 30 cm

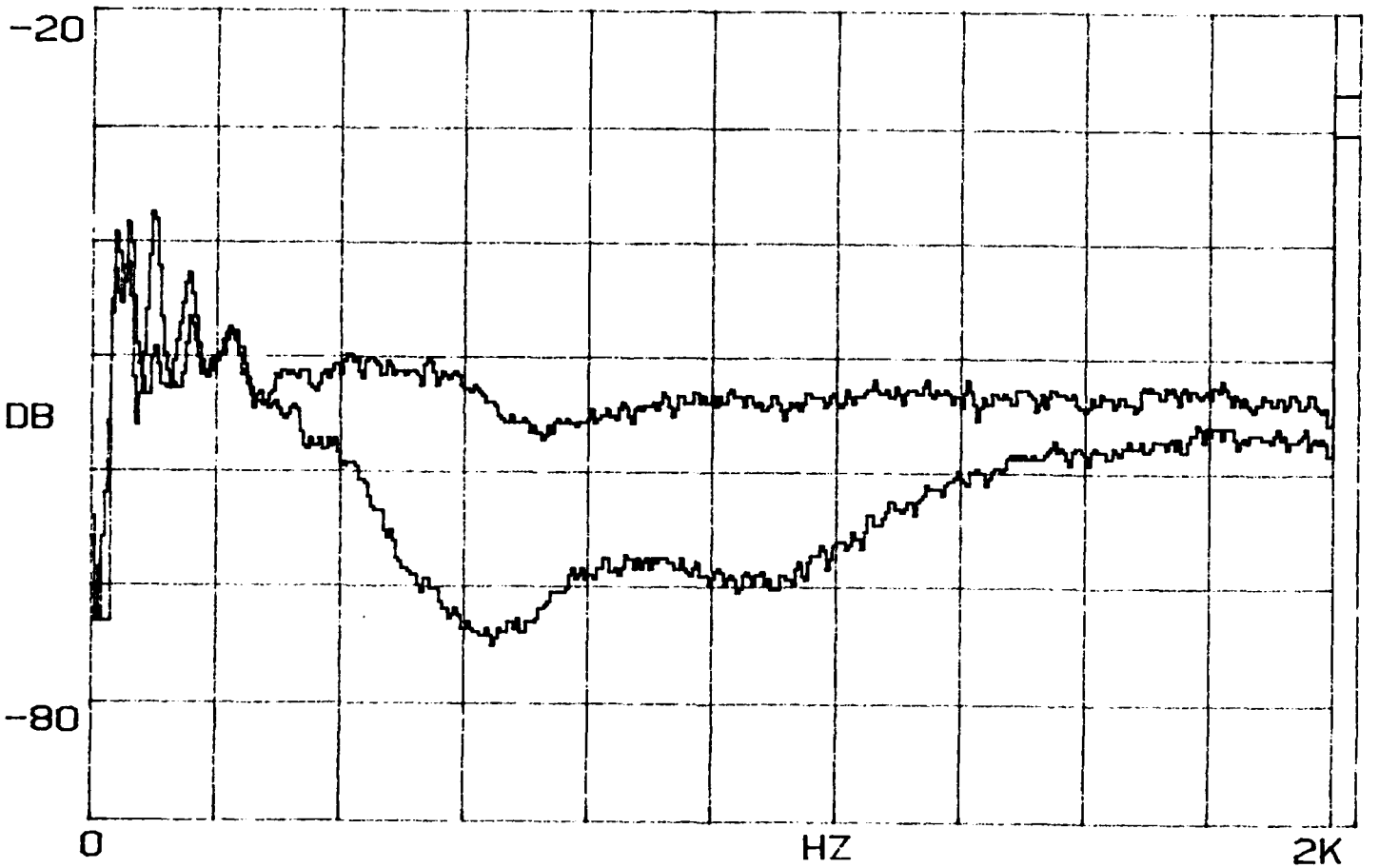

FIGURE K8

β_1=0.69, R'_1=0.47; β_2=1.75, R'_2=0.45

l = 32.5 cm

REFERENCES

1. Cremer, L., Heckl, M., and Ungar, E.E., Structure-Borne Sound, Springer-Verlag, New York, 1973.

2. Dyer, Ira, Notes, Massachusetts Institute of Technology, November 1984.

3. Meirovitch, Leonard, Elements of Mechanical Vibration, McGraw-Hill, New York, 1975.

4. Thompson, William T., Theory of Vibration with Application, Prentice-Hall, New Jersey, 1972.

5. Den Hartog, J.P., Mechanical Vibrations, McGraw-Hill, New York, 1947.

6. Bruel and Kjaer, Measuring Vibration, K. Larsen and Sons, Denmark, September 1982.

7. McGoldrick, R.T., "Ship Vibration," David Taylor Model Basin Report 1451, Carder Rock, Virginia, 1960.

8. Junger, M.C. and Garrelick, J.M., "Ship Silencing and Shock Hardening," Draper Laboratory, Inc., Cambridge, Massachusetts, February 1974.

9. Heckl, M., "Wave Propagation on Beam-Plate Systems," Journal of the Acoustical Society of America, May 1961.

10. Mace, B.R., "Wave Reflection and Transmission in Beams," Journal of Sound and Vibration, 1984.

END

FILMED

11-85

DTIC